UNIVERSITY OF MARIBOR

FACULTY OF CHEMISTRY AND CHEMICAL ENGINEERING

Andreja Nemet

SYNTHESIS OF PROCESSES AND PROCESS SUBSYSTEMS FOR ENTIRE LIFETIME

PhD - Doctoral Dissertation

Maribor, 2015

University of Maribor

Faculty of Chemistry and
Chemical Engineering

Andreja Nemet

SYNTHESIS OF PROCESSES AND PROCESS SUBSYSTEMS FOR ENTIRE LIFETIME

PhD - Doctoral Dissertation

Maribor, 2015

University of Maribor

Faculty of Chemistry and
Chemical Engineering

Synthesis of processes and process subsystems for entire lifetime

PhD - Doctoral Dissertation

Student:	Andreja Nemet
Study programme:	III. Stage Doctoral Programme on Chemistry and Chemical Engineering
Field:	Chemical Engineering
Expected scientific title :	Ph.D.
Supervisor:	full prof. Zdravko Kravanja, PhD
Co-supervisor:	full prof. Jiří Jaromír Klemeš,DSc

Maribor, April 2015

Univerza v Mariboru

Fakulteta za kemijo
in kemijsko tehnologijo

Na osnovi 330. člena Statuta Univerze v Mariboru (Ur. l. RS, št. 46/2012) in sklepa Senata 30. redne seje Fakultete za kemijo in kemijsko tehnologijo Univerze v Mariboru z dne 30. 9. 2014

izdajam

SKLEP O IMENOVANJU KOMISIJE ZA ZAGOVOR DOKTORSKE DISERTACIJE

z naslovom

Sinteza procesov in procesnih podsistemov za celotno življenjsko dobo,

ki jo je predložila Nemet Andreja, univ. dipl. inž. kem. tehnol.

V komisijo imenujem naslednje člane:

red. prof. dr. Peter Krajnc, predsednik
red. prof. dr. Zdravko Kravanja, mentor-član
red. prof. dr. Jiři Jaromír Klemeš, Pannonia University Veszprem, Madžarska, somentor-član
red. prof. dr. Željko Knez, član

Zagovor je v četrtek, 23. 10. 2014 ob 14. uri v predavalnici A-103.

Če imenovani član komisije zavrne sodelovanje v komisiji za zagovor doktorske disertacije, mora o tem v roku 5 delovnih dni po prejemu tega sklepa pisno obvestiti dekana članice.

Pravni pouk: Zoper ta sklep je možna pritožba na senat članice univerze v roku 5 delovnih dni.

Datum: 15. 10. 2014
Kraj: Maribor

Dekan:
red. prof. dr. Željko Knez

UNIVERZA V MARIBORU FAKULTETA ZA KEMIJO IN KEMIJSKO TEHNOLOGIJO 3

Obvestiti:

- člane komisije,
- kandidata-tko,
- arhiv.

FAKULTETA ZA KEMIJO IN KEMIJSKO TEHNOLOGIJO

Outline

Acknowledgement

The research work presented in this thesis has been carried out at the Laboratory for Process System Engineering and Sustainable Development at the Faculty of Chemistry and Chemical Engineering, University of Maribor. First and foremost I offer my sincerest gratitude to my supervisor, Dr. Zdravko Kravanja, who guided and supported me throughout my thesis with his knowledge and patience. I would like to express my thank you also to Prof. Dr Jiří Jaromír Klemeš, from Research Laboratory of Process Integration and Intensification (CPI^2), Faculty of Information Technology, University of Pannonia, Hungary, for his useful advice during my study.

For my financial support I would like to gratefully acknowledge the University of Maribor (Contract No. 125/2011-"Inovativna shema za sofinanciranje doktorskega študija za spodbujanje sodelovanja z gospodarstvom in reševanja aktualnih družbenih izzivov-generacija 2010 Univerza v Mariboru").

I would also like to thank my colleagues at the Laboratory for Process System Engineering and Sustainable Development Dr. Mihael Kasaš, Dr. Lidija Čuček, and Iris Varga who gave me a helping hand whenever needed.

Finally, I would like to express my enormous gratitude to my family and friends. Thank you for your understanding and selfless support. Without you I would not have finished this study.

Abstract

Economically viable process designs should be, in addition to other criteria, profitable over their entire process lifetimes not only at the present time. An improved process design can be achieved by establishing an appropriate trade-off between product income, raw material, operating costs, and investment. The full lifetime of the processes and future prices have to be considered rather than optimising them on a yearly basis using current prices. Single-period optimisation and synthesis models for processes reflects current prices only. The prices can fluctuate rather quickly and the optimal solution may be very different from one year to the another. Therefore, the traditional superstructural synthesis approach applying a mixed-integer nonlinear programming model was upgraded: i) over time, by considering an entire lifetime, which can be described by a multi-period model and ii) the whole field of variation regarding uncertain future prices. A stochastic approach considering the statistical distribution of price projections over an entire lifetime was used on different case studies instead of the traditional deterministic approach accounting for nominal future price projection. The objective was the maximisation of the expected net present value of a process or the expected incremental net present value of different process subsystem.

The heat exchanger network has been one of the subsystem, which can significantly contribute to operating costs due to savings of external utility consumption. For this subsystem a deterministic and stochastic multi-period mixed-integer nonlinear programming (MINLP) synthesis models have been developed in order to account for future price projections. Considering higher energy prices gives rise to larger initial investments compared to solutions obtained with current prices. However, due to the uncertainties of utility prices' forecasts, retrofitting using an extension of HEN during future years of the lifespan might be a better strategy. The objective is to identify a design that is the most suitable for effective future extensions and preferably with the lowest sensitivity to energy price fluctuations, as there can be various designs featuring similar initial investment. The results supports that it is economically beneficial to consider future utility prices as the incremental investment is not only paid-off but additional savings are achieved.

Process-to-process Heat Integration can also significantly affect the trade-off between investment and operating cost. The aim of Total Site (TS) HEN synthesis was to develop a model synthesis for the TS that, besides many other important features, would also consider future utility prices. Two strategies for TS synthesis have been developed: i) sequential, when HI is performed within a process during the first step and then after a process-to-process HI has been performed, and ii) simultaneous, where the HI is performed within and between processes simultaneously. The second strategy can reveal additional opportunities for heat recovery that might not be identified when applying the first strategy. Comparison of the results obtained at consideration of current utility prices and forecasted utility prices indicates that is worth to account for future utility prices.

The separation processes also consume a significant amount of energy. The synthesis of a distillation column sequence integrated within its heat exchanger network was used as a case study for the separation of a multi-component stream into pure component products by considering future utility prices. This analysis has been performed in order to evaluate the magnitude of the influence of forecasted utility prices. It can be concluded that forecasted utility prices can be beneficial, however, the technical limits of the systems should be carefully observed.

The price fluctuation can also be observed for other prices not only utility prices, e.g. raw material cost, product price, etc. The expected impact on the trade-off would tend to compensate for the cost variations, for example at higher utility costs a higher investment can be economically viable in order to decrease the operating cost. However, when all the costs and incomes are simultaneously considered, the tendencies of each separate impact can be different, which was indicated in the case study presented.

Keywords: future prices, forecasted prices, stochastic optimisation, mathematical programming, Heat Exchanger Network, Total Site, distillation column sequence, methanol production

UDK: 519.853:547.261(043.3)

Povzetek

Ekonomično upravičeni načrti morajo biti, poleg ostalih kriterijev, tudi dobičkonosni skozi celotno življenjsko dobo procesa, ne samo v sedanjem času. Z vzpostavitvijo primernega trženja med prihodki produkta, stroški surovin, obratovalnimi stroški in investicijo v celotni življenski dobi lahko dosegamo izboljšan načrt procesa. Zato je optimizacija za celotno življenjsko dobo procesa z upoštevanjem napovedanih cen primernejša od optimizacije na letni osnovi. Enoperiodno optimiranje in sinteza za procese odraža le sedanje cene. Optimalna rešitev, dosežena za eno leto, se lahko znatno razlikuje od rešitve za drugo leto, saj se cene spreminjajo precej hitro. Običajni superstrukturni sintezni pristop z uporabo mešano-celoštevilskega nelinearnega programiranja smo zato nadgradili 1) z upoštevanjem celotne življenjske dobe, kar lahko opišemo z večperiodnim modelom in 2) z območjem spreminjanja negotovih prihodnjih cen. Namesto običajnega determinističnega pristopa pri nominalnih projekcijah prihodnjih cen smo uporabili stohastični pristop z upoštevanjem statistične porazdelitve napovedovanja cen za celotno življenjsko dobo. Namen je bil maksimiranje pričakovane neto sedanje vrednosti procesa oz. pričakovane inkrementalne neto sedanje vrednosti izboljšave različnih procesnih podsistemov.

Podsistem, ki znatno prispeva k obratovalnim stroškom zaradi prihrankov pri porabi zunanjih pogonskih sredstev, je omrežje toplotnih prenosnikov. Za sintezo tega podsistema smo razvili tako deterministični kot stohastični večperiodni celoštevilski nelinearni programirni (MINLP) model ob upoštevanju prihodnjih cenovnih projekcij. Z upoštevanjem višjih cen energentov se povečajo začetne investicije v primerjavi z rešitvami, ki jim dosežemo pri sedanjih cenah. Zaradi negotovosti napovedovanja cen se je smiselno povečanju začetne investicije izogniti z načrtovanjem možnosti razširitve omrežja toplotnih prenosnikov v kasnejšem obdobju. Namen je doseči načrt, ki je kar najbolj primeren za učinkovito razširitev v prihodnosti, po možnosti z najmanjšo občutljivostjo na spreminjanje cen.

Toplotna integracija med različnimi procesi lahko tudi znatno vpliva na trženje med investicijo in obratovalnimi stroški. Tako je bil eden od ciljev sinteze omrežja toplotnih prenosnikov prav upoštevanje prihodnjih cen pogonskih sredstev. Razvili smo dve strategiji za sintezo celotnega območja (ang. Total Site), in sicer: i) zaporedno, pri kateri toplotno integracijo izvajamo najprej na nivoju procesa in potem na nivoju celotnega območja, in ii) sočasno, pri kateri izvajamo toplotno integracijo na nivoju procesa in na nivoju celotnega območja hkrati. Slednja strategija omogoča dodatne možnosti prihranka toplote, kar potrjuje primerjava rezultatov doseženih pri sedanjih in prihodnjih cenah pogonskih sredstev.

Separacijski procesi so lahko veliki porabniki energije. Sintezo zaporedja destilacijskih kolon integriranih z lastnim omrežjem toplotnih prenosnikov smo uporabili kot študijski primer za ločevanje večkomponentnega toka v čiste produkte. Analizo smo izvedli tudi z namenom določitve obsega vpliva napovedanih prihodnjih cen pogonskih sredstev. Zaključimo lahko, da z upoštevanjem napovedanih cen lahko dosegamo ekonomsko učinkovitejše procese ali procesne podsisteme, vendar je pri tem potrebno skrbno upoštevati tehnološke omejitve študiranega sistema.

Nihanje cen razen pri pogonskih lahko opazimo tudi pri drugih cenah, npr. pri cenah surovin, in produktov. Pričakujemo lahko, da trženje v postopku optimiranja poskuša kompenzirati ta nihanja cen, npr. višje cene pogonskih sredstev bodo izravnane s povečanjem investicije, s čemer se zmanjšajo prihodnji obratovalni stroški. Vendar, ko upoštevamo vse stroške in prihodke hkrati, so lahko trendi vplivov različni od posameznega vpliva le teh, kar smo pokazali tudi s študijskim primerom.

Ključne besede: prihodnje cene, napovedane cene, stohastično optimiranje, matematično programiranje, omrežje toplotnih prenosnikov, celotno območje (Total Site), zaporedje destilacijskih kolon, proizvodnja metanola

UDK: 519.853:547.261(043.3)

List of tables

List of figures

Nomenclature

Chapter 2

<u>*Abbreviations*</u>

AP	augmented penalty
ER	equality relaxation
MINLP	mixed integer nonlinear programming
OA	outer approximation

<u>*Indexes/ Sets*</u>

n	period of time from the set N
u	price scenario in and earlier period from U
v	price scenario from the set V
ξ	scenario from the set $\{\xi_1 \ldots \xi_v\}$

<u>*Constants*</u>

A, B	matrix of coefficients
$\mathbf{c}^{\mathrm{T}}$	vector of cost coefficients
x_1, x_2, x_3, x_4, x_5	projection level
t_{LT}	lifetime of the process system
pl_{v}	probability level of scenario
r_{D}	sum of discounted rate and inflation, %

<u>*Binary variables*</u>

y	binary variables

<u>*Variables*</u>

CE	certainty equivalent, €
DBP	discounted payback, *y*
ENPV	expected net present value, €
EU	Expected Utility Value, €
$F_{\mathrm{C},n}$	annual cash flow, €
I	investment, €
IRR	internal rate of return
LTDROI	lifetime discounted return on investment
NPV	net present value, €
$p_{n,v}$	combined probability of process system being at a certain price projection and time period n
$tr_{u,v}$	transition probability
$U_{n,v}^{exp}$	Exponential Utility Function, €
$U_{n,v}^{lin}$	linearised Exponential Utilty Function,€
x	continuous variables
Z	objective function
α	variable at constraints when nonlinear objective function is reformulated
s_v^+, s_v^-	positive slack variables

d	design variable
$\Delta aNPV$	incremental annual contribution to the total ΔNPV of a scenario at certain projection in a certain period, €
τ	risk tolerance, €l

<u>*Superscripts*</u>

UP upper bound

LO lower bound

Chapter 3

<u>*Abbreviations*</u>

CE	Certainty Equivalent
ENPV	Expected Net Present Value
HE	heat exchanger
HEN	heat exchanger network
MINLP	mixed integer nonlinear programming
NPV	Net Present Value
OP-C	Operating Cost
RP	Risk Premium
TAC	Total Annual Cost

<u>*Indexes/ Sets*</u>

i	hot streams from the set I
j	cold stream from the set J
k	temperature locations from the set K
n	period from the set N
v	future price projection scenario from the set V

<u>*Constants*</u>

ac	cost exponent for process heat exchangers
AD^{up}	upper bound of the extension area, m^2
cc	cost exponent for heat exchangers between cold utility and process stream
cf^{CU}	fixed charge for heat exchanger between process stream and cold utility, k€
cf^{HU}	fixed charge for heat exchanger between process stream and hot utility, k€
cf	fixed charge for heat exchanger between process streams, k€
CP_i	heat capacity flow-rate of hot stream i, kW/°C
CP_j	heat capacity flow-rate of cold stream j, kW/°C
cv	variable charge of HE between two process streams, k€/(m^2y)
cv^{CU}	variable charge of HE between process stream and cold utility, k€/(m^2y)
cv^{HU}	variable charge of HE between process stream and hot utility, k€/(m^2y)
Ecc_j	heat content of cold stream j, kW
Ech_i	heat excess of hot stream i, kW
EU	Expected Utility value, k€
f_n^D	yearly compounding coefficient for investment
f_n^{DA}	yearly discounting coefficient for investment
h	heat transfer coefficient, W/(m^2 °C)
hc	cost exponent for heat exchangers between cold utility and process stream

k_1	slope of the linearised Utility function for positive $\Delta aNPV_{n,v}$
k_2	slope of the linearised Utility function for positive $\Delta aNPV_{n,v}$
n_{ext}	year of extension, y
NPV^{REF}	net present value of the reference design, k€
NPV_v^{REF}	net present value of the reference design for Scenario v, k€
$p_{n,v}$	probability of projections in period n for scenario v, %
r_D	sum of discounted rate and inflation, %
$T_{in,j}^{\mathrm{C}}$	supply temperature of cold stream, °C
$T_{out,j}^{\mathrm{C}}$	target temperature of cold stream, °C
$T_{in,i}^{\mathrm{H}}$	supply temperature of hot stream, ,°C
$T_{out,i}^{\mathrm{H}}$	target temperature of hot stream, ,°C
t_{LT}	lifetime of the HEN, y
t_{OP}	annual operating hours, h/y
U_i^{CU}	overall heat transfer coefficient for coolers, W/(m^2 °C)
U_i^{HU}	overall heat transfer coefficient for heaters, W/(m^2 °C)
$U_{i,j}$	overall heat transfer coefficient for heat exchangers between process streams, W/(m^2 °C)
ε	small constant, applied at linearisation of Utility function

Binary variables

y^{CU}	matches including cold utility
y^{HU}	matches including hot utility
$y_{i,j,k}$	process stream matches
$yd_{i,j,k}$,	process stream matches for additional area
yd_i^{CU}	matches including cold utility for additional area
yd_j^{HU}	matches including heat utility for additional area

Variables

A_i^{CU}	HE area between cold utility and hot process stream i, m^2
A_{ij}^{HE}	HE area between hot and cold process streams i and j, m^2
A_j^{HU}	HE area between hot utility and cold process stream j, m^2
$AD_{i,n=1,v}^{\mathrm{CU}}$	additional area of cooler, for the first year of lifetime,m^2
$A_{i,n>1,v}^{\mathrm{CU}}$	additional area of cooler, for the years of lifetime besides first year, m^2
$AD_{i,j,k,n=1,v}^{\mathrm{HE}}$	additional area of HE between process streams, for the first year of lifetime, m^2
$AD_{i,j,k,n>1,v}^{\mathrm{HE}}$	additional area of HE between process streams, for the years of lifetime besides first year, m^2
$AD_{j,n=1,v}^{\mathrm{HU}}$	additional area of heater, for the first year of lifetime, m^2
$A_{j,n>1,v}^{\mathrm{HU}}$	additional area of heater, for the years of lifetime besides first year, m^2
$c_{n,v}^{\mathrm{CU}}$	cost of cold utility in n period and v stochastic trend, k€/kW

$c_{n,v}^{\mathrm{HU}}$	cost of hot utility in n period and v stochastic trend, k€/kW
$c_{n,v}^{\mathrm{OP}}$	operating cost in period n for projection v, k€
$F_{\mathrm{C},n}$	annual cash flow in period *n*, k€
$FixC_n$	fix charges of HE in year n, k€
I	investment, k€
$LTDROI$	lifetime return on investment
NPV	net present value, k€
$p_{n,v}$	probability of being a scenario in year n at probability v
pl	average probability level
$Q_{i,n,v}^{\mathrm{CU}}$	energy exchanged between i and the cold utility in period n for projection v, kW
$Q_{j,n,v}^{\mathrm{HU}}$	energy exchanged between j and the hot utility in period n for projection v, kW
$Q_{i,j,k,n}$	energy exchanged between *i* and *j* in stage *k* in period *n* for deterministic approach, kW
$Q_{i,j,k,n,v}$	energy exchanged between i and j in stage k and period n for projection v for stochastic approach, kW
s^+_v, s^-_v	slack variables for positive and negative deviations
$TC_{j,k,n}$	temperature of cold stream *j* as it leaves stage k in period *n* for deterministic approach, K
$TC_{j,k,n,v}$	temperature of cold stream j as it leaves stage k in period n for projection v for stochastic approach, °C
$TH_{i,k,n}$	temperature of hot stream *i* as it enters stage *k* in period *n* for deterministic approach, K
$TH_{i,k,n,v}$	temperature of hot stream i as it enters stage k in period n for projection v for stochastic approach, °C
t_{LT}	HEN lifetime, y
$tr(u,v)$	transition probabilities of transfer from projection *u* to projection *v*
$U_l(x_l)$	Exponential Utility Function, k€
$U_{n,v}^{negative}$	linear Utility function for negative $\Delta aNPV_{n,v}$
$U_{n,v}^{positive}$	linear Utility function for positive $\Delta aNPV_{n,v}$
$U_{n,v}^{lin}(\Delta aNPV_{n,v})$	linearised Utility function
$VarC_n$	varying charges of HE in year n, k€
x_l	wealth of scenario *l*, k€
x_1, x_2, x_3, x_4, x_5	variables for transition probabilities
z	objective function
$\Delta aNPV$	incremental annual contribution to the total ΔNPV of a scenario at certain projection in a certain period, k€
$\Delta ENPV$	Incremental Expected Net Present Value, k€
$\Delta F_{C,n,v}$	incremental annual cash flow, k€
ΔI	incremental investment, k€
ΔNPV	Incremental Net Present Value, k€
$\Delta_{\ln}T_{i,j,k,n,v}$	logarithmic mean temperature difference between *i* and *j* at location *k* in

	period n for projection v, °C
$\Delta T_{i,n}^{\mathrm{CU}}$	approach between i and the cold utility, °C
$\Delta_{\ln} T_{i,n,v}^{\mathrm{CU}}$	logarithmic mean temperature difference between i and cold utility at location k in period n for projection v, °C
$\Delta T_{j,n}^{\mathrm{HU}}$	approach between j and the hot utility, °C
$\Delta_{\ln} T_{j,n,v}^{\mathrm{HU}}$	logarithmic mean temperature difference between j and hot utility at location k in period n for projection v, °C
τ	risk tolerance, k€l

Superscripts

CU	cold utility
HU	hot utility

Chapter 4.1

Abbreviations

CU	cold utility
CS	sink side of Total Site
ENPV	Expected Net Present Value
HE	heat exchanger
HEN	heat exchanger network
HS	source side of Total Site
HU	hot utility
MINLP	mixed-integer nonlinear programming
NPV	Net Present Value

Indexes/ Sets

Ap	all processes included in the Total Site from the set *AP*
ph	processes that have heat surpluses from the set *PH*
pc	processes that have heat demands from the set *PC*
i	hot streams in different processes from the set *I*
j	cold streams in different processes from the set *J*
iu	different intermediate utilities from the set *IU*
k^{HS}	temperature locations within the superstructure on the source side from the set K^{HS}
k^{CS}	temperature locations within the superstructure on the sink side from the set K^{CS}
n	number of periods observed from set *N*
v	different utility prices' projections from the set *V*

Constants

Al	allowance for threading, mechanical strength, and corrosion, m
A, B, C	Antoine constants for pressure/temperature relationship

ac	cost exponent for process to intermediate utility heat exchanges
cc	cost exponent for heat exchangers between cold utility and process stream
c^{y}	coefficient for accounting for the condensate pipeline
cf^{CU}	fixed charge for heat exchanger between process stream and cold utility, €
cf^{HU}	fixed charge for heat exchanger between process stream and hot utility, €
cf	fixed charge for heat exchanger between process streams, €
$CP_{ph,i}$	heat capacity flow-rate of hot stream i for process ph, W/K
$CP_{pc,j}$	heat capacity flow-rate of cold stream j in process pc, W/K
cv	variable charge of HE between two process streams, €/(m^2.y)
cv^{CU}	variable charge of HE between process stream and cold utility, €/(m^2.y)
cv^{HU}	variable charge of HE between process stream and hot utility, €/(m^2.y)
$c_{n,v}^{\mathrm{CU}}$	cost of cold utility in period n and projection v, €/J
$c_{n,v}^{\mathrm{HU}}$	cost of hot utility in period n and projection v, €/J
c^{P1}	pipe cost per unit weight, € /g
c^{P2}	installation cost, €/ m
c^{P3}	right-of-way cost, €/ m
c^{P4}	insulation cost on a volume basis, €/ m^3
f^{rec}	fraction of condensate returned to source side processes
h_{iu}	heat transfer coefficient of hot stream iu, W/(m^2 .K)
$h_{ph,i}$	heat transfer coefficient of hot stream i in process ph, W/(m^2 .K)
$h_{pc,j}$	heat transfer coefficient of cold stream j in process pc, W/(m^2.K)
hc	cost exponent for heat exchangers between cold utility and process stream
$l_{ph,pc}$	length of potential pipeline between source side process ph and sink side process pc, m
Ns	number of stages
$p_{n,v}$	probability of projections in period n, %
$pipe_{ph,pc,iu}^{inst}$	upper bound on variable for calculation of installation cost of source side process ph, to sink side process pc, for intermediate utility iu, m
$q_{ph,pc}^{UP}$	upper bound for amount of heat for transfer from process ph to process pc, W
$q_{ph,pc}^{LO}$	lower bound for amount of heat for transfer from process ph to process pc, W
r_{D}	sum of discounted rate and inflation, %
r_{T}	tax rate, %
SE	maximum allowable stress in material caused by internal pressure and joint efficiency at design temperature, Pa
$T_{pc,j}^{\mathrm{C,in}}$	supply temperature of cold stream j in process pc, °C
$T_{pc,j}^{\mathrm{C,out}}$	target temperature of cold stream j in process pc, °C

$T_{ph,i}^{\mathrm{H,in}}$	supply temperature of hot stream *i* for process *ph* ,°C
$T_{ph,i}^{\mathrm{H,out}}$	target temperature of hot stream *i* for process *ph* ,°C
$T^{\mathrm{CU,out}}$	outlet temperature of cold utility
$T^{\mathrm{HU,out}}$	outlet temperature of hot utility
t_{LT}	lifetime of the HEN, y
t_{OP}	annual operating hours, h/y
$w_{ph,pc,iu}^{tot,UP}$	upper bound of weight of pipeline between source side process *ph* and sink side process *pc* for intermediate utility *iu*, g
$\gamma_{ph,i,iu}^{\mathrm{HS}}$	upper bound for temperature difference between hot stream *i* and intermediate utility *iu* in process *ph*, °C
$\gamma_{ap,iu,j}^{\mathrm{CS}}$	upper bound for temperature difference between intermediate utility *iu* and cold stream *j* in process *pc,* °C
μ	friction factor of pipeline

Binary variables

$y_{ph,i,iu,k^{\mathrm{HS}}}^{\mathrm{HS}}$	for selecting/deselecting matches between hot stream *i* and intermediate utility *iu* in process *ph* at location k^{HS}
$y_{pc,iu,j,k^{\mathrm{CS}}}^{\mathrm{CS}}$	for selecting/deselecting matches between intermediate utility *iu* and cold stream *j* in process *pc* at location k^{CS}
$y_{ph,i}^{\mathrm{CU}}$	for selecting/deselecting matches between hot stream *i* and cold utility in process *ph*
$y_{pc,j}^{\mathrm{HU}}$	for selecting/deselecting matches between hot utility and cold stream *j* in process *pc*
$yt_{ph,pc,iu}$	for selecting/deselecting the pipe between source side process *ph* and sink side process *pc*, for intermediate utility *iu*

Variables

$A_{ph,i}^{\mathrm{CU}}$	HE area between cold utility and hot process stream *i* in process *ph*, m^2
$A_{ph,i,iu,k^{\mathrm{HS}}}^{\mathrm{HS}}$	HE area between hot streams *i* and intermediate utility *iu* at location k^{HS} in process *ph*, m^2
$A_{pc,iu,j,k^{\mathrm{CS}}}^{\mathrm{CS}}$	HE area between intermediate utility *iu* and cold stream *j* at location k^{CS} in process *pc*, m
$A_{pc,j}^{\mathrm{HU}}$	HE area between hot utility and cold process stream *j* in process *pc*, m^2
$c_{n,v}^{\mathrm{OP}}$	operating cost in period *n* for projection *v*, €/y
$CP_{ph,iu,n,v}^{HS}$	heat capacity flow-rate for intermediate utility *iu* in process *ph*, W/K
$CP_{pc,iu,n,v}^{CS}$	heat capacity flow-rate for intermediate utility *iu* in process *pc*, W/K

$d_{ph,pc,iu}$ inner diameter of pipeline between source side process *ph* and sink side process *pc* for intermediate utility *iu*, m

$Ecc^{HS}_{ap,iu}$ heat surplus of intermediate utility on the sink side, W

$Ech^{CS}_{ap,iu}$ heat content of intermediate utility on the source side, W

$Fp^{\mathrm{HS}}_{ap,iu}$ cost correction factor for pressure for heat exchangers on the source side $Fp^{\mathrm{CS}}_{ap,iu}$ cost correction factor for pressure for heat exchangers on the sink side

$h_{ph,pc,iu}$ and specific enthalpy for the steam in pipeline between source side process *ph* sink side process *pc* for intermediate utility *iu,* J/g

I investment, €

$LMTD^{\mathrm{HS}}_{ph,i,iu,k^{\mathrm{HS}},n,v}$ logarithm mean temperature approximation between hot stream *i in* process *ph* and intermediate utility *iu* in stage k^{HS} and period *n* for projection *v*, °C

$LMTD^{\mathrm{CS}}_{pc,iu,j,k^{\mathrm{CS}},n,v}$ logarithm mean temperature approximation between intermediate utility *iu* and cold stream *j* in process *pc*, stage k^{CS} and period *n* for projection *v*, °C

$LMTD^{\mathrm{CU}}_{ph,i,n,v}$ logarithm mean temperature approximation between hot stream *i* in process *ph* and external cold utility in period *n* for projection *v*, °C

$\dot{m}_{ph,pc,iu,n,v}$ mass flow-rate in pipeline between source side process *ph* and sink side process *pc* for intermediate utility *iu* in period *n* for projection *v,* g/s

$p^{drop}_{ph,pc,iu,n,v}$ pressure drop during heat transport from source side process *ph* to sink side process *pc* for intermediate utility *iu* in period *n* for projection *v*, Pa

$p_{n,v}$ probability of a scenario in period *n* at projection *v*

$p^{\mathrm{HS}}_{ph,iu}$ pressure of intermediate utility leaving process *ph* on the source side, Pa

$p^{\mathrm{CS}}_{pc,iu}$ pressure of intermediate utility entering process *pc* on the sink side, Pa

$pipe^{inst}_{ph,pc,iu}$ variable for calculation of installation cost for a pipe of intermediate utility *iu* between source side process *ph* and sink side process *pc*

c^{pipe} total cost of the pipeline, €

$q^{av}_{ph,pc,iu,n,v}$ available amount of heat for transfer from hot process *ph* to cold process *pc* for intermediate utility *iu* in period *n* for projection *v*, W

$q^{loss}_{ph,pc,iu,n,v}$ heat loss during transfer from hot process *ph* to cold process *pc* for intermediate utility *iu* in period *n* for projection *v*, W

$Q^{\mathrm{CU}}_{ph,i,n,v}$ energy exchanged between hot stream *i* and intermediate utility *iu* in period *n* for projection *v*, W

$Q^{\mathrm{HU}}_{pc,j,n,v}$ energy exchanged between cold stream *j* and hot utility in period *n* for projection *v*, W

$Q^{\mathrm{HS}}_{ph,i,iu,k^{\mathrm{HS}},n,v}$ energy exchanged between hot stream *i* and intermediate utility *iu* in process *ph*, stage k^{HS} and period *n* for projection *v*, W

$Q^{\mathrm{CS}}_{pc,iu,j,k^{\mathrm{CS}},n,v}$ energy exchanged between intermediate utility *iu* and cold stream j in process *pc*, in stage k^{CS}, period *n*, for projection *v*, W

$TC_{pc,j,k^{\mathrm{CS}},n,v}$ temperature of cold stream *j* in process *pc* as it leaves stage k^{CS} in period *n* for projection *v*, °C

$TH_{ph,i,k^{\mathrm{HS}},n,v}$ temperature of hot stream *i* in process *ph* as it enters stage k^{HS} in period *n* for projection *v*, °C

$TC^{\mathrm{HS,out}}_{ph,iu,n,v}$ temperature of intermediate utility *iu* as it leaves process *ph*, °C

$TC^{\mathrm{HS,in}}_{ph,iu,n,v}$ temperature of intermediate utility *iu* as it enters process *ph*, °C

$TH^{\mathrm{CS,in}}_{pc,iu,n,v}$ temperature of intermediate utility *iu* as it enters process *pc*, °C

$TH^{\mathrm{CS,out}}_{pc,iu,n,v}$ temperature of intermediate utility *iu* as it leaves process *pc*, °C

$th^{pipe}_{ph,pc,iu}$ pipe thickness for a pipeline between source side process *ph* and sink side process *pc* for intermediate utility *iu,* m

t_{LT} Total Site lifetime, y

$v_{ph,pc,iu,n,v}$ velocity of steam during heat transport in pipeline from source side process *ph* to sink side process *pc* for intermediate utility *iu* in period *n* for projection *v*, m/s

$V_{ph,pc,iu}$ specific volume of steam in pipeline from source side process *ph* to sink side process *pc* for intermediate utility *iu,* m^3/kg

W_{ENPV} Expected Net Present Value, €

$F_{C,n,v}$ annual cash flow, €

$v^{HS}_{ph,iu}$ variable for indication of presence of any heat exchange between process *ph* and intermediate utility *iu*

$v^{CS}_{pc,iu}$ variable for indication of presence of any heat exchange between process *pc* and intermediate utility *iu*

$V^{ins}_{ph,pc,iu}$ volume of insulation of pipeline between source side process *ph* and sink side process *pc* for intermediate utility *iu*, m^3

$w^{tot}_{ph,pc,iu}$ weight of pipeline between source side process *ph* and sink side process *pc* for intermediate utility *iu*, g

$\Delta h^{liq}_{ph,iup,n,v}$ difference of specific enthalpy of water for stream *iup* for source side process *ph* in period *n* for projection *v*, J/g

$\Delta h^{st}_{ph,iue,n,v}$ difference of specific enthalpy of steam for stream *iue* for source side process *ph* in period *n* for projection *v*, J/g

$\Delta T_{ph,i,IU,k^{\mathrm{HS}},n,v}$ approach temperature difference between hot stream *i* and intermediate utility *iu* in process *ph* at location k^{HS} in period *n* for projection *v*, °C

$\Delta T^{\mathrm{CU}}_{ph,i,n,v}$ approach temperature difference between hot stream *i* and the cold utility in period *n* for projection *v*, °C

Chapter 4.2

<u>*Indexes/ Sets*</u>

ap all the processes included in the Total Site from the set *AP*

ic hot streams and condensates for intermediate utilities from the set $IC \subset AP$

hp	hot process streams from the set $HP \subset IC$
ihu	steam intermediate utility as hot streams from the set $IHU \subset IC$
hcond	condensate from hot intermediate utility from the set $HCond \subset IC$
apic	connection of process to its hot process steams and condensates from the set *APIC*
jc	cold streams and condensates from the set *JC*
cp	cold process streams from the set $CP \subset JC$
icue	steam intermediate utility as cold stream from the set $ICUE \subset JC$
icup	water preheat for intermediate utility as a cold stream from the set $icup \in ICUE \subset JC$
icu	intermediate utilities as cold stream including evaporation and preheating from the set $ICU \subset JC$
ccond	condensate required for evaporation from the set *CCond*
acjc	connection of processes to its cold process streams and condensates form the set *ACJC*
iu_iucond	steam mains of intermediate utilities and condensates pipeline from the set *IU_IUCond*
iu	steam mains of intermediate utilities from the set $IU \subset IU\_IUCond$
iucond	pipeline of condensates from the set $IUCond \subset IU\_IUCond$
ul	steam levels of intermediate utilities as steam from the set *IUL*
iuml	assignment of an intermediate utility level to a steam main for the same intermediate utility from the set *IUML*, $IUML \subset (IU \times IUL)$
iuhot	assignment of an intermediate utility as hot stream to the steam main of intermediate utility from the set $IUHOT \subset (IU \times IC)$
iucold	assignment of intermediate utility as cold stream to the steam of intermediate utility form the set $IUCOLD \subset (IU \times JC)$
iucondhcond	assignment of condensate as hot stream to the condensate pipeline from the set $IUCondHCond \subset (IUCond \times HCond)$
iucondccond	assignment of condensate as cold stream to the pipeline of condensate from the set $IUCondCCond \subset (IUCond \times CCond)$
iucondihu	assignment of condensate pipeline to hot process stream from the set $IUCondIHU \subset (IUCond \times IHU)$
icueicup	assignment of cold intermediate utility stream for preheating to evaporation from the set $ICUEICUP \subset (ICUE \times ICUP)$
icueccond	assignment of cold condensate stream to cold evaporation stream from the set $ICUECCond \subset (ICUE \times CCond)$
cpicup	union index/set of cold process stream and streams for preheating from the set $CPICUP = CP \cup ICUP$
iuicu	assignment of steam cold process steam and preheating stream to steam main from the set $IUICU \subset (IU \times ICU)$
iuihu	assignment of hot stream for intermediate utility to the steam main of the inlet process to the main from the set $IUIHU \subset (IU \times IHU)$

iuihu1	assignment of hot stream for intermediate utility to the steam main of the outlet process from the main from the set $IUIHU1 \subset (IU \times IHU)$
k	temperature locations at stage boundaries from the set *K*
s_scond	segments from set *S_SCond*
s	all steam main segments from the set $S \subset S\_SCond$
scond	all condensate pipeline segments from the set *SCond*
snod	all nodes representing one process from the set *Snod*
iuspipe	assignment of mains to the segments, from set $IUSpipe \subset (IU\_IUCond \times S\_SCond)$
ius	assignment of steam mains to the segments from set$IUS \subset (IU \times S)$
iucondscond	assignment of condensate pipeline to the condensate segments from set $IUCondSCond \subset (IUCond \times SCond)$
assigsnod_ap	assignment of process to the node from set $AssignSnod\_AP \subset (Snod \times AP)$
asingsnod_sin	assignment of the steam segment entering the node from the set $AssignSnod\_Sin \subset (Snod \times S)$
asingsnod_sout	assignment of steam segment leaving the node from set $AssignSnod\_Sout \subset (Snod \times S)$
asingsnodcond_sin	assignment of the condensate segment entering the node $AssignSnodCond\_Sin \subset (Snod \times SCond)$
asingsnodcond_sou	assignment of steam segment leaving the node from set $AssignSnod\_Sout \subset (Snod \times SCond)$
n	periods in time from set *N*
v	different price projections from set *V*

<u>*Constants*</u>

aexp	varying cost exponent
$c_{n,v}^{HU}$	prices of hot utility within period *n* for scenario *v* , €/J
$c_{n,v}^{CU}$	prices of cold utility within period *n* for scenario *v*,€/J
$c_{n,v}^{\mathrm{tot}}$	annual operating cost within period n and scenario v, without any heat integration, €
CP_{cp}	heat capacity flow-rate of cold process stream, W/K
CP_{hp}	heat capacity flow-rate of hot process stream, W/K
cf	fixed cost of heat exchanger between process streams and/or intermediate utility stream, €
cf^{HU}	fixed cost of heat exchanger between cold process streams or preheating and external hot utility,€
cf^{CU}	fixed cost of heat exchanger between hot process streams and external cold utility, €

cf^{pump}	fixed cost of pump for intermediate utility, €
cv	varying cost of heat exchanger between process streams and/or intermediate utility stream, €
cv^{HU}	varying cost of heat exchanger between cold process streams or preheating and/or external hot utility, €
cv^{CU}	varying cost of heat exchanger between hot process streams and external cold utility, €
cv^{pump}	varying cost of pump for intermediate utility, €/J
Ech_{hp}	heat content of hot process stream *hp,* W
Ecc_{cp}	heat duty of cold process stream *c* ,W
$f^{cond,rec}$	condensate recovery rate
f_{cond}^{fric}	friction factor for condensate
f_{steam}^{fric}	friction factor for steam
f_{cp}^{fric}	friction factor for cold process stream
Ki	thermal conductivity of insulation, W /(m^2 K)
$L_{hp,cp}$	distance between hot process stream *hp* and cold process stream *cp,* m
L_{s_scond,iu_iucond}	length of steam main or condensate pipeline *iu_iucond* for segment *s_scond*, m
$p_{n,v}$	probability of utility prices being in period *n* and scenario *v*
$Q_{hp,cp,k}^{tc,UP}$	upper bound on heat exchange between hot process *hp* and cold process *cp* in stage *k,*W
$q_{m,cp}^{tot}$	total mass flow-rate of cold process stream *cp,* g/s
r_{D}	inflation and interest rate together
r_{T}	tax rate
$T_{cp}^{\mathrm{C,in}}$	inlet temperature of cold process stream, K
$T_{icup}^{c,in}$	inlet temperature of freshwater for preheating, K
$T_{cp}^{\mathrm{C,out}}$	outlet temperature of cold process stream, K
T^{G}	temperature of pipe surrounding , K
$T_{hp}^{\mathrm{H,in}}$	inlet temperature of hot process stream, K
$T_{hp}^{\mathrm{H,out}}$	outlet temperature of hot process stream, K
$T^{\mathrm{HU,out}}$	outlet temperature of hot utility, K
$T^{\mathrm{CU,out}}$	outlet temperature of cold utility, K
t^{op}	annual operating hours, s
t_{LT}	lifetime of the Total Site, s

V_{cond}^{spec}	specific volume of condensate, m^3/g
$\gamma_{hp,cp}$	upper bound on heat exchange between hot process stream *hp* and cold process stream *cp* , W
$\gamma_{hp,icu}$	upper bound on heat exchange between hot process stream *hp* and cold streams icu for intermediate utility ,W
$\gamma_{ihu,cp}$	upper bound on heat exchange between intermediate utility as hot stream *ihu* and cold process stream *cp* ,W
ρ_{cp}	density of cold process stream, g/m^3
η	pump efficiency

Binary variables

$y_{hp,cp,k}$	selection/deselection of heat exchange match between hot process stream *hp* and cold process stream *cp* in stage k
$y_{hp,icu,k}$	selection/deselection of heat exchange match between hot process stream *hp* and cold intermediate utility stream including preheating in stage k
$y_{ihu,cp,k}$	selection/deselection of heat exchange match between hot intermediate utility stream *ihu* and cold process stream *cp* in stage k
y_{hp}^{CU}	selection/deselection of heat exchanger between external cold utility and hot process stream *hp*
y_{cp}^{HU}	selection/deselection of heat exchanger between external hot utility and cold process stream cp
$y_{hp,cp,k}^{dir}$	selection/deselection of pipeline between hot process *hp* and *cp* in stage *k*
ys_{s_scond,iu_iucond}	selection/deselection of steam main or condensate pipeline *iu_iucond* for segment *s_scond*
y_{iu}^{pump}	selection/deselection of pump for steam main *iu*

Variables

$A_{hp,cp,k}$	heat exchanger area between hot process stream *hp* and cold process stream *cp* within stage *k,* m^2
$A_{hp,icue,k}$	heat exchanger area between hot process stream *hp* and intermediate utility stream as cold stream, including preheating *icu,* within stage *k,* m^2
$A_{ihu,cp,k}$	heat exchanger area between intermediate utility stream as hot stream *ihu* and cold process stream *cp*, within stage *k,* m^2
A_{hp}^{CU}	heat exchanger area between hot process stream *hp* and external cold utility, m^2
A_{cp}^{HU}	heat exchanger area between cold process stream *cp* and external hot utility, m^2

CP_{icup}^{var}	heat capacity flow-rate of stream for preheating, W/K
$c^{pipe,dir}$	investment of pipes for direct process-to-process heat integration, €
$c^{pipe,indir}$	investment of pipes for indirect process-to-process heat integration, €
$d_{hp,cp,k}^{HSCS}$	diameter of pipe directed from hot process stream *hp* to cold process stream *cp*, for the heat exchanger in stage k, m
$d_{hp,cp,k}^{CSHS}$	diameter of pipe for cold process stream when directed from cold process stream *cp* to hot process stream *cp*, for the heat exchanger in stage *k*, m
$d_{s,iu}$	diameter of steam main *iu* for segment *s,* m
$d_{scond,iucond}$	diameter of condensate pipeline *iucond* for segment *scond,* m
$EC_{ap,ccond}^{cond,tot}$	total amount of heat required in water for an evaporation, W
$EC_{ap,ccond}^{cond}$	amount of heat recovered in condensate from other process, W
$Ecp_{ap,icup}$	amount of heat required for preheating of fresh water stream *icup* in process *ap,* W
$Ecc_{ap,iu}^{HS}$	amount of heat transferred to steam mean *iu* from process *ap,* W
$Ech_{ap,iu}^{CS}$	amount of heat transferred from steam mean *iu* to process *ap,* W
I_{iu}^{pump}	investment of pump for steam main *iu,* €
$I^{pump,dir}$	investment of pump for direct process-to-process heat exchanges, €
$h_{s,iu}$	specific enthalpy for steam in steam main *iu* for segment *s*, J/g
$h_{scond,iucond}^{spec}$	specific enthalpy in condensate pipeline *iucond* for segment *scond,*, J/g
$Ls_{s\_scond,iu\_iucond}^{\mathrm{var}}$	variable for distance of steam main or condensate pipeline *iu_iucond* for segment *s_scond,* m
$L_{hp,cp,k}^{\mathrm{var}}$	variable for distance between hot process stream *hp* and cold process stream *cp*, for heat exchanger occurring in stage *k*, m
$TC_{cp,k}$	temperature of cold process stream *cp* at temperature location *k,* K
$TC_{icup,k}$	temperature of cold preheating stream *icup* at temperature location *k,* K
$TH_{hp,k}$	temperature of hot process stream *hp* at temperature location *k*, K
$T_{icup}^{C,iu}$	outlet temperature of preheating stream *icup,* K
TH_{ihu}^{IU}	temperature of intermediate utility as hot stream *ihu,* K
$th_{s,iu}^{pipe}$	pipe thickness of steam main *iu* for segment *s,* m
$th_{scond,iucond}^{pipe}$	pipe thickness of condensate pipeline *iucond* for segment *scond,* m
p_{ihu}^{CS}	pressure in hot stream *ihu* for intermediate utility, bar
p_{icue}^{HS}	pressure in cold stream *icue* for intermediate utility, bar

$p_{hp,cp,k}^{drop,HSCS}$	pressure drop in cold process stream *cp,* when directed from hot process *hp*, for heat exchange within stage *k,* bar
$p_{hp,cp,k}^{drop,CSHS}$	pressure drop in cold process stream *cp,* when directed from cold process stream towards hot process *hp*, for heat exchange within stage *k,* bar
$ps_{s,iu}$	pressure in steam main *iu* for segment *s,* bar
$p_{s,iu}^{drop}$	pressure drop in steam main *iu* for segment *s,* bar
$Q_{hp,cp,k}$	amount of heat transferred from hot process stream *hp* to cold process stream *cp* in stage k, including heat losses, W
$Q_{hp,cp,k}^{tc}$	amount of heat transferred from hot process stream *hp* to cold process stream *cp* in stage k, excluding heat losses, W
$Q_{hp,icu,k}$	amount of heat transferred from hot process stream *hp* to cold intermediate utility stream *icu* (including streams for evaporation and preheating) in stage *k*, W
$Q_{ihu,cp,k}$	amount of heat transferred from hot intermediate utility stream *iu* to cold process stream *cp,* W
Q_{hp}^{CU}	amount of heat transferred to external cold utility from hot process stream *hp,* W
$Q_{hp,cp,k}^{loss,CSHS}$	amount of heat loss during transport of cold process stream *cp* to hot process stream *hp*, W
$Q_{hp,cp,k}^{loss,HSCS}$	amount of heat loss during transport of cold process stream *cp* from hot process stream *hp*, W
Q_{cp}^{HU}	amount of heat transferred from hot utility to cold process stream *cp*, W
$Qs_{sond,iucond}$	amount of heat in pipeline for condensate *iucond* in segment *scond*, W
$Qs_{s,iu}$	amount of heat in steam main *iu* for segment *s*, W
$Qs_{scond,iucond}^{loss}$	heat loss during transport of condensate in pipeline *iucond* in segment *scond,* W
$Q_{s,iu}^{loss,tot}$	total heat loss in steam main *iu* during transport in segment *s,* W
$V_{s,iu}^{spec}$	specific volume of steam in steam main iu in segment s, m^3/g
$R_{iu}^{liq\_st}$	ratio between the enthalpy of water preheating and evaporation
w_{iu}^{pump}	work of pump for steam main *iu,* W
$w_{hp,cp,k}^{pump,CSHS}$	work of pump on cold stream for direction from cold to hot stream at any stage of *k,* W
$w_{hp,cp,k}^{pump,HSCS}$	work of pump on cold stream for direction from hot stream at any stage of *k,* W
$\Delta F_{\mathrm{C},n,v}$	annual cash flow within period *n* for scenario *v,* €
ΔI	investment, €

$\Delta h_{iu}^{liq,spec}$	specific enthalpy of water preheating for steam main *iu,* J/g
$\Delta h_{iu}^{st,spec}$	specific enthalpy of evaporation for steam main *iu,* J/g
$\Delta T_{hp,cp,k}$	approach temperature difference between hot process stream *hp* and cold process stream *cp* in stage *k*, K
$\Delta T_{hp,icu,k}$	approach temperature difference between hot process stream hp and cold intermediate utility stream *icu*, that includes evaporation as well as the preheating, in stage *k,* K
$\Delta T_{ihu,cp,k}$	approach temperature difference between hot stream for intermediate utility *ihu* and cold process stream *cp* in stage *k*, K
$\Delta T_{cpicup}^{\mathrm{HU}}$	approach temperature difference between external hot utility and cold process stream *cp* or cold stream for preheating *icup*, K
$\Delta T_{hp}^{\mathrm{CU}}$	approach temperature difference between external cold utility and hot process stream *hp*, K
ΔW_{ENPV}	expected net present value of savings, €

1 Introduction

The topic of the dissertation is the optimisation of the process systems and subsystems accounting besides other characteristics for forecasted utility prices when optimising energy-related subsystems as well as prices for raw materials, utilities and products, when considering the whole process systems.

1.1 Problem description

The profitability of a company depends on revenues, expenditures and the required investment. Appropriate planning of production processes and subsystem is indispensable in order to obtain economically viable processes. The required amount of heat can be one of the key factors that impacts the sustainable developments of the companies. Nowadays, numerous methods are available for the enhancement of heat recovery. The result from the mathematical programming approach are obtained by trade-offs between operating cost and investment. The planning has usually been carried out using the objective of minimising Total Annual Cost (TAC). The TAC considers that operating cost factors are constant during the entire process lifetime. This assumption is quite dubious, as the analysis of historical prices indicated, that the utility prices have varied considerably in the past and a growing tendency can be observed on average. Therefore, applying an assumption of constant prices over the whole lifetime leads to solutions that underestimates the operating costs. Moreover, the previously mentioned variation of prices is invalid except only for the utility prices, but also for other prices regarding process operation, e.g. raw material cost or other energy sources. A methodology that accounts for all those mentioned price variations should be applied during process synthesis.

1.1.1 Heat exchanger network

The proper HEN synthesis targets improves the process profitability. The Heat Integration (HI) has been pioneered from the 70s of the last century (Linnhoff, 1994). Over the time it has been still considerably developing by number of researchers worldwide. Nowadays, there are three main directions of the research regarding HI: the thermodynamical based on Pinch Technology, mathematical programming (MP) and the combination of these two approaches. The basis of Heat Integration started to emerge with Composite Curves (Linnhoff, 1994). The following larger described discoveries were the Pinch Point and the Problem Table Algorithm (Linnhoff and Flower, 1978). All the described discoveries are still routinely used but have been extended by the Grand Composite Curve. Pinch Analysis (Linnhoff and Hindmarsh, 1983) determines thermodynamically feasible minimum energy targets, which are sometimes unachievable due to technical reasons.

Yee and Grossmann (1990) developed another approach - an MINLP model based on mathematical programming for the synthesis of HENs. The calculation of heat exchanger area in this approach is simplified and is assumed as an area of heat transfer, where the overall heat transfer coefficient is determined by contribution of heat transfer coefficient of the streams on the both side of the heat exchanger. More advance approach is described by Soršak and Kravanja (1999), where the mentioned model was extended, for the case of shell and tube heat exchanger, accounting for the pressure drops, to enable a proper heat and power integration. Additionally, the heat transfer coefficients were determined from the shell and tube heat exchanger design variables. Another approach of optimising shell and tube is by reducing total cost, which is a sum of operating and investment cost, by improving overall heat transfer coefficient using constructal theory (Azad and Amidpour, 2011). A more recent work about retrofit HEN analysis, which accounts for pressured drops was presented by Soltani and Shafiei (2011). It uses combination of genetic algorithm, linear programming and integer linear programming methods, where the genetic algorithm obtains the best structural modification. Mizutani et al. (2003) made a more detailed optimisation based on trade-off between the heat transfer area and pumping cost. Soršak and Kravanja (2004) developed also a mathematical model, which account for different type of heat exchangers not only the shell and tube. Aaltola (2002) created a multi-period MINLP model for flexible HEN, where the flow-rates and temperatures of the streams change within different periods. The objective function of this model consists of the unit costs for matches, mean area costs for stream matches, mean area costs for hot and cold utilities' matches, and mean hot and cold utilities cost. This model underestimates the total area cost and overestimates the heat exchanger area. Because of the use of mean values for areas within different periods, Verheyen and Zhang (2006) upgraded the multi-period MINLP model for flexible HEN by using the maximum area per period during MINLP formulation. All these models account for time periods of the same length. Isafiade and Fraser (2010) in their model accounted for a HEN design with an unequal time-horizon of different periods.

Besides the mentioned approaches, there are meta-heuristic approaches as well. A genetic algorithm has been applied for synthesis and optimisation of HEN. It can be applied for a small size HEN, when no stream splitting is considered (Lewin et al., 1998) or considering stream splitting and the economic trade-off (Lewin, 1998). It has been further extended to be able to synthesize and optimise large HENs (Dipama et al., 2008). There are also different approaches of global optimisation techniques, e.g. with the application of an Outer Approximation for Global Optimization Criterion (Björk and Westerlund, 2002).

1.1.2 Total Site

The applications of Heat Integration (HI) are becoming increasingly more important, as they are contributing significantly to the solution of some the most severe problems of our modern society. Heat Integration of processes can notably contribute to their sustainability by decreasing their energy consumption. This contribution is even more significant when process-level integration is extended to the Total Site (TS) level. The concept of TS includes various processes connected through a central utility system that enables heat recovery between these different processes. The concept of TS was pioneered by Dhole and Linnhoff (1993). In their work Site Sink and Site Source Profiles were introduced based on graphical tools applied for the evaluation of fuel consumption, cogeneration, emissions, and the cooling needs of an industrial site. Klemeš et al. (1997) extended this methodology by introducing Total Site Profiles (TSPs) and Site Utility Grand Composite Curves (SUGCCs). These curves serve for evaluating the heat recovery potentials between different processes. In earlier times the TS concept was only applied for industrial processes. Perry et al. (2008) further developed the concept of TS by also including processes from other sectors – residential, business, service, and agricultural. Fodor et al. (2010) extended Total Site Profile methodology by considering individual temperature differences for utilities and processes. Liew et al. (2012) presented four different tables in order to assess the sensitivity of TS with respect to operational changes, by applying a Total Site Sensitivity Table. Chew et al. (2013) listed numerous effects that can significantly affect the Heat Integration of a Total Site. A heuristic approach was used for developing a matrix containing these effects. The different impacts are weighted against each other. These methodologies are based on thermodynamic approach. An example is a Total Site Profile for a large steel plant was presented by Matsuda et al. (2012). Hackl and Harvey (2013) applied the TS Analysis as part of a holistic approach using a framework of industrial clusters for energy efficiency improvement. Another possibility for utilizing TS Analysis is for cogeneration potential, as presented by Bandypadhyay et al. (2010). Power Integration of processes might be additionally performed by applying the Power Pinch Analysis (PoPA) (Wan Alwi et al., 2012). However, not only the economic, but also the environmental aspect should also be a focus of interest. An example of methodology for setting CO_2 emission targets for energy resource planning and utility system optimisation is presented in Al-Mayyahi et al. (2013), where two composite curves are constructed as targeting tools.

In these works, both the thermodynamic and the mathematical programming approaches have proved to be useful methods, especially for setting targets for heat recovery. However, these targets need further adjustment by taking into account heat exchanges types and related area cost in order to obtain optimal trade-offs between utility consumptions and investments. This is especially the case for a Total Site where heat, transferred from one process to another, has to pass two steps of heat exchanges, and the streams need a pipeline connecting the processes.

The steam system in coal based poly-generation plant can serve as an example. When analysed as a Total Site, the heat recovery is conducted between processes by a central utility system (Zhang et al., 2014). The heat exchanges are determined within each heat recovery steam generation process separately and the process-to-process heat exchange is designed after. However, no heat or pressure drop has been assumed in this work.

They are also many mathematical programming (MP) models available for optimising the Heat Integration at the process level. A numerous extension of these models have been made. On the other side, the earliest applications of mathematical programming to Total Site were devoted to the synthesis of steam networks and process-to-process heat recovery targeting. In particular, a numerous studies have been performed approaching the synthesis problem as a steam turbine network synthesis. A conceptual design and setting the targets regarding steam level, with respect to pressure and temperature of saturation was presented by Mavromatis and Kokossis (1998). The objective was economical, namely to obtain optimal trade-off between the revenue raised by the production of power and the capital cost incurred with the installation of turbine units. Bagajewicz and Rodera (2000) developed a systematic procedure based on linear programming and mixed integer linear programming model that has been used to identify the energy saving targets and to find the location of intermediate fluid circuits. The previously mentioned turbine hardware model was supplemented by the boiler hardware model in order to describe boilers performance. Additionally, for TS analysis a transshipment model was developed in order to describe the interaction between the placement of the steam levels and steam loads of site processes by Shang and Kokossis (2004). The model presented was later improved by Varbanov et al. (2004) by which a better description of part-load performance has been given compared to the previously published model. Based on the turbine and boiler hardware model together with the transshipment model a multi period MILP model for minimisation of total utility cost for TS under multiple operation scenarios was developed by Shang and Kokossis (2005). One of the applications of the mathematical programming approach combined with Pinch Analysis for optimal energy targeting between processes was proposed by (Kovač Kralj et al., 2002) The developed methodology consisted of three steps. The first step was to perform retrofit analysis at the process level by applying any non-linear programming or mixed-integer non-linear programming algorithms. In the second step the analysis of possible heat transfer was performed by constructing Cold Composite Curve and Hot Composite Curve. This analysis considered waste heat and external utility heat demand for the case of retrofitted or non-retrofitted processes. A superstructure containing all these possible heat transfers was constructed, based on the information attained during the second step. The optimal energy target from all possible heat transfers is obtained by solving a mixed-integer nonlinear programming model. The methodology presented has been extended, thus including possible heat transfers, where heat integration at the process level could or could not be performed (Kovač Kralj et al., 2005). The further development of TS design focused on the flexibility of site utility system through optimisation of TS heat recovery subject to variable conditions. The modelling framework was presented in Aguilar et al. (2007), while the methodology and application in Aguilar et al. (2007). Also the multi objective optimisation was applied in order to combine the minimisation of cost with the minimisation of the environmental impact, assessed in life cycle environmental burdens (Papandreou and Shang, 2008). Kim et al. (2010) presented a MILP model for optimisaton of utility system in an industrial complex considering fuel tank, splitter, mixer, boiler, turbine, steam header, letdown unit, water and electricity unit. In addition, an economic/environmental analysis of the results were performed. Velasco-Garcia et al. (2011) considered not only the running cost of the utility system but also the costs association with the starting-up the operating units. Chen and Lin (2012) combined a heat recovery system model with a steam system model. Ghannadzadeh et al. (2012) presented an Iterative Bottom-to-Top model for shaftwork targeting, applying which a temperature of steam main, steam flow-rate and shaft power generated. Luo et al. (2012) developed a MILP model for designing a multiple interconnected steam power plants, where the objective was to minimize the total cost of steam power system including the economic operation cost and environmental cost. The basic elements of the model is the multi-fuel boilers and complex turbine, which enables to keep the problem linear instead of using nonlinear model. The dust, NO_x and SO_x emission from coal-fired boiler was considered for the environmental impact. Zhang et al. (2013) developed a mathematical model consisting from three part as follows: heat integration of process plants, optimisation of the utility system and the coupling equations for the site-scale steam integration. For Heat Integration a global temperature intervals were used similarly as in pinch analysis and the duty is determined within those set intervals.

In order to account for heat exchange area cost, Laukannen et al. (2012) extended the model by Yee and Grossmann (1990), originally developed for the syntheses of heat exchanger networks (HENs), for indirect heat transfer between processes. Similarly to the original HEN model, all the temperature-driven forces in HEN are treated as optimisation variables, which enables the obtaining of appropriate trade-offs between utility consumption and investment. However, the pressure levels of intermediate utilities have to be selected a priori and fixed during the optimisation. The investment cost of the pipeline can only be included only as a certain increase in fixed cost regarding heat exchangers. Furthermore, it does not account for heat losses, neither for incomplete condensate recovery, nor for pressure drops during the heat transportation. Although it is in many respects simplified and it does not represent the whole TS.

The Total Site is considered as a set of processes linked together through a central utility. These different processes can include industrial, residential, service, business, agricultural sectors or any other process with heat or electricity demand (Figure 1-1).

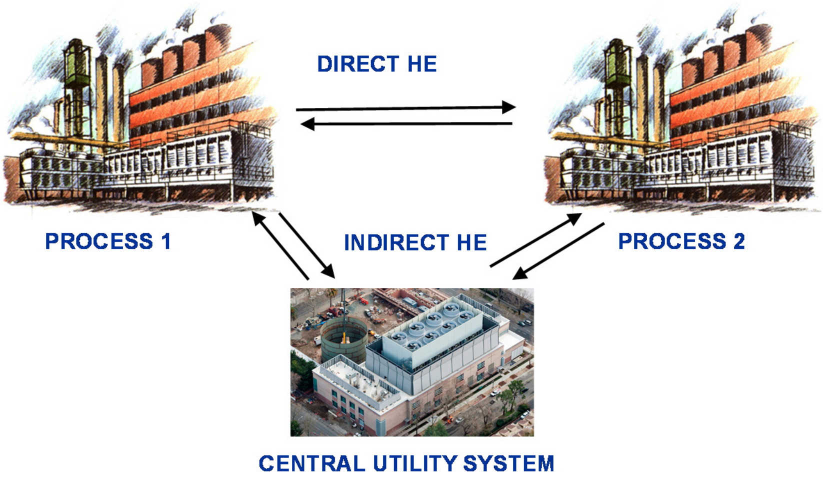

Figure 1-1: Scheme of a Total Site

Therefore, heat recovery can be performed within each processes and additionally, when Total Site concept is applied the process-to-process heat recovery is considered. In this concept it is obtained via two heat exchanges. First heat exchange occurs between process stream with heat surplus and intermediate utility and the second between intermediate utility and process stream with heat demand. It should be noted, that within processes the intermediate utility is transported via pipeline, therefore it should be considered when synthesizing the Total Site. An process-to-process heat transfer was also considered by Hipólito-Valencia et al. (2014) who designed an integrated trigeneration system for eco-industrial parks. The inter process heat transfer took place directly between process streams. Steam Rankine cycle, organic Rankine cycle, and the absorption-refrigeration cycle were additionally integrated in the system.

1.1.3 Distillation column sequence with its heat exchanger network

Optimally designing distillation columns in order to ensure energy efficiency is a complex task, which has a significant effect on process profitability, since separation processes require large amounts of utilities. In fact, the energy requirements for separation processes represent quite a high rate of overall world energy consumption. Similarly as during the heat integration, there are two main directions for distillation columns synthesis. One direction is the thermodynamic approach. Descriptions about sequencing the distillation columns, and about the heat integration of distillation columns, can be found in different sources (for example Smith, 2005).

An example of retrofit design regarding methanol plant was presented by Demirel (2006) by applying a Column Grand Composite Curve and an Exergy Loss Profile. Soares Pinto et al. (2011) developed a novel approach for temperature-enthalpy profile when determining a target for the usage of side condensers and side reboilers, based on a thermodynamic analysis. They introduced a minimum driving force, which was considered as an exergy loss distribution of the existing column similar to temperature driving force in the case of HEN. By applying the thermodynamic approach, the target for processes is set. However, the rate of integrating the distillation column and HEN depends on the trade-off between the operating cost and the capital cost.

A mathematical programming approach was developed, in order to establish this trade-off. For example, Novak et al. (1996) presented a compact superstructure for the optimisation of distillation column's sequence integrated with its heat exchanger network. A nonlinear short-cut method was applied, in order to overcome the problems with singularities (Yeomans and Grossmann, 1999). A combination of state task network and state equipment network superstructure was suggested for this purpose. A nonlinear disjunctive programming model was proposed for the synthesis of the heat integrated distillation column sequence. Another problem relating to solving MINLP problems is to ensure a feasible initial guess for the optimisation, on which the solution can be highly dependent, not to mention that the objective function and constraints usually have to be continuously differentiable twice. An alternative method for solving these problems is the natural hybrid evolutionary/local search method. Using this approach, the continuous design parameters for the units the local search method are applied, whilst for the optimisation procedure regarding the heat exchanger design an evolutionary optimisation procedure can be used (Fraga and Žilinskas, 2003). Proios et al. (2005) presented a generalised modular framework for the heat integrated distillation column. It is a three-stage systematic procedure that uses logical modelling in order to generate tight and accurate structural models. Grossmann et al. (2005) presented a rigorous model for the synthesis of a complex distillation column. Two models were described - a mixed-integer nonlinear model and a generalised disjunctive programming model. Both models applied tray-by-tray formulation. However, these models are quite complex. A novel approach for obtaining solution for the heat integrated distillation column sequence is the genetic algorithm (Wang and Li, 2010) for the non-sharp separation of the components.

1.1.4 Methanol production process

The annual production of methanol is above 40 Mt and still shows a growth tendency with approximately 4 % increase each year (Aasberg-Petersen et al., 2013). It is used as a feed for producing a range of chemicals such as acetic acid and formaldehyde amongst others. There are many different raw materials utilised for methanol production; e.g. a mixture of natural gas and biomass can be used (Li et al., 2010), or methane by applying the Ammonia-Oxidizing Bacteria process (Taher and Chandran, 2013). A different approach for utilising steel-work off-gases, either with or without the addition of a biomass, for the production of methanol was presented recently by Lundgren et al. (2013). Despite different possible sources methanol is still mainly produced from natural gas. However, the production from coal is increasing significantly, especially in regions where natural gas is unavailable or is expensive, e.g. in China (Aasberg-Petersen et al., 2013). Due to the sharp competition between various raw materials - mainly between natural gas and coal - the design of a methanol production plant should be performed by considering several aspects. A proper trade-off between operating costs and investment should be established for obtaining an optimal process design. Kordabadi and Jahanmiri (2005) used a genetic algorithm for designing a methanol plant under varying conditions in regard to the length and temperature of a stage in within a two-stage methanol synthesis reactor. A super-structural approach to the synthesis of a methanol process was presented some time ago by Kravanja and Grossmann (1990), by applying a MINLP model using PROSYN – a MINLP process synthesizer.

1.2 Basic aims of the research and methodology

The aim of the dissertation is to develop a methodology for forecasting prices and considering them at the syntheses of process systems and subsystems. In regards to subsystems only those are evaluated, that might significantly affects the economical viability of the whole process system. Therefore, the more specific aims of the research can be described using the following points:

Aim 1: The development of a methodology for synthesising and optimising processes and process subsystems for entire lifetimes that accounts for forecasted utility prices. Two steps are required to achieve this aim. In first step, the price forecast should be performed and in the second step, the synthesis models should be upgraded in order to account for the forecasted prices obtained during the previous step.

Aim 2: An application of the developed methodology for an entire lifetime by considering future utility prices for optimisation Heat Exchanger Network (HEN). The aim of this optimisation is to propose a network design that would meet the respective trade-offs between investment and operating costs during all periods over entire lifetime as closely as possible. However, the price forecast is always somewhat uncertain; therefore, additionally a HEN extension at a later time during the lifetime should also be enabled additionally.

Aim 3: An application of the developed methodology for an entire lifetime by considering future utility prices for the synthesis of a Total Site (Heat Integration within and between different processes). This synthesis can be performed by applying one of two different strategies. A sequential strategy is a step-wise approach. In the first step the Heat Integration at process level is optimised first and then at the Total Site level in second step. The simultaneous strategy is performed at both levels simultaneously, and might be more beneficial. Both strategies are performed by considering forecasted utility prices.

Aim 4: An application of the methodology for an entire lifetime with considered future utility prices, for the synthesis of a distillation column sequence together with its Heat Exchanger Network by considering forecasted utility prices. A stochastic multi-period models for the synthesis of the heat integrated distillation column sequence by considering forecasted utility prices have to be developed.

Aim 5: An application of the methodology to the synthesis of overall process flow-sheets by considering the forecasted prices of raw materials, utilities and products. The aim is to develop an approach that accounts for different forecasted prices that might have an impact on the trade-off of the whole process system. As the profitability of the whole process depends on the operating cost as well as on revenues, all price variations should be considered simultaneously instead of focusing on one price variation.

1.3 Outline of Dissertation

This dissertation consists of seven chapters: i) Introduction, ii) Theoretical background and the development of the solution procedure, iii) Heat Exchanger Network synthesis on the process level for entire lifetimes, iv) Process-to-process Heat Integration for entire lifetimes, v) Syntheses of distillation columns' sequences and their HENs over entire lifetimes, vi) Process syntheses for entire lifetimes, vii) Conclusions and future work. The basic aim of the dissertation was to optimise or synthesize different processes and process subsystems by considering price variations. This phenomena of price variations has been evaluated for four different cases: i) Optimisation of Heat Exchanger Networks within processes, ii) Total Site synthesis including heat integration within processes as well as between processes, iii) Distillation columns' sequence optimisations with their HENs and iv) synthesis of process for the production of methanol.

The introduction and a state-of-art regarding processes and studied process subsystems are provided in Chapter 1. The following Chapter 2 provides a theoretical background and the development of the solution procedure. The general procedure of obtaining solutions is developed and described. It consists of the methodology for price forecasting, the multi-period and stochastic MINLP model formulations, together with the definitions of different objective functions, as well as the procedure for solving MINLP problems.

Chapter 3 presents the optimisation of a Heat Exchanger Network (HEN) for an entire lifetime by considering future utility prices. Two different approaches for obtaining solutions have been developed: i) when the HEN is built at the beginning of the lifetime, without any possibilities of later extensions during its lifetime, and ii) when there is an opportunity to extend (retrofit) the initial HEN design once over its lifetime. The initial model for HEN optimisation has been firstly upgraded to a stochastic multi–period MINLP model. Further enhancement of the model has been required in order to enable extensions at later times over the lifetime. Both solutions were analysed by applying various economic criteria.

Chapter 4 describes a Total Site synthesis by considering future utility prices, besides other important properties. A Sink Source Model has been developed for Heat Integration between processes and after achieving the optimal heat recoveries within processes. The developed model enables process-to-process Heat Integration (HI) by also taking into account various properties regarding heat transfer, pipeline design etc. However, it could only be applied for HI between processes by excluding the HI during the process level. Therefore, a Total Site Compact model has been developed. It enables synthesis of an entire Total Site for heat recovery within processes and between different processes simultaneously accounting for the required heat exchangers and also the pipelines.

Chapter 5 deals with the impact of varying utility prices on the optimisation of a distillation column sequence together with its HEN. This chapter discusses the potential for future utility prices effecting optimal design. It also indicates the boundaries of the developed procedure.

Chapter 6 extends the synthesis methodology by also considering several future prices, i.e. forecasted product prices, raw materials' prices, and various utilities' prices. The methodology was applied to an example of a methanol production process. This chapter provides an evaluation of the simultaneous effects of different price variations.

In Chapter 7, the conclusion obtained from the current work is summarised and some proposals for future research directions.

2 Theoretical background and the development of the solution procedure

2.1 Theoretical background

2.1.1 Superstructural approach

The superstructural approach can be regarded as an activity when from a certain structure that contains different automatically generated structural design alternatives, the better ones are selected based on a certain criterion (Kravanja et al., 1998). The superstructural synthesis thus comprises the generation and the selection of different structural alternatives as well as decisions on which structural elements to integrate within the final structure and how they are interconnected. This can be regarded as discrete decision-making. However, also the geometry, sizes, temperature, enthalpy flow-rate, pressure has to determined. The latter implies making choices within the continuous spaces of the parameters. Therefore, from the conceptual point of view a design synthesis problem corresponds to a discrete/continuous optimisation problem. For solving this problem a mathematical programming approach can be applied, namely mixed-integer linear programming (MILP) or mixed-integer non-linear programming (MINLP). The majority of chemical engineering problems are non-linear, therefore the MINLP optimisation approach is utilised for these problems. Therefore, solving synthesis problems consist of three step (Kravanja et al., 1998):

1. Generation of a synthesis superstructure for different structure/topology and other design alternatives that are all candidates for a feasible and optimal solution.
2. Development of a special MINLP model formulation for the generated superstructure within an equation-oriented environment. This formulation consists of continuous variables that are used for continuous decisions (dimensions, size, levels) and a set of integer (binary) variables that are denoted for the potential existence of structural elements, their connectivity, and standard dimensions.
3. Solution of a defined MINLP model, performed by a suitable MINLP algorithm and strategies, which during the simultaneous MINLP optimisation approach yields a solution with an optimal topology and continuous parameters.

An optimal structure design is proposed that would be obtained by accomplishing the above MINLP activity steps.

2.1.2 General MINLP optimisation model

In chemical engineering the vast majority of the problems involves continuous and integer (discrete) variables. The values of process parameters, e.g. temperature, enthalpy flow-rate, pressure etc., are the continuous variables. The integer variables presents the decision regarding design, e.g. selected matches for heat exchange, connections between different process units, selection/deselection of certain process unit or operation etc. A mixed-integer nonlinear programming (MINLP) model presents a mathematical formulations of a given synthesis problem that contains a objective function to be minimised or maximised subjected to mixed-integer linear and nonlinear constraints.

The problem formulation for maximisation is the following one:

$$\begin{aligned}
&\max \ Z = \mathbf{c}^{\mathrm{T}}\mathbf{y} + f(\mathbf{x}) \\
&s.t. \\
&\mathrm{A}\cdot\mathbf{y} + \mathbf{h}(\mathbf{x}) = 0 \\
&\mathrm{B}\cdot\mathbf{y} + \mathbf{g}(\mathbf{x}) \le 0 \qquad\qquad\qquad\qquad \text{(MINLP)} \\
&\mathbf{x} \in \mathbf{X} = \left\{\mathbf{x} \middle| \mathbf{x} \in \mathbf{X} \subseteq \mathbb{R}^n, \mathbf{x}^{\mathrm{LO}} \le \mathbf{x} \le \mathbf{x}^{\mathrm{UP}}\right\} \\
&\mathbf{y} \in \{0,1\}^m
\end{aligned}$$

Where:

Z – objective function

$\mathbf{y}$ – vector of binary variables

$f(\mathbf{x})$ – f continuous scalar function of vector variables $\mathbf{x}$, that is a vector of continuous variables

$\mathbf{h}(\mathbf{x})$ – system of equality constraints,

$\mathbf{g}(\mathbf{x})$ – system of inequality constraints.

A, B – matrix of coefficients

$\mathbf{c}^{\mathrm{T}}$ – vector of cost coefficients

2.1.3 Solving MINLP problems

All the presented aims requires a methodology for forecasting prices. As the forecast is uncertain, different price projections have been arrived at, based on historical prices. A Gaussian statistical distribution has served as a basis, when determining the probabilities of prices for certain projections over certain periods. The mathematical programming approach has been used for determining probabilities and for the syntheses of process systems and subsystems. The probabilities have been determined using a nonlinear programming model solved by the commercially-available program CONOPT/GAMS. The MINLP models can be solved by applying various algorithms. In the current work in MIPSYN (Kravanja, 2010) a Modified Outer Approximation/Equality Relaxation algorithm (Kravanja and Grossmann, 1994) was used. It is an extension of the Outer Approximation/Equality Relaxation (OA/ER) algorithm (Duran and Grossmann, 1986; Kocis and Grossmann, 1987) and Outer Approximation/Equality Relaxation/Augmented Penalty (OA/ER/AP) (Viswanathan and Grossmann, 1990) algorithm. In DICOPT solver of GAMS programme OA/ER/AP algorithm was applied.

All of these algorithms are decomposing MINLP problem to a sequence of nonlinear subproblems and master mixed-integer linear problems (MILP). The algorithm of Outer Approximation/Equality Relaxation is schematically represented in Figure 2-1.

The MINLP problem is reformulated to a master MILP problem in two steps. First, the objective function is reformulated in such a way, that all nonlinear are moved into constraints by a variable α.

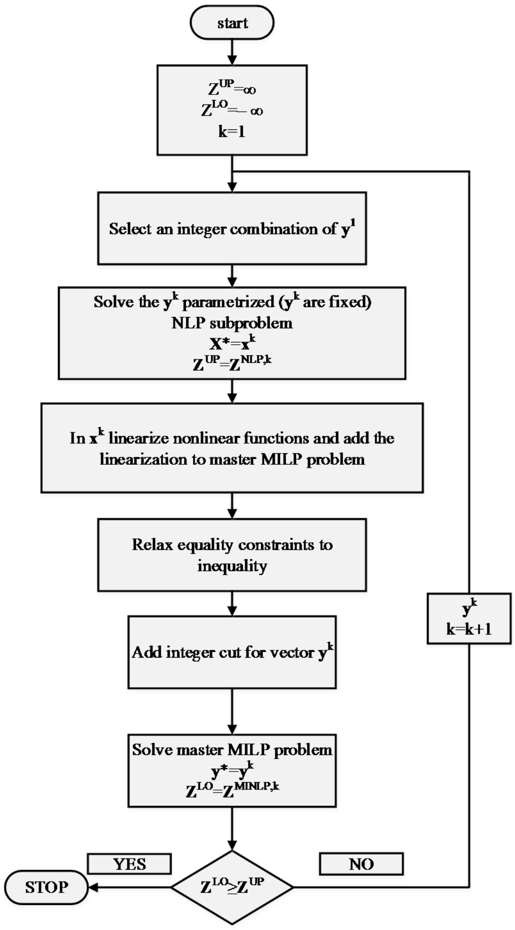

Figure 2-1: Schematic representation of AO/ER (minimisation of objective function)

$$
\begin{aligned}
&Z = \min_{\mathbf{x},\mathbf{y}}(f(\mathbf{x}) + \mathbf{c}^{\mathrm{T}}\mathbf{y}) \\
&\text{s.t.} \\
&\mathbf{Ay} + \mathbf{g}(\mathbf{x}) \le \mathbf{0} \\
&\mathbf{Ey} \le \mathbf{e} \\
&\mathbf{y} \in \{0,1\}^m, \mathbf{x} \in \mathbb{R}^n
\end{aligned}
\qquad
\begin{aligned}
&Z = \min_{\alpha,\mathbf{y}}(\alpha + \mathbf{c}^{\mathrm{T}}\mathbf{y}) \\
&s.t. \\
&f(x) \le \alpha \\
&\mathbf{Ay} + \mathbf{g}(\mathbf{x}) \le \mathbf{0} \\
&\mathbf{Ey} \le \mathbf{e} \\
&\mathbf{y} \in \{0,1\}^m, \mathbf{x} \in \mathbb{R}^n, \alpha \in \mathbb{R}
\end{aligned}
$$

The objective function is now linear and all the nonlinearities are present only in the constraints. If functions $f(\mathrm{x})$ and $g(\mathrm{x})$ are continuous, differentiable and convex, the following relationship can be written.

$$
\begin{aligned}
f(\mathrm{x}) &\ge f(\mathrm{x}^{\mathrm{k}}) + \nabla f(\mathrm{x}^{\mathrm{k}})^{\mathrm{T}}\left(x - x^k\right) \\
g(\mathrm{x}) &\ge g(\mathrm{x}^{\mathrm{k}}) + \nabla g(\mathrm{x}^{\mathrm{k}})^{\mathrm{T}}\left(x - x^k\right)
\end{aligned}
\tag{2-1}
$$

The essential meaning of the above relationship is that the linearisation of nonlinear convex function saves the initial nonlinear search space (Figure 2-2a). If the linearisation is performed infinitely, it can be observed that the initial search space is precisely preserved (Figure 2-2b).

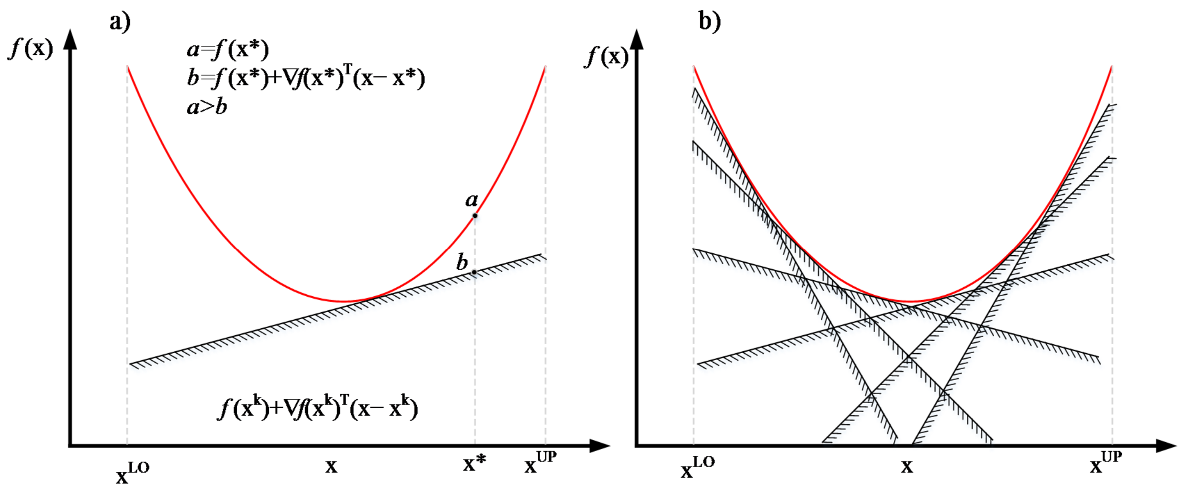

Figure 2-2: a) linearisation of nonlinear convex function. b) Approximation of nonlinear convex function with its linearisation.

The above problem relationship is a basis for of conversion of the original MINLP problem into an MILP master problem.

$$
\begin{aligned}
&Z = \min(\alpha + \mathbf{c}^T \mathbf{y})\\
&\text{s.t.}\\
&\left.\begin{aligned}
&f(\mathrm{x}^k) + \nabla f(\mathrm{x}^k)^T(\mathrm{x}-\mathrm{x}^k) - \alpha \le 0\\
&\mathbf{g}(\mathrm{x}^k) + \nabla \mathbf{g}(\mathrm{x}^k)^T(\mathrm{x}-\mathrm{x}^k) - \mathbf{A}\mathbf{y} \le 0
\end{aligned}\right\} \qquad k \in \mathbb{R}^n\\
&E(x) \le \mathrm{e}\\
&\mathrm{y} \in \{0,1\}, x \in \mathbb{R}^n, \mathrm{x}^{\mathrm{LO}} \le \mathrm{x} \le \mathrm{x}^{\mathrm{UP}}, \alpha \in \mathbb{R}
\end{aligned}
$$

The above formulation has one main drawback, that there is an infinite number of linear constraints. However, in order to avoid an infinite number of linearisation, linearisation are derived only at some selected points, which are the solutions of the NLP subproblems. If we assume there is K solutions of NLP subproblems, then the master MILP problem can be written as follows:

$$
\begin{aligned}
&Z = \min(\alpha + \mathbf{c}^T \mathbf{y})\\
&\text{s.t.}\\
&\left.\begin{aligned}
&f(\mathrm{x}^k) + \nabla f(\mathrm{x}^k)^T(\mathrm{x}-\mathrm{x}^k) - \alpha \le 0\\
&\mathbf{g}(\mathrm{x}^k) + \nabla \mathbf{g}(\mathrm{x}^k)^T(\mathrm{x}-\mathrm{x}^k) - \mathbf{A}\mathbf{y} \le 0
\end{aligned}\right\} \qquad k = 1,\ldots,K\\
&E(x) \le \mathrm{e}\\
&\mathrm{y} \in \{0,1\}, x \in \mathbb{R}^n, \mathrm{x}^{\mathrm{LO}} \le \mathrm{x} \le \mathrm{x}^{\mathrm{UP}}, \alpha \in \mathbb{R}
\end{aligned}
$$

In cases, when MINLP problems, besides inequality constraints, contain also nonlinear equality constraints $\mathbf{h}(\mathbf{x})=\mathbf{0}$, the equality constraints are relaxed into inequalities ones by considering signs of Lagragian multiplicatiors μ_i:

$$h_i(\mathbf{x}) = \begin{cases} h_i(\mathbf{x}) \le 0, & if\, \mu_i > 0 \\ h_i(\mathbf{x}) \ge 0, & if\, \mu_i < 0 \\ neglected & if\, \mu_i = 0 \end{cases} \tag{2-2}$$

The relaxed linearization of nonlinear functions $h_i(\mathbf{x})=0$ that are added to the master MILP problem formulation have the following form :

$$\mathbf{T}^k \left(\nabla h\left(\mathbf{x}^k\right)\left(\mathbf{x}-\mathbf{x}^k\right)\right) \le 0 \tag{2-3}$$

where $\mathbf{T}^k$ is a diagonal matrices with terms:

$$t_{ij}^k = \begin{cases} 1, & if\, \mu_i > 0 \\ -1 & if\, \mu_i < 0 \\ 0 & if\, \mu_i = 0 \end{cases} \tag{2-4}$$

Repetition of the same linearisations is avoided by applying the following integer cut:

$$\begin{aligned} &\sum_{i \in \mathrm{B}^k} y_i - \sum_{i \in \mathrm{N}^k} y_i \le \left|\mathrm{B}^k\right| - 1, \qquad k = 1, \dots, K \\ &\mathrm{B}^k = \left\{ i \middle| y_i^k = 1 \right\}, \mathrm{N}^k = \left\{ i \middle| y_i^k = 0 \right\}, \end{aligned} \tag{2-5}$$

2.2 Development of solution procedure

2.2.1 Price projections

The utility prices have to be forecasted for the time horizon regarding the expected operation of the plant under analysis (Nemet et al., 2013). The price projections are based on the historical data, e.g. depending on gasoline prices (Index Mundi, 2012). A monthly basis can be applied in order to obtain more precise data for projections. The data time period was 10 y in Figure 2-1. The forecasting has to be performed for all prices that can vary. Different projections, at different probability levels, using Gaussian distribution for cost coefficients are derived at, in order to consider the uncertainties of future prices: a very optimistic one for underestimated price coefficients at probability level $p = 0.068$ (Projection 1 – P1), optimistic at 0.2417 (Projection 2 – P2), average at 0.383 (Projection 3 – P3), pessimistic at 0.2417 (Projection 4 – P4), and very pessimistic projection for overestimated price coefficients at probability level 0.0668 (Projection 5 – P5), Figure 2-3.

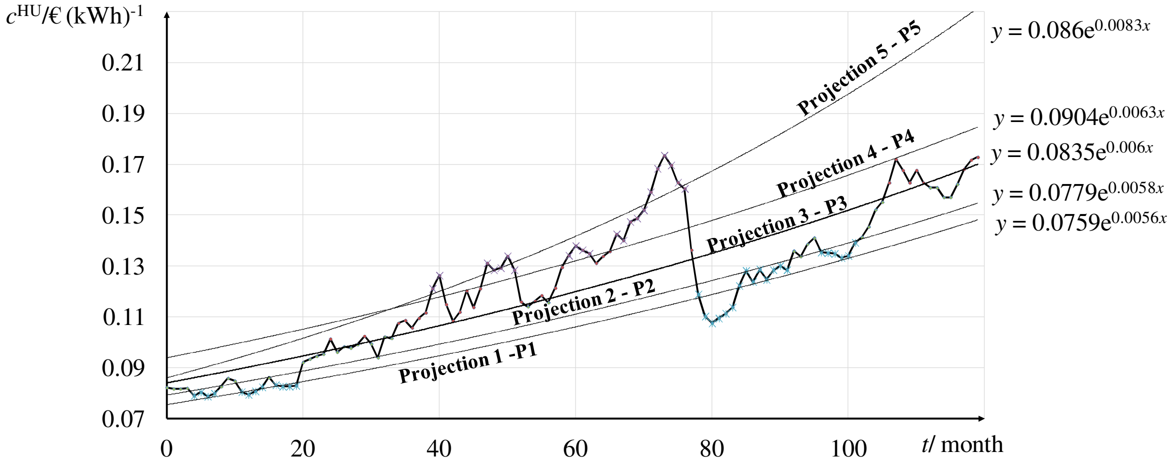

Figure 2-3: Different basis for further projections for hot oil

The procedure for obtaining probabilities for certain time periods at certain probabilities is the following. Starting from the current price, the utility price can follow many different price scenarios over the process lifetime, jumping from one to another price projections, Figure 2-4a.

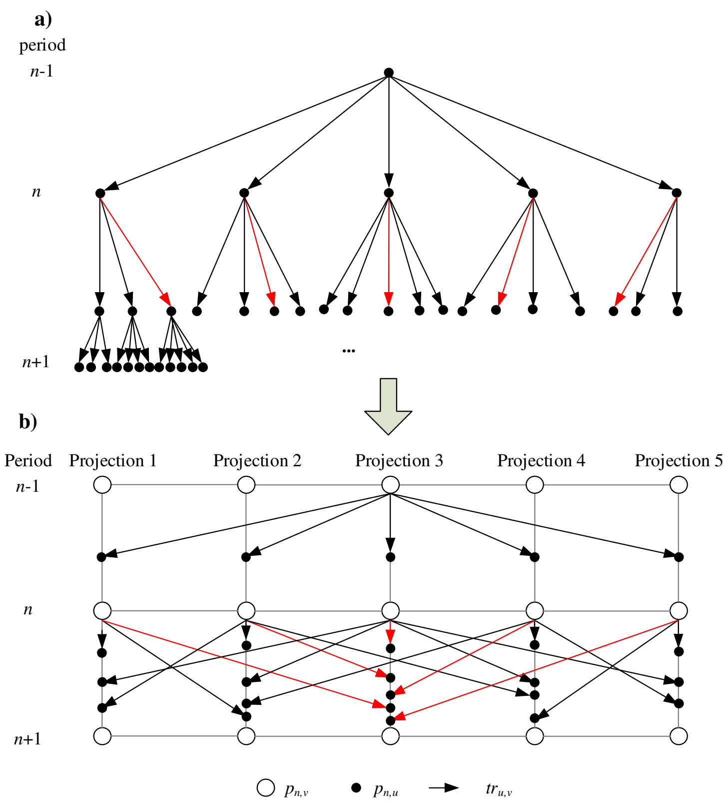

Figure 2-4: Time-projection grid for the determination of probabilities for a) traditional and b) novel approach

There are approximately $3 \cdot 10^{10}$ different scenarios (determined as $5^{15,}$), if 5 different utility price projections are proposed and 15 y of lifetime is assumed (Figure 2-3a). As the *ENPV* is defined as a sum of their individual *ENPV*s multiplied by their probabilities, the corresponding optimisation model would be too large to be solved even for shorter lifetimes. Rather than considering these scenarios separately with their individual probabilities (Figure 2-4a), combined probabilities $p_{n,v}$ (Figure 2-4b) were proposed. It is a probability for a process system design being at a certain price projection v and time period n, which were determined, in order to perform stochastic multi-period synthesis of process system. The probabilities are now determined as a sum of the individual probabilities of all the scenarios being at a certain price projection and time period. By utilising this approach the individual scenarios are composed into combined ones, one for each projection. The number of scenarios for 15 y is now significantly reduced - down to 5. The combined probabilities are defined in the following way. Each of the price transitions, from any current price projection u to any other projection v in the next period, has its own transition probability, $tr_{u,v}$. The probability of a specific price projection within a certain period, $p_{n,v}$, is defined as the sum of the probabilities, that a price scenario will follow the projection on a current position from all projections during the previous period. The probability of the jump from a previous projection u to the current one v is defined as a multiplication of previous probability $p_{n-1,u}$ by the corresponding transition probability, $tr_{u,v}$. (see e.g. for Projection 3 - highlighted transitions, Figure 2-4b). The calculation of probabilities $p_{n,v}$ starts from the root node (Figure 2-4b). If the current, starting price lies on one of the projections, the probability $p_{0,v}$ for this projection is 1, and it is 0 for the rest of projections. If the price lies somewhere in-between of two projections, it can be expressed as a linear combination of the adjacent projections' prices. The coefficients from the linear combination then represent probabilities $p_{0,v}$ for the two projections. An NLP model is formulated in order to obtain the combined probabilities of each projection for every time period. As in principle probabilities of staying or jumping down or up for one or two projection levels (x_1, x_2, x_3, x_4, x_5) can be regarded as being independent of the current node position, **u**×**v** different transition probabilities $\boldsymbol{tr}_{\mathrm{u,v}}$ can be expressed as a function of 5 variables only (Eq. 2-6):

$$\boldsymbol{tr}(u,v)=\begin{bmatrix} \frac{x_1}{x_1+x_2+x_3} & \frac{x_2}{x_1+x_2+x_3} & \frac{x_3}{x_1+x_2+x_3} & 0 & 0 \\ \frac{x_4}{x_4+x_1+x_2+x_3} & \frac{x_1}{x_4+x_1+x_2+x_3} & \frac{x_2}{x_4+x_1+x_2+x_3} & \frac{x_3}{x_4+x_1+x_2+x_3} & 0 \\ x_5 & x_4 & x_1 & x_2 & x_3 \\ 0 & \frac{x_5}{x_5+x_4+x_1+x_2} & \frac{x_4}{x_5+x_4+x_1+x_2} & \frac{x_1}{x_5+x_4+x_1+x_2} & \frac{x_2}{x_5+x_4+x_1+x_2} \\ 0 & 0 & \frac{x_5}{x_5+x_4+x_1} & \frac{x_4}{x_5+x_4+x_1} & \frac{x_1}{x_5+x_4+x_1} \end{bmatrix} \qquad (2\text{-}6)$$

The probability at certain projection and period is determined as the multiplication of the probability in the previous period by transition probabilities, summed up for each projection from where the transition can be done to the observed projection:

$$p_{n,v}=\sum_{u}(p_{n-1,u}\cdot tr_{u,v}) \qquad \forall n\in N=\{1,2,..t_{\mathrm{LT}}\}, v\in V \qquad (2\text{-}7)$$

The sum of probabilities of all transitions from each projection to all projections in the next period should be equal to 1:

$$\sum_{v} tr_{u,v}=1 \qquad \forall u\in U \qquad (2\text{-}8)$$

The objective for each projection is to minimise the difference between its average probability and its probability level pl_v (0.0668, 0.2417, 0.383, 0.2417, 0.0668):

$$\frac{\sum_{n\in\{1,2..t_{LT}\}} p_{n,v}}{t_{LT}} - pl_v = s_v^+ - s_v^- \qquad \forall v \in V \qquad (2\text{-}9)$$

where s^+_v and s^-_v are positive slack variables used to account for the difference. The objective function is then defined as minimisation of these differences for all price projections:

$$z = \sum_v (s_v^+ + s_v^-) \qquad (2\text{-}10)$$

2.2.2 Multi-period programming

The traditional MINLP has to be upgraded over time in order to consider the entire lifetime. It can be obtain by multi-period programming.

$$\begin{aligned}
&\max \ \ Z = \mathbf{c}^{\mathrm{T}}\mathbf{y} + f(\mathbf{x}_n) \\
&\text{s.t.} \\
&\mathrm{A}_n \cdot \mathbf{y} + \mathbf{h}_n(\mathbf{x}_n) = 0 \\
&\mathrm{B}_n \cdot \mathbf{y} + \mathbf{g}_n(\mathbf{x}_n) \le 0 \\
&\mathbf{d} \ge \mathbf{d}_n^e(x) \\
&(\mathbf{x}_n,\mathbf{d}) \in \mathbf{X} = \left\{(\mathbf{x}_n,\mathbf{d}) \middle| (\mathbf{x}_n,\mathbf{d}) \in \mathbf{X}, \mathbf{x}_n^{\mathrm{LO}} \le \mathbf{x}_n \le \mathbf{x}_n^{\mathrm{UP}}, d^{\mathrm{LO}} \le d \le d^{\mathrm{UP}}\right\} \\
&\mathbf{y} \in \{0,1\}^m
\end{aligned} \qquad (\text{MINLP-MP})$$

The multi-period programming model formulation can be applied when the problem contains parameters that varying throughout some periods. Therefore, instead of original MINLP model formulation the problem is disaggregated into periods as follows.When the utility price variations are considered, the periods presents a time intervals within which the prices are constant (Figure 2-5).

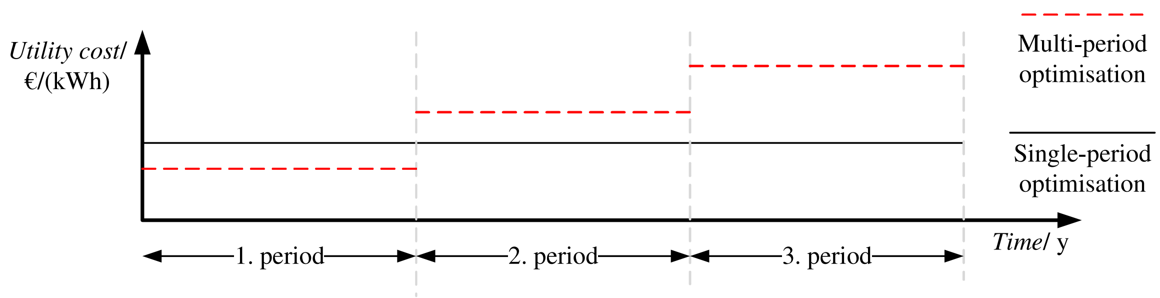

Figure 2-5: Graphical representation of time period of the multi-period optimisation

2.2.3 Stochastic programming

In order to consider variability of future prices, the traditional MINLP has to be upgraded to a stochastic MINLP programming considering future prices as uncertain parameters. Parameters (data) are usually considered at nominal fixed values as known values, when formulating a mathematical programming model. However, in reality the parameters are uncertain and thus often given within certain bounds. The stochastic programming refers to mathematical programming where problems involve uncertainties of some of the data. In the case of uncertain data, their probability distribution should be known. The aim of the stochastic optimisation is to obtain an optimal solution that is feasible for all possible combination of uncertain parameters within their given bounds. A stochastic problem can be solved numerically through discretisation of the vector of uncertain parameters ξ to a finite number of possible realisations, called scenarios, e.g. $\xi_1,\ldots,\ \xi_v$, with respect to their probabilities $p_1,\ldots,\ p_v$, where index of scenarios is denoted by v. The approach with known scenarios and their probabilities is also called the deterministic equivalent. Therefore, the basic MINLP formulation is upgraded to the following form:

$$
\begin{aligned}
&\max\ \ Z = \sum_{v} \Big(p_v \cdot (\mathbf{c}_v^{\mathrm{T}} \mathbf{y} + f_v(\mathbf{x}_\mathbf{v}, \xi_v) \Big) \\
&s.t. \\
&\mathrm{A}_\mathrm{v} \cdot \mathbf{y} + \mathbf{h}_\mathbf{v}(\mathbf{x}_\mathbf{v}, \xi_\mathbf{v}) = 0 && \forall v \in V \\
&\mathrm{B}_v \cdot \mathbf{y} + \mathbf{g}_v(\mathbf{x}_v, \xi_v) \le 0 && \forall v \in V && \text{(MINLP-S)} \\
&\mathbf{x}_\mathbf{v} \in \mathbf{X}_\mathbf{v} = \left\{ \mathbf{x}_\mathbf{v} \middle| \mathbf{x}_\mathbf{v} \in \mathbf{X}_\mathbf{v} \subseteq \mathbb{R}^n, \mathbf{x}_v^{\mathrm{LO}} \le \mathbf{x}_v \le \mathbf{x}_v^{\mathrm{UP}} \right\} \\
&\mathbf{y} \in \{0,1\}^m
\end{aligned}
$$

The stochastic problem (MINLP-S) as multi-scenario problem can be represented graphically, e.g. for three scenario in Figure 2-6 where all different scenarios are available at the same time. These scenarios can be transformed into a deterministic equivalent by composing them through their multiplication by their own probability.

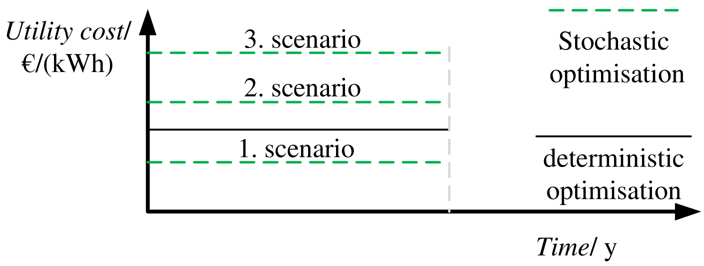

Figure 2-6: Graphical representation of stochastic programming scenarios

2.2.4 Multi-period stochastic programming

Finally, when MINLP problem is defined for several uncertain parameters over various time periods, the multi-period stochastic MINLP problem (MINLP-MPS) is thus obtained:

$$\max\ Z = \sum_{v}\left(p_v \cdot (\mathbf{c}_{n,v}^{\mathrm{T}}\mathbf{y} + f_{n,v}(\mathbf{x}_{\mathbf{n,v}},\xi_v)\right)$$

$$s.t.$$

$$\mathrm{A}_{n,v} \cdot \mathbf{y} + \mathbf{h}_{n,v}(\mathbf{x}) = 0$$

$$\mathrm{B}_{n,v} \cdot \mathbf{y} + \mathbf{g}_{n,v}(\mathbf{x}) \leq 0 \qquad \text{MINLP-MPS}$$

$$\mathbf{d} \geq \mathbf{d}_{n,v}^{e}(\mathbf{x})$$

$$\mathbf{x}_{n,v} \in \mathbf{X}_{n,v} = \left\{\mathbf{x}_{n,v} \middle| \mathbf{x}_{n,v} \in \mathbf{X}_{n,v} \subseteq \mathbb{R}^n, \mathbf{x}_{n,v}^{\mathrm{LO}} \leq \mathbf{x}_{n,v} \leq \mathbf{x}_{n,v}^{\mathrm{UP}}\right\}$$

$$\mathbf{y} \in \{0,1\}^m$$

In the synthesis, a future price, e.g. for hot utility, was represented by different price projections, each by its own probability, over a certain number of time periods. Performing MINLP synthesis of a process over its entire lifetime thus corresponds to solving the corresponding (MINLP-MPS) problem. The multi-period stochastic programming can be graphically presented as can be seen in Figure 2-7.

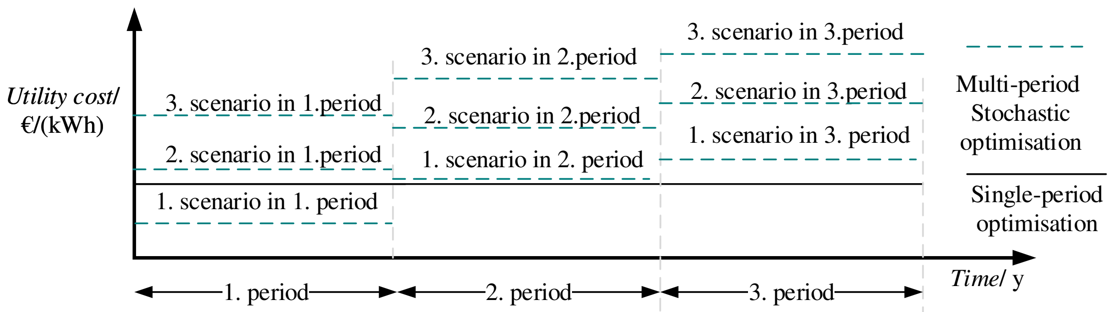

Figure 2-7: Graphical representation of multi-period stochastic programming

2.2.5 Definition of the objective functions

Different criteria are available in order to evaluate economic viability of processes. The most common criteria are the following: Net Present Value (*NPV*), Internal Rate of Return (*IRR*), Discounted Payback (*DPB*), and Lifetime Discounted Return on Investment (*LTDROI*) (Novak Pintarič and Kravanja, 2006).

2.2.5.1 Net Present Value

The Net Present Value (*NPV*) criterion can be considered as a compromise criterion between quantitative criterion (e.g. total annual cost, profitability before tax) and qualitative criterion (e.g. payback time, internal rate of return). The solutions of quantitative criteria have lower profitability compared to qualitative criteria and higher investment. On the other hand, qualitative criteria selects solutions, where the profitability is higher and the investment is lower. Therefore, the quantitative criteria is appropriate only for a long-term planning, whilst the quantitative criteria only for a short-term planning (Novak Pintarič and Kravanja, 2006). The *NPV* contains terms of quantitative as well as the qualitative criteria, therefore, it can be considered as compromised criteria where the solutions obtained have moderate profitability and medium size investment. *NPV* of the processes is the arithmetic sum of all the cash flows' present values (Eq. 2-11)

$$\max NPV(x,y) = -I(x,y) + \sum_{n=1}^{t_{\mathrm{LT}}} \frac{F_{\mathrm{C},n}(x,y)}{(1+r_{\mathrm{D}})^n} \tag{2-11}$$

where I is the investment, $F_{\mathrm{C},n}$ the annual cash flow for each period separately, t_{LT} the lifetime of the process or process subsystem and r_{D} the discount rate and inflation together.

2.2.5.2 Internal Rate of Return

IRR (Novak Pintarič and Kravanja, 2006) is the discount rate, at which the *NPV* of a project under consideration is zero (Eq. 2-12). When *NPV* is zero, the investment is exactly the same as the present value of those savings over the project's lifetime. The calculated *IRR* (Eq. 2- 12) presents the marginal discount rate when a project is still economically viable. If *IRR* is higher than the actual discount rate, the project will be profitable.

$$-I(x,y) + \sum_{n=1}^{t_{\mathrm{LT}}} \frac{F_{\mathrm{C},n}(x,y)}{(1+IRR)^n} = 0 \tag{2-12}$$

2.2.5.3 Discounted Payback

A discounted payback (*DPB*) (Accounting Explained, 2014) is a ratio between the cumulative discounted annual cash flow, and the initial investment. In contrast to the evaluation of a simple payback, the annual cash flows are discounted at first and after cumulated in order to consider the value of money. When applying *DPB* to the synthesis of HEN, the cumulative discounted annual cash flow is the cumulative discounted saving realised from the reduced utility consumption obtained when optimising the HEN with future rather than current utility prices. It is the time required to pay-off the investment by savings obtained by investment, accounting for the value of money. The *DPB* is determined from Eq. 2-13:

$$-I(x,y) + \sum_{n=1}^{\mathrm{DPB}} \frac{\Delta F_{\mathrm{C},n}(x,y)}{(1+r_D)^n} = 0 \tag{2-13}$$

2.2.5.4 Lifetime discounted return on investment

LTDROI is a financial ratio between the cumulative discounted annual cash flow, summed up throughout the entire lifetime, and the investment. The values indicate how many times the additional investment will be returned during the entire lifetime of the system or HEN. It is determined from Eq. 2-14:

$$\max LTDROI(x,y) = \sum_{n=1}^{t_{\mathrm{LT}}} \frac{\Delta F_{\mathrm{C},n}(x,y)}{(1+r_{\mathrm{D}})^n} \cdot \frac{1}{I(x,y)} \tag{2-14}$$

2.2.6 Risk assessment of additional investment in HEN

The utility prices can only be forecasted and consequently the uncertainties can be rather significant. A risk assessment should be performed in order to estimated whether or not a higher investment is reasonable due to probably higher utility prices. For this purpose the Certainty Equivalent (*CE*) criterion is applied. It is a small, zero-risk returned amount of money, that a decision maker may trade for a larger potential return with an associated risk. An Exponential Utility Function for the for the determination utility related scenario was applied. In the case of HEN synthesis the "profit" is presented as the incremental annual contribution $\Delta aNPV$ of a scenario at certain projection in a certain period, to the total ΔNPV. Specific case of HEN is defined as follows:

$$U_{n,v}^{exp}(\Delta aNPV_{n,v}) = 1 - e^{-\frac{\Delta aNPV_{n,v}}{\tau}} \tag{2-15}$$

where $\Delta aNPV_{n,v}$is the wealth or evaluation measure of the scenario v and τ is the risk tolerance. Then Expected Utility Value (EU) it evaluated as a sum of different scenarios' utilities, multiplied with their assigned probability:

$$EU = \sum_{n,v}\left(p_{n,v} \cdot U_{n,v}\left(\Delta aNPV_{n,v}\right)\right) \tag{2-16}$$

The relation between the CE and EU is the following:

$$CE = -\tau \cdot ln(1 - EU) \tag{2-17}$$

However, the exponential relation between utility function and caused numerical problems during the optimisation. Therefore, a linearised variation of the utility function has been proposed, where the exponential function is expressed as two linear functions:

$$U_{n,v}^{lin}(\Delta aNPV_{n,v}) = \begin{cases} U_{n,v}^{positive} = max\{0, k_1 \cdot \Delta aNPV_{n,v}\}, \Delta aNPV_{n,v} \geq 0 \\ U_{n,v}^{negative} = min\{0, k_2 \cdot \Delta aNPV_{n,v}\} = max\{0, -k_2 \cdot \Delta aNPV_{n,v}\}, \Delta aNPV_{n,v} < 0 \end{cases} \tag{2-18}$$

The slopes k_1 and k_2 of the linear functions for positive and negative $\Delta aNPV_{n,v}$ can be determined from the mean positive and mean negative $\Delta aNPV_{n,v}$ obtained in the specific case. As the slope of the negative function is steeper than the one of the positive function, the contribution of negative $\Delta aNPV_{n,v}$ affect the optimisation more than the contribution of positive $\Delta aNPV_{n,v}$. Therefore, the optimisation tends to identify HEN design with less $\Delta aNPV_{n,v}$. Both linear functions are merged into a single one. A smoothing approximation was applied in order to avoid discontinuity of the max operator:

$$max\{0, x\} = 0.5 \cdot \sqrt{x^2 + \varepsilon^2} + 0.5 \cdot x \tag{2-19}$$

where ε is a very small constant, e.g. 10^{-4}. Note that in the case when $x > 0$ both terms in the approximation are halved and positive and therefore the result is the positive x. If $x < 0$, the first term equals to the positive half of x, whilst the second term to the negative half of x, both resulting in zero (Figure 2.6). This smoothing function was applied to the sum of both linear functions:

$$\begin{aligned} &U_{n,v}^{lin}(\Delta aNPV_{n,v}) = max\{0, k_1 \cdot \Delta aNPV_{n,v}\} + max\{0, -k_2 \cdot \Delta aNPV_{n,v}\} = \\ &\left(0.5 \cdot \sqrt{k_1 \cdot \Delta aNPV_{n,v}{}^2 + k_1{}^2 \cdot \varepsilon^2} + 0.5 \cdot k_1 \cdot \Delta aNPV_{n,v}\right) + \\ &\left(0.5 \cdot \sqrt{\left(-k_2 \cdot \Delta aNPV_{n,v}\right)^2 + k_2{}^2 \cdot \varepsilon^2} - 0.5 \cdot k_2 \cdot \Delta aNPV_{n,v}\right) \end{aligned} \tag{2-20}$$

After rearrangement of Eq. 2-16, the linearised utility function of the following form was applied:

$$U_{n,v}^{lin}(\Delta aNPV_{n,v}) = 0.5\cdot(k_1 + k_2)\cdot\sqrt{\Delta aNPV_{n,v}{}^2 + \varepsilon^2} + 0.5\cdot(k_1 - k_2)\cdot\Delta aNPV_{n,v} \qquad (2\text{-}21)$$

All the functions $U_{n,v}^{exp}$, $U_{n,v}^{positive}$, $U_{n,v}^{negative}$, and $U_{n,v}^{lin}$ are presented in Fig. 2-6.

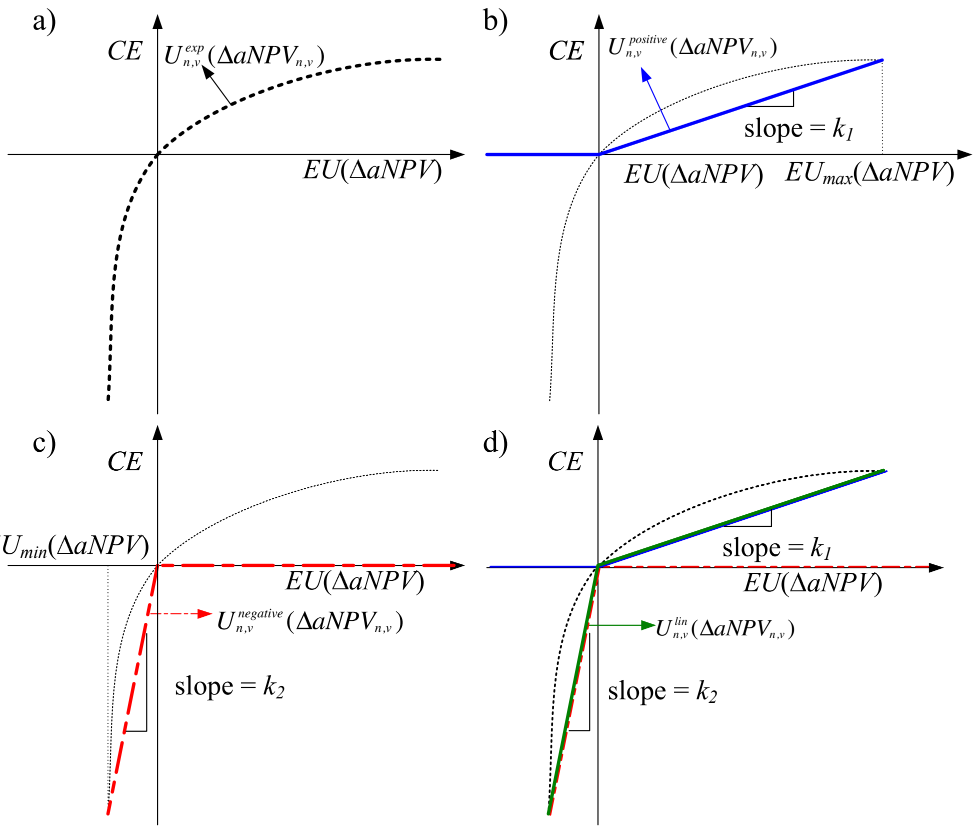

Figure 2-8: Linearisation of Utility Function: a) Exponential Utility function $U_{n,v}^{exp}$, b) Positive Linear Utility function $U_{n,v}^{positive}$, c) Negative Linear Utility function $U_{n,v}^{negative}$, and d) Linearised Utility function $U_{n,v}^{lin}$

The final form of equations is obtained by supplementing Eq. 2-21 to Eq. 2-11.

$$max\, EU(x,y) = \sum_{n,v}\left(p_{n,v}\cdot\left(0.5\cdot(k_1 + k_2)\cdot\sqrt{\left(\Delta aNPV_{n,v}\cdot(x,y)\right)^2 + \varepsilon^2} + 0.5\cdot(k_1 - k_2)\cdot\Delta aNPV_{n,v}\left(x,y\right)\right)\right) \qquad (2\text{-}22)$$

3 Heat exchange network synthesis on process level for entire lifetime

3.1 No extensions

The flowchart of the optimisation is presented in Figure 3-1. The optimisation process begins with the collection of the input data for the optimisation.

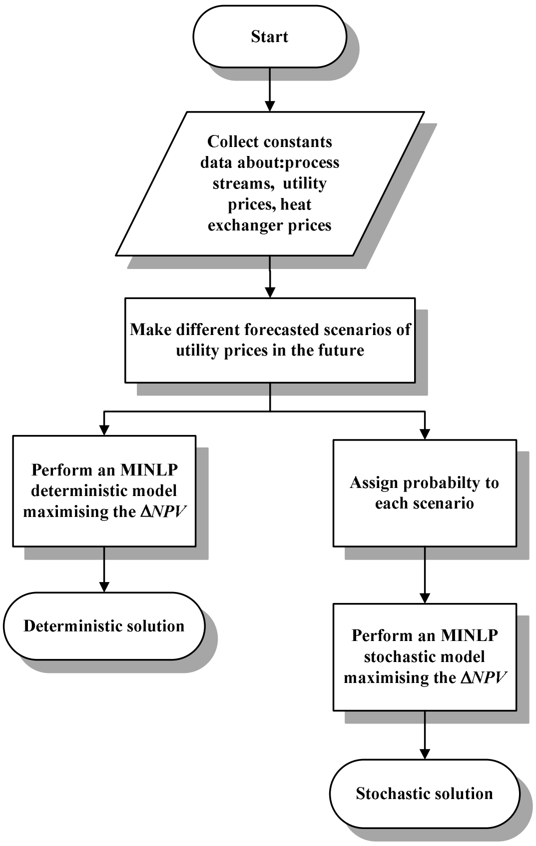

Figure 3-1: Flowchart of process optimisation

These data are related to the process stream input and output temperatures, heat capacity flow rates and different prices of utility and heat exchangers, and some coefficients on the variable cost of heat exchangers. In order to account for forecasted utility prices a projection of prices, based on the prices in the past, has to be performed. Different scenarios of the future price are projected, because of the uncertainty of the projections. After data on future utility price is obtained an optimisation of the HEN design is performed. There are two approaches considered in this work. One is the deterministic model, where the result is optimal, considering only one scenario of utility price in the future. To consider all scenarios, a stochastic model is developed. In this model each scenario has its own probability of realization.

3.1.1 Superstructure

The superstructure of the model developed by Yee and Grossmann (1990) was used. In a typical superstructure each hot stream can be potentially matched with each cold stream. The utilities are placed at the extreme ends of the process streams, as can be seen in Figure 3-2, where a two-stage superstructure is shown. An isothermal mixing of streams at the outlets of the matches is imposed within this superstructure.

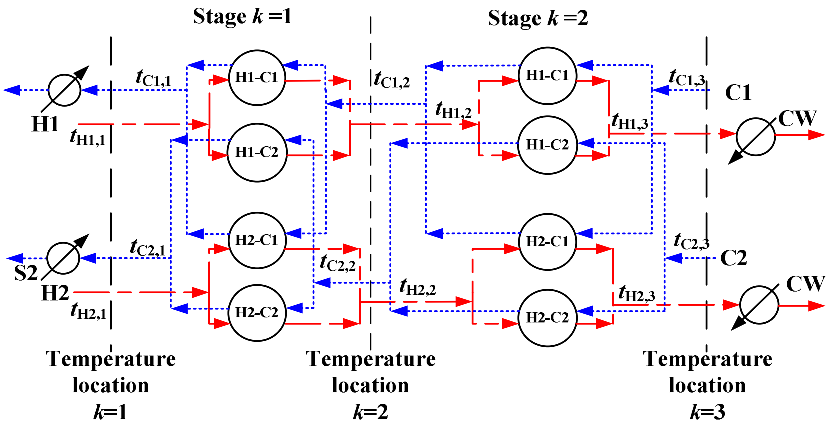

Figure 3-2: Two-stage superstructure (Yee and Grossmann, 1990)

3.1.2 Multi-period deterministic MINLP model formulation

A multi-period optimisation model was developed in order to account for this tendency regarding utility prices, where the coefficients for utility prices are growing through the periods, too. The stage-wise model by Yee and Grossmann (1990) has been extended to a multi-period model for considering different prices over different periods. The following indexes and sets are defined within this model and superstructure:

- Index i for hot streams, $i \in I$
- Index j for cold streams, $j \in J$
- Index k for temperature location within the superstructure, $k \in K$
- A new index n for the number of periods observed, $n \in N$

Note that N_S is the number of stages. The number of temperature location is one more than N_S as the stages present an interval and the temperature locations presents the boundaries of these stages.

A detailed description of the original single-period model is given elsewhere and only a more compact description of this multi-period model follows. Note that all the constraints and most of the variables in the model are now indexed by n since the model has to present every period $n \in N$. The description begins by calculating the duty for each stream in each period n, which is the summation of heat exchanged between process streams and utility consumption within the same period:

$$(T_{in,i}^{\mathrm{H}} - T_{out,i}^{\mathrm{H}}) \cdot CP_i = \sum_j \sum_k Q_{i,j,k,n} + Q_{i,n}^{\mathrm{CU}} \qquad \forall i \in I,\ n \in N \qquad (3\text{-}1)$$

$$(T_{out,j}^{\mathrm{C}} - T_{in,j}^{\mathrm{C}}) \cdot CP_j = \sum_i \sum_k Q_{i,j,k,n} + Q_{j,n}^{\mathrm{HU}} \qquad \forall j \in J,\ n \in N \qquad (3\text{-}2)$$

The heat exchanged between process streams within a stage in each period n is the temperature difference between two consecutive stage temperatures multiplied by the heat capacity flowrate (CP):

$$CP_i \cdot \left(TH_{i,k,n} - TH_{i,k+1,n}\right) = \sum_j Q_{i,j,k,n} \qquad \forall i \in I,\ k \in K,\ n \in N \qquad (3\text{-}3)$$

$$CP_j \cdot \left(TC_{j,k,n} - TC_{j,k+1,n}\right) = \sum_i Q_{i,j,k,n} \qquad \forall j \in J,\ k \in K,\ n \in N \qquad (3\text{-}4)$$

To calculate a cold utility duty of a hot process stream, the difference between the stream's last stage temperature and its outlet temperature is multiplied by its heat capacity flowrate:

$$CP_i \cdot \left(TH_{i,k=N_S+1,n} - T^{\mathrm{H}}_{out,i}\right) = Q^{\mathrm{CU}}_{i,n} \qquad \forall i \in I,\ n \in N \qquad (3\text{-}5)$$

and similarly to calculate the hot utility duty of a cold process stream, the difference between the stream's outlet temperature and its first stage temperature is multiplied by its heat capacity flowrate:

$$CP_j \cdot \left(T^{\mathrm{C}}_{out,j} - TC_{j,k=1,n}\right) = Q^{\mathrm{HU}}_{j,n} \qquad \forall j \in J,\ n \in N \qquad (3\text{-}6)$$

The first stage temperatures are equal to the input temperatures of the hot streams (Eq. 3-7) and the last stage temperature is determined by the input temperatures of the cold streams (Eq. 3-8):

$$T^{\mathrm{H}}_{in,i} = TH_{i,k=1,n} \qquad \forall i \in I,\ n \in N \qquad (3\text{-}7)$$

$$T^{\mathrm{C}}_{in,j} = TC_{j,k=N_S+1,n} \qquad \forall j \in J,\ n \in N \qquad (3\text{-}8)$$

The temperatures over the consecutive stages should have a monotonically decreasing tendency:

$$TH_{i,k,n} \geq TH_{i,k+1,n} \qquad \forall i \in I,\ k \in K,\ n \in N \qquad (3\text{-}9)$$

$$TC_{j,k,n} \geq TC_{j,k+1,n} \qquad \forall j \in J,\ k \in K,\ n \in N \qquad (3\text{-}10)$$

The last stage temperature $\forall i \in I$ is greater than or equal to the outlet temperature of the hot stream:

$$TH_{i,k=N_S+1,n} \geq T^{\mathrm{H}}_{out,i} \qquad \forall i \in I,\ n \in N \qquad (3\text{-}11)$$

The first stage temperature $\forall j \in J$ is less than or equal to the outlet temperature of the cold stream:

$$T^{\mathrm{C}}_{out,j} \geq TC_{j,k=1,n} \qquad \forall j \in J,\ k \in K \qquad (3\text{-}12)$$

Logical constraints and binary variables are used when selecting the stream match at stage *k*:

$$Q_{i,j,k,n} - min(Ech_i, Ecc_j) \cdot y_{i,j,k} \leq 0 \qquad \forall i \in I, j \in J,\ k \in K,\ n \in N \qquad (3\text{-}13)$$

$$Q^{\mathrm{CU}}_{i,n} - Ech_i \cdot y_i \leq 0 \qquad \forall i \in I,\ n \in N \qquad (3\text{-}14)$$

$$Q^{\mathrm{HU}}_{j,n} - Ecc_j \cdot y_j \leq 0 \qquad \forall j \in J,\ n \in N \qquad (3\text{-}15)$$

The binary variables in the following equations are used to activate or deactivate the constraints for the approaching temperatures, in order to ensure feasible driving forces for the heat exchange:

$$\Delta T_{i,j,k,n} \leq TH_{i,k,n} - TC_{j,k,n} + \gamma_{i,j} \cdot (1 - y_{i,j,k}) \qquad \forall i \in I, j \in J, k \in K, n \in N \qquad (3\text{-}16)$$

$$\Delta T_{i,j,k+1,n} \leq TH_{i,k+1,n} - TC_{j,k+1,n} + \gamma_{i,j} \cdot (1 - y_{i,j,k}) \qquad \forall i \in I, j \in J, k \in K, n \in N \qquad (3\text{-}17)$$

The approach temperatures between the process streams and utilities are always positive:

$$\Delta T_{i,n}^{\mathrm{CU}} \leq T_{i,k=N_\mathrm{S}+1,n} - T_{\mathrm{out}}^{\mathrm{CU}} \qquad \forall i \in I, n \in N \qquad (3\text{-}18)$$

$$\Delta T_{j,n}^{\mathrm{HU}} \leq T_{\mathrm{out}}^{\mathrm{HU}} - T_{j,k=1,n} \qquad \forall j \in J, n \in N \qquad (3\text{-}19)$$

The temperature differences and heat loads can vary during different periods and, consequently, the optimal heat exchange area (A) can be different in each period. However, once the HEN is built, the structure of the HEN and the areas of the heat exchangers are constant over its entire lifetime. For each heat exchanger unit, a maximal area to be minimised in the objective function is selected from all those possible when using the following inequalities:

$$A_{ij}^{\mathrm{HE}} \geq \frac{Q_{i,j,k,n}}{U_{i,j} \cdot (\Delta T_{i,j,k,n} \cdot \Delta T_{i,j,k+1,n} \cdot (\frac{\Delta T_{i,j,k,n} + \Delta T_{i,j,k+1,n}}{2}))^{0.333}} \qquad \forall i \in I, j \in J, n \in N \qquad (3\text{-}20)$$

$$A_{i}^{\mathrm{CU}} \geq \frac{Q_{i,n}^{\mathrm{CU}}}{U_{i}^{\mathrm{CU}} \cdot ((T_{\mathrm{out},j}^{\mathrm{H}} - T_{\mathrm{in}}^{\mathrm{CU}}) \cdot \Delta T_{i,n}^{\mathrm{CU}} \cdot (\frac{T_{\mathrm{out},j}^{\mathrm{H}} - T_{\mathrm{in}}^{\mathrm{CU}} + \Delta T_{i,n}^{\mathrm{CU}}}{2}))^{0.333}} \qquad \forall i \in I, n \in N \qquad (3\text{-}21)$$

$$A_{j}^{\mathrm{HU}} \geq \frac{Q_{j}^{\mathrm{HU}}}{U_{j}^{\mathrm{HU}} ((T_{\mathrm{in}}^{\mathrm{HU}} - T_{\mathrm{out},j}^{\mathrm{C}}) \cdot \Delta T_{j,n}^{\mathrm{HU}} \cdot (\frac{T_{\mathrm{in}}^{\mathrm{HU}} - T_{\mathrm{out},j}^{\mathrm{C}} + \Delta T_{j,n}^{\mathrm{HU}}}{2}))^{0.333}} \qquad \forall j \in J, n \in N \qquad (3\text{-}22)$$

Note that Chen's approximation (Chen, 1987) was used for logarithmic mean differences in order to overcome the numerical problems of the logarithmic differences when the approach temperatures on both sides of the exchanger are equal. The objective is to maximise the ΔNPV between the model, which accounts for the projected prices and the model, which has fixed cost for utilities:

$$\Delta NPV = -I + \sum_{n} \frac{F_{\mathrm{C},n}}{(1 + r_\mathrm{D})^n} - NPV^{\mathrm{REF}} \qquad (3\text{-}23)$$

where NPV^{REF} is the NPV of the optimised model with a fixed current cost for utilities. The $F_{\mathrm{C},n}$ is the annual cash flow after taxes, r_T:

$$F_{\mathrm{C},n} = \left((1 - r_\mathrm{T}) \left(0 - \left(c_n^{\mathrm{OP}} \right) \right) + r_\mathrm{T} \frac{I}{t_{\mathrm{LT}}} \right) \qquad \forall n \in N \qquad (3\text{-}24)$$

where the annual utility cost with varying prices is calculated for every period during the lifetime as:

$$c_n^{\mathrm{OP}} = \sum_j t_{\mathrm{OP}} \cdot Q_{j,n}^{\mathrm{HU}} \cdot c_n^{\mathrm{HU}} + \sum_i t_{\mathrm{OP}} \cdot Q_{i,n}^{\mathrm{CU}} \cdot c_n^{\mathrm{CU}} \qquad \forall n \in N \qquad (3\text{-}25)$$

and the last term in Eq. 3-24 is a straight-line depreciation allowance.

The investment I is further calculated as a sum of the fixed and variable charges:

$$I = \sum_i \sum_j \sum_k cf \cdot y_{i,j,k} + \sum_i cf^{\mathrm{CU}} \cdot y_i^{\mathrm{CU}} + \sum_j cf^{\mathrm{HU}} \cdot y_j^{\mathrm{HU}} + cv \cdot A_{ij}^{\mathrm{HE}} + cv^{\mathrm{CU}} \cdot A_i^{\mathrm{CU}} + cv^{\mathrm{HU}} \cdot A_j^{\mathrm{HU}} \qquad (3\text{-}26)$$

Note that in the presented model, the investment coefficients for heat exchangers are held constant throughout the whole lifetime of the process because the investment is assumed as being paid in its entirety, when the HEN is built.

3.1.3 Multi-period stochastic MINLP model formulation

The multi-period deterministic model can be a powerful tool for evaluating the different scenarios available. However, one design has to be chosen for building the HEN. A one-stage multi-period stochastic MINLP model was used to account for, as much as possible, the probabilities of future price variations, p. The model is similar to the deterministic multi-period model. Its modifications are the following:

Additional index v, $v \in V$, for different future price projection scenarios is included in the model. The variables that are now also indexed to v are:

$$Q_{i,j,k,n,v},\ Q_{j,n,v}^{\mathrm{HU}},\ Q_{i,n,v}^{\mathrm{CU}},\ \Delta_{\ln} T_{i,j,k,n,v}, \Delta_{\ln} T_{j,n,v}^{\mathrm{HU}},\ \Delta_{\ln} T_{i,n,v}^{\mathrm{CU}}$$

and Equations from Eq. 3-1 to Eq. 3-19 are indexed by v, too.

The objective function is multiplied by the probability - p_v of the scenarios $v \in V$

$$\Delta NPV = \sum_v p_v \cdot \left[\left(\left((1 - r_{\mathrm{T}}) \left(0 - \sum_n \frac{c_{v,n}^{\mathrm{op}}}{(1 + r_D)^n} \right) + r_{\mathrm{T}} \cdot \frac{(1 + r_D)^{t_{LT}} - 1}{r_D \cdot (1 + r_D)^{t_{LT}}} \frac{I}{t_{\mathrm{LT}}} \right) - I \right) - NPV_v^{\mathrm{REF}} \right] \qquad (3\text{-}27)$$

where I is calculated from Eq. 3-26 and c^{OP} is modified by Eq. 3-28:

$$c_{v,n}^{\mathrm{OP}} = \sum_j t_{\mathrm{OP}} \cdot Q_{j,n,v}^{\mathrm{HU}} \cdot c_{n,v}^{\mathrm{HU}} + \sum_i t_{\mathrm{OP}} \cdot Q_{i,n,v}^{\mathrm{CU}} \cdot c_{n,v}^{\mathrm{CU}} \qquad \forall n \in N,\ v \in V \qquad (3\text{-}28)$$

3.1.4 Case study 1

The input data for the process streams and utilities are shown in Table 3-1. For the heat exchanger between two process stream the fixed charge coefficient was cf =46.0 k€ and a variable coefficient cv =2.742 k€/m^2; while for the heat exchanger between cold or hot utilities and process stream the fixed-charge coefficients were cf^{HU}, cf^{CU} = 121.4 k€ and the variable coefficients cv^{CU}, cv^{HU} = 0.193 k€/m^2. Note that the exponent for the variable charge of investment was 1. The number of operating hours was t_{OP} = 8,500 h/y. The forecasted prices of utilities were based on the price fluctuation from January 2001 to December 2010. Based on these prices the hot and cold utility yearly prices for five scenarios were determined.

Different optimal HEN designs with maximal incremental net present value obtained were compared with each other.

Table 3-1: Input data for HEN design with no extension

Streams	T_{in} / °C	T_{out}/°C	CP/kW °C^{-1}	h/kW m^{-2} °C^{-1}
Hot 1	376.85	96.85	10	1
Hot 2	316.85	96.85	20	1
Cold 1	136.85	376.85	15	1
Cold 2	76.85	226.85	13	1
Hot oil	406.85	376.85	-	5
Cooling water	26.85	46.85	-	1

The HEN design obtained with current utility prices was used as reference one. Table 2 shows its NPVs when the design, optimised with fixed prices of utility, underwent different future price scenarios for lifetimes 5 and 15 y. To determine *NPV* for a reference design, a deterministic multi-period model was used. The objective function was the maximisation of the *NPV*, where fixed current prices of utilities were considered.

Table 3-2: HEN designs at different lifetimes with current fixed prices of utility and its reference *NPV*s at different future price scenarios in Case Study

Lifetime /y	*I / k€*	*Obj. func. / k€*	NPV_1^{REF} */k€ Scenario 1*	NPV_2^{REF} */k€ Scenario 2*	NPV_3^{REF} */k€ Scenario 3*	NPV_4^{REF} */k€ Scenario 4*	NPV_5^{REF} */k€ Scenario 5*
5	1,654.58	-4,189.92	-4,046.12	-4,213.52	-4,617.418	-5,485.21	-5,795.30
15	1,929.92	-7,574.03	-9,076.066	-9,636.569	-11,104.23	-14,806.29	-15,977.38

3.1.4.1 Influence of lifetime

As the model's objective function was the maximisation of the *ΔNPV*, the lifetime of the HEN had a great effect on the optimisation. Figure 3-3 shows the comparison between the different lifetimes of the HEN (1, 5, 10 and 15 y).

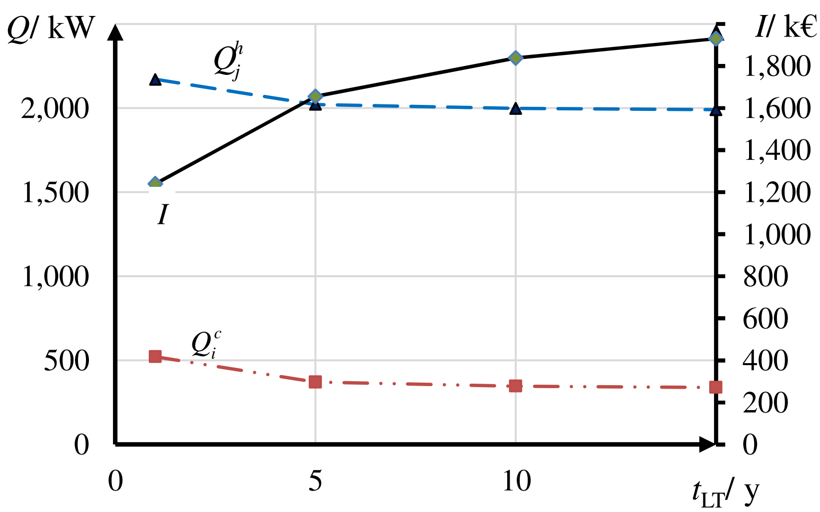

Figure 3-3: Investment and utility loads vs. lifetime of HEN

For this comparison, current utility costs were fixed throughout the entire lifetime and a single-period model was applied. As can be seen in Figure 3-3, when the lifetime increased, the investment of HEN increased too, whilst the loads of utilities (Q_j^h and Q_i^c) decreased. Within the lifetime, the cumulative utility cost increases and the trade-offs between operating cost and investment moved towards smaller utility loads and larger investment. Larger investment stands for a larger heat exchanger, which means that a higher amount of heat can be recovered. As a consequence of better heat integration, the utility consumption reduced.

Table 3-3: Areas of heat exchangers optimised with fixed current prices of utility for different lifetimes

Heat exchanger match hot/cold stream	$t_{LT} = 1\ y$	$t_{LT} = 5\ y$	$t_{LT} = 10\ y$	$t_{LT} = 15\ y$
A_{11}^{HE} /m^2	64.034	131.377	157.204	169.874
A_{12}^{HE} /m^2	69.382	66.015	64.221	63.544
A_{21}^{HE} /m^2	130.937	218.803	261.442	283.254
TOTAL A_{ij}^{HE} /m^2	264.353	416.195	482.867	516.672
A_{1}^{CU} /m^2	4.891	5.575	5.960	6.108
A_{2}^{CU} /m^2	38.171	36.003	35.504	35.320
TOTAL A_{i}^{CU} /m^2	43.062	41.578	41.464	41.428
TOTAL A_{1}^{HU} /m^2	19.350	16.328	15.782	15.587

The Table 3-3 presents the areas of the heat exchangers optimised for different HEN lifetime. As can be seen, the heat exchanger areas for the process heat recovery are increasing with the longer lifetime of HEN. In contrary, the areas of coolers and heaters are decreasing with the increased lifetime.

3.1.4.2 Deterministic multi-period model results

A deterministic multi-period model was used to account for utility price variation. It determined the optimal HEN designs $\mathrm{D}_{\mathrm{f2}}^{\mathrm{HEN}}$ - $\mathrm{D}_{\mathrm{f4.8}}^{\mathrm{HEN}}$ (see Figure 3-4) depending on the considered scenario of future price projections, where the utility price increase factors *f*2 - *f*4.8 (see Figure 3-4) are also determined. The number at *f* is the ratio between the price of the utility at the end of the lifetime and its current price. The designs were optimised at certain future price projection. However, the future prices can be different than the projection considered during the optimisation. For this reason, each obtained design was analysed at each considered possible future price projection and its performance determined by a comparison with the solution for fixed current prices (Table 3-2). The corresponding *ΔNPV*, *ΔIRR, DPB, LTDROI* and incremental investment (*ΔI*) were obtained.

Figure 3-4 shows the curves of *ΔNPV* versus *ΔI* obtained for different HEN designs ($\mathrm{D}_{\mathrm{f2}}^{\mathrm{HEN}}$ to $\mathrm{D}_{\mathrm{f4.8}}^{\mathrm{HEN}}$) at various future price realizations (e.g. *f*2 to *f*4.8). The *NPV* is the subtraction of the initial investment from the present value of the future cash flows. In the case study work the *ΔNPV* is an economic criterion, which analyses, if the additional investment, obtained by optimisation at different scenarios of future price, is economically viable. As can be seen, the

ΔNPV was positive at each considered future prices realisation for the D_{f2}^{HEN}, $D_{f2.5}^{HEN}$ and $D_{f2.8}^{HEN}$ designs. All these designs were economically viable as the additional investment is paid-off by savings on the utility costs.

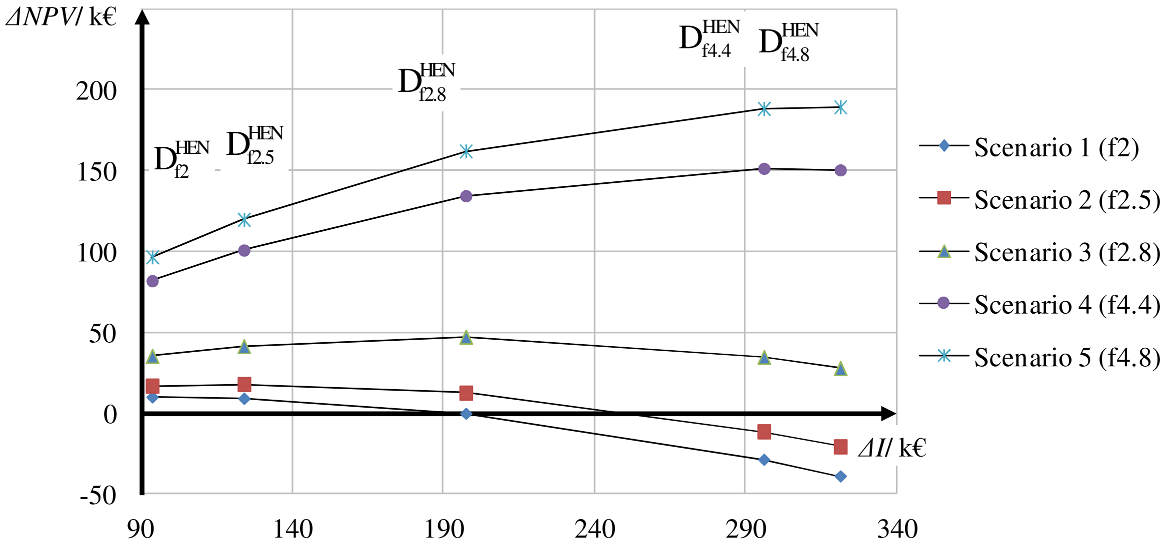

Figure 3-4: Incremental net present value vs. incremental investment (t_{LT}=15)

The most reliable solution with the highest *ΔNPV* would be the one where the curve at the lowest future price realization (f2) crosses the X axis, since it would satisfy economic viability at any future price accomplishment. In this case it was the HEN design close to $D_{f2.8}^{HEN}$ where *ΔI* was about 195 k€ (Figure 3-4) for which *ΔNPV*s was the highest for Scenario 3.

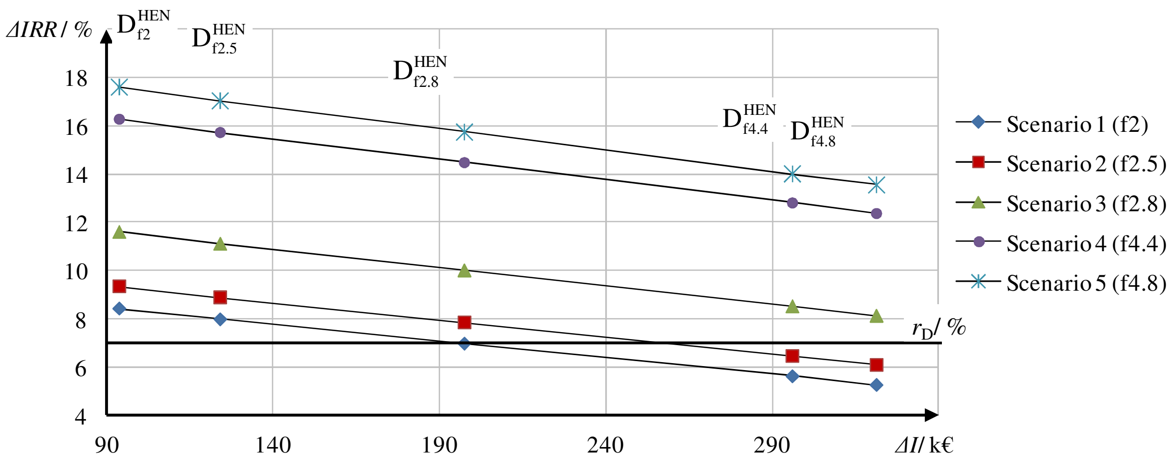

Figure 3-5: Incremental internal rate of return vs. incremental investment (t_{LT}=15)

A different economic criterion is the *ΔIRR*. In this case study it presents the marginal discount rate and inflation (r_D) together, at which the additional investment is paid-off and there is no profit. However, the *ΔIRR* should be higher than r_D as this is the expected rate, and if the *ΔIRR* is lower the investment would not be paid off. Similar results were obtained when the

ΔIRRs were determined. It is the marginal discount rate, which should be greater or equal to 7%, in this case the sum of the discount rate and inflation - the horizontal line in Figure 3-5, in order that the design can be economically viable. Figure 3-5 presents the *ΔIRR* versus incremental investment for 15 y of HEN lifetime.

For a 15 y lifetime of HEN, the *ΔIRRs* of the two designs ($D_{f4.8}^{HEN}$, and $D_{f4.4}^{HEN}$ in Figure 3-5) were unacceptable, as in Scenarios 1 and 2 they were less than the sum of the discount rate and inflation. For the other three designs (D_{f2}^{HEN}, $D_{f2.5}^{HEN}$ and $D_{f2.8}^{HEN}$), the *ΔIRR* was acceptable for each projection of utility below an *ΔI* of about 195 k€. Although Figure 3-5 indicates that the highest *ΔIRRs* were realised at the smallest *ΔIs*, the corresponding *ΔNPV*s were, however, the smallest (Figure 3-4). The most reliable design with the highest *ΔNPV* was the one with the lowest allowable *ΔIRR*, which was again the one located at *ΔI* where the *ΔIRRs* for all the scenarios were greater than or equal to the sum of the discount rate and inflation. In our case it was a design close to the $D_{f2.8}$ design at an *ΔI* of about 195 k€.

A further economic analysis can determine the lifetime discounted return on investment (*LTDROI*). This is an economic criterion, which indicates how many times the incremental investment will be returned throughout the entire lifetime, when considering the time value of money. At *LTDROI*=1 the additional investment was precisely equal to the discounted cumulative annual cash flow (horizontal line in Figure 3-6).

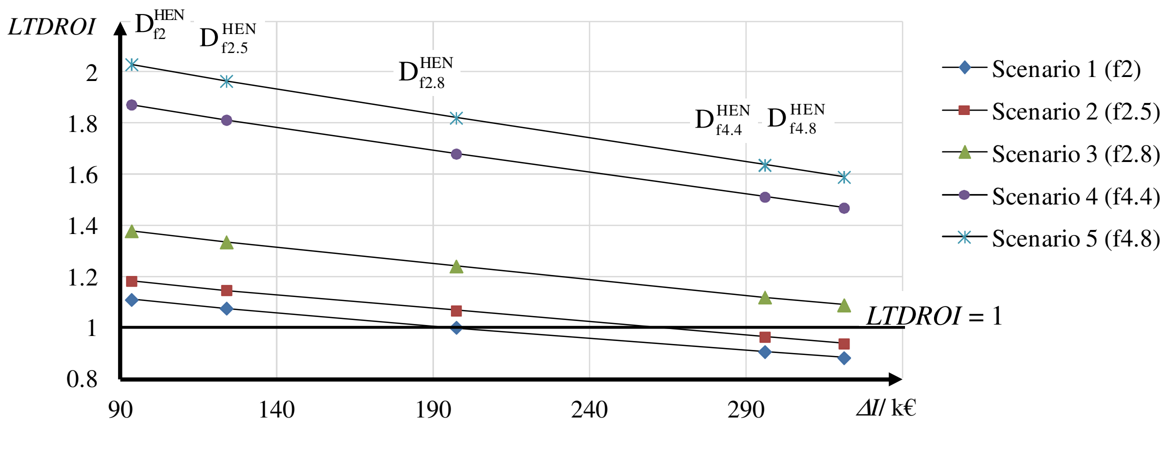

Figure 3-6: Lifetime discounted return on investment vs. incremental investment (t_{LT}=15)

As can be seen in Figure 3-6, when increasing the investment, *LTDROI* decreased. If the ratio *LTDROI* was less than 1, the savings were less than the additional investment and the design was not economically viable. When t_{LT} =15 y the designs D_{f2}^{HEN}, $D_{f2.5}^{HEN}$ and $D_{f2.8}^{HEN}$ had *LTDROI*s higher than 1 for each price projection. All these designs can be economically viable solutions. Similarly, as was the case with *ΔIRR*, higher *LTDROI*s were obtained at smaller *ΔNPV*s, and vice versa. Thus, the most reliable design with the highest *ΔNPV* was the one at the smallest allowable *LTDROI*=1. It was the one close to the $D_{f2.8}$ design at an *ΔI* of about 195 k€.

The alternative criterion for justifying additional investment is the discounted payback. It is the time required to return the investment, also accounting for the value of money. It should be less than or equal to the lifetime of HEN in order to obtain an economically viable solution (horizontal line at 15 y in Figure 3-7).

For the 15 y lifetime, the three designs D_{f2}^{HEN}, $D_{f2.5}^{HEN}$ and $D_{f2.8}^{HEN}$ had less than 15 years of *DPB*. It corresponded to the other presented criteria. The other two designs $D_{f4.4}^{HEN}$ and $D_{f4.8}^{HEN}$ were not economically viable as the *DPB* at Scenarios 1 and 2 was longer than the lifetime of HEN (Figure 3-7). The most reliable design with the highest *ΔNPV*, again close to the $D_{f2.8}$ design at an *ΔI* of about 195 k€, was the one at the highest *DPB*=15.

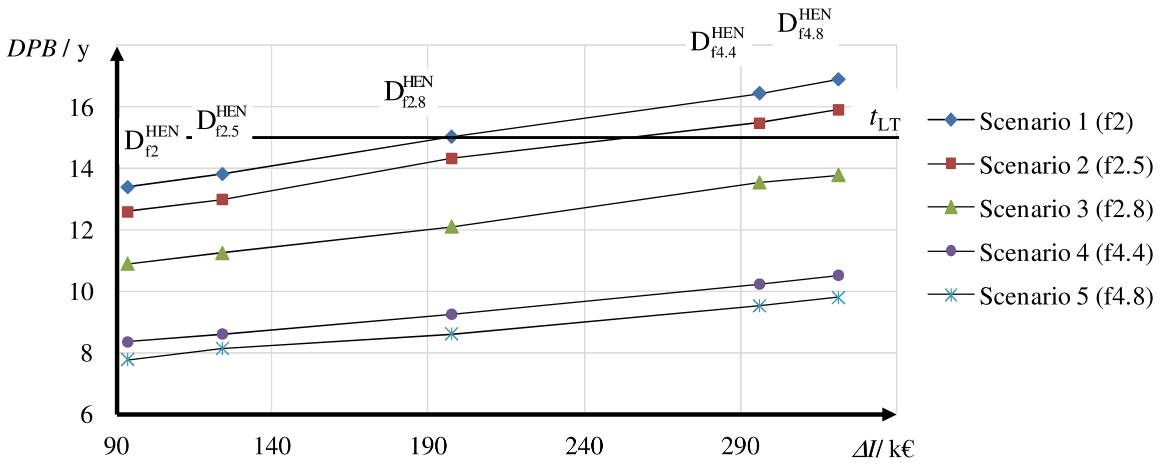

Figure 3-7: Discounted payback time vs. incremental investment (t_{LT}=15 y)

As presented, the lifetime of the HEN also had a great effect on the economic viability of the incremental investment. When the designs were optimised for a 5 y lifetime, the solutions obtained were very different from those at a 15 y lifetime. As can be seen in Figure 3-8, none of the designs optimised had positive *ΔNPV*s for all future price scenarios.

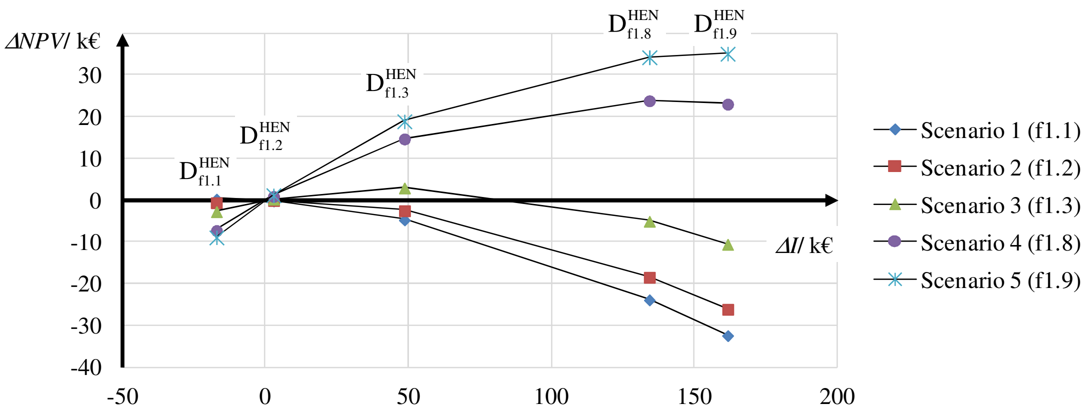

Figure 3-8: Incremental net present values vs. incremental investment (t_{LT} = 5y)

For Case Study 1 the obtained result suggests that the additional investment for a 5 y of lifetime is not economically viable, as the additional investment may not be paid-off during this lifetime. Also, the additional investments were significantly lower compared to those obtained at an optimisation for 15 y (Figures 3-4 and 3-8). For the longer lifetime there were three designs, which were economically viable. Design $D_{f2.8}$ had the highest *ΔNPV* for Scenarios 3, 4 and 5 compared to the other two viable designs (D_{f2}, $D_{f2.5}$), and it had the lowest *ΔIRR* and *LTDROI*, and the highest *DPB*.

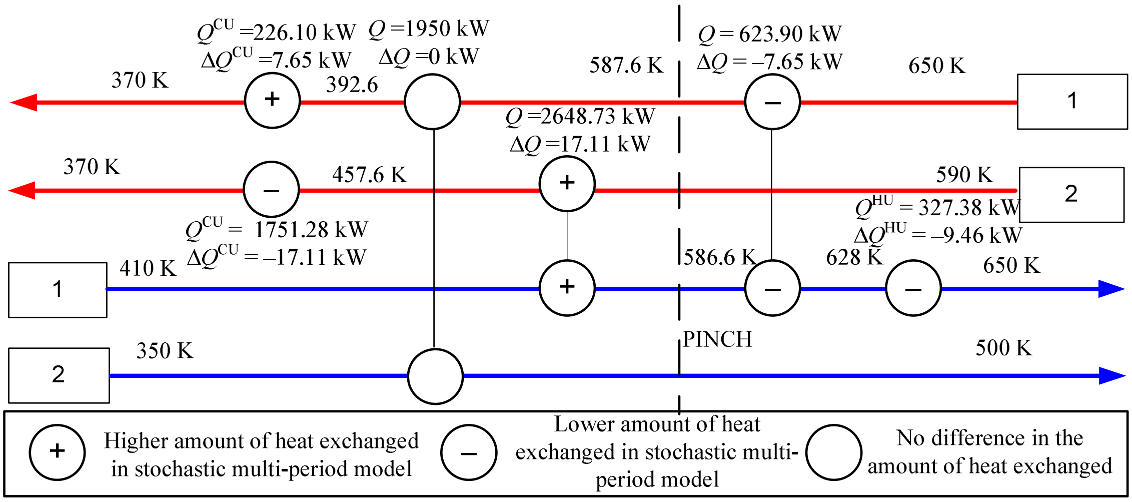

Figure 3-9: Comparison of the multi-period deterministic model at Scenario 3 and the model developed by (Yee & Grossmann, 1990) for Case Study 1 for 15 y lifetime

To evaluate the improvement that can be gained by the use of the proposed multi-period model considering future utility prices and maximizing *NPV*, a comparison of the result obtained by Yee and Grossmann model and the results of the multi-period deterministic model, for Scenario 3 with 15 y lifetime, was performed. The results obtained by the novel model are better compared to the model developed by Yee and Grossmann as the *NPV* increased by ΔNPV of 29 k€ from –-11,086 k€ to –11,057 k€ (0.26 % of improvement). The *NPV* increased because the utility consumption decreased for both hot and cold utility by 9.5 kW. In the case of hot utility it means a decrease from 336.5 to 327 (2.8 %) and in the case of cold utility from 1986.8 to 1977.3 (0.5 %). The decrease of the utility consumption was achieved by better process heat integration in larger heat exchangers, which increased the investment by ΔI of 159 k€ from 1,968 k€ to 2,127 k€ (8%). The comparison of both HEN designs is shown in Figure 3-9.

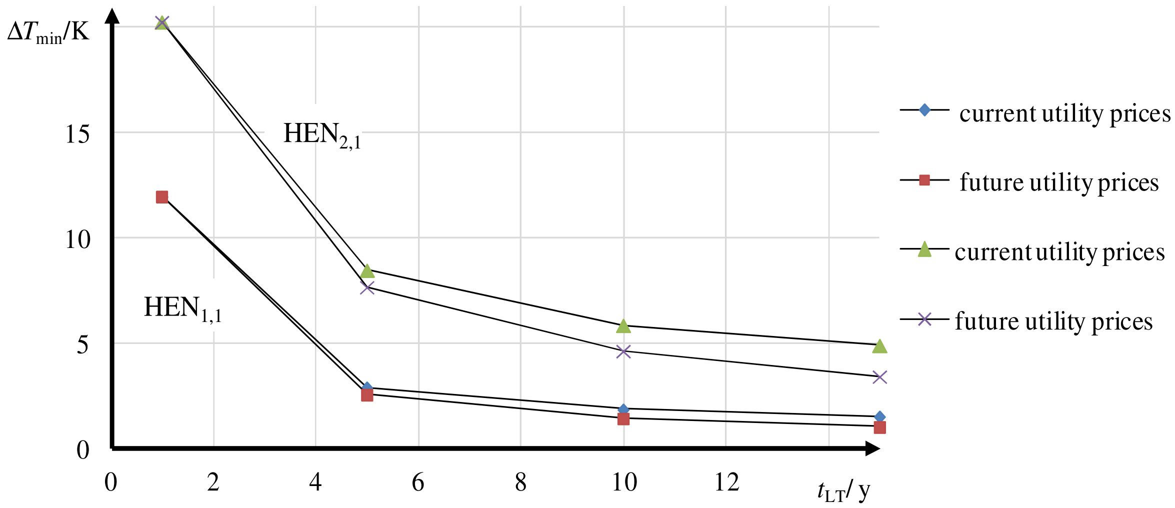

Figure 3-10: The relation between ΔT_{min} and the lifetime and considering current and future utility prices of the process for Case study 1

It is interesting also to show the relation between the lifetime and ΔT_{min} of heat exchangers located at the pinch point (HEN$_{1,1}$, HEN$_{2,1}$). As expected, the ΔT_{min} decreases with the lifetime (Figure 3-10) and heat recovery improves, enabling a larger investment to become economically viable. Note that when future utility prices are considered rather than the current ones, some savings from additional heat recovery is obtained by the further decrease of $\Delta T_{\min}$.

3.1.4.3 Multi-period stochastic results

The multi-period stochastic model was applied, in order to consider all future price scenarios simultaneously. The comparison was done similarly to the deterministic model, to the design optimised by the fixed current prices of utilities. The expected *ΔNPV*s at different scenarios are presented in Table 3-4.

Table 3-4: Expected *ΔNPV*s and *ΔNPV*s from different scenarios of HEN designs optimised with multi-period stochastic approach for Case Study 1

HEN Design	*Expected ΔNPV*	*ΔNPV /k€ Scenario 1 p=0.07*	*ΔNPV/k€ Scenario 2 p=0.24*	*ΔNPV/k€ Scenario 3 p=0.38*	*ΔNPV/k€ Scenario 4 p=0.24*	*ΔNPV/k€ Scenario 5 p=0.07*
t_{LT} =5 y	5.114	-7.3058	-4.431	2.688	18.054	23.581
t_{LT} =15 y	65.43	-5.682	8.532	46.434	142.379	172.903

For both lifetimes the expected *ΔNPV*s were positive. Only for t_{LT}= 5 y in Scenario 1, where the increase of utility price is the lowest and Scenario 2, with a bit higher increase of prices, the additional investment is not economically viable. With the increase of lifetime to t_{LT}= 15 y also in Scenario 2 the additional investment is justified.

The difference between designs of deterministic multi-period model, Scenario 3, and stochastic multi-period model was low. The *NPV* for a 15 y of lifetime decreased by –0.75 k€ for a stochastic model. The investment was increased by 26.26 k€. The hot and cold utility savings was – 1.24 kW.

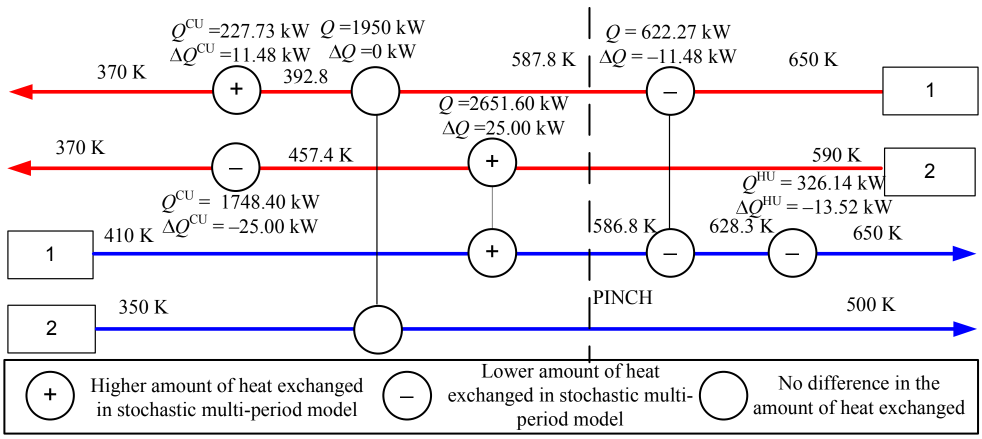

Figure 3-11: Comparison of HEN designs and heat loads results obtained by the multi-period deterministic model with fixed current utility prices and the multi-period stochastic model with future utility prices for Case study 1 for 15 y lifetime

In order to evaluate the influence of the forecasted utility prices, the comparison between the solution of stochastic multi-period model with future prices and the solution of multi-period model with fixed current utility prices was performed. The *NPV* at the most probable

Scenario 3 was increased by 46 k€ from -7,574 k€ to -7,528 k€ (6 %), and investment by 224 k€ from 1,930 to 2,154 k€ (11.6 %). This additional investment reduced the consumption of hot and cold utilities by 13.5 kW, from 339.5kW to 326 kW (4 %) for hot and from 1,989.5 to 1,976 (0.7 %) for cold one (Figure 3-11).

3.1.5 Case study 2

Case Study 2 consisted of 3 hot and 4 cold process streams. The data for process stream and external utilities included in the case study is presented in Table 3-5.

Table 3-5: Input data for HEN design in Case study 2

Streams	T_{in} /°C	T_{out} /°C	CP /kW °C^{-1}	h /kW m^{-2} °C^{-1}
Hot 1	352.85	312.85	9.802	1.25
Hot 2	346.85	245.85	2.931	0.05
Hot 3	254.85	79.85	6.161	3.20
Cold 1	225.85	339.85	7.179	0.65
Cold 2	15.85	302.85	0.641	0.25
Cold 3	52.85	112.85	7.627	0.33
Cold 4	39.85	292.85	1.69	3.20
Hot oil	406.85	376.85	-	3.5
Cooling water	26.85	46.85	-	3.5

The fixed-charge coefficients and variable coefficients for heat exchangers, heaters and coolers, the exponent for the variable charge of investment, and the number of annual operating hours were the same as in the previous case study.

Firstly, the reference HEN designs were obtained for the lifetimes of 5 and 15 y, and their reference *NPV*s were calculated for different future price scenarios (Table 3-6). Then, the results from the multi-period deterministic approach were compared with these reference *NPV*s.

Table 3-6: HEN designs at different lifetimes with current fixed prices of utilities and its reference NPVs at different future price scenarios in Case Study 2

Lifetime /y	*I / k€*	*Obj. func. / k€*	NPV_1^{REF} */k€ Scenario 1*	NPV_2^{REF} */k€ Scenario 2*	NPV_3^{REF} */k€ Scenario 3*	NPV_4^{REF} */k€ Scenario 4*	NPV_5^{REF} */k€ Scenario 5*
5 y	1,251.300	-2,050.66	-2,000.71	-2,059.12	-2,203.76	-2,516.17	-2,628.69
15 y	1,682.887	-3,118.54	-3,540.97	-3,694.15	-4,103.78	-5,141.27	-5,471.62

3.1.5.1 Multi-period deterministic results

Only *ΔNPV* and *ΔIRR* are shown for Case Study 2. In Figure 3-12 it can be seen that the *ΔNPV*s for lifetime 15 y were positive for all designs D_{f2}^{HEN} - $D_{f4.8}^{HEN}$, and all scenarios. Note that *ΔNPV* increased until design $D_{f4.4}^{HEN}$ and that further incremental investment would decrease the ΔNPV. Based on this observation the best solution would be around design $D_{f4.4}^{HEN}$ (Figure 3-12).

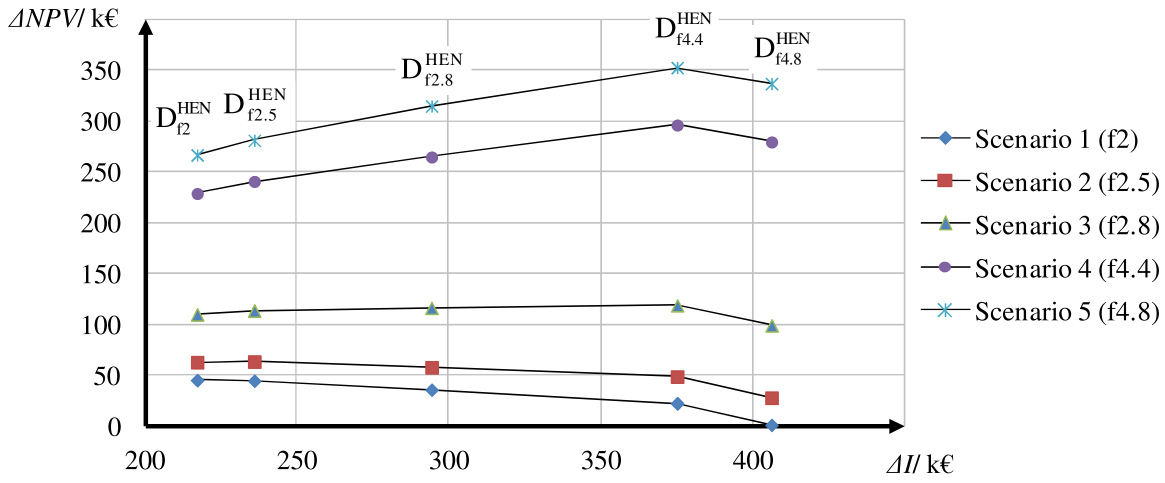

Figure 3-12: Incremental net present value vs. incremental investment (t_{LT} = 15 y)

The ΔIRR was the highest at design D_{f2}^{HEN} whereas ΔI was the smallest (Figure 3-13). However, every design was economically viable, as their ΔIRRs were acceptable for all scenarios, even for Scenario 1.

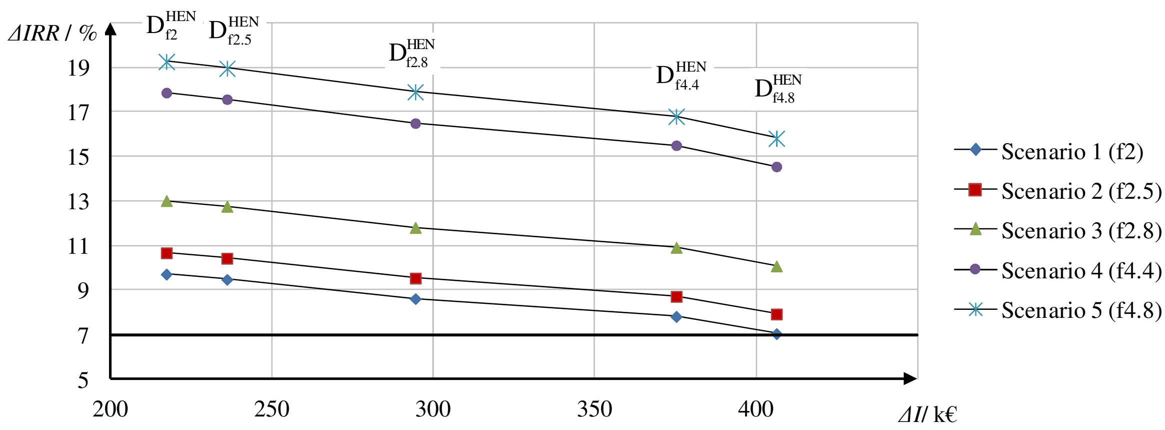

Figure 3-13: Incremental internal rate of return vs. incremental investment (t_{LT} = 15 y)

When the 5 year lifetime of HEN was considered, none of the design could be economically justified because none of the designs had positive ΔNPVs at all scenarios (Figure 3-14).When the design of the multi-period deterministic approach is compared to the one of the model by Yee and Grossmann (1990) for the utility prices following Scenario 3 and 15 y lifetime, there is a difference even in a number of heat exchangers. Additional heat exchangers between the hot stream 2 and cold stream 2 and between hot stream 3 and cold stream 4 are presented in the design of the novel model. Two other heat exchangers between hot stream 1 and cold stream 2 and hot stream 1 and cold stream 4 are moved to different temperature level, and the splitting of hot stream 1 is different. The investment was increased by ΔI of 235 k€ from 1,742 to 1,977 k€ (13.5 %) and the consumptions of hot and cold utilities were reduced from

163 to 133kW (18.4 %) and from 92 kW to 62 kW (32.6 %) yielding *ΔNPV* of 338 k€ from –4,325 to –3,987 k€ (7.8 %). The comparison of both designs is shown in Figure 3-15.

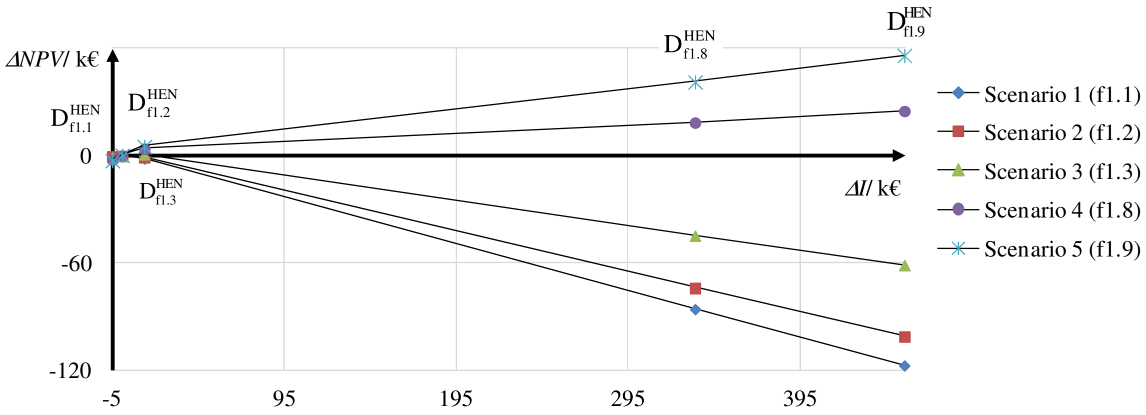

Figure 3-14: Incremental net present value (t_{LT} = 5 y) vs. incremental investment

3.1.5.2 Multi-period stochastic results

The multi-period stochastic model was applied also for Case study 2.

Table 3-7: Expected *ΔNPV*s and *ΔNPV*s from different scenarios of HEN designs optimised with multi-period stochastic approach for Case Study 2

HEN Design	*Expected ΔNPV*	*ΔNPV /k€ Scenario 1 p=0.07*	*ΔNPV/k€ Scenario 2 p=0.24*	*ΔNPV/k€ Scenario 3 p=0.38*	*ΔNPV/k€ Scenario 4 p=0.24*	*ΔNPV/k€ Scenario 5 p=0.07*
t_{LT} = 5 y	1.520	-2.024	-1.221	0.762	5.043	6.585
t_{LT} =15 y	146.46	31.22	54.26	115.68	271.15	320.61

It can be seen from Table 7 that the expected *ΔNPV*s were positive for both cases, which indicates that most likely their additional investments would be justified. When looking at the outcomes from different scenarios, the probabilities that the design would not be economically justified are low: 31 % for the design with 5 y, and no evidence for a negative outcome for the design with the 15 y lifetime.

The difference between the stochastic and deterministic multi-period models was not significant. The *NPV* was 0.71 k€ higher at the deterministic model and the investment was higher at the stochastic model by 22.05 k€. The utility load differences were low –1.04 kW

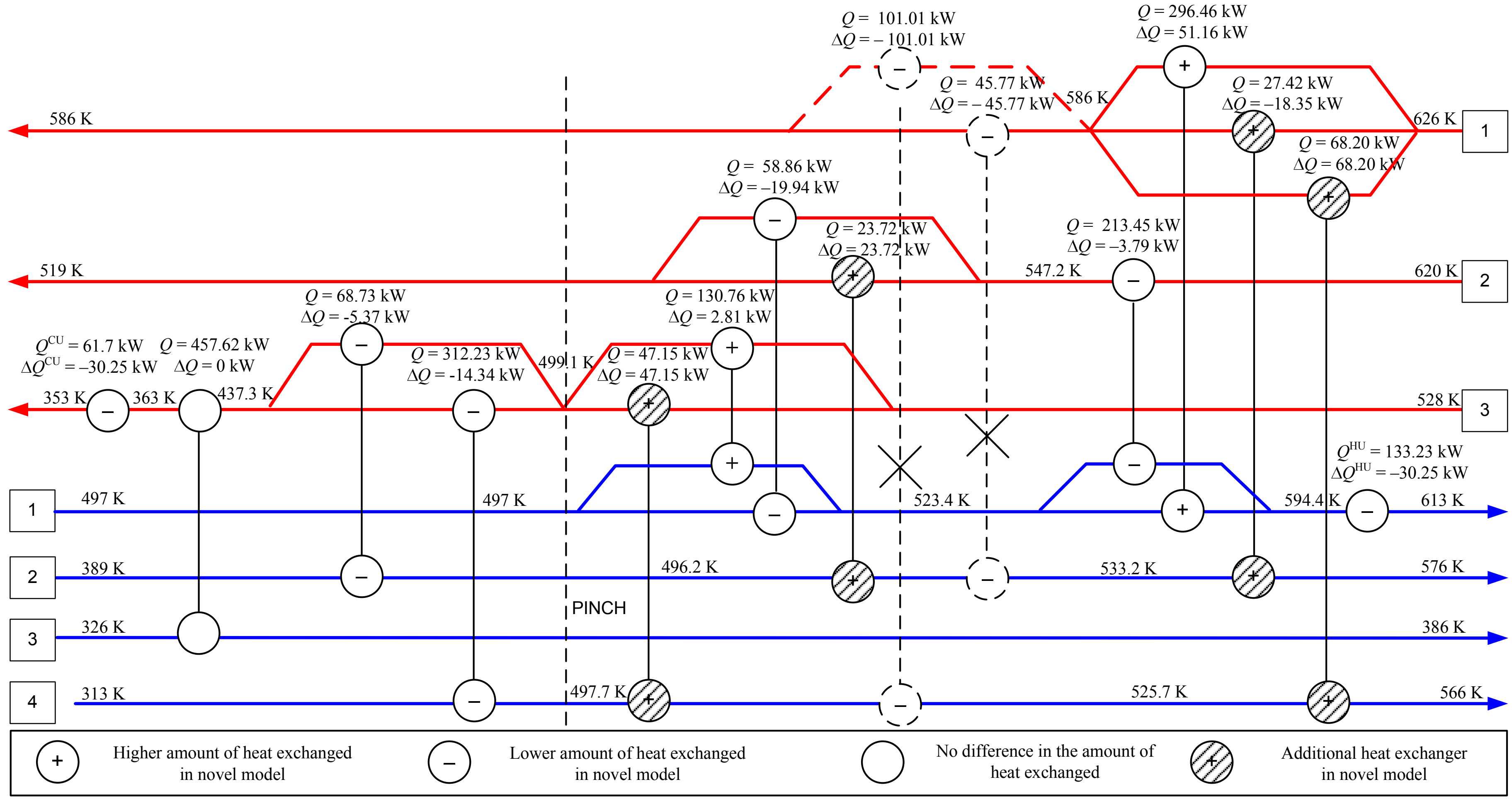

Figure 3-15:Comparison of the multi-period deterministic model at Scenario 3 and the model developed by Yee and Grossmann (1990) for Case study 2 for 15 y lifetime

The comparison of HEN designs and heat loads results (Figure 3-16) obtained by the multi-period deterministic model with fixed current utility prices and the multi-period stochastic model with future utility prices for 15 y lifetime showed that the investment increased by 316 from 1,683 k€ to 1,999 k€ (18.7 %) which yielded ΔNPV of 115 k€ from –4,103 k€ to –3,988 k€ (3%) if the most probable Scenario 3 would occur in the future. Utilities decreased by 22 kW, from 154 kW to 132 kW (14.3 %) for hot and from 83 kW to 61 kW (26.5 %) for cold utility.

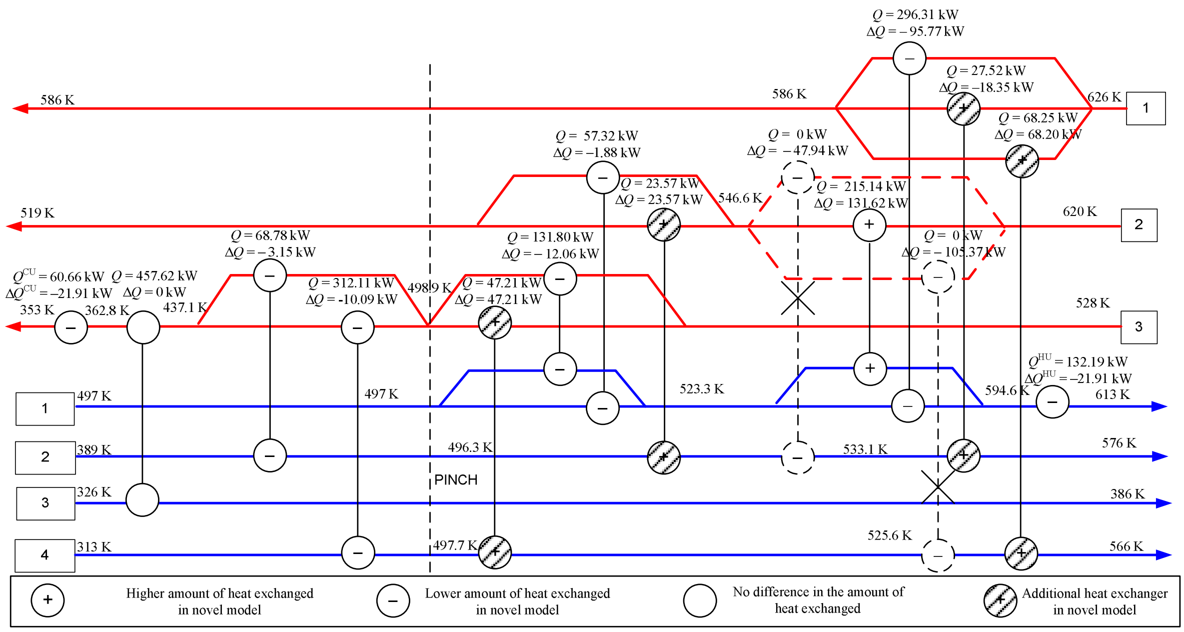

Figure 3-16: Comparison of HEN designs and heat loads results obtained by the multi-period deterministic model with fixed current utility prices and the multi-period stochastic model with future utility prices for Case study 2 for 15 y lifetime

The results obtained by this stochastic approach are more compact than those from the deterministic multi-period approach. It should also be noted, that the results presented are local optima because the problems are non-convex. The optimisations were carried out using the General Algebraic Modelling System (GAMS) using solver DICOPT for MINLP with Conopt for solving NLP subproblems and GUROBI for MILP master problems

3.2 With extensions

3.2.1 Stochastic multi-period MINLP model for HEN

The HEN synthesis can be performed, after obtaining the combined probability of each projection in each period as described in Chapter 2.1. The Yee and Grossmann's (1990) model is upgraded to a stochastic multi-period MINLP model in order to account for future utility prices, similarly as for HEN model with no extension. Therefore, here only the difference between the models without and with extensions are presented. The temperature differences and heat loads can vary during different periods and, consequently, the optimal heat exchange area (A) can be different in each period for every projection. However, the heat exchanger area is a fixed area except during period when extension are allowed. For each heat exchanger unit, a maximal area to be minimised in the objective function is selected from all those possible:

$$A_{i,j,k,n,v}^{\mathrm{HE}} \geq \frac{Q_{i,j,k,n,v}}{U_{i,j} \cdot (\Delta T_{i,j,k,n,v} \cdot \Delta T_{i,j,k+1,n,v} \cdot (\frac{\Delta T_{i,j,k,n,v} + \Delta T_{i,j,k+1,n,v}}{2}))^{0.333}}$$

$$\forall i \in I, j \in J, k \in K, n \in N, v \in V \tag{3-29}$$

$$A_{i,n,v}^{\mathrm{CU}} \geq \frac{Q_{i,n,v}^{\mathrm{CU}}}{U_{i}^{\mathrm{CU}} \cdot ((T_{\mathrm{out},j}^{\mathrm{H}} - T_{\mathrm{in}}^{\mathrm{CU}}) \cdot \Delta T_{i,n,v}^{\mathrm{CU}} \cdot (\frac{T_{\mathrm{out},j}^{\mathrm{H}} - T_{\mathrm{in}}^{\mathrm{CU}} + \Delta T_{i,n,v}^{\mathrm{CU}}}{2}))^{0.333}} \quad \forall i \in I, n \in N, v \in V \tag{3-30}$$

$$A_{j,n,v}^{\mathrm{HU}} \geq \frac{Q_{j,n,v}^{\mathrm{HU}}}{U_{j}^{\mathrm{HU}} \cdot ((T_{\mathrm{in}}^{\mathrm{HU}} - T_{\mathrm{out},j}^{\mathrm{C}}) \cdot \Delta T_{j,n,v}^{\mathrm{HU}} \cdot (\frac{T_{\mathrm{in}}^{\mathrm{HU}} - T_{\mathrm{out},j}^{\mathrm{C}} + \Delta T_{j,n,v}^{\mathrm{HU}}}{2}))^{0.333}} \quad \forall j \in J, n \in N, v \in V \tag{3-31}$$

When considering extension of the HEN in the future, new exchangers or additional area of existing exchanger can be installed. However, once it is implemented, it is costly to be removed. Therefore, the area cannot be easily decreased. For this purpose additional variables $AD_{i,j,k,n,v}^{\mathrm{HE}}$, $AD_{i,n,v}^{\mathrm{CU}}$ $AD_{j,n,v}^{\mathrm{HU}}$ for new or additional areas of existing exchangers, coolers, and heaters, respectively, were introduced. It should be noted that in the first year the additional areas of a HE correspond to the actual areas of the initial HEN:

$$AD_{i,j,k,n=1,v}^{\mathrm{HE}} = A_{i,j,k,n=1,v}^{\mathrm{HE}} \qquad \forall i \in I, j \in J, k \in K, n \in N, v \in V \tag{3-32}$$

$$AD_{i,n=1,v}^{\mathrm{CU}} = A_{i,n=1,v}^{\mathrm{CU}} \qquad \forall i \in I, n \in N, v \in V \tag{3-33}$$

$$AD_{j,n=1,v}^{\mathrm{HU}} = A_{j,n=1,v}^{\mathrm{HU}} \qquad \forall j \in J, n \in N, v \in V \tag{3-34}$$

In the following years the total areas are calculated as the areas of the previous year extended for additional areas:

$$A_{i,j,k,n>1,v}^{\mathrm{HE}} = A_{i,j,k,n-1,v}^{\mathrm{HE}} + AD_{i,j,k,n>1,v}^{\mathrm{HE}} \qquad \forall i \in I, j \in J, k \in K, n \in N, v \in V \tag{3-35}$$

$$A_{i,n>1,v}^{\mathrm{CU}} = A_{i,n-1,v}^{\mathrm{CU}} + AD_{i,n>1,v}^{\mathrm{CU}} \qquad \forall i \in I, n \in N, v \in V \tag{3-36}$$

$$A_{j,n>1,v}^{\mathrm{HU}} = A_{j,n-1,v}^{\mathrm{HU}} + AD_{j,n>1,v}^{\mathrm{HU}} \qquad \forall j \in J, n \in N, v \in V \tag{3-37}$$

In order to be able to determine fixed and variable charges for the extended or newly built exchangers, coolers and heaters, new binary variables $yd_{i,j,k}$, yd_{i}^{CU} and yd_{j}^{HU} are proposed. They are activated, when additional areas are proposed to be installed in the year of extension, noted as n_{ext}. An upper bound AD^{up} for extensions has been introduced. Besides its mathematical meaning, it can also have various practical significances in the industry, e.g. the availability of space in the plant, etc.

$$AD^{\mathrm{HE}}_{i,j,k,n=n_{ext},v} \le AD^{up} \cdot yd_{i,j,k,n=n_{ext},v} \qquad \forall i\in I, j\in J, k\in K, n\in N, v\in V \qquad (3\text{-}38)$$

$$AD^{\mathrm{HU}}_{i,n=n_{ext},v} \le AD^{up} \cdot yd^{\mathrm{HU}}_{i,n=n_{ext},v} \qquad \forall i\in I, n\in N, v\in V \qquad (3\text{-}39)$$

$$AD^{\mathrm{CU}}_{j,n=n_{ext},v} \le AD^{up} \cdot yd^{\mathrm{HU}}_{j,n=n_{ext},v} \qquad \forall j\in J, n\in N, v\in V \qquad (3\text{-}40)$$

In addition, the model developed by Yee and Grossmann (1990) is upgraded also for the use of Expected Net Present Value (*ENPV*) as an objective function. The original model when considering current fixed utility prices during the whole lifespan, served for obtaining a reference solution for comparison with those obtained by newly developed model. Thus, the actual objective was the maximisation of the Expected Incremental Net Present Value ($\Delta ENPV$) (Novak Pintarič and Kravanja, 2006) between the HEN design considering the future prices and the one at current prices, where *ENPV* for a particular price scenario is the sum of the yearly cash flows' present values minus investment. $\Delta ENPV$ is obtained when all scenarios' ΔNPVs are combined using the corresponding probabilities $p_{n,v}$:

$$\Delta ENPV = -\Delta I + \sum_{n=1}^{t_{\mathrm{LT}}} \sum_{v} p_{n,v} \cdot \frac{\Delta F_{\mathrm{C},n,v}}{(1+r_{\mathrm{D}})^{n}} \qquad (3\text{-}41)$$

ΔI is the incremental investment, t_{LT} the lifetime of the HEN, r_{D} the sum of discount rate and inflation together, and $\Delta F_{\mathrm{C},n,v}$ the incremental annual cash flow for each period separately after taxes, r_{T}:

$$\Delta F_{\mathrm{C},n,v} = \left((1-r_{\mathrm{T}})\left(0-\left(\Delta c^{\mathrm{OP}}_{n,v}\right)\right) + r_{\mathrm{T}} \frac{\Delta I}{t_{\mathrm{LT}}}) \right) \qquad \forall n\in N, v\in V \qquad (3\text{-}42)$$

where the annual utility cost with varying prices is calculated for every period during the lifetime as:

$$c^{\mathrm{OP}}_{n,v} = \sum_{j} t_{\mathrm{OP}} \cdot Q^{\mathrm{HU}}_{j,n,v} \cdot c^{\mathrm{HU}}_{n,v} + \sum_{i} t_{\mathrm{OP}} \cdot Q^{\mathrm{CU}}_{i,n,v} \cdot c^{\mathrm{CU}}_{n,v} \qquad \forall n\in N, v\in V \qquad (3\text{-}43)$$

The investment *I* is further calculated as a sum of the fixed and variable charges; however, also for additional units and areas. There are two types of fixed charges: i) for the newly installed HE units and ii) for additional areas on existing HE units:

$$\begin{aligned} FixC_n = {} & \sum_i \sum_j \sum_k cf_n \cdot y_{i,j,k} + \sum_i cf^{\mathrm{CU}}_n \cdot y^{\mathrm{CU}}_i + \sum_j cf^{\mathrm{HU}}_n \cdot y^{\mathrm{HU}}_j \\ & + \sum_i \sum_j \sum_k cfd_n \cdot yd_{i,j,k} + \sum_i cfd^{\mathrm{CU}}_n \cdot yd^{\mathrm{CU}}_i + \sum_j cfd^{\mathrm{HU}}_n \cdot yd^{\mathrm{HU}}_j \end{aligned} \qquad \forall i\in I, j\in J, k\in K \quad (3\text{-}44)$$

Similarly, the variable charges consist of the part built at the beginning of lifetime and when the extensions occur:

$$VarC_n = cv \cdot AD^{\mathrm{HE}}_{i,j,n} + cv^{\mathrm{CU}} \cdot A^{\mathrm{CU}}_{i,n} + cv^{\mathrm{HU}} \cdot A^{\mathrm{HU}}_{j,n} \qquad \forall i\in I, j\in J \qquad (3\text{-}45)$$

The variable charges are determined for all time periods including the first year since, as it has been already mentioned. The actually installed areas of the initial HEN design correspond to additional areas in the first year. The investment is therefore calculated as the sum of these charges over the entire lifespan, discounted to the present value:

$$I = \sum_{n} (FixC_n + VarC_n) \cdot f_n^{DA} \cdot f_n^{D} \tag{3-46}$$

where f_n^{DA} denotes a yearly discounting coefficient:

$$f_n^{DA} = \frac{1}{(1+r_D)^{n-1}} \tag{3-47}$$

and f_n^{D} a yearly compounding coefficient for investment:

$$f_n^{D} = (1+r_{\mathrm{C}})^{n-1} \tag{3-48}$$

where r_{D} denotes a compound interest rates, which in our case was an inflation rate. Note that the investment is charged at the beginning of year n, therefore, its discounting and compounding is raised to power n-1.

3.2.2 Model description

In the case studies comparisons of solutions obtained by different models are performed, therefore a short description of these models and their abbreviation are presented in the following section:

MINLP-D-CP-NE. In this deterministic (D) MINLP model current utility prices (CP) were considered and no extension (NE) of HEN design is allowed in the future.

MINLP-D-FP-NE. This is a multi-period MINLP model applying deterministic approach, where the HEN design is fixed during the whole lifetime and optimised at a certain future price (FP) projection.

MINLP-D-FP-E. It is a deterministic MINLP model, where optimisation was performed accounting for one of the future utility price projections. The initial investment is restricted to be at most as high as in the solution obtained with the model MINLP-D-CP-NE considering current prices. Extension (E) of HEN designs are allowed in a certain selected year.

MINLP-S-FP-NE. This stochastic (S) multi-period MINLP model accounts for future price projections scenarios simultaneously. The HEN design is optimised for whole lifetime, without extensions.

MINLP-S-FP-E. It is the proposed stochastic multi-period MINLP model, allowing extension in a certain year of the lifetime. The initial investment is restricted to be less or equal to the investment of a solution obtained with MINLP-D-CP model considering current prices.

3.2.3 Case study 1

The Case study 1 presented in Chapter 3.1.4 are applied, under different time period, therefore under different utility prices. The current prices were taken for April 2012, and the projection has been made on the basis of historical prices from April 2002 to April 2012

3.2.3.1 Deterministic optimisation with MINLP-D-CP-NE

First, the solution of deterministic model with current fixed energy prices is obtained. This solution provided a reference HEN design for the comparison. As the criterion the *NPV* for the whole lifetime was selected and the obtained current prices' NPV_{CP} was recalculated to future energy prices projections (*P1 - P5*), Table 3-9.

Table 3-8: Reference solutions of model MINLP-D-CP-NE for Case Study 1

I	NPV_{CP}	NPV_{P1}	NPV_{P2}	NPV_{P3}	NPV_{P4}	NPV_{P5}
1957.6	-7,984.5	-10,260.1	-10,840.9	-11,919.2	-13,501.3	-19,959.6

3.2.3.2 Optimisation without extensions with MINLP-D-FP-NE and MINLP-S-NE models considering future utility prices

The next step of the evaluation was to obtain a HEN design, which accounts for future utility prices. For this purpose two models are applied. One is the deterministic MINLP-D-FPNE and the other is the stochastic MINLP-S-FP-NE model. All the investment is installed at the beginning of the lifetime, hence, future extensions are not needed. The solution of these models indicated that HEN design with significantly better economic performance can be obtained when accounting for future utility price projection (Nemet et al., 2012). However, it also indicated that the improvement was a consequence of a larger investment at the beginning of the lifetime.

3.2.3.3 Deterministic optimisation with MINLP-D-FP-E, allowing for extensions

Rather than installing all the investment at the beginning of the lifetime, another approach is to start with an initial HEN and allowing for extensions as utility prices increase, thus reducing the risk related to the uncertainty of forecasted prices. As we start with current prices, the investment obtained with current prices serves as initial investment. Therefore, the investment of the initial design is restricted to the current prices' investment. The deterministic MINLP-D-FP-E model was applied to this strategy. When considering different future utility price projections, the optimal solutions with extensions vary significantly. Figure 3-17 presents the Δ*NPV*s between the obtained MINLP-D-FP-E solutions and the reference solutions of model MINLP-D-CP-NE, for different price projections. As can be seen from Figure 3-17, the largest improvement in *NPV* could be obtained, when the extension of the HEN was performed at the beginning of the first year. It can be seen that the highest savings due to extensions in HEN are to be potentially obtained, if the utility prices follow the most pessimistic projection with the highest prices (*P5*). At this projection both, the energy savings and money savings per unit of energy are the highest. The Δ*NPV* value is decreasing when the year of extension is shifted to the future, until it reaches a break-even period, when no extension of HEN is economically viable. In the most pessimistic scenario (*P5*) this break-even period was at year thirteen; however, in the case of the most optimistic future prices (*P1*) it is already at the sixth year.

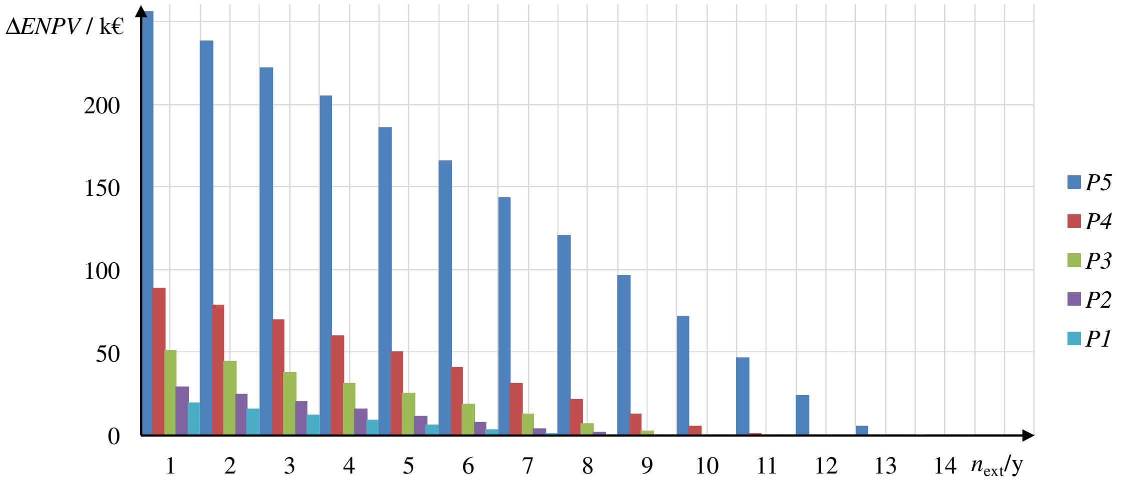

Figure 3-17: Impact of the year of extension on the Δ*NPV* at different utility price projections for Case Study 1

3.2.3.4 Stochastic optimisation with MINLP-S-FP-E, considering future utility prices and allowing for extensions

In order to consider all the projections simultaneously, a stochastic approach is applied and the probabilities of a HEN design being at certain projections in certain time periods have to be determined.

Table 3-9: Calculated probabilities ($p_{n,v}$) of projections v=1,..,5 in period n, n = 0,...,15

Period	*Projection 1*	*Projection 2*	*Projection 3*	*Projection 4*	*Projection 5*
0			0.890	0.110	
1	0.00089	0.089	0.730	0.169	0.011
2	0.010	0.145	0.615	0.204	0.025
3	0.025	0.180	0.531	0.223	0.042
4	0.041	0.201	0.468	0.233	0.058
5	0.057	0.214	0.420	0.237	0.073
6	0.073	0.221	0.382	0.237	0.086
7	0.088	0.225	0.353	0.236	0.098
8	0.102	0.226	0.329	0.234	0.109
9	0.115	0.226	0.310	0.231	0.118
10	0.126	0.226	0.294	0.228	0.126
11	0.136	0.225	0.281	0.225	0.133
12	0.145	0.224	0.270	0.222	0.139
13	0.153	0.223	0.261	0.219	0.144
14	0.160	0.222	0.253	0.217	0.148
15	0.166	0.221	0.247	0.215	0.151

The current price of oil (April 2012) 0.172 €/kWh is located between initial prices of Projection 3 (0.1705 €/kWh), and Projection 4 (0.1913 €/kWh) and can be expressed as a linear combination of the adjacent projections: 0.172 = 0.89·0.170 + 0.11·0.191. Based on the initial probabilities of Projection 3 and 4 being $p_{0,3} = 0.89$ and $p_{0,4} = 0.11$, the probabilities for all projections in the subsequent periods were calculated by the proposed MINLP–P probability, Table 3-10. The HEN synthesis with stochastic approach was performed applying the model MINLP-S-FP-E, using the above probabilities. The corresponding criterion is *ENPV*. The *ENPV* of the stochastic HEN design obtained with this model is compared to the *ENPV* which would be realised, if the reference HEN design, synthesised by the MINLP-D-CP-NE model, is exposed to the same future prices and probabilities as the stochastic HEN design. Note that the reference *ENPV* was -12,774.3 k€. Considering all possible future price scenarios simultaneously in this stochastic approach, the extension becomes economically unreasonable after eleventh year of lifetime (Figure 3-18), as this would lead to higher incremental investment compared to the money savings achieved from the reduction of utility consumption.

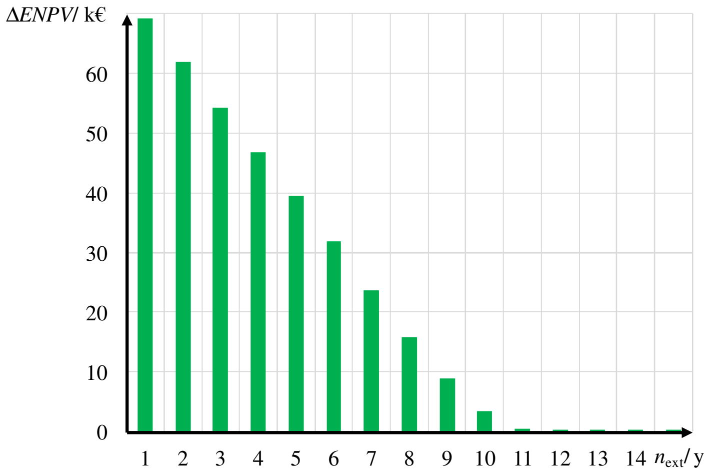

Figure 3-18: Impact of the year of extension on the Δ*ENPV* when applying the stochastic approach to Case Study 1

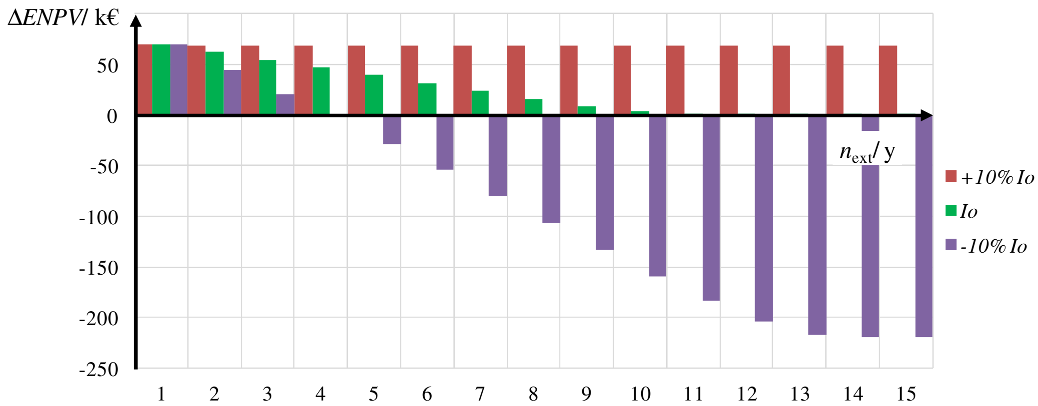

Figure 3-19: Comparison of Δ*ENPV* of HEN designs with different initial investment for Case Study 1

A set of calculations, considering different initial investment has been analysed, in order to analyse the sensitivity of the economic performance of a HEN design as a function of initial investment. The initial investment obtained at current energy prices (April 2012) of energy I_o was altered by -10 % and +10 %. Note that solutions at 100 % investment (Figure 3-18) were taken as reference solutions through the lifetime. Figure 3-19 clearly indicates that the initial investment should be selected carefully, as it influences the future economic performance of the HEN substantially. A general conclusion is that even a small underestimation of the initial investment can seriously affect the future economic performance of HEN. This is true even in cases when extensions of HEN are allowed to be performed.

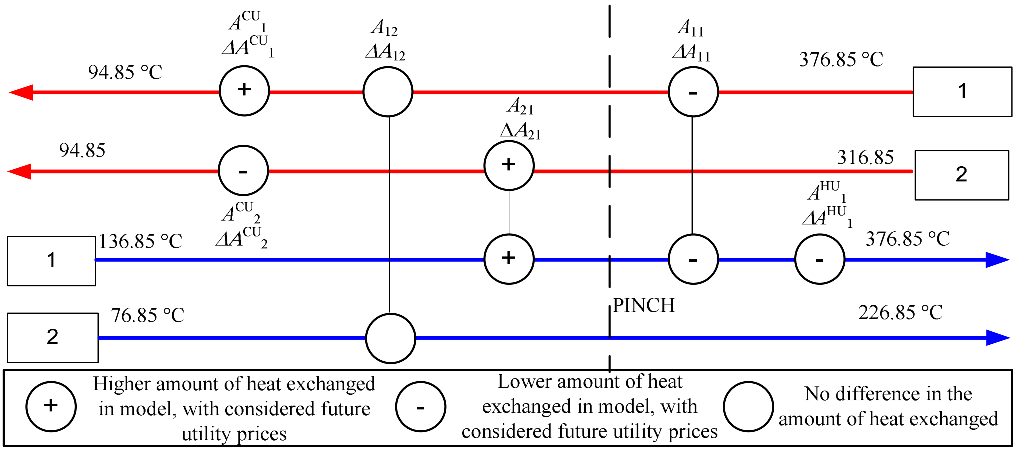

Figure 3-20: Optimal HEN structure for Case Study 1

It is interesting to note that in this case study all HEN deigns obtained by different optimisations exhibit the same structure, Figure 3-20. However, their initial and extended exchanger areas varied notable under different conditions, Table 3-11.

Table 3-10: Heat transfer area before A/m^2 and after ΔA extension, when optimised at different year of extension (n_{ext}) for Case Study 1

	A_{11}	ΔA_{11}	A_{12}	ΔA_{12}	A_{21}	ΔA_{21}	A^{HU}_1	A^{CU}_1	A^{CU}_2
Initial structure	173.63		63.37		289.79		15.54	6.15	35.27
n_{ext}/ y									
2	155.26	42.89	62.22	0	309.30	33.45	15.56	6.41	35.15
3	164.45	33.75	62.79	0	299.53	41.22	15.54	6.40	35.21
4	167.79	30.45	63.00	0	295.99	43.65	15.54	6.39	35.23
5	169.38	28.98	63.10	0	294.30	41.16	15.54	6.37	35.24
6	170.40	28.06	63.16	0	293.21	38.59	15.54	6.35	35.25
7	171.07	26.26	63.21	0	292.50	34.31	15.54	6.32	35.25
8	171.55	22.46	63.24	0	292.00	28.67	15.54	6.29	35.26
9	171.91	17.94	63.26	0	291.62	21.34	15.54	6.26	35.26
10	172.18	12.45	63.28	0	291.33	11.94	15.54	6.21	35.26
11	172.99	4.36	63.33	0	290.48	2.45	15.54	6.16	35.27
12	173.63	0	63.37	0	289.79	0	15.54	6.15	35.27

As the investment in the first year is restricted to the one obtained at current utility prices by the model MINLP-D-CP-NE, the initial HEN design is the same as the reference design. As the table indicates, extensions are larger in the beginning of the lifetime. It also indicates that

HEN is integrated more if extensions are performed in early stages of lifetime. The utility consumption is increasing if extensions are applied later. In Case study 1, it increases from 325.5 at the first year to 337.6 kW at the 12th year. This leads to a conclusion that the earlier the extension is installed, the higher heat recovery and the smallest utility consumption could be achieved. However, premature additional investments may not be justified due to the uncertainty of the future utility prices.

3.2.3.5 Selection of initial HEN

One way of deciding, which initial HEN should be selected is in regards to the risk related to a possible loss if an extension is not implemented, when future prices do not support this decision. A quick assessment can be made in the following way. The initial structure selected, when no extension is considered, should perform economically at least as well as the HEN, optimised at current energy prices. Then $\Delta ENPV$ obtained as the difference between $ENPV$ of the initial HEN without extension at a given year and $ENPV$ of HEN optimised at current energy prices can be used as a possible measurement of the risk involved. The $\Delta ENPV$ or risk involved selecting an initial HEN can be seen from the Figure 3-21.

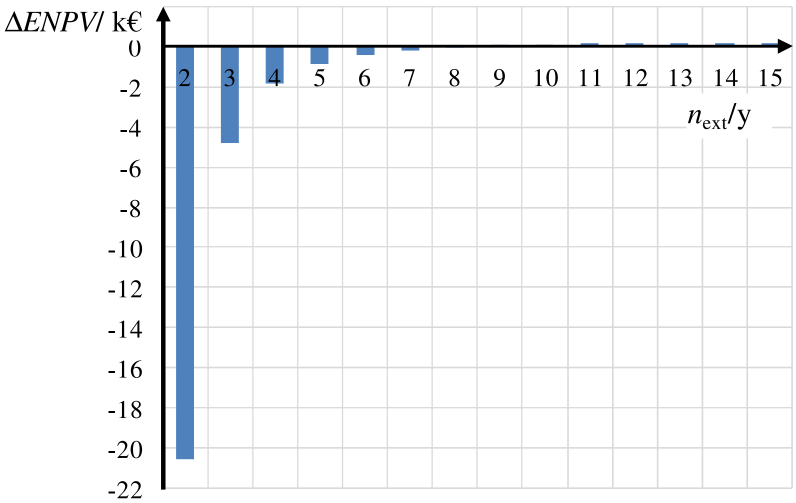

Figure 3-21: Comparison of the different initial structure economic performance at future energy prices of energy without extensions for Case Study 1

Only the initial HEN design, when extension is executed in second year of lifetime has relatively poorer economic performance compared to the HEN design obtained at current prices of energy. The possible loss, when the initial HEN design is optimised for an extension in year three, is relatively small, -4.8 k€ (0.037%), compared to the overall $ENPV$ of -12,779 k€. Therefore, design for an extension in year three can be selected as an initial HEN design. Further evaluation was focused on optimisation with this fixed initial HEN design, allowing extensions in other years (Figure 3-22).

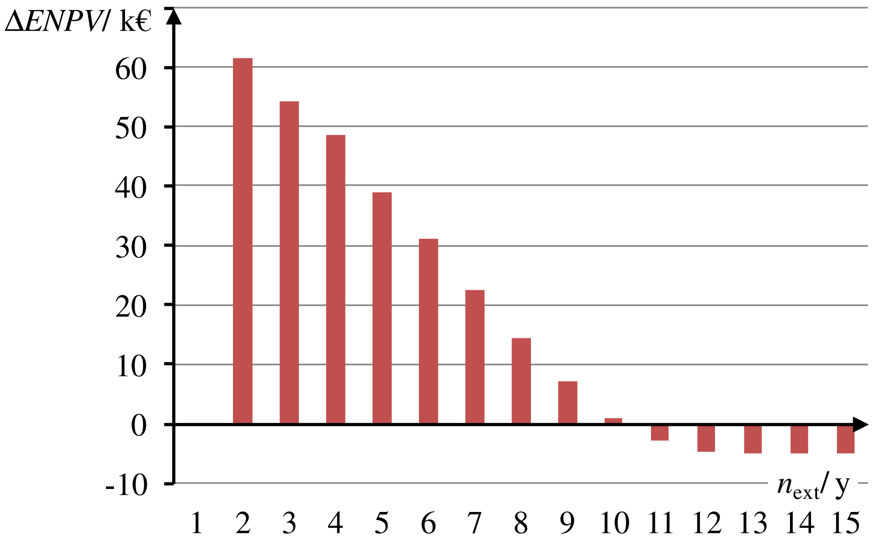

Figure 3-22: Economic performance of initial structure optimised for an extension at year 3, when allowing for extensions in other years

Observing Figure 3-22 it can be concluded that if the initial HEN design optimised for extension in the third year is extended after year three (comparison of Figure 3-22 and Fig Figure 3-18), the economic performance become worse, however not significantly. Even with no economically viable extension, the losses are negligible, especially when compared to the overall *ENPV*. On the other hand, when accounting for an extension early, especially at the beginning of the lifetime, the economic benefit can be significant. However, the uncertainty of meeting the optimal structure is thus higher, due to a longer span of the forecast. In cases when extensions are performed later, the risk is lower; however, the savings could be negligible.

3.2.3.6 Risk assessment with Certainty Equivalent

Another approach considering risk would be applying the assessment of the Certainty Equivalent (*CE*). First step in the assessment is to determine the Linearised Exponential Utility Function $U_{n,v}^{lin}$, in order to avoid numerical problems of the original Exponential Utility Function. A risk tolerance τ should reflect an individual decision about negative money outcome, which an investor can tolerate in his or her portfolio. The slope of the $U_{n,v}^{lin}(\Delta aNPV_{n,v})$ depends on the selected τ and the mean positive and negative $\Delta aNPV_{n,v}$ determined. However, as slope k_2 of negative outcomes is larger than k_1 of positive ones, the negative values are therefore maximised with a higher weights during the optimisation, when maximising the Δ*ENPV*, than the positive values. As a result, the optimisation tends to avoid large negative values and the risk is thus minimised. The risk premium (*RP*) is the difference between the Δ*ENPV* and the *CE*. Figure 3-23 presents a solution when different τ was selected: 25 k€, 50 k€, 75 k€, 100 k€ and 200 k€. As can be seen, when τ = 25 k€ the *CE* is small compared to the Δ*ENPV* and the *RP* is 25.32 k€ (maximal for the observed τ). This is a solution, where practically no risk is taken; however, the possible saving is significantly lower than in cases with higher τ, where the *CE*s are also higher and consequently the *RP*s are thus lower. For comparison the Δ*ENPV* when no risk assessment was performed can be seen in Figure 3-23. It indicates, that τ=200 k€ is very close to the tolerance, where all the possible Δ*ENPV* might be achieved.

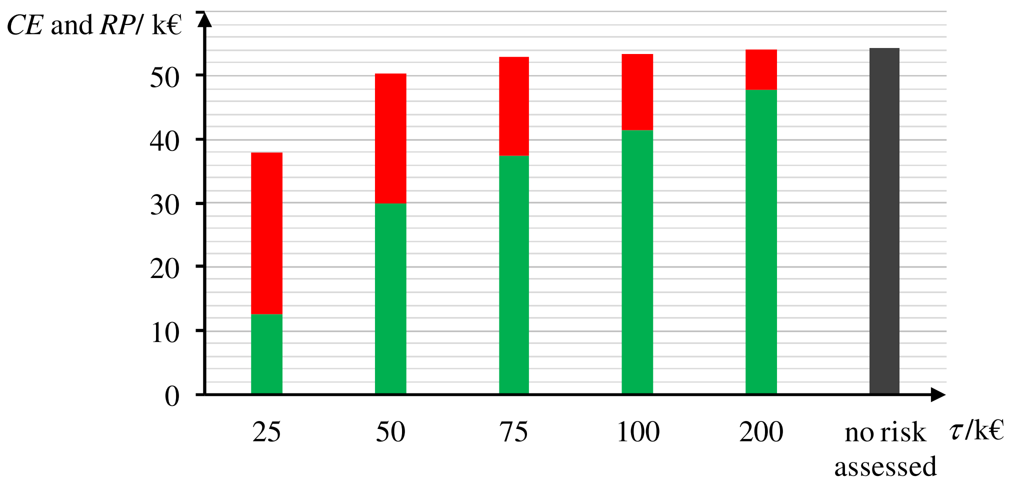

Figure 3-23: *CE* and *RP* versus τ

Another indicator, which provides the insight in the degree of HI is the $\Delta T_{\min}$ obtained at different optimisations. From Figure 3-24 it can be concluded, that the extensions performed in later years of the lifetime lead to smaller additional exchanger areas and, hence, larger $\Delta T_{\min}$ and larger consumption of utilities. Also, including risk assessment in the optimisation leads to solutions, with higher $\Delta T_{\min}$ compared to the case, when no risk assessment is made.

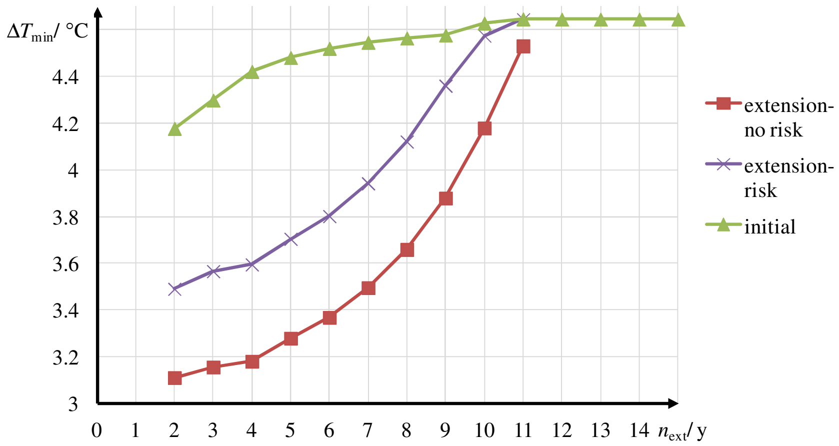

Figure 3-24: $\Delta T_{\min}$ for initial and extended HEN designs with and extended design without risk assessment depending on the year of extension for Case Study 1

3.2.4 Case study 2

Case study 2 consists of 3 hot and 4 cold process streams and is includes the same process streams, utilities as already described in Chapter 3.1.5 except utility prices, where the current prices has been taken for April 2012 and the basis for future prices projection was from April 2002 to April 2012.

The *ENPV* of the reference HEN design obtained at optimisation with current energy prices and recalculated for the future prices was -4,368.920 k€. When considering future energy prices and allowing for an extension in the fourth year of the lifetime using the stochastic approach, the optimisation yielded *ENPV* of -4,322.100 k€, which results in 46.820 k€ (1.1 %) savings.

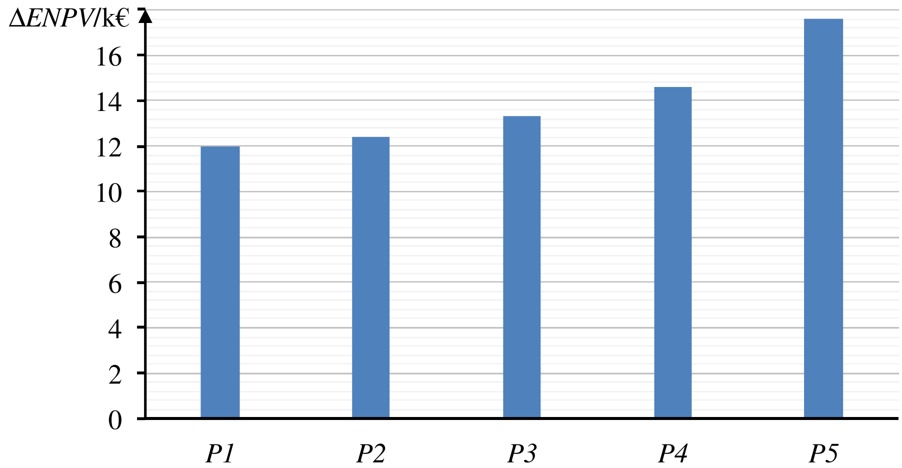

Figure 3-25:Difference in the economic performance of two initial structures, one obtained by optimisation with current and another with future utility prices, allowing for extension at the fourth year for Case Study 2

This case study was performed in order to evaluate the economic performance of two initial HEN designs: (i) the one obtained with model MINLP-D-CP-NE and (ii) the other obtained with MINLP-S-FP-E and the same investment as the first design.

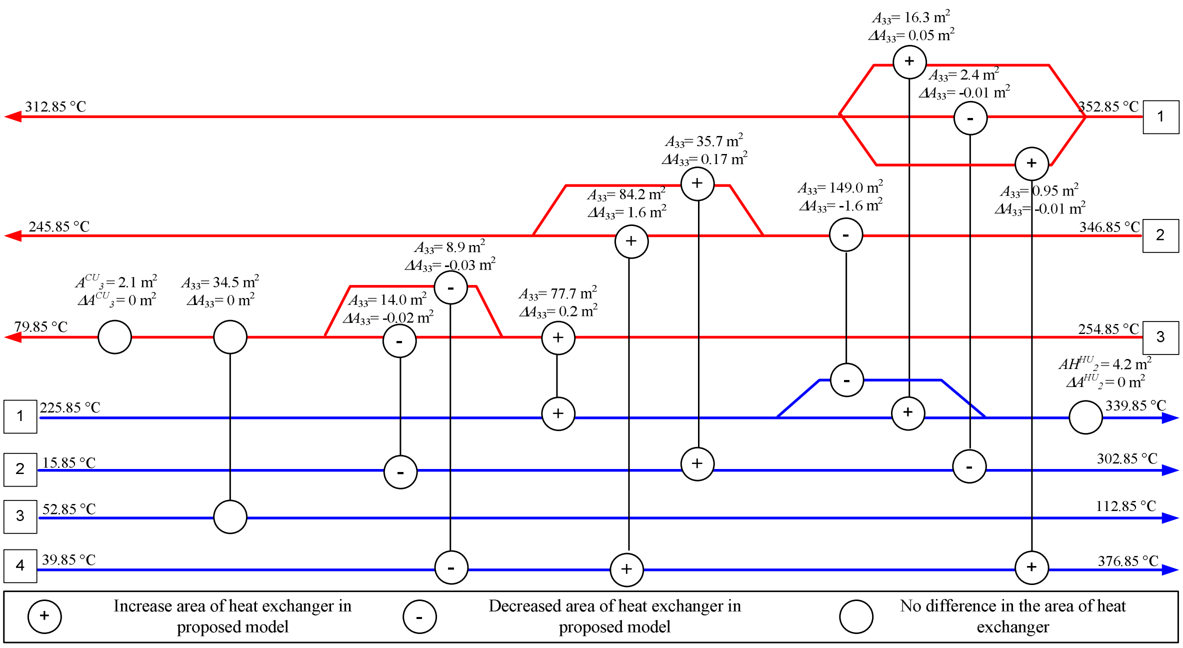

Figure 3-26: Difference between the structure obtained by optimisation at current prices and initial structure at stochastic approach when considered extension at fourth year of extension for Case study 2

As was indicated in Case study 1, the initial HEN design can have a significant impact on the HENs' future economic performance. In order to indicate, how significant this impact is, both initial designs underwent extensions in the fourth year of the lifespan. The comparison was performed for each utility price projection separately. The results are shown in Figure 3-25, where it can be seen that the overall economic performance of the initial design obtained by the stochastic model and future prices is better than the one of the deterministic model at current prices - at least 11.9 k€ at the optimistic and 17.6 k€ at the pessimistic utility price projection. The results indicate that it is reasonable to apply the stochastic model with extensions considering future prices. The difference between initial designs is presented in Figure 3-26.

In addition, the comparison was evaluated between two optimisation criteria - minimisation of Total Annual Cost (*TAC)* and maximisation of *NPV*. In order to simplify the case, both optimisations were performed using the deterministic approach (Figure 3-27). When analysing the results of Figure 3-27a, it can be concluded that worst economic performance was achieved when the criteria of *TAC* minimisation at current utility prices was used (*TAC-CP*). For this case the *ENPV*, recalculated for future utility prices, was -6,144 k€. A better solution *ENPV* of -5,870 k€ was obtained when minimising *TAC* considering future utility prices and allowing for extensions (*TAC-E*). It indicates that it is profitable accounting for future utility prices. The *ENPV* of the HEN design obtained by maximising *NPV* at current utility prices (*NPV-CP*) and recalculated to the future utility prices was -4,342.53 k€. The overall optimal solution with the highest *ENPV* of -4,311.10 k€ was obtained when the objective was maximisation of *NPV* considering future utility prices and allowing for extensions (*NPV-E*). Note that solutions when minimising *TAC* were significantly worse, compared to those obtained by maximising *NPV*. The use of *NPV* when current utility prices were considered resulted in about 1,800 k€ (29.3 %) savings, and when it was applied to a HEN design with extensions and future prices, about 1,500 k€ (26.6 %) savings were achieved, compared to the solutions obtained by minimising *TAC* (Figure 3-27b). Figure 3- 27b indicates that most of the savings with *NPV* were achieved due to a significantly lower consumption of utilities (OP-C in Figure 3-27b).

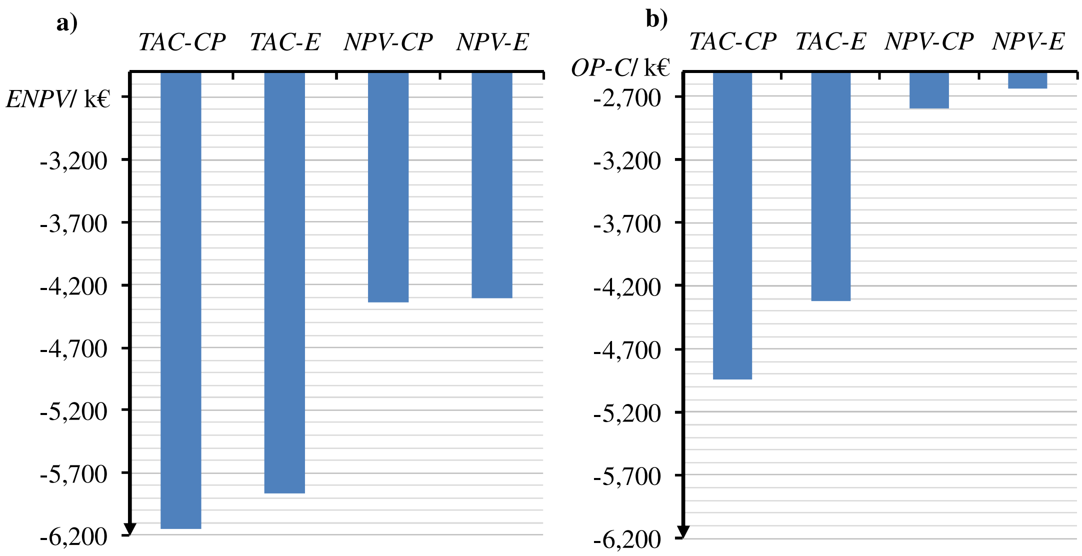

Figure 3-27: Comparison of a) Expected Net Present Value and b) operating cost for the whole lifetime, when considering the future utility prices of those solutions obtained by minimisation of Total Annual Cost and maximisation of Net Present Value at utility price projection P3

4 Process-to-process Heat Integration for Total Site for entire lifetime

4.1 Sequential Heat Integration within process and process-to-process

4.1.1 Scheme of Total Site

The first step of the TS Integration is to perform Heat Integration within each process individually (Figure 4-1a). For this purpose the original model developed by Yee and Grossmann (1990) can be applied. The external utility requirement can be obtained as a result of this optimisation. The input data for TS Integration are those process streams or their parts that remain as non-integrated after performing Heat Integration at the process level. This input data is defined within two sets, namely: (i) those parts of the hot streams which require cooling - a heat source in TS (Figure 4-1a, COOLING), and (ii) those parts of the cold streams which require heating - a heat sink in TS (Figure 4-1, HEATING). TS Heat Integration can then be performed between several processes by applying the corresponding TS superstructure; e.g. Figure 4-1b presents a superstructure for two hot and two cold streams, and two intermediate utilities. In Figure 4-1b, H1 and H2 denote the whole or parts of hot streams, while C1 and C2 the whole or parts of cold streams, included within the Total Site heat recovery analysis.

The intermediate utilities firstly collect the excessive heat from the heat source side (Figure 4-1b, Source Side), represented as hot streams of different processes, and afterwards they are sent to the heat sink side (Figure 4-1b, Sink Side) to cover as much as the heating demands, represented by the cold streams of different processes. As intermediate utilities are usually saturated or slightly superheated steams, they exchange heat isothermally. They are thus in superstructure matches arranged in parallel to each stream at each stage. Intermediate utilities are available at different temperature/pressure levels in order to maximize the heat recovered between the Source and Sink Sides. Within the superstructure of Figure 4-1b medium-pressure (MP) and low-pressure (LP) steams are presented as intermediate utilities. Each number of stages, on the Source and Sink Sides, is proportional to the minimum number of either process streams or intermediate utilities. The temperatures of the hot streams on the Source Side decrease at temperature locations (e.g. from temperature location $k^{HS} = 1$ to $k^{HS} = 3$ in Fig. 1b), whilst those of the cold streams on the sink side increase (e.g. from temperature location $k^{CS} = 3$ to $k^{CS} = 1$ in Figure 4-1b). After performing heat recovery between the source and sink sides, the remaining heating and cooling demands are supplied by an external hot and external cold utility.

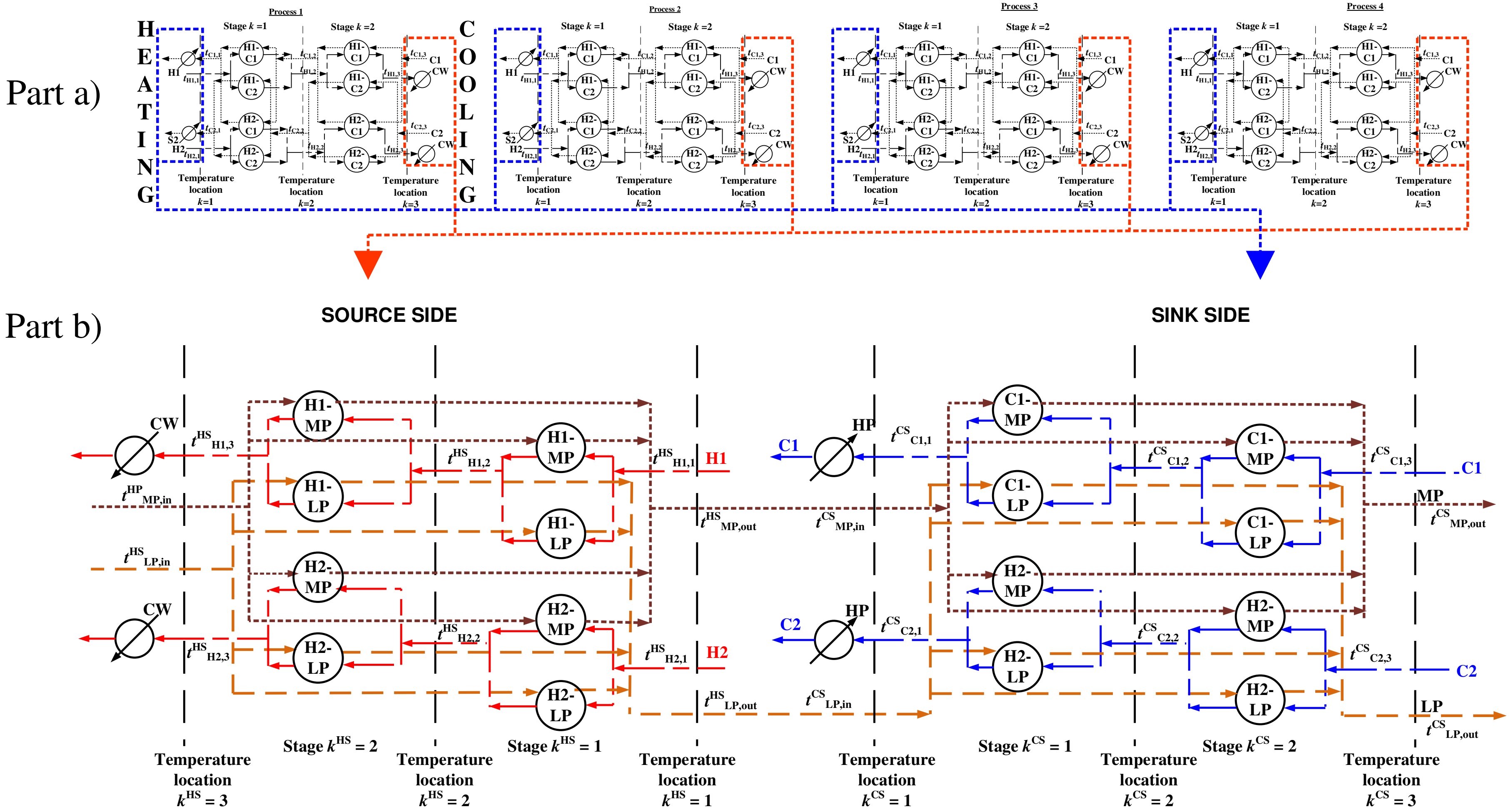

Figure 4-1: Total Site Heat Integration: a): scheme of Source and Sink Sides, b): Total Site superstructure for two hot, two cold streams, and two intermediate utilities.

4.1.2 Stochastic multi-period MINLP model for Total Site

A stochastic multi-period MINLP model has been developed in order to optimize a Total Site. The following sets and indexes have been introduced within this model:

- Index *ap* for all the processes included in the Total Site, $ap \in AP$
- Index *ph* for processes that have heat surpluses, $ph \in PH \subset AP$
- Index *pc* for processes that have heat demands, $pc \in PC \subset AP$
- Index *i* for hot streams in different processes, $i \in I$
- Index *j* for cold streams in different processes, $j \in J$
- Index *iu* for different intermediate utilities, $iu \in IU$
- Index k^{HS} for temperature locations within the superstructure on the source side, $k^{\mathrm{HS}} \in K^{\mathrm{HS}}$
- Index k^{CS} for temperature locations within the superstructure on the sink side, $k^{\mathrm{CS}} \in K^{\mathrm{CS}}$
- Index *n* for the number of periods observed , $n \in N=\{1,2,..,t_{\mathrm{LT}}\}$, where t_{LT} is the lifetime
- Index *v* for different utility prices' projections, $v \in V$

The model can be partitioned into two complementary parts: (i) the Source Side (Hot Side - HS) where the heat is transferred from hot streams to intermediate utilities, and the external cold utility (CU) and (ii) Sink Side (Cold Side - CS), where the heat demand of the cold streams is covered by intermediate utilities and the external hot utility (HU) connected through the modelling of a pipeline for transferring heat from the source side to the sink side.

Note that the model was indexed twice, once by periods observed over the entire lifetime ($n \in N=\{1, 2 \ldots t_{\mathrm{LT}}\}$), and secondly by utility prices' projections ranging from the more pessimistic to the more optimistic prices, ($v \in V$). The utility prices for these projections could be forecasted as described in Nemet et al. (2012) based on historical utility prices, and probabilities determined by NLP, as described in Nemet et al. (2013).

Source Side Equations

The duties of the hot streams during each process are calculated as the difference between its inlet $T_{ph,i}^{\mathrm{H,in}}$ and its outlet $T_{ph,i}^{\mathrm{H,out}}$ temperature multiplied by the heat capacity flow-rate $CP_{ph,i}$ (Eq. 4-1). The heat surpluses of the hot streams are transferred either to an intermediate $Q_{ph,i,iu,k^{\mathrm{HS}},n,v}^{\mathrm{HS}}$ or external cold utility $Q_{ph,i,n,v}^{\mathrm{CU}}$.

$$(T_{ph,i}^{\mathrm{H,in}} - T_{ph,i}^{\mathrm{H,out}}) \cdot CP_{ph,i} = \sum_{iu} \sum_{k^{\mathrm{HS}}} Q_{ph,i,iu,k^{\mathrm{HS}},n,v}^{\mathrm{HS}} + Q_{ph,i,n,v}^{\mathrm{CU}} \quad \forall\ ph \in PH,\ i \in I,\ ui \in IU,\ n \in N,\ v \in V \tag{4-1}$$

The heat duty of hot stream *i* of process *ph* within each stage is a result of multiplication between heat capacity flow-rate $CP_{ph,i}$ and temperature difference between the two consecutive temperature locations *k* and *k*+1, $TH_{ph,i,k^{\mathrm{HS}},n,v}$. It is equal to the amount of heat transferred to the intermediate utilities $Q_{ph,i,iu,k^{\mathrm{HS}},n,v}^{\mathrm{HS}}$ (Eq. 4-2) and the heat transferred to the external cold utility $Q_{ph,i,n,v}^{CU}$ (Eq. 4-3).

$$CP_{ph,i} \cdot (TH_{ph,i,k^{\mathrm{HS}},n,v} - TH_{ph,i,k^{\mathrm{HS}}+1,n,v}) = \sum_{iu} Q_{ph,i,iu,k^{\mathrm{HS}},n,v}^{\mathrm{HS}}\ \forall\quad ph \in PH,\quad i \in I,\quad k^{\mathrm{HS}} \in K^{\mathrm{HS}},\quad n \in N,\quad v \in V \tag{4-2}$$

$$CP_{ph,i} \cdot (TH_{ph,i,k^{\mathrm{HS}}=Ns+1,n,v} - T_{ph,i}^{H,out}) = Q_{ph,i,n,v}^{CU} \; \forall \qquad ph \in PH, \qquad i \in I, \qquad n \in N, \qquad v \in V \tag{4-3}$$

The heat duty of each intermediate utility $Ecc_{ph,iu,n,v}^{HS}$ is determined as the amount of heat exchanged between the hot streams and intermediate utilities $Q_{ph,i,iu,k^{\mathrm{HS}},n,v}^{\mathrm{HS}}$ (Eq. 4-4). Note that the heat transfer is assumed to be isothermal, therefore the inlet $TC_{ph,iu,n,v}^{\mathrm{HS,in}}$ and outlet $TC_{ph,iu,n,v}^{\mathrm{HS,out}}$ temperatures are equal (Eq. 4-5).

$$Ecc_{ph,iu,n,v}^{HS} = \sum_{i} \sum_{k^{\mathrm{HS}}} Q_{ph,i,iu,k^{\mathrm{HS}},n,v}^{\mathrm{HS}} \qquad \forall ph \in PH,\; iu \in IU,\; n \in N,\; v \in V \tag{4-4}$$

$$TC_{ph,iu,n,v}^{\mathrm{HS,out}} = TC_{ph,iu,n,v}^{\mathrm{HS,in}} \qquad \forall ph \in PH,\; iu \in IU,\; n \in N,\; v \in V \tag{4-5}$$

The first stage temperature of a hot stream $TH_{ph,i,k^{\mathrm{HS}}=1,n,v}$ is equal to its inlet temperature $T_{ph,i}^{\mathrm{H,in}}$ (Eq. 4-6) and the remaining ones $TH_{ph,i,k^{\mathrm{HS}},n,v}$ monotonically decrease during the next stages (Eq. 4-7).

$$T_{ph,i}^{\mathrm{H,in}} = TH_{ph,i,k^{\mathrm{HS}}=1,n,v} \qquad \forall\, ph \in PH,\; i \in I,\; n \in N,\; v \in V \tag{4-6}$$

$$TH_{ph,i,k^{\mathrm{HS}},n,v} \geq TH_{ph,i,k^{\mathrm{HS}}+1,n,v} \qquad \forall\, ph \in PH,\; i \in I,\; k^{\mathrm{HS}} \in K^{\mathrm{HS}},\; n \in N,\; v \in V \tag{4-7}$$

The temperature during the last stage $TH_{ph,i,k^{\mathrm{HS}}=Ns+1,n,v}$ is greater than or equal to the outlet temperature of the hot stream $T_{ph,i}^{\mathrm{H,out}}$.

$$TH_{ph,i,k^{\mathrm{HS}}=Ns+1,n,v} \geq T_{ph,i}^{\mathrm{H,out}} \qquad \forall\, ph \in PH,\; i \in I,\; n \in N,\; v \in V \tag{4-8}$$

A logical constraint for selecting (binary variable $y_{ph,i,iu,k^{\mathrm{HS}}}^{\mathrm{HS}}$ is set to 1) or rejecting ($y_{ph,i,iu,k^{\mathrm{HS}}}^{\mathrm{HS}}$ is set to 0) a match between the hot stream and the intermediate utility is defined by Eq. 4-9, where $Ech_{ph,i}$ is the heat content of hot stream, which represents the upper bound of heat exchange. Similarly, a binary variable $y_{ph,i}^{\mathrm{CU}}$ for selection or rejections of the eventual final cooling of the hot stream by the external cold utility is determined in Eq. 4-10.

$$Q_{ph,i,iu,k^{\mathrm{HS}},n,v}^{HS} - Ech_{ph,i} \cdot y_{ph,i,iu,k^{\mathrm{HS}}}^{\mathrm{HS}} \leq 0 \quad \forall ph \in PH,\; i \in I,\; iu \in IU, k^{\mathrm{HS}} \in K^{\mathrm{HS}},\; n \in N,\; v \in V \tag{4-9}$$

$$\sum_{v} Q_{ph,i,n,v}^{\mathrm{CU}} - Ech_{ph,i} \cdot y_{ph,i}^{\mathrm{CU}} \leq 0 \qquad \forall ph \in AP,\; i \in I,\; n \in N,\; n \in N,\; v \in V \tag{4-10}$$

The binary variables are used to activate or deactivate both the right and left stage approach temperature differences, $\Delta T_{ph,i,iu,k^{\mathrm{HS}},n,v}$ and $\Delta T_{ph,i,iu,k^{\mathrm{HS}}+1,n,v}$. The right ones are defined as the differences between the hot stream temperatures at the temperature locations k ($TH_{ph,i,k^{\mathrm{HS}},n,v}$) and the outlet intermediate utility temperatures $TC_{ph,iu,n,v}^{\mathrm{HS,out}}$ (Eq. 4-11), and the left ones as the differences between the hot stream temperatures at the temperature locations k+1 and the inlet intermediate utility temperatures $TC_{ph,iu,n,v}^{\mathrm{HS,in}}$ (Eq. 4-12). All the temperature driving forces are optimization variables, where the lower bound was set at 0.1 °C. The $\gamma_{ph,i,iu}^{\mathrm{HS}}$ is the maximal possible negative temperature difference between intermediate utility and hot stream.

$$\Delta T_{ph,i,iu,k^{\mathrm{HS}},n,v} \le TH_{ph,i,k^{\mathrm{HS}},n,v} - TC^{\mathrm{HS,out}}_{ph,iu,n,v} + \gamma^{\mathrm{HS}}_{ph,i,iu} \cdot (1 - y^{\mathrm{HS}}_{ph,i,iu,k^{\mathrm{HS}}})$$

$$\forall\ ph \in PH,\ i \in I,\ iu \in IU,\ k^{\mathrm{HS}} \in K^{\mathrm{HS}},\ n \in N,\ v \in V \qquad (4\text{-}11)$$

$$\Delta T_{ph,i,iu,k^{\mathrm{HS}}+1,n,v} \le TH_{ph,i,k^{\mathrm{HS}}+1,n,v} - TC^{\mathrm{HS,in}}_{ph,iu,n,v} + \gamma^{\mathrm{HS}}_{ph,i,iu} \cdot (1 - y^{\mathrm{HS}}_{ph,i,iu,k^{\mathrm{HS}}})$$

$$\forall\ ph \in HP,\ i \in I,\ iu \in IU,\ k^{\mathrm{HS}} \in K^{\mathrm{HS}},\ n \in N,\ v \in V \qquad (4\text{-}12)$$

The temperature of the external cold utility $T^{\mathrm{CU,out}}$ is chosen so that the approach temperature difference in cooler $\Delta T^{\mathrm{CU}}_{ph,i,n,v}$ between the hot stream and this cold utility is always positive.

$$\Delta T^{\mathrm{CU}}_{ph,i,n,v} \le TH_{ph,i,k^{\mathrm{HS}}=Ns+1,n,v} - T^{\mathrm{CU,out}} \qquad \forall\ ph \in PH,\ i \in I, n \in N,\ v \in V \qquad (4\text{-}13)$$

When determining the heat exchanger area to be minimized in the objective functions, the maximal area is selected from among those belonging to different price projections v and period n. The heat exchanger area for the heat exchange between hot streams and intermediate utility is denoted by $A^{\mathrm{HS}}_{ph,i,iu,k^{\mathrm{HS}}}$ (Eq. 4-14). The logarithmic mean difference $LMTD_{ph,i,iu,k^{HS},n,v}$ for these types of matches are determined from Eq. 4-15. The heat exchanger area between hot streams and external utility is determined separately $A^{\mathrm{CU}}_{ph,i}$ (Eq. 4-16) where the logarithmic mean temperature ($LMTD^{\mathrm{CU}}_{ph,i,n,v}$) is determined from Eq. 4-17.

$$A^{\mathrm{HS}}_{ph,i,iu,k^{\mathrm{HS}}} \ge \frac{Q^{\mathrm{HS}}_{ph,i,iu,k^{\mathrm{HS}},n,v}}{\left(\frac{1}{h_{ph,i}} + \frac{1}{h_{iu}}\right) \cdot LMTD_{ph,i,iu,k^{HS},n,v}}$$

$$\forall\ ph \in PH,\ i \in I,\ iu \in IU,\ k^{HS} \in K^{HS},\ n \in N,\ v \in V \qquad (4\text{-}14)$$

$$LMTD^{\mathrm{HS}}_{ph,i,iu,k^{HS},n,v} = \left(\Delta T_{ph,i,iu,k^{\mathrm{HS}},n,v} \cdot \Delta T_{ph,i,iu,k^{\mathrm{HS}}+1,n,v} \cdot \left(\frac{\Delta T_{ph,i,iu,k^{\mathrm{HS}},n,v} + \Delta T_{ph,i,iu,k^{\mathrm{HS}}+1,n,v}}{2} \right) \right)^{0.333}$$

$$\forall\ ph \in PH,\ i \in I,\ iu \in IU,\ k^{\mathrm{HS}} \in K^{\mathrm{HS}},\ n \in N,\ v \in V \qquad (4\text{-}15)$$

$$A^{\mathrm{CU}}_{ph,i} \ge \frac{Q^{\mathrm{CU}}_{ph,i,n,v}}{\left(\frac{1}{h_{ph,i}} + \frac{1}{h^{\mathrm{CU}}}\right) \cdot LMTD_{ph,i,n,v}} \qquad \forall\ ph \in PH,\ i \in I,\ n \in N,\ v \in V \qquad (4\text{-}16)$$

$$LMTD^{\mathrm{CU}}_{ph,i,n,v} = \left(\left(T^{\mathrm{H,out}}_{ph,i} - T^{\mathrm{CU}}_{in} \right) \cdot \Delta T^{\mathrm{CU}}_{ph,i,n,v} \cdot \left(\frac{T^{\mathrm{H,out}}_{ph,i} - T^{\mathrm{CU}}_{in} + \Delta T^{\mathrm{CU}}_{ph,i,n,v}}{2} \right) \right)^{0.333}$$

$$\forall\ ph \in PH,\ i \in I,\ n \in N,\ v \in V \qquad (4\text{-}17)$$

Sink Side equations

Process-to-process heat recovery occurs when the heat collected on the Source Side is transferred to the sink side to provide the heat demands of the cold streams.

The heat contents of the intermediate utilities $Ecc^{\mathrm{CS}}_{pc,iu,n,v}$ are equal to the heat transferred to the cold streams $Q^{\mathrm{CS}}_{pc,iu,j,k^{\mathrm{CS}},n,v}$ (Eq. 4-18). Note again that there is no temperature difference between the inlet $TH^{\mathrm{CS,in}}_{pc,iu,n,v}$ and outlet $TH^{\mathrm{CS,out}}_{pc,iu,n,v}$ temperatures since isothermal heat exchange is assumed (Eq. 4-19).

$$Ecc^{\mathrm{CS}}_{pc,iu,n,v} = \sum_{j}\sum_{k^{\mathrm{CS}}} Q^{\mathrm{CS}}_{pc,iu,j,k^{\mathrm{CS}},n,v} \qquad \forall\, pc\in PC,\ iu\in IU,\ n\in N,\ v\in V \qquad (4\text{-}18)$$

$$TH^{\mathrm{CS,\,out}}_{pc,iu,n,v} = TH^{\mathrm{CS,\,in}}_{pc,iu,n,v} \qquad \forall\, pc\in PC,\ iu\in IU,\ n\in N,\ v\in V \qquad (4\text{-}19)$$

The heat demand of a cold stream is determined as a temperature difference between outlet $T^{\mathrm{C,out}}_{pc,j}$ and inlet $T^{\mathrm{C,in}}_{pc,j}$ temperature multiplied by the heat capacity flow-rate $CP_{pc,j}$. It can be provided by the intermediate utilities $Q^{\mathrm{CS}}_{pc,iu,j,k^{\mathrm{CS}},n,v}$ and/or an external hot utility $Q^{\mathrm{HU}}_{pc,j,n,v}$ (Eq. 4-20).

$$(T^{\mathrm{C,out}}_{pc,j} - T^{\mathrm{C,in}}_{pc,j}) \cdot CP_{pc,j} = \sum_{iu}\sum_{k^{\mathrm{CS}}} Q^{\mathrm{CS}}_{pc,iu,j,k^{\mathrm{CS}},n,v} + Q^{\mathrm{HU}}_{pc,j,n,v} \qquad \forall\, pc\in PC,\ iu\in IU,\ n\in N,\ v\in V \qquad (4\text{-}20)$$

The amount of the cold stream's heating demand within a stage is a multiplication of heat capacity flow-rate and temperate difference between two consecutive temperature locations k^{CS} $TC_{pc,j,k^{\mathrm{CS}},n,v}$ and $k^{\mathrm{CS}}+1$, $TC_{pc,j,k^{\mathrm{CS}}+1,n,v}$. This amount is equal to the sum of the heat supplied by the intermediate utilities $Q^{CS}_{pc,iu,j,k^{\mathrm{CS}},n,v}$ (Eq. 4-21) or is provided by an external hot utility $Q^{\mathrm{HU}}_{pc,j,n,v}$ (Eq. 4-22).

$$CP_{pc,j} \cdot (TC_{pc,j,k^{\mathrm{CS}},n,v} - TC_{pc,j,k^{\mathrm{CS}}+1,n,v}) = \sum_{iu} Q^{CS}_{pc,iu,j,k^{\mathrm{CS}},n,v}$$
$$\forall\, pc\in PC,\ j\in J,\ k^{\mathrm{CS}}\in K^{\mathrm{CS}},\ n\in N,\ v\in V \qquad (4\text{-}21)$$

$$CP_{pc,j} \cdot (T^{\mathrm{C,out}}_{pc,j} - TC_{pc,j,k^{\mathrm{CS}}=1,n,v}) = Q^{\mathrm{HU}}_{pc,j,n,v} \qquad \forall\, pc\in PC,\ j\in J,\ n\in N,\ v\in V \qquad (4\text{-}22)$$

The inlet temperature of the cold process stream $T^{\mathrm{C,in}}_{pc,j}$ is equal to the temperature at the last temperature location $TC_{pc,j,k^{\mathrm{CS}}=Ns+1,n,v}$ (Eq. 4-23) and the location temperatures $TC_{pc,j,k^{\mathrm{CS}},n,v}$ decrease monotonically with any increase in the stage number (Eq. 4-24).

$$T^{\mathrm{C,in}}_{pc,j} = TC_{pc,j,k^{\mathrm{CS}}=Ns+1,n,v} \qquad \forall\, pc\in PC,\ j\in J,\ n\in N,\ v\in V \qquad (4\text{-}23)$$

$$TC_{pc,j,k^{\mathrm{CS}},n,v} \geq TC_{pc,j,k^{\mathrm{CS}}+1,n,v} \qquad \forall\, pc\in AP,\ j\in J,\ k^{\mathrm{CS}} \in K^{\mathrm{CS}},\ n\in N,\ v\in V \qquad (4\text{-}24)$$

The outlet temperature of the cold stream $T^{\mathrm{C,\,out}}_{pc,j}$ is greater than or equal to the temperature at the first temperature location $TC_{pc,j,k^{\mathrm{CS}}=1,n,v}$ (Eq. 4-25).

$$T^{\mathrm{C,\,out}}_{pc,j} \geq TC_{pc,j,k^{\mathrm{CS}}=1,n,v} \qquad \forall\, pc\in PC,\ j\in J,\ k^{CS} \in K^{CS},\ n\in N,\ v\in V \qquad (4\text{-}25)$$

A logical constraint for the selection of a match between a cold stream and an intermediate utility by binary variable $y^{\mathrm{CS}}_{pc,iu,j,k^{\mathrm{CS}}}$ is defined in Eq. 4-26. The $Ecc_{pc,j,n,v}$ is the heat demand of cold streams that also represents the upper bound of the heat exchanged and $Q^{\mathrm{CS}}_{pc,iu,j,k^{\mathrm{CS}},n,v}$ is the amount of heat exchanged between intermediate utility and cold stream. For the heat exchange between the remaining part of the cold stream and an external hot utility the logical constrain for selection is made by $y^{\mathrm{HU}}_{pc,j}$ (Eq. 4-27), where the $Q^{\mathrm{HU}}_{pc,j,n,v}$ is the amount of heat demand covered by external utility.

$$Q^{\mathrm{CS}}_{pc,iu,j,k^{\mathrm{CS}},n,v} - Ecc_{pc,j,n,v} \cdot y^{\mathrm{CS}}_{pc,iu,j,k^{\mathrm{CS}}} \leq 0 \qquad \forall\, pc\in PC,\ iu\in IU,\ j\in J,\ n\in N,\ v\in V \qquad (4\text{-}26)$$

$$Q^{\mathrm{HU}}_{pc,j,n,v} - Ecc_{pc,j,n,v} \cdot y^{\mathrm{HU}}_{pc,j} \leq 0 \qquad \forall\, pc\in PC,\, j\in J,\, n\in N,\, v\in V \tag{4-27}$$

The binary variable from Eq. 4-26 is used to activate or deactivate the temperature approach differences at the left and right stage temperature locations, $\Delta T_{pc,iu,j,k^{\mathrm{CS}},n,v}$ in Eq. 4-28 and $\Delta T_{pc,iu,j,k^{\mathrm{CS}}+1,n,v}$ in Eq. 4-29. $\gamma^{\mathrm{CS}}_{pc,iu,j}$ is the maximal possible negative temperature difference between the temperature of the intermediate utility and the cold process stream.

$$\Delta T_{pc,iu,j,k^{\mathrm{CS}},n,v} \leq TH^{CS,in}_{pc,iu,n,v} - TC_{pc,j,k^{\mathrm{CS}},n,v} + \gamma^{\mathrm{CS}}_{pc,iu,j} \cdot (1 - y^{\mathrm{CS}}_{pc,iu,j,k^{\mathrm{CS}}})$$
$$\forall\, pc\in PC,\, iu\in IU,\, j\in J,\, n\in N,\, v\in V \tag{4-28}$$
$$\Delta T_{pc,i,iu,k^{\mathrm{CS}}+1,n,v} \leq TH^{\mathrm{CS,out}}_{pc,iu,n,v} - TC_{pc,j,k^{\mathrm{CS}}+1,n,v} + \gamma^{\mathrm{CS}}_{pc,iu,j} \cdot (1 - y^{CS}_{ap,iu,j,k^{\mathrm{CS}}})$$
$$\forall\, pc\in PC,\, iu\in IU,\, j\in J,\, k^{\mathrm{CS}} \in K^{\mathrm{CS}},\, n\in N,\, v\in V \tag{4-29}$$

The temperature difference between the outlet temperatures of hot utility and cold stream $\Delta T^{\mathrm{HU}}_{pc,j,n,v}$ is defined by Eq. 4-30. The user should provide consistent data for the temperatures of external utilities, e.g. the temperatures of the external hot utilities should be greater than the outlet temperatures of the external cold utilities.

$$\Delta T^{\mathrm{HU}}_{pc,j,n,v} \leq T^{\mathrm{HU,out}} - TC_{pc,j,k^{\mathrm{CS}}=1,n,v} \qquad \forall\, pc\in AP,\, j\in J,\, k^{\mathrm{CS}} \in K^{\mathrm{CS}},\, n\in N,\, v\in V \tag{4-30}$$

On the sink side the calculation of area is performed similarly as on the source side; for a heat exchange between the intermediate utility and/or external cold stream the area $A^{\mathrm{CS}}_{pc,iu,j,k^{\mathrm{CS}}}$ is determined from Eq. 4-31. For this heat exchanger, the logarithmic mean temperature difference $LMTD^{\mathrm{CS}}_{pc,iu,j,k^{\mathrm{CS}},n,v}$ is determined from Eq. 4-32. For the heat exchanger between hot utility (Eq. 33) and a cold stream the area $A^{\mathrm{HU}}_{pc,j}$ is determined from Eq. 4-33. For this match the logarithmic mean temperature difference $LMTD^{\mathrm{HU}}_{pc,j,n,v}$ is determined by applying Eq. 4-34.

$$A^{\mathrm{CS}}_{pc,iu,j,k^{\mathrm{CS}}} \geq \frac{Q^{\mathrm{CS}}_{pc,iu,j,k^{\mathrm{CS}},n,v}}{(\frac{1}{h_{pc,j}} + \frac{1}{h_{IU}}) \cdot LMTD^{\mathrm{CS}}_{pc,iu,j,k^{\mathrm{CS}},n,v}}$$
$$\forall pc\in PC,\, j\in J,\, iu\in IU,\, k^{\mathrm{CS}} \in K^{\mathrm{CS}},\, n\in N,\, v\in V \tag{4-31}$$
$$LMTD^{\mathrm{CS}}_{pc,iu,j,k^{\mathrm{CS}},n,v} = \left(\Delta T_{pc,iu,j,k^{\mathrm{CS}},n,v} \cdot \Delta T_{pc,iu,j,k^{\mathrm{CS}}+1,n,v} \cdot \left(\frac{\Delta T_{pc,iu,j,k^{\mathrm{CS}},n,v} + \Delta T_{pc,iu,j,k^{\mathrm{CS}}+1,n,v}}{2} \right) \right)^{0.333}$$
$$\forall\, pc\in PC,\, j\in J,\, iu\in IU,\, k^{\mathrm{CS}} \in K^{\mathrm{CS}},\, n\in N,\, v\in V \tag{4-32}$$
$$A^{\mathrm{HU}}_{pc,j} \geq \frac{Q^{\mathrm{HU}}_{pc,j,n,v}}{\left(\frac{1}{h_{pc,j}} + \frac{1}{h^{\mathrm{HU}}} \right) \cdot LMTD^{\mathrm{HU}}_{pc,j,n,v}} \quad \forall\, pc\in PC,\, j\in J,\, iu\in IU,\, n\in N,\, v\in V \tag{4-33}$$

$$LMTD^{\mathrm{HU}}_{pc,j,n,v} = \left(\left(T^{\mathrm{HU}}_{in} - T^{\mathrm{C,out}}_{pc,j} \right) \cdot \Delta T_{pc,j,n,v} \cdot \left(\frac{\left(T^{\mathrm{HU}}_{in} - T^{\mathrm{C,out}}_{pc,j} \right) + \Delta T_{pc,j,n,v}}{2} \right) \right)^{0.333}$$

$$\forall\ pc\in PC,\ j\in J,\ iu\in IU,\ n\in N,\ v\in V \qquad (4\text{-}34)$$

Pressure-temperature correlation of saturated steam

Increased investment for higher pressures in the heat exchangers and pipes needs to be considered as the pressure of the intermediate utility can be relatively high. The pressures are determined using the Antoine pressure/temperature relationship applying Antoine constants A, B and C for water. Eq. 4-35 defines the pressure of the source side $p^{\mathrm{HS}}_{ph,iu}$ as a function of the outlet temperature of generated intermediate utility *iu*.

$$p^{\mathrm{HS}}_{ph,iu} = 10^{A-B/\left(C+TC^{\mathrm{HS,out}}_{ph,iu,n,v}\right)} \qquad \forall\ ph\in PH,\ iu\in IU,\ n\in N,\ v\in V \qquad (4\text{-}35)$$

The pressure on the Sink Side $p^{CS}_{pc,iu}$ is determined as the pressure on the source side $p^{HS}_{ph,iu}$ decreased by pressure drop in the pipeline $p^{drop}_{ph,pc,iu,n,v}$ (Eq. 4-36).

$$p^{CS}_{pc,iu} = p^{HS}_{ph,iu} - p^{drop}_{ph,pc,iu,n,v} \quad \forall ph\in PH,\ pc\in PC,\ iu\in IU,\ n\in N,\ v\in V \qquad (4\text{-}36)$$

Finaly, the temperature of the intermediate utility *iu* entering the sink side is related to the pressure of the Sink Side $p^{\mathrm{CS}}_{pc,iu}$ (Eq. 4-37).

$$p^{\mathrm{CS}}_{pc,iu} = 10^{A-B/\left(C+TH^{\mathrm{CS,in}}_{pc,iu,n,v}\right)} \qquad \forall\ pc\in PC,\ iu\in IU,\ n\in N,\ v\in V \qquad (4\text{-}37)$$

Pipeline layout

The amount of steam produced during any certain hot process $Ecc^{HS}_{ph,iu,n,v}$ is equal to the sum of those steam portions $q^{av}_{ph,pc,iu,n,v}$ available for transfer to all the cold processes on the sink side (Eq. 4-38). At the Sink Side, however, the amount of the steam used $Ech^{CS}_{pc,iu,n,v}$ during any cold process is equal to the sum of available steam portions $q^{av}_{ph,pc,iu,n,v}$ from all hot processes, each portion now reduced by a certain heat loss $q^{loss}_{ph,pc,iu,n,v}$ when being transported along a pipeline from one process to another (Eq. 39).

$$Ecc^{HS}_{ph,iu,n,v} = \sum_{pc} q^{av}_{ph,pc,iu,n,v} \qquad \forall ph\in PH,\ iu\in IU,\ n\in N,\ v\in V \qquad (4\text{-}38)$$

$$Ech^{CS}_{pc,iu,n,v} = \sum_{ph} (q^{av}_{ph,pc,iu,n,v} - q^{loss}_{ph,pc,iu,n,v}) \qquad \forall pc\in PC,\ iu\in IU,\ n\in N,\ v\in V \qquad (4\text{-}39)$$

It is assumed in this model that steam can be transferred from any process with heat surplus to each process with heat demand (see the superstructure of Figure 4-2) under the condition that the temperature difference for the match is positive. Big-M formulation of the temperature difference in relation with the selection of heat exchange matches is applied (Source Side Eq. 4-11 and Eq. 4-12, while on the Sink Side Eq. 4-28 and Eq. 4-29). If the temperature difference does not support heat exchange, the binary variable for matching will be forced to zero, meaning that this match is forbidden.

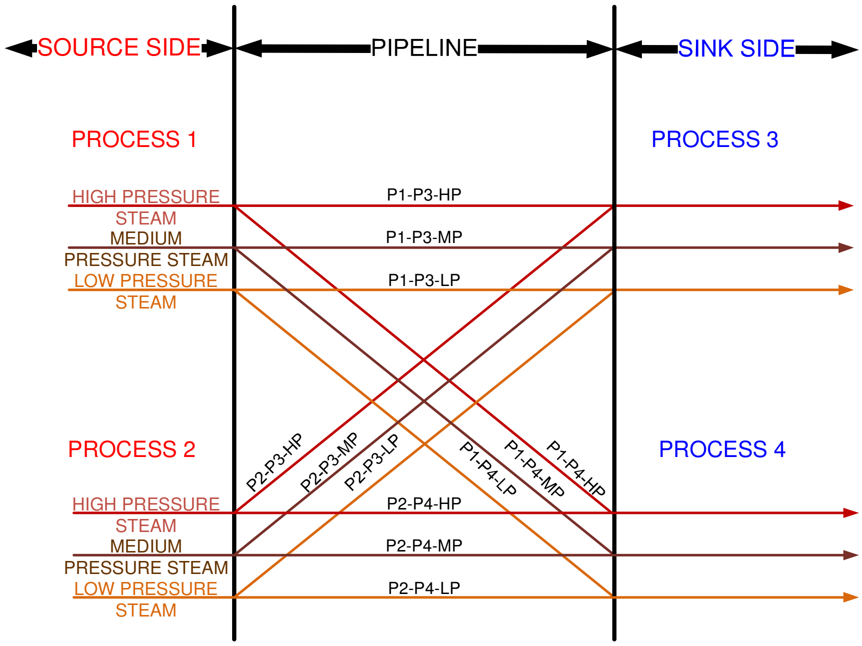

Figure 4-2: Scheme of pipeline for the heat transported from the source side processes to the sink side processes

A binary variable $yt_{ph,pc,iu}$ has been introduced for the selection/rejection of a certain hot-cold process pipeline. $q^{UP}_{ph,pc}$ is the upper bound on the heat exchange between hot and cold processes.

$$q^{av}_{ph,pc,iu,n,v} - yt_{ph,pc,iu} \cdot q^{UP}_{ph,pc} \leq 0 \qquad \forall ph \in PH,\ pc \in PC\ ,iu \in IU,\ n \in N,\ v \in V \qquad (4\text{-}40)$$

The lower bound of the heat transfer has also been set for practical reasons, in order to avoid the heat transfers being too small.

$$q^{av}_{ph,pc,iu,n,v} - yt_{ph,pc,iu} \cdot \left(0.1 \cdot q^{up}_{ph,pc}\right) \geq 0 \qquad \forall ph \in PH,\ pc \in PC\ ,iu \in IU,\ n \in N,\ v \in V \qquad (4\text{-}41)$$

Further logical constraints have been used for pipeline selection. Positive variables $v^{HS}_{ph,iu}$ and $v^{CS}_{pc,iu}$ with upper bounds being 1 have been set at 1 if a heat exchange occurs between any hot stream of a hot process and an intermediate utility at any stage (Eq. 4-42) or between an intermediate utility and any cold stream of a cold process at any stage (Eq. 4-43), respectively.

$$v^{HS}_{ph,iu} \geq y^{HS}_{ph,i,iu,k^{HS}} \qquad \forall ph \in PH\ ,i \in I,\ iu \in IU,\ k^{HS} \in K^{HS} \qquad (4\text{-}42)$$

$$v^{CS}_{pc,iu} \geq y^{CS}_{pc,iu,j,k^{CS}} \qquad \forall pc \in PC\ ,j \in J,\ iu \in IU,\ k^{CS} \in K^{CS} \qquad (4\text{-}43)$$

The binary variable for the existence of a hot-cold process pipeline $yt_{ph,pc,iu}$ has been set to zero, when there is no heat exchange between the processes and an intermediate utility (Eq. 4-44 and Eq. 4-45).

$$yt_{ph,pc,iu} \leq v^{HS}_{ph,iu} \qquad \forall ph \in PH,\ pc \in PC,\ iu \in IU \qquad (4\text{-}44)$$

$$yt_{ph,pc,iu} \le v^{CS}_{pc,iu} \qquad \forall ph \in PH,\ p \in PC,\ iu \in IU \qquad (4\text{-}45)$$

Heat losses during transport

Heat losses can be determined depending on the insulation thickness $th^{ins}_{ph,pc,iu}$ only, as the heat convection through the pipe wall is usually high. The original design equation had to be relaxed into two inequality constraints (Eq. 4-46 and 4-47) in order to avoid numerical problems at zero steam flows. Note, that when the pipeline was selected, both inequalities were enforced and the equality condition re-established, otherwise they would become redundant. In the latter case an additional constraint (Eq. 4-48) sets the heat losses to zero.

$$q^{loss}_{ph,pc,iu,n,v} \ge 2\cdot\pi\cdot k^{ins}\cdot L_{ph,pc}\frac{TC^{HS,out}_{ph,iu,n,v}-T_g}{ln\left(\dfrac{th^{ins}_{ph,pc,iu}+d_{ph,pc,iu}/2+th^{pipe}_{ph,pc,iu}}{d_{ph,pc,iu}/2+th^{pipe}_{ph,pc,iu}}\right)}-\left(1-yt_{ph,pc,iu}\right)\cdot q^{loss,UP}_{ph,pc,iu,n,v}$$

$$\forall ph \in PH,\ pc \in PC,\ iu \in IU,\ n \in N,\ v \in V \qquad (4\text{-}46)$$

$$q^{loss}_{ph,pc,iu,n,v} \le 2\cdot\pi\cdot k^{ins}\cdot L_{ph,pc}\frac{TC^{HS,out}_{ph,iu,n,v}-T_g}{ln\left(\dfrac{th^{ins}_{ph,pc,iu}+d_{ph,pc,iu}/2+th^{pipe}_{ph,pc,iu}}{d_{ph,pc,iu}/2+th^{pipe}_{ph,pc,iu}}\right)}+\left(1-yt_{ph,pc,iu}\right)\cdot q^{loss,UP}_{ph,pc,iu,n,v}$$

$$\forall ph \in PH,\ pc \in PC,\ iu \in IU,\ n \in N,\ v \in V \qquad (4\text{-}47)$$

$$q^{loss}_{ph,pc,iu,n,v} \le yt_{ph,pc,iu}\cdot q^{loss,UP}_{ph,pc,iu,n,v} \qquad \forall ph \in PH,\ pc \in PC,\ iu \in IU,\ n \in N,\ v \in V \qquad (4\text{-}48)$$

Pressure drop

The pressure drop $p^{drop}_{ph,pc,iu,n,v}$ depends on the pipe friction factor μ, the length of the pipeline $L_{ph,pc}$, velocity of the steam $v_{ph,pv,iu,n,v}$, inner diameter $d_{ph,pc,iu}$ and the specific volume of steam $V^{spec}_{ph,iu,n,v}$ (TLV, 2013):

$$p^{drop}_{ph,pc,iu,n,v} = \frac{\mu\cdot L_{ph,pc}\cdot {v_{ph,pc,iu,n,v}}^2}{2\cdot d_{ph,pc,iu}\cdot V^{spec}_{ph,iu,n,v}} \qquad \forall ph \in PH,\ pc \in PC,\ iu \in IU,\ n \in N,\ v \in V \qquad (4\text{-}49)$$

where velocity is determined from the following Eq. 4-50 (TLV, 2013):

$$v_{ph,pc,iu,n,v} = \frac{\dot{m}_{ph,pc,iu,n,v}}{3600}\cdot\frac{V^{spec}_{ph,iu,n,v}}{\left(d_{ph,pc,iu}/2\right)^2\cdot\pi} \qquad \forall ph \in PH,\ pc \in PC,\ iu \in IU,\ n \in N,\ v \in V \qquad (4\text{-}50)$$

The mass flow-rate $\dot{m}_{ph,pc,iu,n,v}$ can be determined as the ratio between the heat transferred from a process to an intermediate utility, and the specific enthalpy of the saturated steam (Eq. 4-51).

$$\dot{m}_{ph,pc,iu,n,v} = \frac{q^{av}_{ph,pc,iu,n,v}}{h_{ph,pc,iu}} \qquad \forall ph \in PH,\ pc \in PC,\ iu \in IU,\ n \in N,\ v \in V \qquad (4\text{-}51)$$

Two correlation equations have been derived from steam tables (available in e.g. Koretsky, 2013) for the specific volume and specific enthalpy of the steam in the temperature interval 120 °C – 330 °C (Figure 4-3).

$$V^{spec}_{ph,iu,n,v} = 1{,}790 \cdot e^{-0.002 \cdot TC^{\mathrm{HS,out}}_{ph,iu,n,v}} \qquad \forall ph \in PH,\ iu \in IU,\ n \in N,\ v \in V \qquad (4\text{-}52)$$

$$h_{ph,iu,n,v} = -2.55 \cdot 10^{-6} \cdot \left(TC^{\mathrm{HS,out}}_{ph,iu,n,v}\right)^2 + 0.002549 \cdot TC^{\mathrm{HS,out}}_{ph,iu,n,v} + 0.1418$$
$$\forall ph \in PH,\ iu \in IU,\ n \in N,\ v \in V \qquad (4\text{-}53)$$

A relation between the diameter and thickness of the pipe (Eq. 4-54) is needed in order to allow a pipe design (Stovall, 1981).

$$th^{pipe}_{ph,pc,iu} \cdot 39.37 = p^{HS}_{ph,iu} \cdot 14.5 \cdot (d_{ph,pc,iu} + 2 \cdot th^{pipe}_{ph,pc,iu}) \cdot 39.37 / (2 \cdot (SE + p^{HS}_{ph,iu} \cdot c^{y})) + Al$$
$$\forall ph \in PH,\ pc \in PC,\ iu \in IU \qquad (4\text{-}54)$$

where SE denotes maximum allowable stress in material and Al allowance for threading, mechanical strength, and corrosion.

Pipe cost

Once the design variables had been defined, the next step was to determine pipe investment. In the literature calculation of pipe cost is slightly different in various handbooks (see e.g. (Nayyar, 2000), therefore, only the main elements of pipe cost are included in the calculation (each element is described by McAllister, 2014).

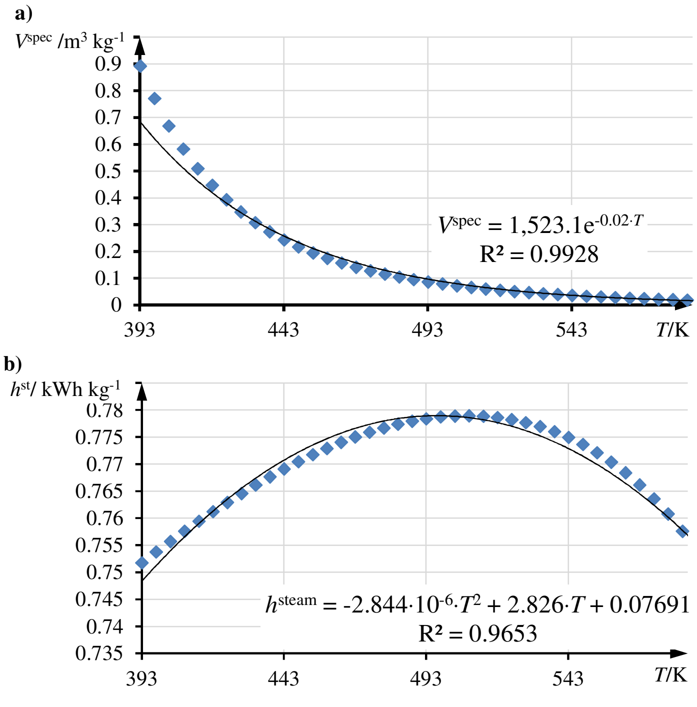

Figure 4-3: Derivation of equation for: a) specific volume and b) specific enthalpy depending on temperature

It is comprised of pipe material cost, cost of installation, right-of-way cost, and insulation cost. Note that the right-of-way cost presents the charge of utilising the land for the pipeline, where it is installed. Each of these cost terms, declared as positive variables, is formulated as having logical inequality by the binary variable $yt_{ph,pc,iu}$. Note that the inequalities (Eq. 4-55, Eq. 4-56 and Eq. 4-57) at the minimum solution point become active (the left hand sided of the inequalities become equal to the right hand sides) when a certain pipeline is selected, and redundant otherwise, thus rendering the cost term to obtain a zero value.
The weight of a pipe $w^{tot}_{ph,pc,iu}$ is defined by the following inequality (Eq. 4-55).

$$w^{tot}_{ph,pc,iu} \geq 1.49 \cdot \left(10.68 \cdot th^{pipe}_{ph,pc,iu} \cdot 39.37 \cdot d_{ph,pc,iu} \cdot 39.37\right) \cdot L_{ph,pc} \; -(1-yt_{ph,pc,iu}) \cdot w^{tot,UP}_{ph,pc,iu}$$
$$\forall ph \in PH, pc \in PC, iu \in IU \qquad (4\text{-}55)$$

A pipe's installation cost $pipe^{inst}_{ph,pc,iu}$ depends on the outer diameter of the pipe and its length as presented in Eq. 4-56.

$$pipe^{inst}_{ph,pc,iu} \geq \left(d_{ph,pc,iu} + 2 \cdot th^{pipe}_{ph,pc,iu}\right)^{0.43} \cdot L_{ph,pc} - \left(1 - yt_{ph,pc,iu}\right) \cdot pipe^{inst,UP}_{ph,pc,iu}$$
$$\forall ph \in PH, pc \in PC, iu \in IU \qquad (4\text{-}56)$$

The volume of the insulation $V^{ins}_{ph,pc,iu}$ has to be determined (Eq. 4-57), in order to calculate the insulation cost.

$$V^{ins}_{ph,pc,iu} \geq \pi \cdot \left(\left(d_{ph,pc,iu}/2 + th^{pipe}_{ph,pc,iu} + th^{ins}_{ph,pc,iu}\right)^2 - \left(d_{ph,pc,iu}/2 + th^{pipe}_{ph,pc,iu}\right)^2\right) \cdot L_{ph,pc}$$
$$-\left(1 - yt_{ph,pc,iu}\right) \cdot V^{ins,UP}_{ph,pc,iu}$$
$$\forall ph \in PH, pc \in PC, iu \in IU \qquad (4\text{-}57)$$

The cost of a pipeline is the sum of the material cost, installation cost, right-of-way cost, and the insulation cost of the pipe (Eq. 4-58).

$$c^{pipe} = c^{P1} \cdot \sum_{ph,pc,iu} w^{tot}_{ph,pc,iu} + c^{P2} \cdot \sum_{ph,pc,iu} pipe^{inst}_{ph,pc,iu} + c^{P3} \cdot \sum_{ph,pc,iu} yt_{ph,pc,iu} \cdot L_{ph,pc} + c^{P4} \cdot \sum_{ph,pc,iu} V^{ins}_{ph,pc,iu} \qquad (4\text{-}58)$$

Preheating due to unrecovered condensate

In the model presented so far it had been assumed that the condensate at the sink side would be completely recovered and recycled back to the source side. However, when running a Total Site, only a certain fraction of condensed water is returned to the source side processes. The preheating of fresh water is thus needed in order to compensate for the condensate losses. Note, that preheating can considerably decrease the amount of intermediate utilities that can be produced and transferred to the Sink Side. The set *IU* that had so far represented intermediate utilities' cold streams for steam boiling was extended by additional cold streams in order to account for the preheating of intermediate utilities. *IU* is now composed of two subsets and the indexes are defined:

- Index *iup* for cold streams presenting the needs of preheating, $iup \in IUP \subset IU$
- Index *iue* for cold streams presenting the evaporation, $iue \in IUE \subset IU$

Additional constraint makes the outlet temperature of the condensate equal to the inlet temperature of the intermediate utility on the Source Side.

$$TC^{HS,out}_{ph,iup,n,v} = TC^{HS,in}_{ph,iue,n,v} \qquad \forall ph \in PH,\ iup \in IUP,\ iue \in IUE,\ iue{=}iup,\ n \in N,\ v \in V \qquad (4\text{-}59)$$

The heat utilised for preheating is related to the heat for boiling according to their specific enthalpies, more precisely by the differences according to their specific enthalpies accounting for the preheating from a certain temperature and boiling at another temperature:

$$Ecc^{HS}_{ph,iup,n,v} / Ecc^{HS}_{ph,iue,n,v} = \Delta h^{liq}_{ph,iup,n,v} / \Delta h^{st}_{ph,iue,n,v}$$
$$\forall ph \in PH,\ iup \in IUP,\ iue \in IUE,\ iup{=}iue,\ n \in N,\ v \in V \qquad (4\text{-}60)$$

If the specific enthalpy for water h^{liq} in kWh/kg is defined as a function of temperature by the following correlation (Figure 4-4 and Eq. 4-61) derived from the steam tables (Koretsky, 2013):

$$h^{liq}_{ph,iup,n,v} = \left(1.321 \cdot 10^{-3} \cdot T^{HS}_{ph,iup,n,v} - 0.3853\right) \qquad \forall ph \in PH,\ iup \in IUP,\ n \in N,\ v \in V \qquad (4\text{-}61)$$

then the enthalpy difference between the outlet and inlet temperatures is:

$$\Delta h^{liq}_{ph,iup,n,v} = 1.321 \cdot 10^{-3} \cdot \left(TC^{\mathrm{HS,out}}_{ph,iup,n,v} - TC^{\mathrm{HS,in}}_{ph,iup,n,v}\right) \ \forall ph \in PH,\ iup \in IUP,\ n \in N,\ v \in V \ (4\text{-}62)$$

Similarly, the specific enthalpy for steam was already defined by Eq. 4-53. and the specific heat of the evaporation as the difference between the specific heats of steam and liquid:

$$\Delta h^{st}_{ph,iue,n,v} = \left(-2.55 \cdot 10^{-6} \cdot \left(TC^{HS,in}_{ph,iue,n,v}\right)^2 + 0.002549 \cdot TC^{HS,in}_{ph,iue,n,v} + 0.1418\right) -$$
$$\left(1.321 \cdot 10^{-3} \cdot T^{out,HS}_{ph,iup,n,v} - 0.3853\right)$$
$$\forall ph \in PH,\ iup \in IUP,\ iue \in IUE,\ iup{=}iue,\ n \in N,\ v \in V \qquad (4\text{-}63)$$

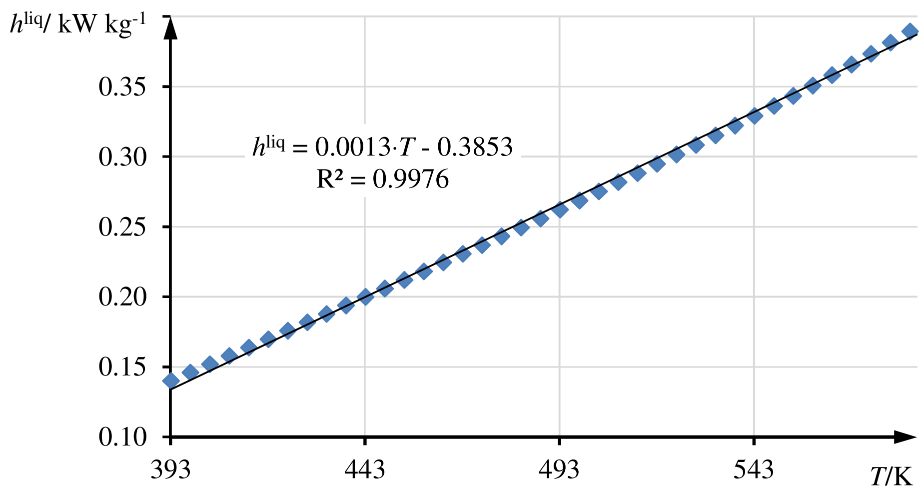

Figure 4-4: Derivation of equation for specific enthalpy of liquid depending on the temperature

Finally, as a fraction of condensate (f^{rec}) is reused, the preheating must be proportional to the condensate loss ($1-f^{\mathrm{rec}}$) and Eq. 4-60 is upgraded to Eq. 4-64.

$$Ecc^{HS}_{ph,iup,n,v} = \frac{\Delta h^{liq}_{ph,iup,n,v}}{\Delta h^{st}_{ph,iue,n,v}} \cdot Ecc^{HS}_{ph,iue,n,v} \cdot \left(1 - f^{rec}\right)$$
$$\forall ph \in PH,\ iup \in IUP,\ iue \in IUE,\ iup = iue,\ n \in N,\ v \in V \qquad (4\text{-}64)$$

Objective function and future utility prices

The Expected Net Present Value W_{ENPV} has been selected as an objective function,

$$W_{\mathrm{ENPV}} = -I + \sum_{n=1}^{t_{\mathrm{LT}}} \sum_{v} p_{n,v} \cdot \frac{F_{\mathrm{C},n,v}}{(1+r_{\mathrm{D}})^{n}} \qquad (4\text{-}65)$$

where $p_{n,v}$ are the probabilities related to periods n and price projections v. The after tax annual cash flow $F_{\mathrm{C},n,v}$ consists of operating cost savings and depreciation.

$$F_{\mathrm{C},n,v} = \left((1 - r_{\mathrm{T}}) \cdot \left(c^{tot}_{n,v} - c^{OP}_{n,v}\right) + r_{\mathrm{T}} \frac{I}{t_{\mathrm{LT}}}) \right) \qquad \forall n \in N,\ v \in V \qquad (4\text{-}66)$$

The savings are defined as the difference between the total cost $c^{tot}_{n,v}$ for external utilities as there was no Total Site heat integration and the actual cost $c^{OP}_{n,v}$ of external utilities. The total cost is further defined as:

$$c^{tot}_{n,v} = Ecc_{pc,j} \cdot t_{OP} \cdot c^{\mathrm{HU}}_{n,v} + Ech_{ph,i} \cdot t_{OP} \cdot c^{\mathrm{CU}}_{n,v} \qquad \forall n \in N,\ v \in V \qquad (4\text{-}67)$$

and the operating cost for the actual consumptions of external hot and cold utilities as:

$$c^{\mathrm{OP}}_{n,v} = \sum_{pc} \sum_{j} t_{\mathrm{OP}} \cdot Q^{\mathrm{HU}}_{pc,j,n,v} \cdot c^{\mathrm{HU}}_{n,v} + \sum_{ph} \sum_{i} t_{\mathrm{OP}} \cdot Q^{\mathrm{CU}}_{ph,i,n,v} \cdot c^{\mathrm{CU}}_{n,v} \qquad \forall n \in N,\ v \in V \qquad (4\text{-}68)$$

Note, that the trade-off between the investment and operating costs is usually obtained at current energy prices. However, energy prices have fluctuated considerably in the past and shown a progressive tendency to increase. As a similar trend is expected in the future, it would be more appropriate to perform the optimization of TS by considering future rather than current energy prices. Notable savings could thus be obtained. Therefore, cost coefficients for hot $c^{\mathrm{HU}}_{n,v}$, and cold utilities $c^{\mathrm{CU}}_{n,v}$, and probabilities $p_{n,v}$ are forecasted over time periods n and different price projections v for an entire lifetime (Nemet et al., 2013).

$$\begin{aligned} I = &\sum_{ph}\sum_{i}\sum_{iu}\sum_{k^{\mathrm{HS}}} cf_{iu} \cdot y^{HS}_{ph,i,iu,k^{HS}} + \sum_{pc}\sum_{iu}\sum_{j}\sum_{k^{\mathrm{CS}}} cf_{iu} \cdot y^{CS}_{ph,iu,j,k^{CS}} + \sum_{ph}\sum_{i} cf^{\mathrm{CU}} \cdot y^{\mathrm{CU}}_{ph,i} + \sum_{pc}\sum_{j} cf^{\mathrm{HU}} \cdot y^{\mathrm{HU}}_{pc,j} \\ &+ \sum_{ph}\sum_{i}\sum_{iu}\sum_{k^{\mathrm{HS}}} cv \cdot Fp^{\mathrm{HS}}_{ph,iu} \cdot A^{\mathrm{HS}}_{i,iu,k^{\mathrm{HS}}} + \sum_{pc}\sum_{iu}\sum_{j}\sum_{k^{\mathrm{CS}}} cv \cdot Fp^{\mathrm{CS}}_{pc,iu} \cdot A^{\mathrm{CS}}_{iu,j,k^{\mathrm{CS}}} \\ &+ \sum_{ph}\sum_{i} cv^{\mathrm{CU}} \cdot A^{\mathrm{CU}}_{ph,i} + \sum_{pc}\sum_{j} cv^{\mathrm{HU}} \cdot A^{\mathrm{HU}}_{pc,j} + c^{pipe} \end{aligned} \qquad (4\text{-}69)$$

Finally, the investment cost is accounted for by higher pressures regarding both the fixed and variable cost terms - the fixed cost coefficients being increased for higher pressure steam productions and the selected exchanger areas being multiplied by the pressure correction factor on the source side $Fp^{\mathrm{HS}}_{ph,iu}$ and the sink side $Fp^{\mathrm{CS}}_{pc,iu}$.

4.1.3 Case study 3

An illustrative case study based on a real case data was performed in order to demonstrate the developed methodology. It consisted of four processes P1-P4. Process P1 represents streams from a sulphuric acid production plant, while processes P2-P4 are a part of a refinery complex. The input data of the case study is presented in Table 4-1.

Table 4-1: Input data for process stream for case study

Process	stream	Type	T_{in}/°C	T_{out}/°C	CP/kW °C^{-1}	h/kW m^{-2} °C^{-1}
Process 1	P1-H1	Hot	980	430	19.92	0.065
	P1-H2	Hot	604	450	20.23	0.065
	P1-H3	Hot	518	190	20.23	0.065
	P1-H4	Hot	477	190	18.77	0.065
	P1-H5	Hot	433	180	15.10	0.065
Process 2	P2-C1	Cold	255	368	33.81	6.2
	P2-C2	Cold	75	561	2.44	6.2
Process 3	P3-C1	Cold	27	557	4	0.065
	P3-C2	Cold	274	366	141.6	6.2
Process 4	P4-C1	Cold	75	95	450	6.2

There were four intermediates available: (i) low-pressure steam, (ii) medium-pressure steam (iii) high-pressure steam, and (iv) ultra-high-pressure steam and two external utilities: (i) hot oil and (ii) a cold external utility. Table 4-2 contains the detailed input data on utilities together with the input data for the pipeline and other data. For the two external utilities, the forecasts of prices were made based on the historical prices from June 1986 until April 2014. Those prices were determined from gasoline prices (Index Mundi, 2012) by applying the methodology described in Ulrich and Vasudevan (2006). A curve showing the historical hot utility prices is presented in Figure 5a, while those for cold utility prices in Figure 5b with bases for five different projections. As can be seen in Figure 4-5, the current hot utility price is 0.1981 €/kWh, which could be expressed as a linear combination of Projection 3 (0.1940 €/kWh) and Projection 4 (0.2150 €/kWh), 0.1981=0.80*0.1940+0.20*0.2150, where 0.80 and 0.20 are the initial probabilities of the two projections. The probabilities of each projection in each year were derived at from these two initial probabilities by applying the MINLP model, as described in Appendix B. The pressure correction factor was 1 for the low-pressure steam, 1.1 for medium-pressure steam, 1.25 for high-pressure steam, and 1.5 for ultra-high-pressure stream (Viguri Fuente, 2013). The assumed life span of the Total Site was 15 y. In the objective function a 5 % discount rate and 2 % inflation was considered resulting in 7 % r_{D}. The tax rate r_{T} has been assumed at 20 %. When the optimization was performed at fixed pressure levels, the selected pressures were 3 bar for low-pressure steam, 10 bar for medium-pressure steam, 30 for high-pressure steam, and 70 bar for ultra-high-pressure steam.

Table 4-2: Input data for utilities and pipeline for the case study

Available utilities			
Utility type	Utility level	T/ °C	h/ kW/(m^2·°C)
intermediate utility	low pressure steam	120 – 148	10
	medium pressure steam	148 – 208	10
	high pressure steam	208 – 252	11
	ultra high pressure steam	252 –310	11
external utility	hot oil	382	15
	cold external utility	27 – 47	8

Pipeline		
Data	Value	Unit
thermal conductivity of insulation (Devki Energy Consultancy, 2006)	0.03	W/(m °C)$^{-1}$
coefficient for accounting the condensate pipeline, c^y	1.1	
friction factor of pipeline, μ	0.01885	
pipe cost per unit weight (Alibaba, 2014)	1.3	k€/t
installation cost (McAllister, 2014)	0.26	k€/m
right of way cost (McAllister, 2014)	80	k€/km

Distance between processes /km		
P1-P2	P1-P3	P1-P4
2.5	1.25	3.0

Other mechanical constants		
Data	Value	Unit
allowance for threading, mechanical strength, and corrosion, Al (Stovall, 1981)	0.065	in
Antoine constants for pressure/temperature relationship (valid for: 99-374°C) (DDBST, 2014)	A = 10.265, B= 1810.94 C= -28.655	Pa and K
maximum allowable stress in material, SE (Stovall, 1981)	0.4	psig

Other economical constants		
cost exponent, for different heat exchangers ac, cc, hc	1	
fixed charge for HE between process stream and cold utility, cf^{CU}	121.4	k€
fixed charge for HE between process stream and hot utility, cf^{HU}	121.4	k€
fixed charge for HE between process streams, cf	46.0	k€
variable charge of HE between two process streams, cv	2.742	k€/(m^{2}y)
variable charge of HE between process stream and cold utility, cv^{CU}	0.193	k€/(m^{2}y)
variable charge of HE between process stream and hot utility, cv^{HU}	0.193	k€/(m^{2}y)
Lifetime of the TS, t_{LT}	15	y
Annual operating hours, t_{OP}	8,500	h/y

The results are presented as follows. The solution obtained using the sequential approach, where Source and Sink Side HENs and the pipeline were optimised sequentially, is presented at fixed pressure levels. Further, these results were compared to those results when the Source and Sink Side HENs and the pipeline were synthesized simultaneously – the simultaneous approach. The comparison was made at fixed pressure levels at current utility prices. In the next step the pressure levels were flexible and considered as optimization variables. Therefore, the comparison is presented between the results of the model when optimized at fixed and flexible pressure levels. The comparisons between the results obtained at current or future utility prices are analysed next in order to evaluate their impact on the trade-off between investment and operating cost. In the last section, an example is discussed by considering the preheating of water due to unrecovered condensate.

The results are presented as follows. The solution obtained using the sequential approach, where source and sink side HENs and the pipeline were optimized sequentially, is presented at fixed pressure levels. Further, these results were compared to those results when the source and sink side HENs and the pipeline were synthesized simultaneously – the simultaneous approach. The comparison was made at fixed pressure levels at current utility prices. In the next step the pressure levels were flexible and considered as optimization variables. Therefore, the comparison is presented between the results of the model when optimized at fixed and flexible pressure levels. The comparisons between the results obtained at current or future utility prices are analysed next in order to evaluate their impact on the trade-off between investment and operating cost. In the following section an example is discussed by considering the preheating of water due to unrecovered condensate.

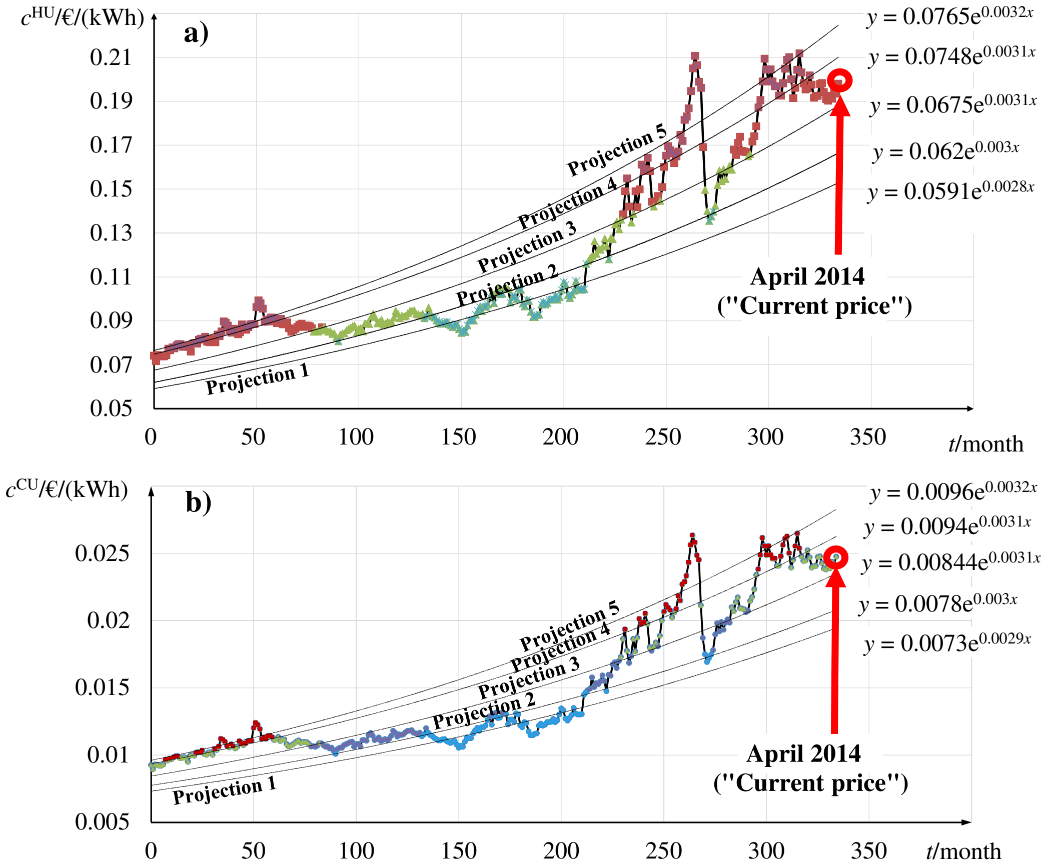

Figure 4-5: Historical data (from June 1986 until April 2014) for a) hot utility and b) cold utility price forecast projections

Synthesis of TS with sequential pipeline design

The sequential approach was performed over two steps. In the first step the optimization of TS was performed without considering the pipeline's design, when only the syntheses of the heat exchanger networks on both the source and sink sides were performed using some preselected temperature drops during transportation. The average ratio between the temperature changes on a unit of pressure change was determined from steam tables as 3 °C per 1 bar. 2 bar pressure drop were assumed, which resulted in 6 °C temperature drop. Note that pressure drop was estimated according to the rule of thumb the pressure drop of 1 bar/km.

In the second step the variables of the source side were fixed to the values obtained during the first step (the heat exchanger areas, heat loads, and the selected heat exchanger network matches). The optimisation was then performed using those fixed values; however, by considering now the pipeline design and also re-optimising the sink side HEN separately in order to adjust it to the overall TS heat balance updated for heat losses along the pipes. Table 3 presents the results obtained using the described sequential approach. The presented solution was taken as a reference solution, and then matched against the solutions obtained over the next simultaneous steps. The obtained solution for HEN for overall Total Site is presented in Fig. 4-6.

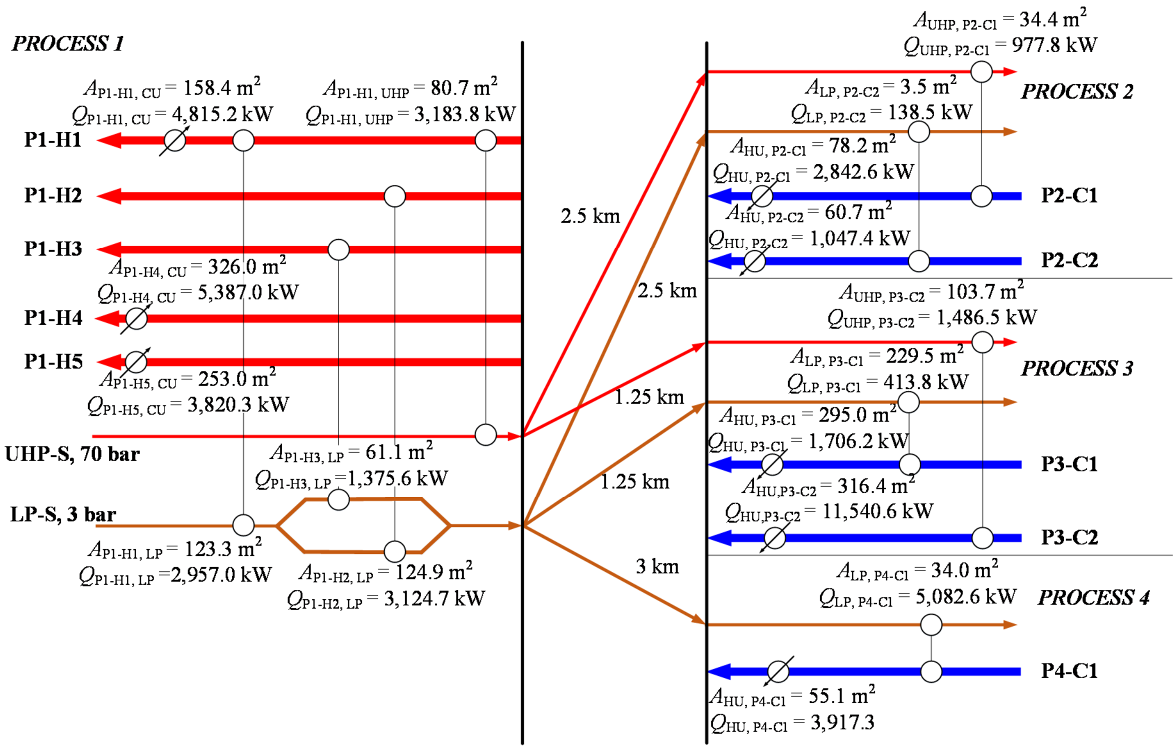

Figure 4-6: Solutions obtained by the sequential approach, which accounted for pipeline design by considering current utility prices with fixed pressure levels

Table 4-3: Comparison between the solutions obtained by the extended model at current utility prices with fixed and flexible pressure levels and those at future prices with flexible pressure levels.

OPTIMISATION	**ENPV /k€**	q^{REC_HS}/ kW	q^{loss}/ kW	q^{REC_CS}/ kW	$T^{c,in}$/°C	I^{HEN}/ k€	I^{pipe}/ k€	I^{Vins}/ k€	***I*/ k€**	q^{CU}/kW	q^{HU}/kW
		$q^{REC\_HS} - q^{loss} = q^{REC\_CS}$				$I^{HEN} + I^{pipe} + I^{Vins} = I$					
SEQUENTIAL APPROACH											
Case a) Current prices Fixed pressures Reference result	**140,116.3**	10,641.1	2,541.8	**8,099.3**	LP: 134.2 UHP: 285.9	4,246.6	2,285.0	113.1	**6,644.7**	**14,022.5**	**21,054.2**
SIMULTANOUES APPROACH											
Case b) Current prices Fixed pressures	**230,555.3**	22,913.3	10,273.9	**12,639.5**	LP: 134.2 MP: 180.7 UHP: 285.9	7,036.6	3,664.7	16.5	**10,717.8**	**1,750.3**	**16,514.1**
Case c) Current prices Flexible pressures	**306,012.4**	22,657.6	5,147.4	**17,510.2**	LP: 143.0 MP: 160.7 UHP 310.6	7,758.2	2,293.5	9.4	**10,061.1**	**2,006.0**	**11,643.4**
Case d) Future prices Flexible pressures	**360,664.8**	22,018.3	788.5	**21,229.9**	LP: 140,9 MP: 171.7 UHP:330	9,354.0	2,491.9	132.2	**11,978.1**	**2,645.3**	**7,923.7**
Difference between cases											
(b-a)	**90,439**	12,272.2	7,732.1	**4,540.2**		2,790.0	1379,7	-96,6	**4,073.1**	**-12,272.2**	**-4,540.2**
(c-b)	**75,457.1**	-255,7	-5,126.5	**4,870.7**		721.6	-1371,2	-7,1	**-656.7**	**255.7**	**-4,870.7**
(d-c)	**54,652.4**	-639,3	-4,358.9	**3,719.7**		1,595.8	198,4	122,8	**1,917.0**	**639.3**	**-3,719.7**
Total (d-a)	**220,548.5**	11,377.2	-1,753.3	**13,130.6**		5,107.4	206,9	19,1	**5,333.4**	**-11,377.2**	**-13,130.6**
Relative difference between cases/%											
(b-a)	**64.5**	115.3	304.2	**56.1**		65.7	60.4	-85.4	**61.3**	**-87.5**	**-21.6**
(c-b)	**32.9**	-1.1	-49.9	**38.5**		10.3	-37.4	-43.0	**-6.1**	**14.6**	**-29.5**
(d-c)	**17.9**	-2.8	-84.7	**21.2**		20.6	8.7	130.6	**19.1**	**31.9**	**-31.9**
Total (d-a)	**157.4**	106.9	69.0	**162.1**		120.3	9.1	16.9	**80.2**	**-81.1**	**-62.4**
Contribution of cases in total change of (d-a)											
(b-a)	**41.0**	107.9	-441.0	**34.6**		54.6	666.8	-505.8	**76.4**	**107.9**	**34.6**
(c-b)	**34.2**	-2.3	292.4	**37.1**		14.1	-662.7	-37.1	**-12.3**	**-2.3**	**37.1**
(d-c)	**24.8**	-5.6	248.6	**28.3**		31.3	95.9	642.9	**35.9**	**-5.6**	**28.3**

4.1.3.1 Synthesis of TS with simultaneous pipeline design

During further research the optimization of the pipeline design and layout was performed simultaneously with the synthesis of the Source and Sink Side HENs. Note that the cost of the pipeline for the recycling the condensate was estimated to be 10 % of the investment in the steam pipeline. In addition the amounts of heat and temperatures at which the produced steam was available for the Sink Side could significantly differ when the pipeline was included within the modelling. Further, the heat losses were also evaluated by optimizing the insulation thickness.

The solution obtained by the simultaneous approaches can be observed from Table 4-3 and the TS network arrangements can be seen in Figure 4-7 at fixed pressure level. It is reasonable to use the simultaneous approach, as the *ENPV* increased from 140,116 k€ to 230,555 k€ which is by 90,439 k€ (64.5 %). The fraction of heat loss along the pipeline compared to the amount of heat gained on the source side was in the case of the sequential approach 23.9 %, whilst for the simultaneous it reached 55.1 %. Note that the amount of heat gained on the source side by the simultaneous approach was significantly higher (12,272 kW or 115.3 %) than the one of the sequential approach (22,913.3 kW vs. 10,641.1 kW). When comparing the pipelines of the two different approaches it can be seen that the total lengths of the pipelines increased by 3 km (28.5 %) from 10.5 km to 13.5 km and the weight by 220.95 t (289.5 %), when using the simultaneous approach. However, despite the longer pipelines, the insulation volume decreased by 293.06 m^3 (85.5 %).

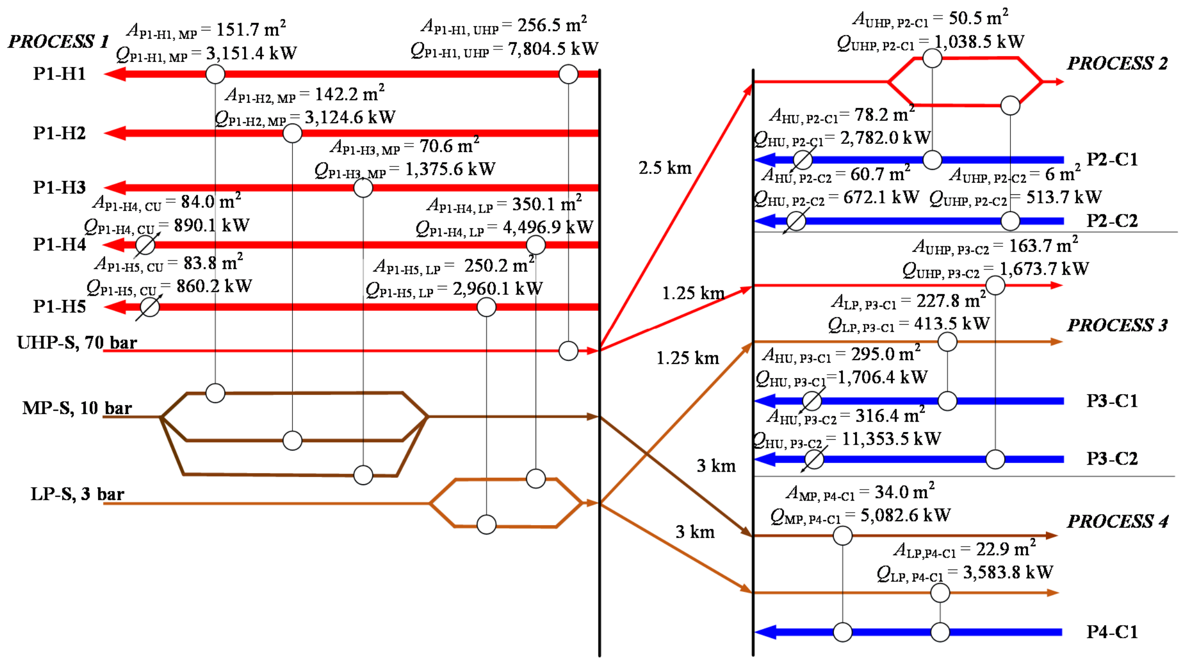

Figure 4-7: Solution obtained by the simultaneous approach, which accounted for pipeline design by considering current utility prices with a fixed pressure levels

From all these results it can be concluded that the simultaneous approach enables better heat recovery between processes. The difference occurs mainly because during the sequential approach the heat losses are neglected at the first step, where the amount of gained heat is reduced. The lower heat transfer regarding the source side results is compensated somewhat by the increased insulation. However, it does not enable to achieve the same heat recovery rate as the simultaneous approach. Modifications of the heat exchangers on the Source Side should also be considered in order to achieve better economic and heat recovery performances. The details about the network changes can be observed by comparison of networks obtain at the sequential approach in Figure 4-6 and the simultaneous approach presented in Figure 4-7.

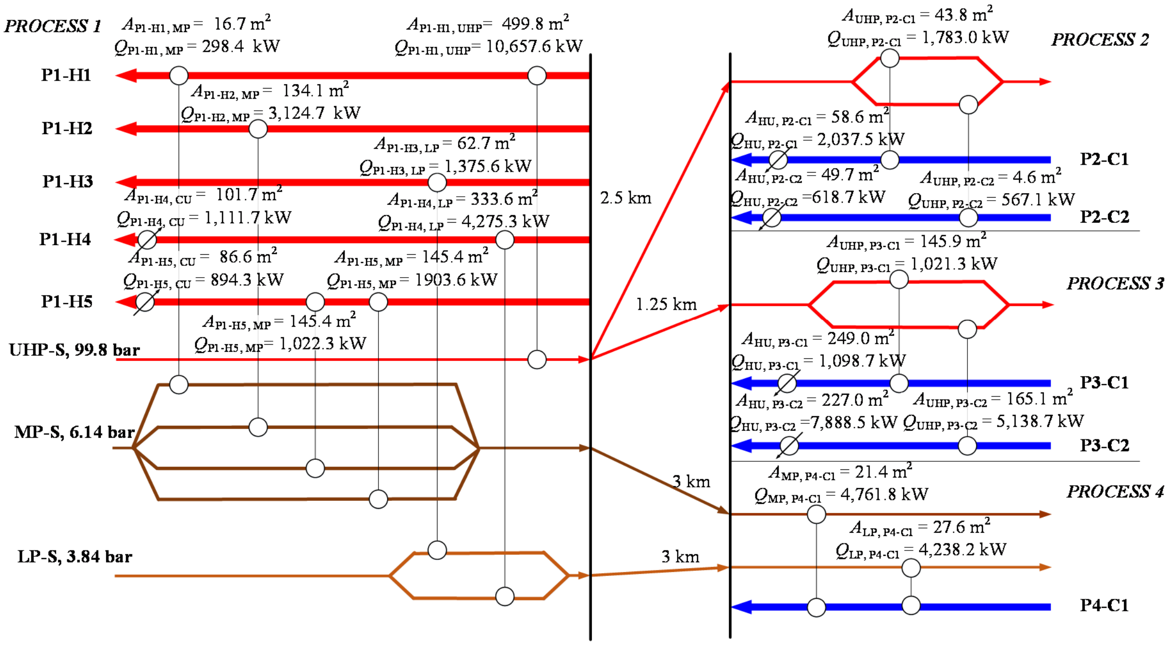

Figure 4-8: Solutions obtained by the simultaneous approach, which accounted for pipeline design by considering current utility prices with a flexible pressure levels

Table 4-3 also presents the results of the optimisation obtained by the simultaneous model at fixed and flexible pressure levels, and it confirmed the necessity of allowing pressure levels to be flexible during the synthesis of Total Site as the *ENPV* increased from 230,555 to 306,012 k€ (32.7 %). Besides the economic viability the result also indicates the improvement regarding external hot utility as it decreased by 4,870.7 kW (29.5 %), while the external cold utility consumption increased slightly by 255.7 kW (14.6 %). However, the increase in the cold utility consumption is more than balanced out with the decrease of external hot utility consumption. The layout of the pipeline has changed (Fig. 8) and the length decreased by 3.75 km from 13.5 km for the case with fixed pressure level to 9.75 km, when optimised at flexible pressure level. Also the heat losses were well reduced, when flexible pressure levels were considered, namely by 49.9 %.

The synthesis of Total Site including pipeline design considering future utility prices was also performed in order to evaluate the influence of the prices. The results are presented in Table 4-3 and the optimal TS network in Figure 4-9. As can be seen, significantly better economic performance was achieved when considering future prices as the *ENPV* additionally increased by 54,652 k€ (17.9 %). This was a result of better heat recovery for which higher investment (19.1 %) was needed. However, the external hot utility consumption decreased significantly, namely by 3,719 kW (31.9 %), while the cold utility consumption increased by 639 kW (31.8 %). However, the overall heat integration was better and one should take into account that external cold utility was cheaper. In the optimization, when considering future utility prices the heat losses were significantly lowered by 4,359 kW (84.7 %) compared to the optimisation at current utility prices. In the case of future utility prices at flexible pressure levels the heat losses represent only 3.6 % of the total heat generated, while in the case of current utility prices at flexible pressure level 22.7 %. This difference in the heat loss serves also for the explanation of the slightly decreased amount of heat generated in the case at future utility prices. A significant part of the investment represents the pipeline cost. When the TS was optimized at current energy prices with fixed pressure levels, the pipeline investment was 3,665 k€ or 34.2 % of the total investment and when the pressure levels were optimized, the pipeline investment considering current utility prices was decreased to 2,294 k€ or 22.8 % of the total investment, and enlarged to 2,492 k€ or 20.8 % when considering future prices.

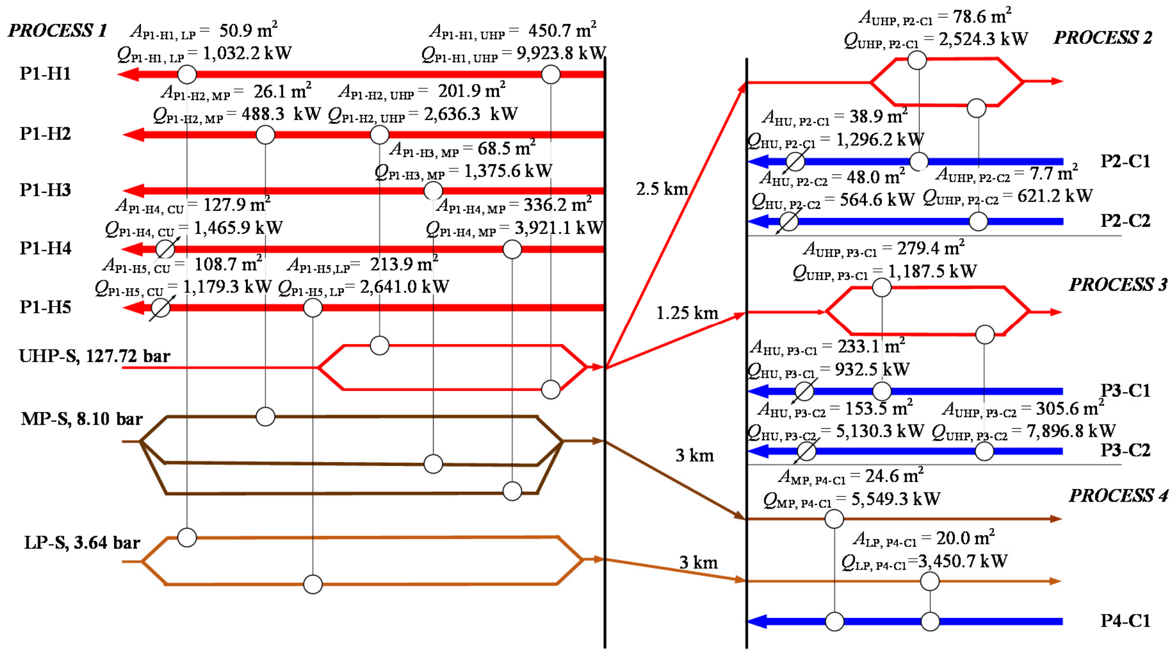

Figure 4-9: Solutions obtained by the simultaneous approach, which accounted for pipeline design by considering future utility prices with flexible pressure levels

The Total Site network differs, when it is synthesize at current energy prices (Figure 4-8) or at future energy prices (Figure 4-9) with flexible pressure levels. A structural change appeared, despite the same pipeline layout. In process P1, an on stream P1-H2 medium-pressure heat exchanger was moved to an ultra-high-pressure heat exchanger. However, the area of the heat exchangers for generating steam increased with the exception of the heat exchanger in P4 between low-pressure steam and process stream P4-C1. All these observations indicated that the trade-off moved towards higher investment and lower operational costs. The comparison between the pipeline design, when optimised at current prices and flexible pressure levels and future prices with flexible pressure levels, is presented in Table 4. The total length of the pipeline did not change and it was 9.75 km for both cases. However, the total weight of the pipe was increased by 94.5 t (73.8 %), due to thicker pipelines. As can be seen in Table 4-4 the average thickness of the insulation increased which resulted in a substantial increase in the insulation volume by 372.026 m^3 (1,307.7 %) and, hence, a significant decrease in heat loss (Table 4-3). The pressure drop and consequently the temperature drop had on average decreased when considering future energy prices, which additionally increased the amount of heat transferred.

Table 4-4: Comparison between the pipe design optimised at future utility prices with flexible pressure levels and current utility prices with flexible pressure levels.

	Pipeline segment	*d*/ cm	th^{pipe}/ mm	*L*/ km	*w*/ t	th^{ins}/ cm	V^{ins}/ m^3	p^{drop}/ bar	$T^{HS,out}$/ °C	$T^{CS,in}$/ °C
Case a) Future prices	P1-P2-UHP	12.7	10	2.5	76.517	8.2	147.261	0.239	330	329,9
	P1-P3-UHP	20.6	1.5	1.25	92.91	8.7	110.129	0.089	330	329,8
	P1-P4-LP	17.8	2	3	25.749	3.4	69.467	1.691	140.9	120
	P1-P4-MP	16.3	4	3	27.337	3.8	73.618	3.695	171.7	148
	TOTAL			**9.75**	**222.5**		**400.475**			
Case b) Current prices	P1-P2-UHP	4.4	4	2.5	10.508	0.5	2.218	3.516	330	308,5
	P1-P3-UHP	17.1	10	1.25	52.815	0.5	3.852	0.193	330	311.0
	P1-P4-LP	20.6	2	3	30.716	0.5	11.107	1.890	140.9	120
	P1-P4-MP	20.6	2	3	33.976	0.6	11.272	1.739	171.7	148
	TOTAL			**9.75**	**128.0**		**28.449**			
Difference (b-a)				0	94,5		**372,026**			
Difference/ %				0	73.8%		1,307.7%			

Further, the computational requirements were analysed. The results of different models were obtained by the General Algebraic Modelling System (GAMS) using the DICOPT solver, where the optimality gap was set at 0. The model consists of 78,000 constraints with approximately 30,000 continuous and 1,000 binary variables. This model size corresponds to the model, where the model reduction was applied by defining only 5 time periods over 15 years of lifetime rather than 15. The *ENPV* was calculated by setting the sum of discounted rate and inflation to the middle year of the period. Note that the model size was the same for all the optimisation since the same superstructure was applied to them. There was some difference in CPU time. The first step of the sequential approach required 403 s on Intel® Core™ i7-4770 CPU @ 3.4 GHz processor while the second step 222 s resulted altogether in 625 s. In comparison, the CPU time of the simultaneous approach with fixed pressure level considering current utility prices was 418 s. Obtaining a solution when allowing for flexible pressure was even faster as only 344 s of CPU time was required, whilst when considering future utility prices it doubled to 897 s.

4.1.3.2 Preheating of intermediate utilities because of unrecovered condensate

Hereby, the result is presented of the synthesis of Total Site by additionally considering a certain fraction of unrecovered condensate accounting for future prices of energy. The fraction f^{rec} was assumed as 70 %. Therefore, only 30 % of the water must be preheated. The result of optimization is presented in Table 4-5 and the optimal TS network in Fig. 4-10, where the dashed line represents the path of the condensate. Additional cold streams were introduced in order to tackle the preheating. The number of process streams in this study was 10 (5 hot at one hot side processes and 5 cold streams at three cold side processes). For each intermediate utility at each source side process one cold stream for preheating and one for evaporation were added (4x1x2 cold intermediate utility streams) and for each intermediate utility at each sink side processes one hot stream for condensation was added (4x3x1 hot intermediate utility streams). Altogether the problem had 17 hot and 13 cold streams.

Table 4-5: Solution of optimization using a simultaneous approach for future utility prices at flexible pressure level by considering preheating of unrecovered condensate

ENPV /k€	q^{REC_HS}/ kW	q^{loss_tot}/ kW	q^{REC_CS}/ kW	$T^{c,in}$/°C	*I*/ k€	q^{CU}/kW	q^{HU}/kW
321,165.0	**22,471.8**	q^{loss_tot}= **3,871,2** q^{loss}= 229.8 q^{cond} 3,641.4	**18,600.6**	LP: 138.7 MP: 157.8 UHP: 316.5	***I*= 11,619.5** I^{AHE}= 8,527.9 I^{PIPE}= 2,204.4 I^{Vins}= 887.2	**2,191.8**	**10,553.0**

The *ENPV* of the obtained solution was decreased to 321,165 k€, which is 39,500 k€ (11.0 %) lower compared to the solution without preheating (Table 4-3, Case d). This difference clearly indicates the necessity of considering the preheating; otherwise the consumption of external utilities could be significantly underestimated. Now, the cold utility consumption was decreased to 2,192 kW (17.1 %) and hot utility increased to 10,553 kW (33.2 %) compared to the solution assuming complete recover of the condensate obtained by the extended model with future utility prices. The heat transferred from hot streams to intermediate utility was 22,472 kW, while the heat transferred from intermediate utility to cold streams was 18,601 kW. The heat recovery within the Total Site was now decreased due to the heat losses, which were twofold.

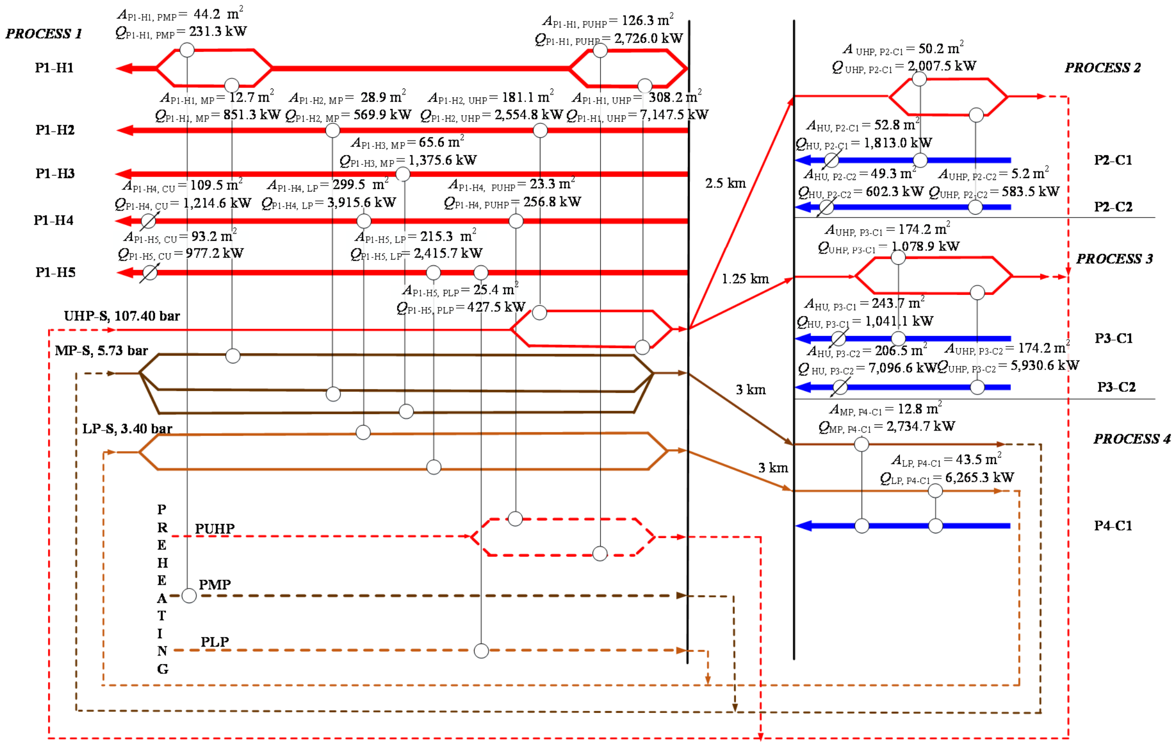

Figure 4-10: Synthesized network for Total Site obtained by the simultaneous model accounted for preheating and future utility prices.

There were heat losses during the steam transportation from the Source to the Sink Sides and, moreover, there are heat loss which occurred due to incomplete recovery of the condensate.

In the case presented the total heat loss during transportation along the pipeline was 230 kW, whilst the heat loss related to the unrecovered portion of condensate was 3,641 kW, which is 15.8 times higher than those through the pipeline. Altogether, the losses were 3,871 kW which represented 17.2 % of the total amount generated at the source site. It is interesting to note that the total investment was slightly decreased to 11,620 k€ and decreased by 359 k€ (3.0 %).

4.2 Simultaneous heat integration within process and process-to-process

4.2.1 Scheme of Total Site

The previously presented MINLP model approach considers only a part of the Total Site synthesis, as only segments after heat recovery at the process level are the input data. Therefore, the model can only be applied when sequential strategy is considered. Moreover, in the previously presented model the process are considered to be either source of heat or sink of heat that is selected during process of collecting input data. Altough, usually it is possible to estimate, which process could represent source and which sink side, there are situation, when this selection is not so straightforward. A new superstructure is required in order to address internal and process-to-process Heat Integration simultaneously as well as to consider the same process as source and sink of energy simultanously. A new Compact Superstructure enables to synthesising of Total Site following either sequential or simultaneous strategy.

4.2.1.1 Sequential Total Site Heat Integration.

The superstructure of the sequential approach is shown in Figure 4-11. Note that intermediate utilities are presented in the superstructures as additional cold and hot streams.

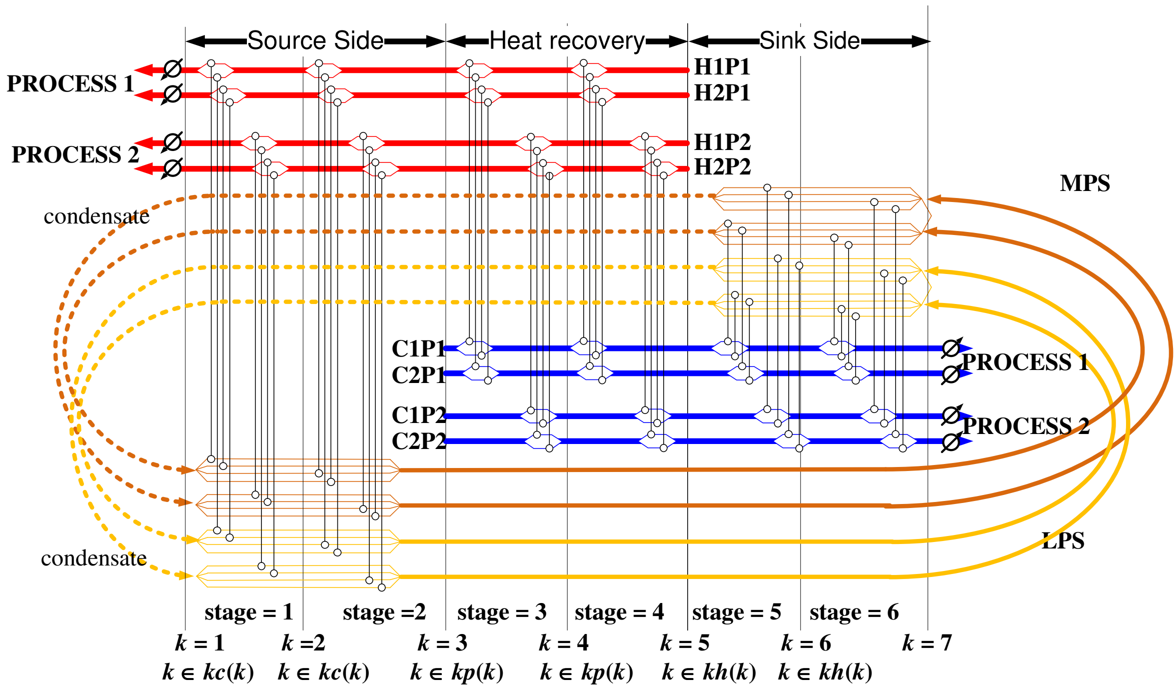

Figure 4-11: HEN superstructure for sequential Total Site Heat Integration for two processes, each with a pair of hot and cold process streams, and two intermediate utilities

They are produced at the Source Side from the residual heat, supplied by the process hot streams, and consumed at the Sink Side as intermediate hot utilities by the process cold streams. The synthesis applying the sequential approach is completed over two steps. In the first step, Heat Integration at the process levels within each process is achieved. For this purpose, only the hot process-cold process matches in the middle stages ($k \in kp(k)$) and the process stream-utility matches at the extreme ends of the superstructure are allowed for heat exchange, whilst matches between process streams and intermediate utility streams are forbidden. The residual parts of the hot and cold streams that represent Source and Sink Sides are identified in this way for each process. Then, the integration of those matches between the residual parts of the process streams on the one side and intermediate utilities on the other side is performed ($k \in kh(k)$ and $k \in kc(k)$) during the second step.

4.2.1.2 Simultaneous Total Site Heat Integration.

When Total Site synthesis is applied to both the process and the Total Site levels simultaneously (Figure 4-12), all possible matches between hot and cold process streams within each process, as well as between the hot process and the cold intermediate streams, and hot intermediate and cold process streams, are proposed within each stage in the simultaneous superstructure.

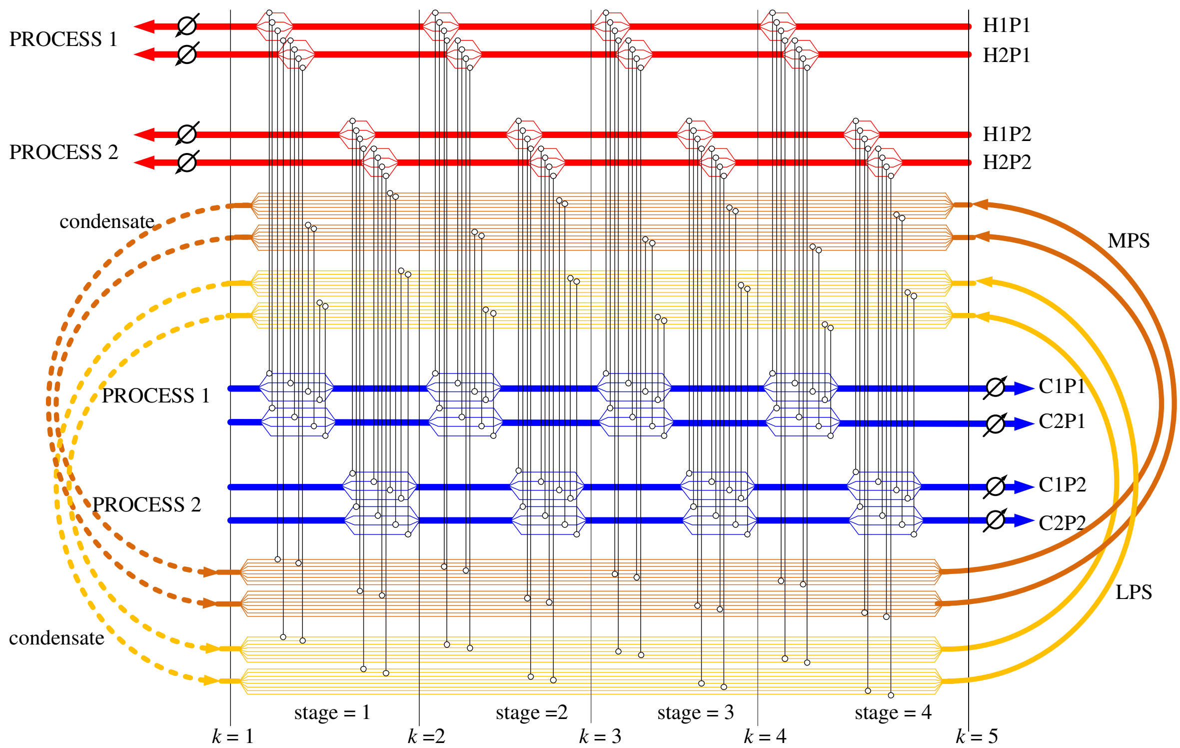

Figure 4-12: HEN superstructure for simultaneous Total Site Heat Integration for two processes, each with a pair of hot and cold process streams, and two intermediate utilities

The MINLP model developed in this work combines the simultaneous and sequential Heat Integration. The process-to-process heat exchange is traditionally performed via intermediate utility, however direct heat transfer between processes should also be considered. Therefore, the Compact Model has been upgraded in order to include also direct process-to-process heat transfer. The superstructure now considers heat exchanger and Heat Integration: i) within and between processes, and the selection of ii) indirect and/or iii) direct heat transfer between processes. Figure 4-13 presents a superstructure for two processes each with one hot and one cold process within one stage with two intermediate utilities (medium pressure steam –MPS and low pressure steam- LPS) available for indirect process-to-process heat transfer. The heat exchanger areas are determined from HE design equation on the basis of the amount of exchanged heat and the logarithm mean temperature difference, enabling optimisation of the temperature-driving forces for all types of heat exchange arrangements.

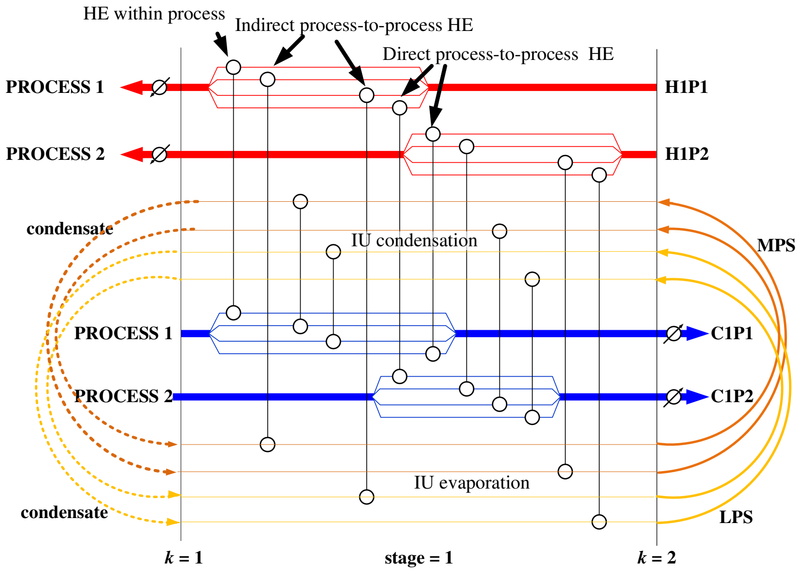

Figure 4-13: Superstructure for Total Site synthesis for two processes including one hot and cold process stream for one stage

4.3 Indirect process-to-process heat exchange

For an indirect process-to-process heat recovery two steps of heat exchanges occurs: the one from hot process streams to intermediate utilities and the other from intermediate utilities to cold process streams. The energy carrier of intermediate utilities is usually water steam at different pressures and temperatures with its latent heat taking advantage of rather high specific heat of evaporation/condensation. As this latent heat and its availability at different temperature very much depend on the pressure level, the pressure levels are also subjects of optimisation in order to gain as much heat as possible from one process and transferred it to other. The overall MINLP model besides HEN model includes also basic design equations for the pipeline considering its pressure levels, heat and pressure losses, and the diameters and thicknesses of pipes and insulation, in order to simultaneously achieve the optimal trade-off between investment of the pipes and heat exchangers and the heat transferred. Steam mains at different pressures are defined by segments (arks) between different processes (nodes) (Figure 4-14a). Heat balances for a Source node and a Sink node are schematically presented in Figure 4-14b. In a Source node the heat is transferred from hot process streams to an intermediate utility, providing heat for generation of that utility. In a Sink node cold process streams are then heated up by transferring the heat from the generated intermediate utility. Similarly, to steam transfer for condensate pipeline there is a Source and Sink node connected via segments, as well. Those nodes for condensate are complementary to the steam node. Hence, node for steam Source node is a Sink node for condensate and vice versa (Figure 4-14a). It should be noted that a process can be in principle Source and Sink with regards of intermediate utilities at the same time. However, in order to enable indirect process-to-process heat exchange in both direction, as from Process 1 to Process 2 in Figure 2a and vice versa, two alternative segments needs to be defined, one for each direction. Note that at most one of the segments can be selected for one intermediate utility level (Figure 4-14a).

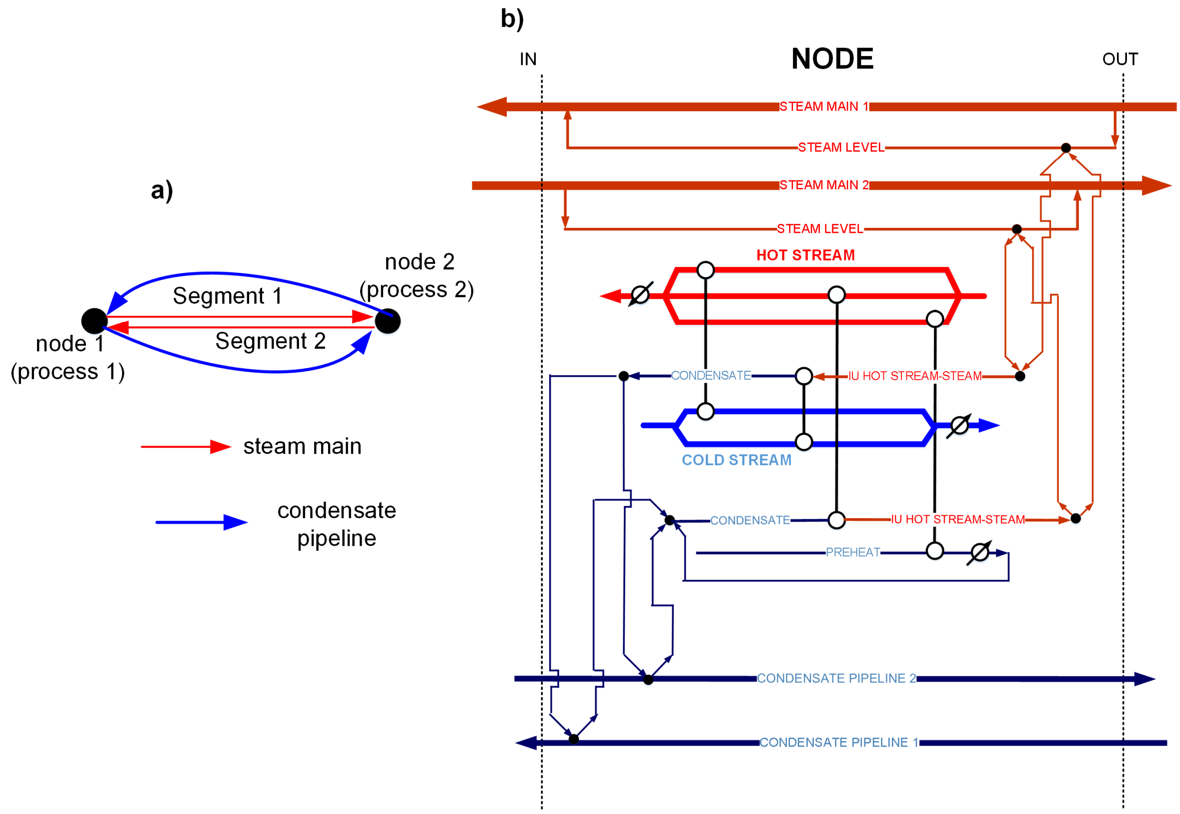

Figure 4-14: Nodes in indirect process-to-process heat exchange

4.4 Direct process-to-process heat exchange

For a direct process-to-process heat exchange it is assumed that cold process streams of one process are to be directed through pipes to hot process streams of another process because temperature differences between the pipes and the surrounding and the corresponding heat losses would be lower, compared to the situation when hot streams are directed to another process' cold streams. The heat losses along cold streams pipes should be considered in the stage heat balances as they significantly affect inlet and outlet temperatures of cold streams and, consequently also heat exchanger areas. The heat losses needs to be taken into account in both directions along the pipes: i) from cold streams to heat exchangers, $Q_{\mathrm{loss\_CSHS}}$, and ii) those from heat exchangers back to cold streams, $Q_{\mathrm{loss\_HSCS}}$ (Figure 4-15). Two sets of temperature losses occur, therefore. Because of the first ones the inlet temperatures of cold streams to heat exchangers are now lower than the left stage-boundary temperatures T_{k} of the superstructure, and because of the second ones the right stage-border temperatures $T_{\mathrm{k+1}}$ are now lower than the outlet temperatures of heat exchangers. Note that these temperature drops are determined as the amounts of heat losses divided by the streams heat capacity flow-rates. Note also that the amount of heat transferred from a hot stream Q_{HP} needs to be high enough to cover both heat losses ($Q_{\mathrm{loss\_CSHS}}$ and $Q_{\mathrm{loss\_HSCS}}$) in addition to the heat supplied to a cold process stream Q_{CP}.

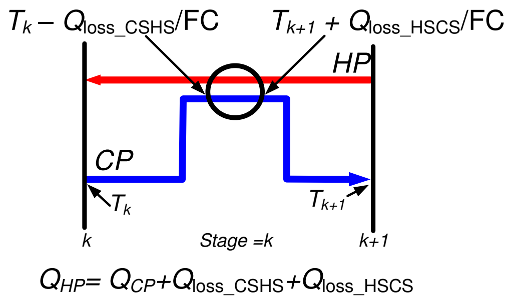

Figure 4-15: Direct process-to-process heat exchange

4.5 Stochastic multi-period MINLP model

The basic model contains the modelling of direct as well as the indirect process-to-process heat exchange, besides the process level heat exchange. A stochastic multi-period MINLP model has been developed in order to optimise a Total Site. The following sets and indexes were introduced within the model:

- Index *ap* for all processes included within the Total Site, $ap \in AP$
- Index *ic* for hot streams and condensates for intermediate utilities , $ic \in IC$
- Index *hp* for hot process streams, $hp \in HP \subset IC$
- Index *ihu* for steam intermediate utility as hot streams, $ihu \in IHU \subset IC$
- Index *hcond* for condensate from a hot intermediate utility, $hcond \in HCond \subset IC$
- Index *apic* for connecting the process to its hot process steams and condensates, $apic \in APIC$
- Index *jc* for cold streams and condensates, $jc \in JC$
- Index *cp* for cold process streams, $cp \in CP \subset JC$
- Index *icue* for steam intermediate utility as cold stream, $icue \in ICUE \subset JC$
- Index *icup* for water preheat for intermediate utility as a cold stream, $icup \in ICUE \subset JC$
- Index *icu* for intermediate utilities as cold stream including evaporation and preheating, $icu \in ICU \subset JC$
- Index *ccond* for condensate required for evaporation, $ccond \in CCond$
- Index *acjc* for connecting processes to their cold process streams and condensates, $acjc \in ACJC$
- Index *iu_iucond* for steam mains of intermediate utilities and the condensates pipeline, $iu\_iucond \in IU\_IUCond$
- Index *iu* for steam mains of intermediate utilities, $iu \in IU \subset IU\_IUCond$
- Index *iucond* for pipeline of condensates, $iucond \in IUCond \subset IU\_IUCond$
- Index *iul* for steam levels of intermediate utilities as steam, $iul \in IUL$
- Index *iuml* for assignment of an intermediate utility level to a steam main for the same intermediate utility, $iuml \in IUML,\ IUML \subset (IU \times IUL)$
- Index *iuhot* for assignment of an intermediate utility as hot stream to the steam main of intermediate utility, $iuhot \in IUHOT \subset (IU \times IC)$
- Index *iucold* for assignment of intermediate utility as cold stream to the steam of intermediate utility, $iucold \in IUCOLD \subset (IU \times JC)$
- Index *iucondhcond* for assignment of condensate as hot stream to the condensate pipeline, $iucondhcond \in IUCondHCond \subset (IUCond \times HCond)$

- Index *iucondccond* for assignment of condensate as cold stream to the pipeline of condensate, $iucondccond \in IUCondCCond \subset (IUCond \times CCond)$
- Index *iucondihu* for assignment of condensate pipeline to hot process stream, $iucondihu \in IUCondIHU \subset (IUCond \times IHU)$
- Index *icueicup* for assignment of cold intermediate utility stream for preheating to evaporation, $icueicup \in ICUEICUP \subset (ICUE \times ICUP)$
- Index *icueccond* for assignment of cold condensate stream to cold evaporation stream, $icueccond \in ICUECCond \subset (ICUE \times CCond)$
- Index *cpicup* for a union set of cold process stream and streams for preheating, $cpicup \in CPICUP = CP \cup ICUP$
- Index *iuicu* for assignment of steam cold process steam and preheating stream to steam main, $iuicu \in IUICU \subset (IU \times ICU)$
- Index *iuihu* for assignment of hot stream for intermediate utility to the steam main of the inlet process to the main, $iuihu \in IUIHU \subset (IU \times IHU)$
- Index *iuihu1* for assignment of hot stream for intermediate utility to the steam main of the outlet process from the main, $iuihu1 \in IUIHU1 \subset (IU \times IHU)$
- Index k for temperature locations at stage boundaries, $k \in K$
- Index *s_scond* for segments, $s\_scond \in S\_SCond$
- Index s for all steam main segments, $s \in S \subset S\_SCond$
- Index *scond* for all condensate pipeline segments, $scond \in SCond$
- Index *snod* for all nodes representing one process, $snod \in SNOD$
- Index *iuspipe* for assignment of mains to the segments, $iuspipe \in IUSpipe \subset (IU\_IUCond \times S\_SCond)$
- Index *ius* for assignment of steam mains to the segments, $ius \in IUS \subset (IU \times S)$
- Index *iucondscond* for assignment of condensate pipeline to the condensate segments, $iucondscond \in IUCondSCond \subset (IUCond \times SCond)$
- Index *assigsnod_ap* for assignment of process to the node, $assigsnod\_ap \in AssignSnod\_AP \subset (Snod \times AP)$
- Index *asingsnod_sin* for assignment of the steam segment entering the node, $asingsnod\_sin \in AssignSnod\_Sin \subset (Snod \times S)$
- Index *asingsnod_sout* for assignment of steam segment leaving the node, $asingsnod\_sout \in AssignSnod\_Sout \subset (Snod \times S)$
- Index *asingsnodcond_sin* for assignment of the condensate segment entering the node, $asingsnodcond\_sin \in AssignSnodCond\_Sin \subset (Snod \times SCond)$
- Index *asingsnodcond_sout* for assignment of steam segment leaving the node, $asingsnodcond\_sout \in AssignSnod\_Sout \subset (Snod \times SCond)$
- Index n for periods over time, $n \in N$
- Index v for different price projections, $v \in V$

The overall duties of hot process streams are calculated from Eqs. 4-70. The heat surplus of the hot streams which is determined as the temperature difference between inlet $T_{hp}^{\mathrm{H,in}}$ and outlet $T_{hp}^{\mathrm{H,out}}$ multiplied by heat capacity flow-rate CP_{hp}. It is transferred to a cold process stream within the same process and/or other process (direct process-to-process HI) $Q_{hp,cp,k}$ and/or to an intermediate or preheating stream (both presented by $Q_{hp,icu,k}$) and/or external cold utility Q_{hp}^{CU}.

$$\left(T_{hp}^{\mathrm{H,in}} - T_{hp}^{\mathrm{H,out}}\right) \cdot CP_{hp} = \sum_{cp}\sum_{k} Q_{hp,cp,k} + \sum_{icu}\sum_{k} Q_{hp,icu,k} + Q_{hp}^{\mathrm{CU}}$$
$$\forall\ hp \in HP,\ cp \in CP,\ k \in K,\ icu \in ICU \qquad (4\text{-}70)$$

The overall duties of cold process streams are determined as the temperature difference between outlet $T_{cp}^{\mathrm{C,out}}$ and inlet $T_{cp}^{\mathrm{C,in}}$ multiplied by its heat capacity flow-rate CP_{cp}. It can be covered from the hot process stream within the same process and/or from other processes $Q_{hp,cp,k}$ and/or intermediate $Q_{ihu,cp,k}$ and/or external Q_{cp}^{HU} hot utility. However, when a direct process-to-process heat exchange occurs, the heat losses in both directions ($Q_{hp,cp,k}^{loss,CSHS}$, $Q_{hp,cp,k}^{loss,HSCS}$) should be subtracted.

$$\left(T_{cp}^{\mathrm{C,out}} - T_{cp}^{\mathrm{C,in}}\right) \cdot CP_{cp} = \sum_{hp}\sum_{k} Q_{hp,cp,k} - \sum_{hp}\sum_{k} Q_{hp,cp,k}^{loss,CSHS} - \sum_{hp}\sum_{k} Q_{hp,cp,k}^{loss,HSCS} + \sum_{ihu}\sum_{k} Q_{ihu,cp,k} + Q_{cp}^{\mathrm{HU}}$$
$$\forall cp \in CP,\ hp \in HP,\ k \in K,\ ihu \in IHU \qquad (4\text{-}71)$$

The heat surplus of hot process stream *hp* during each stage *k* can be transferred to a cold process stream of any process or to an intermediate utility as a cold stream for evaporation as well as for preheating.

$$\left(TH_{hp,k+1} - TH_{hp,k}\right) \cdot CP_{hp} = \sum_{cp} Q_{hp,cp,k} + \sum_{icu} Q_{hp,icu,k}$$
$$\forall\ hp \in HP,\ cp \in CP,\ k \in K,\ icu \in ICU \qquad (4\text{-}72)$$

The heat duty of a cold process stream can be covered either by the heat surplus of a hot process stream or any process or from an intermediate utility as hot stream.

$$\left(TC_{cp,k+1} - TC_{cp,k}\right) \cdot CP_{cp} = \sum_{hp} Q_{hp,cp,k} + \sum_{ihu} Q_{ihu,cp,k} - \sum_{hp} Q_{hp,cp,k}^{loss,CSHS} - \sum_{hp} Q_{hp,cp,k}^{loss,HSCS}$$
$$\forall cp \in CP,\ hp \in HP,\ k \in K,\ ihu \in IHU \qquad (4\text{-}73)$$

The overall heat content for preheating steam $Ecp_{ap,icup}$ is determined as the temperature difference between the evaporation temperature of water $T_{icup}^{C,iu}$ and the inlet temperature of fresh water $T_{icup}^{c,in}$, multiplied by the required heat capacity flow-rate CP_{icup}^{var}.

$$\left(T_{icup}^{C,iu} - T_{icup}^{c,in}\right) \cdot CP_{icup}^{\mathrm{var}} = Ecp_{ap,icup} \qquad \forall icup \in ICUP,\ ap \in AP \qquad (4\text{-}74)$$

The heat duty of a preheating stream during each stage, depending on the temperature at the temperature boundary $TC_{icup,k}$, can be covered by the amount of heat transferred from the hot process stream $Q_{hp,icup,k}$.

$$\left(TC_{icup,k+1} - TC_{icup,k}\right) \cdot CP_{icup}^{\mathrm{var}} = \sum_{hp} Q_{hp,icup,k} \qquad \forall icup \in ICUP,\ hp \in HP,\ k \in K \qquad (4\text{-}75)$$

The non-integrated heat surplus of the hot process stream is transferred to the external cold utility Q_{hp}^{CU} during the last stage of superstructure (Eq. 4-76), whilst the external hot utility requirement is set as the heat transfer required during the first stage of superstructure for heating the cold process steam Q_{cp}^{HU} (Eq. 4-77) or preheating stream Q_{icup}^{HU} (Eq. 4-78).

$$CP_{hp} \cdot (TH_{hp,k=Ns+1} - T_{hp}^{H,out}) = Q_{hp}^{\mathrm{CU}} \qquad \forall\ hp \in HP \qquad (4\text{-}76)$$

$$CP_{cp} \cdot \left(T_{cp}^{\mathrm{C,out}} - TC_{cp,k=1}\right) = Q_{cp}^{\mathrm{HU}} \qquad \forall cp \in CP \qquad (4\text{-}77)$$

$$CP_{icup}^{\mathrm{var}} \cdot \left(T_{icup}^{\mathrm{C,iu}} - TC_{icup,k=1}\right) = Q_{icup}^{\mathrm{HU}} \qquad \forall icup \in ICUP \qquad (4\text{-}78)$$

The temperature variable for the hot stream during the last stage $TH_{hp,k=NS+1}$ is equal to inlet temperature $T_{hp}^{\mathrm{H,in}}$ (Eq. 4- 79), and the remaining ones monotonically decrease (Eq. 4-81). The first stage temperature of the cold stream and cold stream for preheating $TC_{cpicup,k=1}$ is equal to the inlet temperatures of these streams $T_{cpicup}^{\mathrm{C,in}}$ (Eq. 4-80), whilst the remaining ones are monotonically increasing (Eq. 4-82).

$$T_{hp}^{\mathrm{H,in}} = TH_{hp,k=NS+1} \qquad \forall hp \in HP \qquad (4\text{-}79)$$

$$T_{cpicup}^{\mathrm{C,in}} = TC_{cpicup,k=1} \qquad \forall cpicup \in CPICUP \qquad (4\text{-}80)$$

$$TH_{hp,k} \le TH_{hp,k+1} \qquad \forall hp \in HP,\ k \in K \qquad (4\text{-}81)$$

$$TC_{icup,k} \le TC_{icup,k+1} \qquad \forall cpicup \in CPICUP,\ k \in K \qquad (4\text{-}82)$$

The hot process stream's temperature during the first stage $TH_{hp,k=1}$ is greater or equal to the outlet temperature of the hot streams $T_{hp}^{\mathrm{H,out}}$.

$$TH_{hp,k=1} \ge T_{hp}^{\mathrm{H,out}} \qquad \forall hp \in HP \qquad (4\text{-}83)$$

The outlet temperature of the cold process stream $T_{cp}^{\mathrm{C,out}}$ is greater or equal to the temperature during the last stage of the cold stream $TC_{cp,k=NS+1}$.

$$T_{cp}^{\mathrm{C,out}} \ge TC_{cp,k=NS+1} \qquad \forall cp \in CP \qquad (4\text{-}84)$$

The outlet temperature of preheating stream is greater or equal to temperature in the last stage of cold stream.

$$T_{icup}^{\mathrm{C,iu}} \ge TC_{icup,k=NS+1} \qquad \forall cp \in CP \qquad (4\text{-}85)$$

The outlet temperature of preheating stream $T_{icup}^{\mathrm{C,iu}}$ must be equal to the temperature of the cold intermediate utility stream during evaporation $T_{icue}^{\mathrm{C,iu}}$.

$$T_{icup}^{\mathrm{C,iu}} = T_{icue}^{\mathrm{C,iu}}$$
$(iu, icue) \in IUCOLD \wedge (iu, icup) \in IUCOLD \wedge (ap,icue) \in APJC \wedge (ap,icup) \in APJC \wedge (iu,s) \in IUS \wedge (snod, ap) \in AsignSnodAp \wedge (snod, s) \in AsignSnodSout$ (4-86)

A logical constraint for selecting (binary variable $y_{hp,cp,k}$ is set at 1) or if rejecting ($y_{hp,cp,k}$ is set at 0) a match between the hot and cold process streams within the same process is defined by Eq. 4-87 and when a direct process-to-process heat exchange occurs the Eq. 4-87 is modified somewhat, as can be seen in Eq. 4-88.

$$Q_{hp,cp,k} - \min\left(Ech_{hp}, Ecc_{cp}\right) \cdot y_{hp,cp,k} \leq 0 \qquad \forall hp \in HP,\ cp \in CP,\ k \in K, (hp,cp) \in SameAP \qquad (4\text{-}87)$$

$$Q_{hp,cp,k} - Ech_{hp} \cdot y_{hp,cp,k} \leq 0 \qquad \forall hp \in HP,\ cp \in CP,\ k \in K,\ (hp,cp) \in NotSameAP \qquad (4\text{-}88)$$

For the matches $y_{hp,icu,k}$ between the hot process stream and the intermediate utility as a cold process stream, the selection of matches is performed by applying Eq. 4-89.

$$Q_{hp,icu,k} - Ech_{hp} \cdot y_{hp,icu,k} \leq 0 \qquad \forall hp \in HP,\ icu \in ICU,\ k \in K \qquad (4\text{-}89)$$

The selection of matches $y_{ihu,cp,k}$ to cover the heat demand of the cold process stream via intermediate utility is made by employing Eq. 4-90.

$$Q_{ihu,cp,k} - Ecc_{cp} \cdot y_{ihu,cp,k} \leq 0 \qquad \forall ihu \in IHU,\ cp \in CP,\ k \in K \qquad (4\text{-}90)$$

Furthermore, the selection for eventual cooling of the hot stream by external cold utility (y_{hp}^{CU}) is performed by harnessing Eq. 4-91 and for the selection of eventual heating of cold process stream or stream for preheating by the external hot utility (y_{cpicup}^{HU}) by Eq. 4-92.

$$Q_{hp}^{\mathrm{CU}} - Ech_{hp} \cdot y_{hp}^{\mathrm{CU}} \leq 0 \qquad \forall hp \in HP \qquad (4\text{-}91)$$

$$Q_{cpicup}^{\mathrm{HU}} - Ecc_{cpicup} \cdot y_{cpicup}^{\mathrm{HU}} \leq 0 \qquad \forall cpicup \in CPICUP \qquad (4\text{-}92)$$

The binary variables are used to activate and deactivate the approach temperature differences between: i) hot and cold process streams at each temperature location $\Delta T_{hp,cp,k}$ (Eq. 4-93 and Eq. 4- 94), ii) hot process stream and intermediate utility as a cold stream $\Delta T_{hp,icu,k}$ (Eq. 4-95 and Eq. 4-96), and iii) intermediate utility as a hot stream and cold process stream $\Delta T_{ihu,cp,k}$ (Eq. 4-97 and Eq. 4-98). It should be noted that when a direct process-to-process heat exchange occurs the temperature drop due to heat losses ($Q_{hp,cp,k}^{loss\_\mathrm{CSHS}}$ and $Q_{hp,cp,k}^{loss\_\mathrm{HSCS}}$) should be taken into account.

$$\Delta T_{hp,cp,k} \leq TH_{hp,k} - TC_{cp,k} - \frac{Q_{hp,cp,k}^{loss\_\mathrm{CSHS}}}{CP_{cp}} + \gamma_{hp,cp} \cdot \left(1 - y_{hp,cp,k}\right) \qquad \forall hp \in HP,\ cp \in CP,\ k \in K \qquad (4\text{-}93)$$

$$\Delta T_{hp,cp,k+1} \leq TH_{hp,k+1} - TC_{cp,k+1} + \frac{Q_{hp,cp,k}^{loss\_\mathrm{HSCS}}}{CP_{cp}} + \gamma_{hp,cp} \cdot \left(1 - y_{hp,cp,k}\right)$$

$$\forall hp \in HP,\ cp \in CP,\ k \in K \qquad (4\text{-}94)$$

$$\Delta T_{hp,icu,k} \leq TH_{hp,k} - TC_{icu}^{\mathrm{IU}} + \gamma_{hp,icu} \cdot \left(1 - y_{hp,icu,k}\right) \qquad \forall hp \in HP,\ icu \in ICU,\ k \in K \qquad (4\text{-}95)$$

$$\Delta T_{hp,icu,k+1} \leq TH_{hp,k+1} - TC_{icu}^{\mathrm{IU}} + \gamma_{hp,icu} \cdot \left(1 - y_{hp,icu,k}\right) \qquad \forall hp \in HP,\ icu \in ICU,\ k \in K \qquad (4\text{-}96)$$

$$\Delta T_{ihu,cp,k} \leq TH_{ihu}^{IU} - TC_{cp,k} + \gamma_{ihu,cp} \cdot \left(1 - y_{ihu,cp,k}\right) \qquad \forall ihu \in IHU,\ cp \in CP,\ k \in K \qquad (4\text{-}97)$$

$$\Delta T_{ihu,cp,k+1} \leq TH_{ihu}^{IU} - TC_{cp,k+1} + \gamma_{ihu,cp} \cdot \left(1 - y_{ihu,cp,k}\right) \qquad \forall ihu \in HP,\ cp \in CP,\ k \in K \qquad (4\text{-}98)$$

The outlet temperature of the external hot utility $T^{\mathrm{HU,out}}$ is chosen so that the approach temperature difference $\Delta T_{cpicup}^{\mathrm{HU}}$ during the last stage between the cold process stream or cold stream for preheating and hot utility is always positive.

$$\Delta T_{cpicup}^{\mathrm{HU}} \leq T^{\mathrm{HU,out}} - TC_{cpicup,k=NS+1} \qquad \forall cp \in CP \qquad (4\text{-}99)$$

Similarly, the outlet temperature of the external cold utility $T^{\mathrm{CU,out}}$ is chosen so that the approach temperature difference $\Delta T_{hp}^{\mathrm{CU}}$ during the first stage between the hot stream and this cold utility is always positive.

$$\Delta T_{hp}^{\mathrm{CU}} \leq TH_{hp,k=1} - T^{\mathrm{CU,out}} \qquad \forall hp \in HP \qquad (4\text{-}100)$$

Amount of heat transferred from the hot process stream to the intermediate utility within one process $Ecc_{ap,iu}^{HS}$ is a sum of the heat transfers within this process (Eq. 4-101)

$$Ecc_{ap,iu}^{HS} = \sum_{icue \in ICUE \wedge hp \in HP \wedge k \in K \wedge (iu,icue) \in IUCOLD \wedge (hp,icue) \in SameAP \wedge (ap,hp) \in APHP} Q_{hp,icue,k}$$

$\forall ap \in AP$, $iu \in IU$, $snod \in Snod$, $s \in S$, $(iu, s) \in IUS$, $(snod, ap) \in AssignSnodAP$, $(snod, s) \in AssignSnod\_Sout$ (4-101)

Similarly, the amount of heat transferred from the intermediate utility to the cold process streams within one process $Ech_{ap,iu}^{CS}$ is a sum of the heat transfers within this process (Eq. 4-102)

$$Ech_{ap,iu}^{CS} = \sum_{ihu \in IHU \wedge cp \in CP \wedge k \in K \wedge (iu,ihu) \in IUHOT \wedge (ihu,cp) \in SameAP \wedge (ap,cp) \in APJC} Q_{ihu,cp,k}$$

$\forall ap \in AP$, $iu \in IU$, $snod \in Snod$, $s \in S$, $(iu,s) \in IUS$, $(snod, ap) \in AssigSnod\_AP$, $(snod,s) \in AssignSnod\_Sin$ (4-102)

The pressure in the pipeline p_{icue}^{HS} is determined from the outlet temperature of the intermediate utility TC_{icue}^{IU} (Eq. 4-103). The temperature on the utilisation of steam TH_{ihu}^{IU} is determined from the pressure in pipeline p_{ihu}^{CS} after pressure drop is considered (Eq. 4-104).

$$p_{icue}^{\mathrm{HS}} = 10\ \exp\left(\mathrm{A} - \left(\frac{B}{C + TC_{icue}^{\mathrm{IU}}}\right)\right) \qquad \forall ice \in ICU \qquad (4\text{-}103)$$

$$p_{ihu}^{\mathrm{CS}} = 10\ \exp\left(\mathrm{A} - \left(\frac{B}{C + TH_{ihu}^{\mathrm{IU}}}\right)\right) \qquad \forall ihu \in IHU \qquad (4\text{-}104)$$

However, when no pipeline is considered, the temperature of the intermediate utility as a hot stream TH_{ihu}^{IU} is equal to the outlet temperature of the intermediate utility as a cold stream TC_{icu}^{IU}. The same relation is also valid for the pressure (Eq. 4-106).

$$TC_{icu}^{IU} = TH_{ihu}^{IU} \qquad \forall icu \in ICU,\ ihu \in IHU \wedge (ihu, icu) \notin IHUICU1 \qquad (4\text{-}105)$$

$$p_{icu}^{HS} = p_{ihu}^{CS} \qquad \forall icu \in ICU,\ ihu \in IHU \wedge (ihu, icu) \notin IHUICU1 \qquad (4\text{-}106)$$

For pipeline design and condensate-return purposes the ratio $R_{iu}^{liq\_st}$ between the specific enthalpy should be determined between the specific enthalpy of water preheating $\Delta h_{iu}^{liq,spec}$ and evaporation $\Delta h_{iu}^{st,spec}$ at certain temperatures. The water preheating enthaphy was determined as the difference between specific enthaphy of water at evaporation temperature $h_{iu}^{liq,spec}$ and the specific enthalphy of water at the inlet temperature of fresh water hp^{in}. The evaporation enthaphy is determined as the difference between the specific enthaphy of steam $h_{iu}^{st,spec}$ and water at the temperature of evaporation. The specific enthalpy for water $h_{iu}^{liq,spec}$ and for steam $h_{iu}^{st,spec}$ depending on the temperature were derived at from the steam tables, when the temperature is within a temperature range 393-603 K.

$$R_{iu}^{liq\_st} = \frac{\Delta h_{iu}^{liq,spec}}{\Delta h_{iu}^{st,spec}} = \frac{h_{iu}^{liq,spec} - hp^{in}}{h_{iu}^{st,spec} - h_{iu}^{liq,spec}} \qquad \forall\ iu \in IU \qquad (4\text{-}107)$$

The enthalpy difference for saturated liquid can be derived at from steam tables, as presented in Figure 4-16. Therefore, the specific enthalpy difference for liquid depending on temperature can be described using the following equation, where hp^{in} is the specific enthalpy at the inlet temperature of fresh water.

$$\Delta h_{iu}^{liq,spec} = 1.32 \cdot 10^{-3} \cdot \sum_{icue \in ICUE \wedge (iu, icue) \in IUICUE} TC_{icue}^{IU} - 0.3853 - hp^{in}$$

$$\forall iu \in IU,\ icue \in ICUE \qquad (4\text{-}108)$$

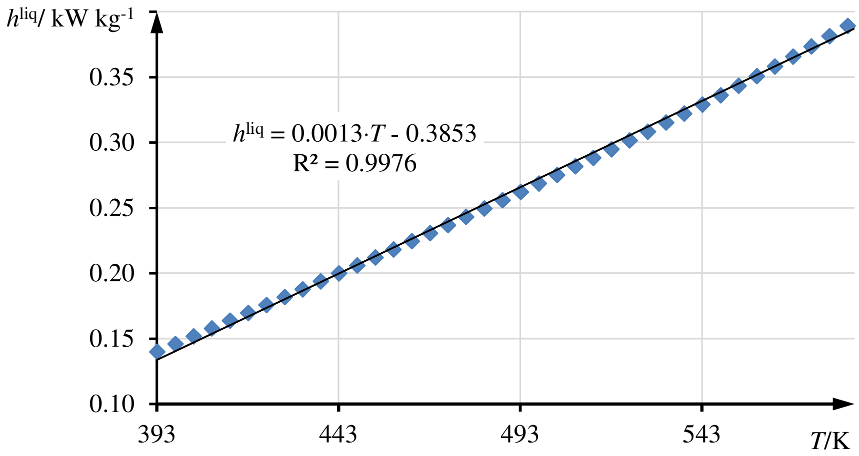

Figure 4-16: Derivation of equation for specific enthalpy for liquid depending on the temperature within temperature range 393-603 K

The specific enthalpy difference for steam is the difference between the specific enthalpy of steam and liquid at a certain temperature. Therefore, the derivation of specific enthalpy of steam is required (Figure 4-17).

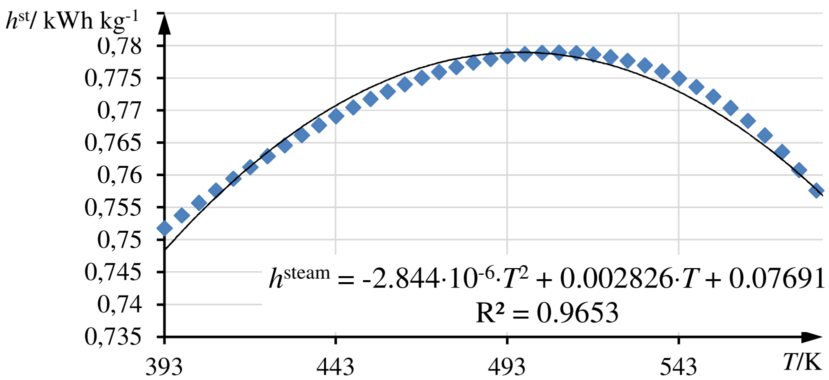

Figure 4-17: Derivation of equation for specific enthalpy of steam depending on temperature

As can be seen in Figure 4-17, the relationship between a specific enthalpy and temperature is nonlinear. However, as the difference between the specific enthalpy of steam and water is required, the derivation of the equation was performed regarding this difference (Figure 4-18). As can be seen, the derivation of specific enthalpy difference is a better option, as the equation derivation can be performed at higher accuracy, especially, when the derivation is made for each intermediate utility level separately. In this case the linear equation derivation can be regarded as acceptably accurate.

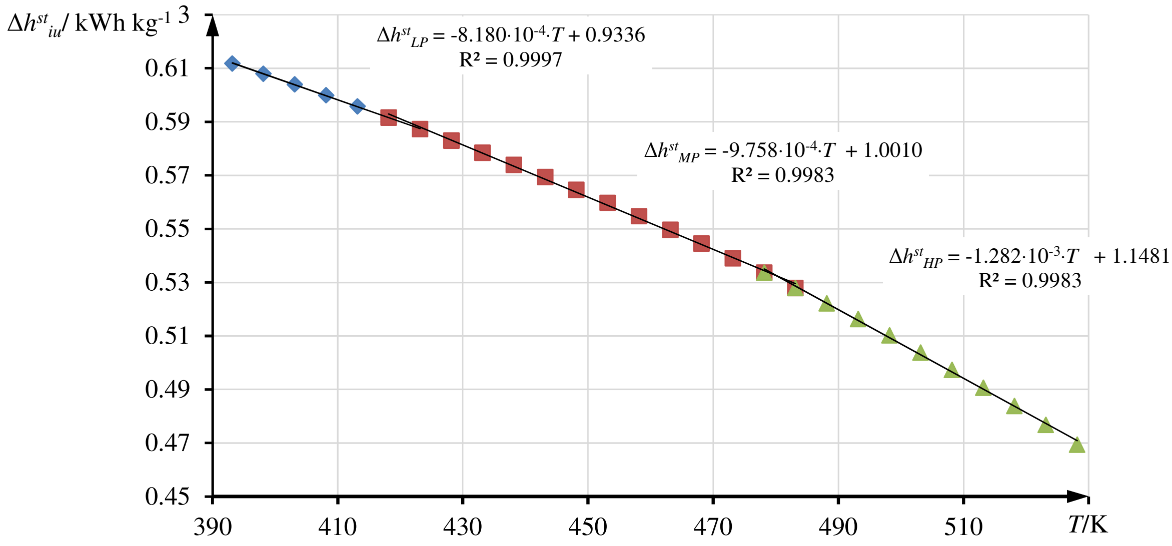

Figure 4-18: Equation derivation of the specific enthalphy of evaporation depending on the temperature

$$\Delta h_{iu}^{st} = -8.180 \cdot 10^{-4} \cdot \sum_{icue \in ICUE \wedge (iu,icue) \in IUICUE} TC_{icue}^{IU} + 0.9336 \qquad \forall iu \in IU,\ icue \in ICUE \tag{4-109}$$

$$\Delta h_{iu}^{st} = -9.758 \cdot 10^{-4} \cdot \sum_{icue \in ICUE \wedge (iu,icue) \in IUICUE} TC_{icue}^{IU} + 1.001 \qquad \forall iu \in IU,\ icue \in ICUE \tag{4-110}$$

$$\Delta h_{iu}^{st} = -1.282 \cdot 10^{-3} \cdot \sum_{icue \in ICUE \wedge (iu,icue) \in IUICUE} TC_{icue}^{IU} + 1.1481 \qquad \forall iu \in IU,\ icue \in ICUE \tag{4-111}$$

The specific enthalpy of evaporation and water preheating were determined, as they are applied in equations for pipeline design optimisation. The ratio between them could be determined as the ratio of the derived equations, however, in this case the inaccuracies of the derivations are multiplying. Therefore, more accurate derivation was obtain (Figure 4-19) by determining an equations of derivation for a certain inlet temperature of fresh water for each intermediate utility separately, as follows:

$$R_{LP}^{liq-st} = 2.291 \cdot 10^{-3} \cdot \sum_{icue \in ICUE \wedge (iu,icue) \in IUICUE} TC_{icue}^{IU} - 0.7015 \qquad \forall iu \in IU,\ icue \in ICUE \tag{4-112}$$

$$R_{MP}^{liq-st} = 2.772 \cdot 10^{-3} \cdot \sum_{icue \in ICUE \wedge (iu,icue) \in IUICUE} TC_{icue}^{IU} - 0.9161 \qquad \forall iu \in IU,\ icue \in ICUE \tag{4-113}$$

$$R_{LP}^{liq-st} = 3.888 \cdot 10^{-3} \cdot \sum_{icue \in ICUE \wedge (iu,icue) \in IUICUE} TC_{icue}^{IU} - 1.4529 \qquad \forall iu \in IU,\ icue \in ICUE \tag{4-114}$$

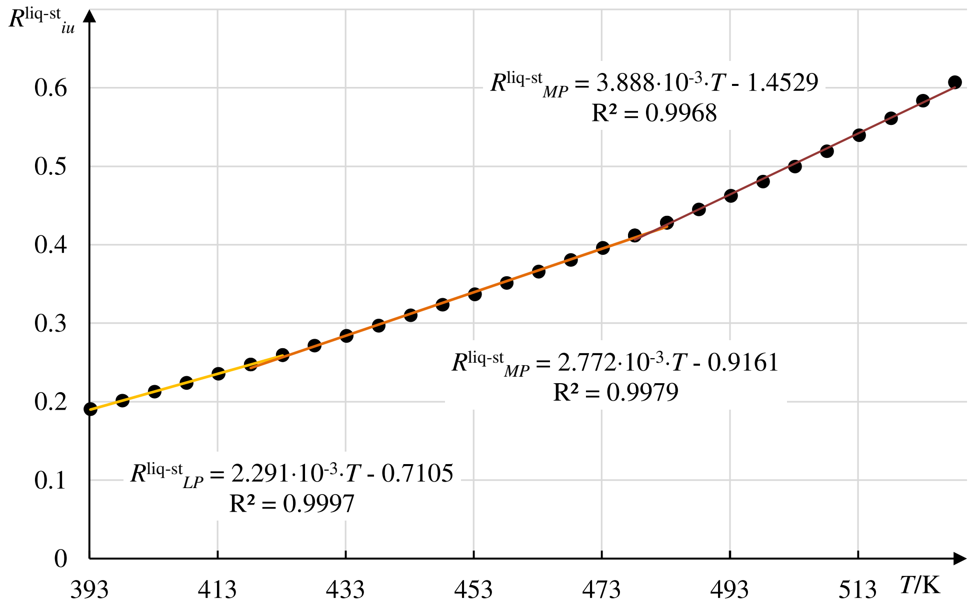

Figure 4-19: Equation derivation for ration between enthaphy of water for preheating and evaporation depending on the temperature for inlet temperature of fresh water at 293 K

In this approach the ratio between the enthalpy difference of water preheating and evaporation can be determined as a linear function of temperature withing each temperature interval of certaing intermediate utility.

4.5.1.1 Condensate heat balances

Water at the required temperature of evaporation should be available, in order to enable feasible heat recovery at Total Site level via intermediate utility. The required enthaphy in water $EC^{cond,tot}_{ap,ccond}$ is determined from the heat content of steam $Ecc^{HS}_{ap,iu}$, from the following equation:

$$EC^{cond,tot}_{ap,ccond} = Ecc^{HS}_{ap,iu} \cdot R^{liq\_st}_{iu}$$

$\forall\ ap \in AP$, $iu \in IU$, $ccond \in CCond$, $s \in S$, $snod \in Snod$, $(ap, ccond) \in APJC$, $(iu, ccond) \in IUCOLD$, $(iu, s) \in IUS$, $(snod, ap) \in AssignSnod\_AP$, $(snod, s) \in AssignSnos\_Sout$ (4-115)

The total amount of heat can be covered from condensate recovery $EC^{cond}_{ap,ccond}$ or from preheating of fresh water $Ecp_{ap,icup}$.

$$EC^{cond,tot}_{ap,ccond} \leq Ecp_{ap,icup} + EC^{cond}_{ap,ccond} + qh_{Ccond}$$

$\forall\ ap \in AP$, $iu \in IU$, $icup \in ICUP$, $ccond \in CCond$, $s \in S$, $snod \in Snod$, $(ap, icup) \in APJC$, $(ap, ccond) \in APJC$, $(iu, icup) \in IUCOLD$, $(iu, ccond) \in IUCOLD$, $(iu, s) \in IUS$, $(snod, ap) \in AssignSnod\_AP$, $(snod, s) \in AssignSnod\_Sout$ (4-116)

The amount of heat available in condensate after condensation $EH_{ap,hcond}^{cond}$ is determined by the multiplication of amount of heat in steam $Ech_{ap,iu}^{CS}$ and the ratio between the enthalpy of water and steam $R_{iu}^{liq\_st}$ and the rate of condensate recovery $f^{cond,rec}$.

$$EH_{ap,hcond}^{cond} = Ech_{ap,iu}^{CS} \cdot R_{iu}^{liq\_st} \cdot f^{cond,rec}$$
$$\forall\ ap \in AP,\ iu \in IU,\ s \in S,\ hcond \in HCond,\ (ap,\ hcond) \in APIC,\ (iu,\ hcond) \in IUHOT,\ (iu,\ s) \in IUS,\ (snod,\ ap) \in AssignSnod\_AP,\ (snod,\ s) \in AssignSnod\_Sin \quad (4\text{-}117)$$

The overall condensate balance at a node is obtained when the sum of the amount of heat entering the node $Qs_{scond,iucond}$ and the condensate produced at the node $EC_{ap,ccond}^{cond}$ is equal to the sum of the amount of heat exiting the node $Qs_{scond,iucond}$ and the utilised condensate $EC_{ap,ccond}^{cond}$. Additionally, heat losses during transport in the pipeline needs to be taken into account $Q_{scond,iucond}^{loss}$.

$$\sum_{scond \in Scond \wedge (snod,scond) \in AsignSnodCond\_Sin \wedge (iucond,scond) \in IUcondScond} \left(Qs_{scond,iucond} - Q_{scond,iucond}^{loss}\right) +$$
$$\sum_{\substack{scond \in SCOND, ap \in AP, hcond \in Hcond \wedge (snod,ap) \in AssigSnodAp \wedge (snod,scond) \in AsingSnodcondSout \wedge \\ (iucond,scond) \in IUcondScond \wedge (iucond,hcond) \in IUcondHcond \wedge (ap,hcond) \in APIC}} EH_{ap,hcond}^{cond} =$$
$$\sum_{\substack{scond \in SCOND, ap \in AP, ccond \in Ccond \wedge (snod,ap) \in AssigSnodAp \wedge (snod,scond) \in AsingSnodcondSin \wedge \\ (iucond,scond) \in IUcondScond \wedge (iucond,ccond) \in IUcondCcond \wedge (ap,ccond) \in APJC}} EC_{ap,ccond}^{cond} +$$
$$\sum_{scond \in Scond \wedge (snod,scond) \in AsignSnodCond\_Sout \wedge (iucond,scond) \in IUcondScond} Qs_{scond,iucond}$$
$$\forall snod \in Snod, iucond \in IUcond \quad (4\text{-}118)$$

4.5.1.2 Pressure drop in condensate pipeline

The pipelines are designed based on a pressure drop, therefore the pressure in pipeline should be deteremined. The inlet pressure is equal to the pressure in the pipeline where condensation is performed.

$$ps_{scond,iucond}^{cond} = \sum_{\substack{hcond \in Hcond \wedge ap \in AP \wedge snod \wedge (ap,hcond) \in APIC \wedge (snod,ap) \in AssigSnodAp \wedge \\ (snod,scond) \in AsingSnodcondSout \wedge (iucond,hcond) \in IUcondHcond}} p_{hcond}^{CS}$$
$$scond \in Scond,\ iucond \in IUcond,\ (iucond,\ scond) \in IUSpipe \quad (4\text{-}119)$$

The outlet pressure from pipeline should be as high as the required pressure for the evaporation, when condensate is reused.

$$\sum_{\substack{ccond \in Ccond \wedge ap \in AP \wedge snod \in SNOD \wedge (ap,snod) \in APJC \wedge (snod,ap) \in AssigSnodAP \wedge \\ (snod,scond) \in AsingSnodcondSin \wedge (iucond,ccond) \in IUcond}} p_{ccond}^{HS} \le ps_{scond,iucond}^{cond} - p_{scond,iucond}^{drop}$$
$$scond \in Scond,\ iucond \in IUcond,\ (iucond,\ scond) \in IUSpipe \quad (4\text{-}120)$$

4.5.1.3 Steam heat balances

The steam balance is made upon each node. The node (process) is in balance when the sum of the inlet amount of heat $Qs_{s,iu}$, contained in the steam, and the amount of heat produced

$Ecc_{ap,iu}^{HS}$ is equal to the amount of outlet heat utilised within the node (process) $Ech_{ap,iu}^{CS}$ and the outlet amount of heat $Qs_{s,iu}$. Additionally, the heat loss during transport $Q_{s,iu}^{loss,tot}$ is considered in the inlet amount of heat.

$$\sum_{s\in S\wedge(snod,s)\in AsignSnodSin\wedge(iu,s)\in IUS} \left(Qs_{s,iu} - Q_{s,iu}^{loss,tot}\right) + \sum_{s\in S\wedge(snod,ap)\in AssigSnodAp\wedge(snod,s)\,AsingSnodSout\wedge(iu,s)\in IUS} Ecc_{ap,iu}^{HS} =$$
$$\sum_{s\in S\wedge(snod,ap)\in AssigSnodAP\wedge(snod,s)\in AsignSnodSin\wedge(iu,s)\in IUS} Ech_{ap,iu}^{CS} + \sum_{s\in S\wedge(snod,s)\in AsignSnodSout\wedge(iu,s)\in IUS} Qs_{s,iu}$$
$$\forall\ ap\in AP,\ iu\in IU,\ s\in S,\ snod\in Snod \qquad (4\text{-}121)$$

4.5.1.4 *Steam mass balances*

In the previous section the calculations for heat balances were presented. Additionally, the mass balances has to be determined as well, in order to obtaine feasible solutions. The mass flow-rate of steam after evaporation $\dot{m}_{ap,iu}^{Ecc\_HS}$ is determined from heat utilised for evaporation Ecc_{iu}^{HS} divided by enthalphy difference between steam and condensate.

$$\dot{m}_{ap,iu}^{Ecc\_HS} = \frac{Ecc_{iu}^{HS}}{\Delta h_{s,iu}} \qquad \forall\ ap\in AP,\ iu\in IU,\ snode\in Snod,\ s\in S,\ (snod,ap)\in AssignSnodAp,$$
$$(snod,\ s)\in AsingSnodSout,\ (iu,\ s)\in IUS \qquad (4\text{-}122)$$

The mass flow-rate decrease due to condensation of the steam during transport as a result of heat loss is determined very similarly. However, it should be taken into account only the part of the heat loss occurring due to condensation.

$$\dot{m}_{s,iu}^{qloss} = \frac{q_{s,iu}^{loss\_st} - q_{s,iu}^{loss}}{\Delta h_{iu}^{st}} \qquad \forall s\in S,\ iu\in IU \qquad (4\text{-}123)$$

The steam mass balance is determined as the mass flowrate $\dot{m}_{s,iu}^{s}$ entering node decreased by the mass flowrate of the condensate in formulated in steam main, due to heat loss $\dot{m}_{s,iu}^{s,\mathrm{q\_loss}}$ summed up by mass flowrate of the steam generated at the process $\dot{m}_{ap,iu}^{Ecc\_HS}$ is equal to steam condensated in the node $\dot{m}_{ap,iu}^{Ech\_CS}$ and mass flowrate of the steam leaving the node.

$$\sum_{s\in S\wedge(snod,s)\in As\sin gSnodSin\wedge(iu,s)\in IUS} \left(\dot{m}_{s,iu}^{s} - \dot{m}_{s,iu}^{s,\mathrm{q\_loss}}\right) +$$
$$\sum_{s\in S\wedge ap\in AP\wedge(snod,ap)\in AssignSnodAp\wedge(snod,s)\in AssignSnodSout\wedge(iu,s)\in IUS} \dot{m}_{ap,iu}^{Ecc\_HS} =$$
$$\sum_{s\in S\wedge ap\in AP\wedge(snod,ap)\in AssignSnodAp\wedge(snod,s)\in AssignSnodSin\wedge(iu,s)\in IUS} \dot{m}_{ap,iu}^{Ech\_CS} +$$
$$\sum_{s\in S\wedge(snod,s)\in AssignSnodSout\wedge(iu,s)\in IUS} \dot{m}_{s,iu}^{s}$$
$$\forall\ snod\in Snod,\ iu\in IU \qquad (4\text{-}124)$$

4.5.1.5 *Pressure drop in steam main*

The pressure in pipe segment $ps_{s,iu}$ is less or equal to the one in the heat exchanger for transferring heat from the hot process stream to the intermediate utility p_{icue}^{HS}.

$$\sum_{icue \in ICUE \wedge (iu,icue) \in IUICU} p_{icue}^{HS} \geq ps_{s,iu} \quad \forall s \in S,\ iu \in IU,\ icue \in ICUE, (iu,s) \in IUS \qquad (4\text{-}125)$$

Pressure balance in the node is determined as the outlet pressure and should be less than any inlet pressure decreased by the pressure drop $p_{ss,iu}^{drop}$. This equation determines the pressure in a following segment of pipeline if no heat is gained from the node (process).

$$ps_{ss,iu} - p_{ss,iu}^{drop} \geq ps_{s,iu} \qquad \forall\ snod \in SNOD, s \in S,\ ss \in S,\ icue \in ICUE \qquad (4\text{-}126)$$

The pressure in the process with heat demand is equal to the pressure in the pipeline segment, decreased p_{ihu}^{CS} by the pressured drop.

$$ps_{s,iu} - p_{s,iu}^{drop} = p_{ihu}^{CS} \qquad \forall s \in S,\ iu \in IU,\ ihu \in IHU, (iu,s) \in IUS,\ (iu,ihu) \in IUIHU1 \qquad (4\text{-}127)$$

4.5.1.6 Pipeline for indirect process-to-process heat recovery

The relationship between pipe diameter $d_{s,iu}$ and thickness $th_{s,iu}^{pipe}$ in the steam main is presented in Eq. 4-128, whilst in the condensate pipeline in Eq. 4-129. The numbers 14.5 and 39.37 in these equations serve as conversion factors between psig and bar (14.5) and between inch and m (39.37).

$$th_{s,iu}^{pipe} \cdot 39.37 = \frac{ps_{s,iu} \cdot 14.5 \cdot \left(d_{s,iu} \cdot 39.37 + 2 \cdot th_{s,iu}^{pipe} \cdot 39.37\right)}{2 \cdot \left(16{,}000 + ps_{s,iu} \cdot 14.5 \cdot 0.4\right)} + 0.065$$

$$\forall s \in S,\ iu \in IU,\ (iu,\ s) \in IUS \qquad (4\text{-}128)$$

$$th_{scond,iucond}^{pipe} \cdot 39.37 = \frac{\left(\sum_{ihu \in (iucond,ihu) \in IUcondIhu} p_{ihu}^{CS} \cdot 14.5\right) \cdot \left(d_{scond,iucond} \cdot 39.37 + 2 \cdot th_{scond,iucond}^{pipe}\right) \cdot 39.37}{2 \cdot \left(16{,}000 + \sum_{ihu \in (iucond,ihu) \in IUcondIhu} p_{ihu}^{CS} \cdot 14.5 \cdot 0.4\right)} + 0.065$$

$$\forall scond \in Scond,\ iucond \in IUcond,\ ihu \in IHU,\ (iucond,\ scond) \in IUcondScond \qquad (4\text{-}129)$$

The binary variable for pipeline ys_{s_scond,iu_iucond} is selected, when the amount of heat Qs_{s_scond,iu_iucond} in the pipe is higher then the lower bound is $Qs_{s\_scond,iu\_iucond}^{LO}$.

$$Qs_{s\_scond,iu\_iucond} \geq Qs_{s\_scond,iu\_iucond}^{LO} \cdot ys_{s\_scond,iu\_iucond}$$

$$\forall\ s\_scond \in S\_SCond,\ iu\_iucond \in IU\_IUCond \qquad (4\text{-}130)$$

A variable for length between the process is introduced in order to avoid using big-M formulations in the model. This variable takes the value of the length of the process, when pipeline is selected and is zero, when pipeline is rejected.

$$Ls_{s\_scond,iu\_iucond}^{\text{var}} = ys_{s\_scond,iu\_iucond} \cdot L_{s\_scond,iu\_iucond}$$

$$\forall\ s\_scond \in S\_SCcond,\ iu\_iucond \in IU\_IUCOND,\ (iu\_iucond, s\_scond) \in IUSpipe \qquad (4\text{-}131)$$

The heat losses $Q_{s,iu}^{loss}$ are determined depending on the insulation thickness. Heat losses can be determined depending on the insulation thickness ($th_{s,iu}^{ins}$) only, as the heat convection through the pipe wall is usually high (Engineering Toolbox, 2013).

$$Q_{s,iu}^{loss} = 2\cdot\pi\cdot Ki\cdot\frac{\sum_{icue\in ICUE\wedge(iu,icue)\in IUICU} TC_{icue}^{IU} - T^{G}}{\ln\left(\frac{th_{s,iu}^{ins}+d_{s,iu}/2+th_{s,iu}^{pipe}}{d_{s,iu}/2+th_{s,iu}^{pipe}}\right)}\cdot Ls_{s,iu}^{var} \quad \forall\ s\in S,\ iu\in IU,\ icue\in ICUE \quad (4\text{-}132)$$

$$Q_{scond,iucond}^{loss} = 2\cdot\pi\cdot Ki\cdot\frac{\sum_{ihu\in IHU\wedge(iucond,ihu)\in IUcondIHU} TH_{ihu}^{IU} - T^{G}}{\ln\left(\frac{th_{scond,iucond}^{ins}+d_{scond,iucond}/2+th_{scond,iucond}^{pipe}}{d_{scond,iucond}/2+th_{scond,iucond}^{pipe}}\right)}\cdot Ls_{scond,iucond}^{var}$$

$$\forall\ scond\in SCond,\ iucond\in IUCond,\ ihu\in IHU \quad (4\text{-}133)$$

The total heat loss for steam $Q_{s,iu}^{loss\_st}$ during transport in pipeline segment is considered as the heat loss due to heat transfer to the ambient increased by the heat losses due to condensation.

$$Q_{s,iu}^{loss\_st} = Q_{s,iu}^{loss}\cdot\left(1+R_{iu}^{liq\_st}\right) \quad \forall s\in S,\ icue\in ICUE \quad (4\text{-}134)$$

The specific volume of steam $V_{s,iu}^{spec}$ in dependence of temperature (Figure 4–20) is determined by equation derivation of the relationship among them from steam tables (Eq.4 – 135 for LP, Eq.4 – 136 for MP and Eq.4 – 137 for HP).

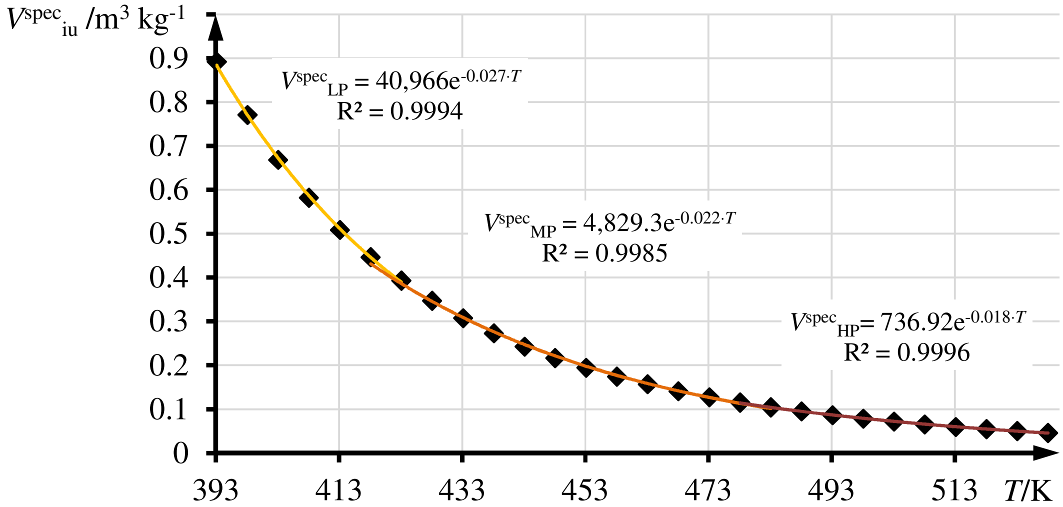

Figure 4-20:Equation derivation for specific volume of steam for each intermediate utility depending on the temperature

$$V_{s,LP}^{spec}=40{,}966\cdot\exp\left(-0.027\cdot\sum_{icue\in ICUE\wedge(iu,icue)\in IUICU}TC_{icue}^{IU}\right)$$

$$\forall\ s\in S,\ icue\in ICUE \qquad (4\text{-}135)$$

$$V_{s,\mathrm{MP}}^{spec}=4{,}829.3\cdot\exp\left(-0.022\cdot\sum_{icue\in ICUE\wedge(iu,icue)\in IUICU}TC_{icue}^{IU}\right)$$

$$\forall\ s\in S,\ icue\in ICUE \qquad (4\text{-}136)$$

$$V_{s,\mathrm{HP}}^{spec}=736.92\cdot\exp\left(-0.018\cdot\sum_{icue\in ICUE\wedge(iu,icue)\in IUICU}TC_{icue}^{IU}\right)$$

$$\forall\ s\in S,\ icue\in ICUE \qquad (4\text{-}137)$$

The pressure drop for steam main $p_{s,iu}^{drop}$ is calculated from Eq. 4-138 and depends of the friction factor for steam f_{steam}^{fric}, amount of heat in the main $Qs_{s,iu}$, specific volume of steam in main V_{iu}^{spec}, diameter of main $d_{s,iu}^{5}$, specific enthalpy difference between steam and water and the length of the pipeline $Ls_{s,iu}^{\mathrm{var}}$.

$$p_{s,iu}^{drop}=\frac{f_{steam}^{fric}\cdot Qs_{s,iu}{}^{2}\cdot V_{iu}^{spec}}{d_{s,iu}{}^{5}\cdot\Delta h_{s,iu}{}^{2}}\cdot Ls_{s,iu}^{\mathrm{var}} \qquad \forall\ s\in S,\ iu\in IU \qquad (4\text{-}138)$$

The pressure drop in the condensate pipeline $p_{scond,iucond}^{drop}$ is determined very similarly, as can be seen from Eq. 4-139 where all the variables are regarded for condensate and the connected pipeline.

$$p_{scond,iucond}^{drop}=\frac{f_{cond}^{fric}\cdot Qs_{scond,iucond}^{2}\cdot V_{cond}^{spec}}{d_{scond,iucond}{}^{5}\cdot h_{scond,iucond}^{spec}{}^{2}}\cdot Ls_{scond,iucond}^{\mathrm{var}}$$

$$\forall\ scond\in Scond,\ iucond\in IUcond \qquad (4\text{-}139)$$

4.5.1.7 Mass balances for condensate

In the previous section the calculations for heat balances were presented. Additionally, the mass balances has to be determined as well, in order to obtaine feasible solutions. The balance of mass-flowrate for condensate is determined in each node separately. The temperature of condesate TH_{hcond}^{IU} after condensation is equal to temperature of the steam temperature TH_{ihu}^{IU} before condensation.

$$TH_{hcond}^{IU}=\sum_{ihu\in IHU\wedge(ihu,hcond)\in IHUHCond}TH_{ihu}^{IU}$$

The mass flow-rate of recovered condensate is determined from the condensation side as a fraction of recovered condensate

$$\dot{m}_{ap,hcond}^{EHcond}=\dot{m}_{ap,iu}^{Ech\_CS}\cdot f^{cond,rec}$$

$\forall\ ap\in AP$, $hcond\in HCond$, $s\in S$, $snod\in SNOD$, $scond\in SCOND$, $(ap, hcond)\in APIC$, $(iu, hcond)\in IUHOT$, $(snod, ap)\in AssigSnodAP$, $(snod, scond)\in AsignSnodCond\_Sout$, $(snod, s)\in AsignSnod\_Sin$, $(iu, s)\in IUS$ (4-140)

The condensate can be recovered from condensate after condensation in heat recovery and additional source of condesate recovery is the condensate generated during transport of steam. The calculation of mass flowrate of condensate recovered from condensate generate during transport can determined from the following equation.

$$\dot{m}_{ap,hcond}^{cond\_st\_pipe} = \sum_{\substack{snod\in Snod \wedge s\in S \wedge iu\in IU \wedge (snod,s)\in AssignSnodSin \wedge \\ (snod,ap)\in AssignSnodAp \wedge (iu,s)\in IUS \wedge (\mathrm{iu,hcond})\in IUHOT}} \left(\dot{m}_{s,iu}^{qloss} \cdot f^{cond,rec}\right)$$

$$\forall\ ap\in AP,\ hcond \in HCond,\ (ap,\ hcond) \in APIC \qquad (4\text{-}141)$$

The sum of inlet mass flow-rate to the node $\dot{m}_{scond,IUcond}^{Scond}$ and mass flow-rate of condensate as a result of condensation in heat exchanger $\dot{m}_{ap,hcond}^{EHcond}$ and in steam main $\dot{m}_{ap,hcond}^{cond\_st\_pipe}$ is equal to outlet mass flow-rate from the node and the condensate utilitsed at evaporation in the node (process) $\dot{m}_{ap,ccond}^{ECcond}$.

$$\sum_{scond\in Scond \wedge (snod,scond)\in AsingSnodcondSin \wedge (IUcond,Scond)\, IUcondScond} \dot{m}_{scond,IUcond}^{Scond} +$$

$$\sum_{\substack{scond\in Scond \wedge ap\in AP \wedge hcond\in Hcond \wedge (snod,ap)\in AssigSnodAp \wedge (snod,scond)\in AsingSnodCondSout \\ (iucond,scond)\in IUCondScond \wedge (iucond,hcond)\in IUCondHcond \wedge (ap,hcond)\in APIC}} \left(\dot{m}_{ap,hcond}^{EHcond} + \dot{m}_{ap,hcond}^{cond\_st\_pipe}\right) =$$

$$\sum_{\substack{scond\in Scond \wedge ap\in AP \wedge ccond\in Ccond \wedge (snod,ap)\in AssigSnodAp \wedge (snod,scond)\in AsingSnodCondSin \\ (iucond,scond)\in IUCondScond \wedge (iucond,ccond)\in IUCondCcond \wedge (ap,ccond)\in APJC}} \dot{m}_{ap,ccond}^{ECcond} +$$

$$\sum_{scond\in Scond \wedge (snod,scond)\in AsingSnodcondSout \wedge (IUcond,Scond)\, IUcondScond} \dot{m}_{scond,IUcond}^{Scond}$$

$$\forall\ snod\in\ Snod,\ iucond\in\ IUcond \qquad (4\text{-}142)$$

Specific heat for the condensate should be determined, in order to determine the temperature drop in condensate pipeline and also the heating requirement for recovered condensate and fresh water. Equations has been derived from steam table for a certain inlet temperature of fresh water within a given temperature range of each intermediate utility separately. An average value of *Cp* for the whole temperature range between inlet temperature and evaporation temperature has been determined at each temperature separately by following procedure:

1. Step: Applying the ratio R_{iu}^{liq-st} the enthaphy for preheating $E_{evap}^{preheat}$ can be determined from $E_{evap}^{evaporation}$ enthaphy as already described.
2. Step: The heat capacity flowrate $CP_{evap}^{preheat}$ can be from $E_{Tevap}^{preheat}$ and the temperature differenc between inlet temperature of fresh water T^{fresh} (used also for determining the R_{iu}^{liq-st}) and the temperature of evaporation T_{evap} as presented in Eq.4-143.

$$CP_{evap}^{preheat} = \frac{E_{evap}^{preheat}}{\left(T_{evap} - T^{fresh}\right)} \qquad \forall\ evap\in EVAP \qquad (4\text{-}143)$$

3. Step: The mass flowrate of steam $\dot{m}_{evap}^{steam}$ is determined from $E_{evap}^{evaporation}$ and the specific enthalphy of evaporation Δh_{evap} (determined as difference between specific enthalphy if steam and condensate).

$$\dot{m}_{evap}^{steam} = \frac{E_{evap}^{evaporation}}{h_{evap}^{steam}} \qquad \forall\ evap \in EVAP \qquad (4\text{-}144)$$

4. Step: In final step the heat capacity flowrate $CP_{evap}^{preheat}$ is divided by $\dot{m}_{evap}^{steam}$ in order to obtain specific heat Cp_{evap} at different temperature of evaporation.

$$Cp_{evap} = \frac{CP_{evap}^{preheat}}{\dot{m}_{evap}^{steam}} \qquad \forall\ evap \in EVAP \qquad (4\text{-}145)$$

5. Step. Linear equations are derivated for Cp_{evap} depending on T_{evap} for each intermediate utility separately, as can be seen in Figure 4-21.

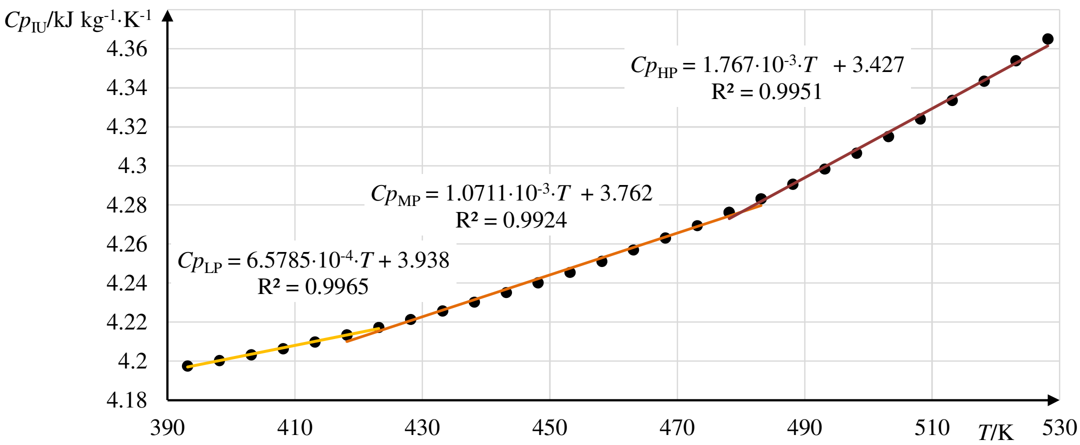

Figure 4-21:Equation derivation for specific heat of preheating water for each intermediate utility depending on the temperature

The same derivation has been applied for Cp_{iucond} and also Cp_{icup}.

The temperature drop in condensate pipeline is determined as the amount of heat loss divided by mass flow-rate in pipeline and specific heat of water (condensate).

$$Ts_{scond,iucond}^{drop,iu} = \frac{Q_{scond,iucond}^{loss}}{\dot{m}_{scond,iucond}^{Scond} \cdot Cp_{iucond}}$$

$\forall$ $scond \in Scond$, $iucond \in IUcond$, $hcond \in Hcond$, $ap \in AP$, $snod \in Snod$, ($iucond$, $scond$) $\in$ $IUcondScond$, ($snod$, ap) $\in$ $AssigSnodAp$, ($snod$, $scond$) $\in$ $AsingScondSout$, ($iucond$, $hcond$) $\in$ $IUcondHcond$ (4-146)

The mass flow-rate for preheating stream is determined as the difference between the required mass flow-rate for evaporation and the mass flow-rate of condensate from recovery pipeline.

$$\dot{m}^{Ecp}_{ap,icup} = \dot{m}^{Ecc\_HS}_{ap,iu} - \dot{m}^{Eccond}_{ap,ccond}$$

$\forall$ *ap*$\in$*AP*, *iu*$\in$*IU*, *icup* $\in$ *ICUP*, *ccond*$\in$*Ccond*, *snod*$\in$*Snod*, *s*$\in$*S*, (*ap*,*icup*)$\in$ *APJC*, (*ap*,*ccond*)$\in$ *APJC*, (*iu*,*ccond*) $\in$ *IUCOLD*, (*iu*,*icup*) $\in$ *IUCOLD*, (*snod*, *ap*)$\in$*AssigSnodAP*, (*snod*, *s*)$\in$*AsingSnodSout*, (*iu*,*s*)$\in$*IUS* (4-147)

The relationship between mass flow-rate for preheating and enthaphy flow is made by the following equation via heat capacity flow-rate of the preheating stream.

$$Ecp_{ap,icup} = \left(TC^{IU}_{icup} - T^{c,in}_{icup}\right)\cdot m^{Ecp}_{ap,icup}\cdot Cp_{icup}$$

$\forall$ (*iu*, *s*)$\in$*IUS,* (*snod, ap*) $\in$ *AsignSnodSout*, (*snod*, *ap*) $\in$ *AssignSnodAP* (4-148)

The temperatures of outlet streams are determined based on equation for mixing of condensates at different temperature. Therefore, the mass flow-rates are multiplied by the temperatures of the associated stream.

$$\sum_{scond\in Scond\wedge(snod,scond)\in AsingSnodcondSin\wedge(IUcond,Scond)\,IUcondScond}\left(\dot{m}^{Scond}_{scond,IUcond}\cdot\left(Ts^{IU}_{scond,iucond} - Ts^{drop,\mathrm{IU}}_{scond,iucond}\right)\right)+$$
$$\sum_{\substack{scond\in Scond\wedge ap\in AP\wedge hcond\in Hcond\wedge(snod,ap)\in AssigSnodAp\wedge(snod,scond)\in AsingSnodCondSout\\(iucond,scond)\in IUCondScond\wedge(iucond,hcond)\in IUCondHcond\wedge(ap,hcond)\in APIC}}\left(\left(\dot{m}^{EHcond}_{ap,hcond} + \dot{m}^{cond\_st\_pipe}_{ap,hcond}\right)\cdot TH^{IU}_{hcond}\right)=$$
$$\sum_{\substack{scond\in Scond\wedge ap\in AP\wedge ccond\in Ccond\wedge(snod,ap)\in AssigSnodAp\wedge(snod,scond)\in AsingSnodCondSin\\(iucond,scond)\in IUCondScond\wedge(iucond,ccond)\in IUCondCcond\wedge(ap,ccond)\in APJC}}\left(\dot{m}^{ECcond}_{ap,ccond}\cdot TC^{IU}_{ccond}\right)+$$
$$\sum_{scond\in Scond\wedge(snod,scond)\in AsingSnodcondSout\wedge(IUcond,Scond)\,IUcondScond}\left(\dot{m}^{Scond}_{scond,IUcond}\cdot Ts^{IU}_{scond,iucond}\right)$$

$\forall$ *snod* $\in$ *Snod*, *iucond* $\in$ *IUcond* (4-149)

The ethalphy required to be covered in condensate due to heat loss in steam main should be covered by external utility in order to satisfy heat balance.

$$q^{cond}_{ap,ccond} = \sum_{\substack{snod\in Snod\wedge s\in S\wedge iu\wedge IU\wedge(snod,s)\in AssingSnodSout\wedge\\(snod,ap)\in AssignSnodAP\wedge(iu,s)\in IUS\wedge(iu,ccond)\in IUCOLD}}\left(q^{loss}_{s,iu}\cdot R^{liq-st}_{iu}\right)$$

$\forall$ *ap* $\in$ *AP*, *ccond* $\in$ *Ccond*, (*ap*, *ccond*) $\in$ *APJC* (4-150)

An external utility is utilised in order to cover heat losses that occurs during transport.

$$qh_{ccond} = \dot{m}^{ECcond}_{ap,ccond}\cdot Cp^{cond}\cdot\sum_{icue\in ICUE\wedge(ap,icue)\in APJC\wedge(icue,ccond)\in ICUECcond}\left(TC^{IU}_{icue} - TC^{IU}_{ccond}\right) + q^{cond}_{ap,ccond}$$

$\forall$ *ap*$\in$*AP*, *ccond*$\in$*Ccond*, *iucond*$\in$*IUcond*, *snod*$\in$*SNOD*, *scond*$\in$*SCOND*, (*ap*, *ccond*) $\in$ *APJC*, (*iucond*, *ccond*)$\in$*IUcondCcond*, (*snod*, *ap*)$\in$*AssignSnodAP*, (*snod*, *scond*)$\in$*AssignSnodCondSin*, (*iucond*, *scond*)$\in$ *IUcondScond* (4-151)

A binary variable for selection/ rejection of heat exchanger between hot utility and condensate in a process, where steam is generate y^{hu}_{ccond}, is set to 1, when there is heat transfer, and is 0 when no heat transfer occurs.

$$qh_{ccond} - ecc_{ccond}\cdot y^{hu}_{ccond} \le 0 \qquad \forall\ ccond \in Ccond \qquad (4\text{-}152)$$

4.5.1.8 Pipeline design and heat loss for direct heat exchange

The pipeline design and heat loss for direct heat exchange are determined by the application of similar equations already presented for steam. The difference between them is the fluid inside. The selection/rejection of the pipeline is performed by binary variable $y^{dir}_{hp,cp,k}$ based on the amount of heat transferred to the cold process excluding heat losses $Q^{tc}_{hp,cp,k}$. The selection of the pipeline is selected only if the amount of heat transferred is larger than a certain lower bound.

$$Q^{tc}_{hp,cp,k} - y^{dir}_{hp,cp,k} \cdot Q^{tc,UP}_{hp,cp,k} \leq 0 \qquad \forall\ hp \in HP,\ cp \in CP,\ k \in K \qquad (4\text{-}153)$$

$$Q^{tc}_{hp,cp,k} \geq y^{dir}_{hp,cp,k} \cdot Q^{tc,LO}_{hp,cp,k} \qquad \forall\ hp \in HP,\ cp \in CP,\ k \in K \qquad (4\text{-}154)$$

Similarly, as at pipeline design for steam main. Therefore,

$$L^{\mathrm{var}}_{hp,cp,k} = y^{dir}_{hp,cp,k} \cdot L_{hp,cp} \qquad \forall\ hp \in HP,\ cp \in CP,\ k \in K \qquad (4\text{-}155)$$

The correlation between pipe thickness and diameter needs to be calculated for the pipeline in both directions from the cold process towards the hot process, and vice versa.

$$th^{pipe,CSHS}_{hp,cp,k} \cdot 39.37 = \frac{p_{cp} \cdot 14.5 \cdot d^{CSHS}_{hp,cp,k} \cdot 39.37 + 2 \cdot th^{CSHS}_{hp,cp,k} \cdot 39.37}{2 \cdot \left(16{,}000 + p_{cp}\right) \cdot 14.5 \cdot 0.4} + 0.065$$

$$\forall\ hp \in HP,\ cp \in CP,\ k \in K \qquad (4\text{-}156)$$

$$th^{pipe,HSCS}_{hp,cp,k} \cdot 39.37 = \frac{p_{cp} \cdot 14.5 \cdot d^{HSCS}_{hp,cp,k} \cdot 39.37 + 2 \cdot th^{HSCS}_{hp,cp,k} \cdot 39.37}{2 \cdot \left(16{,}000 + p_{cp}\right) \cdot 14.5 \cdot 0.4} + 0.065$$

$$\forall\ hp \in HP,\ cp \in CP,\ k \in K \qquad (4\text{-}157)$$

Heat losses are determined by considering the temperature drop during transporting of the cold process. Therefore, when determining heat loss, for the transporting from the cold process stream to the hot process stream the temperature is decreased in comparison to the temperature at the stage boundary.

$$Q^{loss,CSHS}_{hp,cp,k} = 2 \cdot \pi \cdot Ki \cdot \frac{TC_{cp,k} - T^{\mathrm{G}}}{\ln\left(\dfrac{th^{ins,CSHS}_{hp,cp,k} + d^{CSHS}_{hp,cp,k}/2 + th^{pipe,CSHS}_{hp,cp,k}}{d^{CSHS}_{hp,cp,k}/2 + th^{pipe,CSHS}_{hp,cp,k}}\right)} \cdot L^{\mathrm{var}}_{hp,cp,k}$$

$$\forall\ hp \in HP,\ cp \in CP,\ k \in K \qquad (4\text{-}158)$$

However, on the other hand, when the cold process is transferred back to its original process, the temperature at the heat exchanger should be higher compared to the temperature boundary, due to heat losses during transporting.

$$Q^{loss,HSCS}_{hp,cp,k} = 2 \cdot \pi \cdot Ki \cdot \frac{TC_{cp,k} + Q^{loss,HSCS}_{hp,cp,k} / \left(2 \cdot CP_{cp}\right) - T^{\mathrm{G}}}{\ln\left(\dfrac{th^{ins,HSCS}_{hp,cp,k} + d^{HSCS}_{hp,cp,k}/2 + th^{pipe,HSCS}_{hp,cp,k}}{d^{HSCS}_{hp,cp,k}/2 + th^{pipe,HSCS}_{hp,cp,k}}\right)} \cdot L^{\mathrm{var}}_{hp,cp,k}$$

$$\forall\ hp \in HP,\ cp \in CP,\ k \in K \qquad (4\text{-}159)$$

Besides these heat losses, the pressure drop should also be determined. For this purpose the mass flow-rate of the whole cold process stream is determined as the parameter before the optimisation and the mass flow-rate of the cold process stream directed to the hot process stream is recalculated as the initial mass flow-rate multiplied by the ratio between the heat content of the split part versus the total stream.

$$p_{hp,cp,k}^{drop,HSCS} = f_{cp}^{fric} \cdot \frac{\left(q_{m,cp}^{tot} \cdot \frac{q_{hp,cp,k}^{tc}}{\sum_{hp} q_{hp,cp,k}^{tc}} \right)^2}{\rho_{cp} \cdot \left(d_{hp,cp,k}^{HSCS} \right)^5} \cdot L_{hp,cp} \quad \forall\, hp \in HP,\, cp \in CP,\, k \in K \tag{4-160}$$

$$p_{hp,cp,k}^{drop,CSHS} = f_{cp}^{fric} \cdot \frac{\left(q_{m}^{tot} \cdot \frac{q_{hp,cp,k}^{tc}}{\sum_{hp} q_{hp,cp,k}^{tc}} \right)^2}{\rho_{cp} \cdot \left(d_{hp,cp,k}^{CSHS} \right)^5} \cdot L_{hp,cp} \quad \forall\, hp \in HP,\, cp \in CP,\, k \in K \tag{4-161}$$

The total amount of heat transferred from the hot process stream needs to cover not only the cold process duty but in addition also the heat losses occurring during transporting.

$$q_{hp,cp,k}^{tc} = q_{hp,cp,k} - q_{hp,cp,k}^{loss,\mathrm{HSCS}} - q_{hp,cp,k}^{loss,\mathrm{CSHS}} \quad \forall\, hp \in HP,\, cp \in CP,\, k \in K \tag{4-162}$$

4.5.1.9 Pump design

Pumps are considered within the Total Site structure in order to compensate for the pressure drop, occurring during transportation. They are located on each selected main. The work of pumps for the steam main is determined from Eq. 4-163 and depends on the pressure drop $p_{s,iu}^{drop}$, amount of heat transferred $Qs_{s,iu}$, that is then divided by the enthalpy difference $\Delta h_{iu,s}$ and multiplied by the specific volume $V_{s,iu}^{spec}$ in order to obtain the volume flow-rate within the pipe

$$w_{iu}^{pump} \geq \sum_{s \in S} \left(\left(\sum_{iu \in IU \wedge (iu,s) \in IUSpipe} p_{s,iu}^{drop} \right) \cdot \sum_{iu \in IU \wedge (iu,s) \in IUSpipe} \left(\frac{Qs_{s,\mathrm{iu}} \cdot V_{s,\mathrm{iu}}^{spec}}{h_{iu,s} \cdot \eta} \right) \right) - \left(1 - y_{iu}^{pump}\right) \cdot w_{iu}^{pump,UP}$$
$$\forall\, iu \in IU, s \in S \tag{4-163}$$

A similar equation has been used for the condensate pipeline.

$$w_{iucond}^{pump} \geq \sum_{scod \in Scond} \left(\left(\sum_{iucond \in IUcond \wedge (iucond,scond) \in IUSpipe} p_{s,iu}^{drop} \right) \cdot \sum_{iucond \in IUcond \wedge (iucond,scond) \in IUSpipe} \left(\frac{Qs_{scond,iucond} \cdot V_{scond,iucond}^{spec}}{h_{iucond,scond} \cdot \eta} \right) \right)$$
$$-\left(1 - y_{iucond}^{pump}\right) \cdot w_{iucond}^{pump,UP}$$
$$\forall\, iu \in IU, s \in S \tag{4-164}$$

The binary variable for selecting pump existence $y_{iu\_iucond}^{pump}$ depends on the binary variable for the selection/ rejection of the main ys_{s_scond,iu_iucond}.

$$y_{iu\_iucond}^{pump} \geq \sum_{s\_scond \in S\_SCOND \wedge (iu\_iucond,s\_scond) \in IUS} ys_{s\_scond,iu\_iucond}$$
$$\forall\, s\_scond \in S\_SCond,\, iu\_iucond \in IU\_IUCond \tag{4-165}$$

The pipe investment I_{iu}^{pump} consists of fixed cost cf^{pump} and variable cost cv^{pump}.

$$I_{iu}^{pump} = cf^{\,pump} \cdot y_{iu}^{pump} + cv^{pump} \cdot w_{iu}^{pump} \qquad \forall\ iu \in IU \tag{4-166}$$

The pump work ($w_{hp,cp,k}^{pump,CSHS}$, $w_{hp,cp,k}^{pump,HSCS}$) depends on pressure drop ($p_{hp,cp,k}^{drop,CSHS}$, $p_{hp,cp,k}^{drop,HSCS}$) and volume flow-rate. In the case of direct heat transfer the volume flow-rate is determined as the mass flow-rate divided by density ρ_{cp}. The mass flow-rate q_m^{tot} is determined as the parameter before optimization; however, when stream splitting occurs, it is multiplied by the splitting ratio.

$$w_{hp,cp,k}^{pump,CSHS} \geq \frac{p_{hp,cp,k}^{drop,CSHS} \cdot q_m^{tot} \cdot \dfrac{q_{hp,cp,k}^{tc}}{\sum_{hp} q_{hp,cp,k}^{tc}}}{\rho_{cp} \cdot \eta} - \left(1 - y_{hp,cp,k}^{dir}\right) \cdot w_{hp,cp}^{pump,UP} \qquad \forall\ hp \in HP,\ cp \in CP,\ k \in K \tag{4-167}$$

$$w_{hp,cp,k}^{pump,HSCS} \geq \frac{p_{hp,cp,k}^{drop,HSCS} \cdot q_m^{tot} \cdot \dfrac{q_{hp,cp,k}^{tc}}{\sum_{hp} q_{hp,cp,k}^{tc}}}{\rho_{cp} \cdot \eta} - \left(1 - y_{hp,cp,k}^{dir}\right) \cdot w_{hp,cp}^{pump,UP} \qquad \forall\ hp \in HP,\ cp \in CP,\ k \in K \tag{4-168}$$

The whole investment pumping for a direct process-to-process heat exchange accounts for pumps in both directions.

$$I^{pump,dir} = \sum cf^{\,pump} \cdot 2 \cdot y_{\mathrm{hp},cp,k}^{dir} + \sum_{hp,cp,k} cv^{pump} \cdot w_{hp,cp,k}^{pump,CSHS} + \sum_{hp,cp,k} cv^{pump} \cdot w_{hp,cp,k}^{pump,HSCS} \qquad \forall\ hp \in HP,\ cp \in CP,\ k \in K \tag{4-169}$$

4.5.1.10 Objective function

The objective function is the expected net present value of savings ΔW_{ENPV}

$$\Delta W_{ENPV} = -\Delta I + \sum_{n=1}^{t_{\mathrm{LT}}} \sum_{v} p_{n,v} \cdot \frac{\Delta F_{\mathrm{C},n,v}}{(1 + r_{\mathrm{D}})^n} \tag{4-170}$$

It consists of total annual costs $\Delta F_{\mathrm{C},n,v}$:

$$\Delta F_{\mathrm{C},n,v} = \left(\left(1 - r_{\mathrm{T}}\right)\left(c_{n,v}^{\mathrm{tot}} - c_{n,v}^{\mathrm{OP}}\right) + r_{\mathrm{T}} \frac{\Delta I}{t_{\mathrm{LT}}}) \right) \qquad \forall n \in N,\ v \in V \tag{4-171}$$

which contains a term for determining the annual cash flow at forecasted utility prices, when no heat integration is performed $c_{n,v}^{\mathrm{tot}}$. This case can be regarded as the reference case.

$$c_{n,v}^{\mathrm{tot}} = \sum_{cp} Ecc_{cp} \cdot t^{\mathrm{op}} \cdot c_{n,v}^{HU} + \sum_{hp} Ech_{hp} \cdot t^{\mathrm{op}} \cdot c_{n,v}^{CU} \qquad \forall n \in N,\ v \in V \tag{4-172}$$

The difference between the annual cash flow without $c_{n,v}^{\mathrm{tot}}$ and with $c_{n,v}^{\mathrm{OP}}$ heat integration performed (Eq. 4-173) represents the savings due to heat recovery.

$$c_{n,v}^{\mathrm{OP}} = \sum_{cp}\left(Q_{cp}^{HU}\cdot t^{\mathrm{op}}\cdot c_{n,v}^{HU}\right) + \sum_{hp}\left(Q_{hp}^{CU}\cdot t^{\mathrm{op}}\cdot c_{n,v}^{CU}\right) +$$
$$\sum_{icup}\left(Q_{icup}^{HU}\cdot t^{\mathrm{op}}\cdot c_{n,v}^{HU}\right) + \sum_{ccond}\left(Q_{ccond}^{HU}\cdot t^{\mathrm{op}}\cdot c_{n,v}^{HU}\right) +$$
$$\sum_{iu}\left(w_{iu}^{pump}\cdot t^{\mathrm{op}}\cdot c^{el}\right) + \sum_{hp}\sum_{cp}\sum_{k}\left({}_{hp,cp,k}^{pump,HSCS}\cdot t^{\mathrm{op}}\cdot c^{el}\right) + \sum_{hp}\sum_{cp}\sum_{k}\left({}_{hp,cp,k}^{pump,CSHS}\cdot t^{\mathrm{op}}\cdot c^{el}\right)$$
$$\forall n\in N,\ v\in V \qquad (4\text{-}173)$$

However, in order to achieve these savings, additional investment ΔI is needed. The investment would consist of the costs for all types of heat exchangers, pipes, and pumps.

$$\Delta I = \sum_{hp}\sum_{cp}\sum_{k}\left(cf\cdot y_{hp,cp,k} + cv\cdot\left(A_{hp,cp,k}\right)^{aexp}\right) + \sum_{hp}\sum_{icu}\sum_{k}\left(cf\cdot y_{hp,icu,k} + cv\cdot\left(A_{hp,icu,k}\right)^{aexp}\right) +$$
$$\sum_{ihu}\sum_{cp}\sum_{k}\left(cf\cdot y_{ihu,cp,k} + cv\cdot\left(A_{ihu,cp,k}\right)^{aexp}\right) +$$
$$\sum_{hp}\left(cf^{\mathrm{CU}}\cdot y_{hp}^{\mathrm{CU}} + cv\cdot\left(A_{hp}^{\mathrm{CU}}\right)^{aexp}\right) + \sum_{cp}\left(cf^{\mathrm{HU}}\cdot y_{cp}^{\mathrm{HU}} cv\cdot\left(A_{cp}^{\mathrm{HU}}\right)^{aexp}\right) +$$
$$\sum_{ccond}\left(cf^{\mathrm{HU}}\cdot y_{ccond}^{\mathrm{HU}} cv\cdot\left(A_{ccond}^{\mathrm{HU}}\right)^{aexp}\right)$$
$$c^{pipe,indir} + c^{pipe,dir} + \sum_{iu} I_{iu}^{pump} + I^{pump,dir}$$
$$\forall n\in N,\ v\in V \qquad (4\text{-}174)$$

The following heat exchangers and their heat exchanger area calculations are represented within the model:

i) Heat exchange between hot process stream *hp* and cold process stream *cp* $A_{hp,cp,k}$:

$$A_{hp,cp,k} = \frac{Q_{hp,cp,k}\cdot\left(\left(1/hh_{hp}\right)+\left(1/hc_{cp}\right)\right)}{\left(\Delta T_{hp,cp,k}\cdot\Delta T_{hp,cp,k+1}\cdot\dfrac{\left(\Delta T_{hp,cp,k}+\Delta T_{hp,cp,k+1}\right)}{2}\right)^{1/3}}$$
$$\forall\ hp\in\ HP,\ cp\in\ CP,\ k\in\ K \qquad (4\text{-}175)$$

ii) Heat exchange between intermediate utility as hot stream *ihu* and cold process stream *cp* (steam condensation) $A_{ihu,cp,k}$:

$$A_{ihu,cp,k} = \frac{Q_{ihu,cp,k}\cdot\left(\left(1/hh_{ihu}\right)+\left(1/hc_{cp}\right)\right)}{\left(\Delta T_{ihu,cp,k}\cdot\Delta T_{ihu,cp,k+1}\cdot\dfrac{\left(\Delta T_{ihu,cp,k}+\Delta T_{ihu,cp,k+1}\right)}{2}\right)^{1/3}}$$
$$\forall\ ihu\in\ IHU,\ cp\in\ CP,\ k\in\ K \qquad (4\text{-}176)$$

iii) Heat exchange between hot process stream *hp* and intermediate utility as cold process stream *icu* (evaporation and preheating) $A_{hp,icu,k}$:

$$A_{hp,icu,k} = \frac{Q_{hp,icu,k} \cdot \left(\left(1/hh_{hp} \right) + \left(1/hc_{icu} \right) \right)}{\left(\Delta T_{hp,icu,k} \cdot \Delta T_{hp,icu,k+1} \cdot \frac{\Delta T_{hp,icu,k} + \Delta T_{hp,icu,k+1}}{2} \right)^{1/3}}$$

$$\forall\ ihu \in IHU,\ cp \in CP,\ k \in K \qquad (4\text{-}177)$$

iv) Heat exchange between cold process stream *cp* and external hot utility A_{cp}:

$$A_{cp} = \frac{Q_{hp} \cdot (1/hc_{cp} + 1/hhu)}{\left(\left(T^{HU,in} - TC_{cp} \right) \cdot \Delta T_{cp}^{HU} \cdot \frac{\left(T^{HU,in} - TC_{cp} \right) + \Delta T_{cp}^{HU}}{2} \right)^{1/3}} \qquad \forall\ cp \in CP \qquad (4\text{-}178)$$

v) Heat exchange between stream of condensate in process, where steam is generated, and external hot utility A_{ccond}:

$$A_{ccond} = \frac{Q_{cond} \cdot (1/hc_{ccond} + 1/hhu)}{\left(\left(T^{HU,in} - TC_{ccond} \right) \cdot \Delta T_{ccond}^{HU} \cdot \frac{\left(T^{HU,in} - TC_{ccond} \right) + \Delta T_{ccond}^{HU}}{2} \right)^{1/3}}$$

$$\forall\ ccond \in CCond \qquad (4\text{-}179)$$

vi) Heat exchange between hot process stream *hp* and external cold utility A_{hp}:

$$A_{hp} = \frac{Q_{hp} \cdot (1/hh_{hp} + 1/hcu)}{\left(\left(TH_{hp}^{out} - T^{CU,in} \right) \cdot \Delta T_{hp}^{CU} \cdot \frac{\left(TH^{out} - T^{CU,in} \right) + \Delta T_{hp}^{CU}}{2} \right)^{1/3}} \qquad \forall\ hp \in HP \qquad (4\text{-}180)$$

In the literature, calculation of pipe cost is slightly different in various handbooks, see e.g. Nayyar (2000), therefore only the main elements of pipe cost are included in the calculation (each element is described in McAllister, 2014). It is comprised of pipe material cost, cost of installation, right-of-way cost, and insulation cost. The weight of a pipe $w_{s\_scond,iu\_iucond}^{tot}$ is defined by the following equality:

$$w_{s\_scond,iu\_iucond}^{tot} = 1.49 \cdot \left(10.68 \cdot th_{s\_soncd,iu\_iucond}^{pipe} \cdot 39.37 \cdot d_{s\_soncd,iu\_iucond} \cdot 39.37 \right) \cdot Ls_{s\_soncd,iu\_iucond}^{\mathrm{var}}$$

$$\forall\ s\_scond \in S\_SCond,\ iu\_iucond \in IU\_IUCond \qquad (4\text{-}181)$$

A pipe's installation cost $pipe_{s\_scond,iu\_iucond}^{inst}$ depends on the outer diameter of the pipe, (sum of inner diameter d_{s_scond,iu_iucond} and pipe thickness twice $th_{s\_scond,iu\_iucond}^{pipe}$) and its length $Ls_{s\_soncd,iu\_iucond}^{\mathrm{var}}$ as presented in Eq. 4-182.

$$pipe_{s\_scond,iu\_iucond}^{inst} = \left(d_{s\_scond,iu\_iucond} + 2 \cdot th_{s\_scond,iu\_iucond}^{pipe} \right)^{0.43} \cdot Ls_{s\_soncd,iu\_iucond}^{\mathrm{var}}$$

$$\forall\ s\_scond \in S\_SCond,\ iu\_iucond \in IU\_IUCond \qquad (4\text{-}182)$$

The volume of the insulation $V^{ins}_{s\_scond,iu\_iucond}$ besides other presented variables also depends on the insulation thickness $th^{ins}_{s\_scond,iu\_iucond}$ (Eq. 4-183).

$$V^{ins}_{s\_scond,iu\_iucond} = \pi \cdot \Big(\big(d_{s\_scond,iu\_iucond} / 2 + th^{pipe}_{s\_scond,iu\_iucond} + th^{ins}_{s\_scond,iu\_iucond} \big)^2 - \big(d_{s\_scond,iu\_iucond} / 2 + th^{pipe}_{s\_scond,iu\_iucond} \big)^2 \Big) \cdot Ls^{\text{var}}_{s\_scond,iu\_iucond} \quad \forall\ s \in S,\ icue \in ICUE \tag{4-183}$$

The cost of a pipeline is the sum of the material cost , installation cost, right-of-way cost, and the insulation cost of the pipe.

$$c^{pipe,indir} = c^{P1} \cdot \sum_{s,icue} w^{tot}_{s,icue} + c^{P2} \cdot \sum_{s,icue} pipe^{inst}_{s,icue} + c^{P3} \cdot \sum_{s,icue} ys_{s,icue} \cdot Ls_s + c^{P4} \cdot \sum_{s,icue} V^{ins}_{s,icue} \tag{4-184}$$

The weight of a pipe is defined by the following equations:

$$w^{tot,dir,CSHS}_{hp,cp,k} = 1.49 \cdot \big(10.68 \cdot th^{pipe,CSHS}_{hp,cp,k} \cdot 39.37 \cdot d^{pipe,CSHS}_{hp,cp,k} \cdot 39.37 \big) \cdot L^{\text{var}}_{hp,cp,k} \quad \forall\ hp \in HP,\ cp \in CP,\ k \in K \tag{4-185}$$

$$w^{tot,dir,HSCS}_{hp,cp,k} = 1.49 \cdot \big(10.68 \cdot th^{pipe,HSCS}_{hp,cp,k} \cdot 39.37 \cdot d^{pipe,HSCS}_{hp,cp,k} \cdot 39.37 \big) \cdot L^{\text{var}}_{hp,cp,\mathrm{k}} \quad \forall\ hp \in HP,\ cp \in CP,\ k \in K \tag{4-186}$$

A pipe's installation cost depends on the outer diameter of the pipe and its length as presented in Eq. 4-187 and Eq. 4-188.

$$pipe^{inst,CSHS}_{hp,cp,k} = \big(d^{CSHS}_{hp,cp,k} + 2 \cdot th^{pipe,CSHS}_{hp,cp,k} \big)^{0.43} \cdot L^{\text{var}}_{hp,cp,k} \quad \forall\ hp \in HP,\ cp \in CP,\ k \in K \tag{4-187}$$

$$pipe^{inst,HSCS}_{hp,cp,k} = \big(d^{HSCS}_{hp,cp,k} + 2 \cdot th^{pipe,HSCS}_{hp,cp,k} \big)^{0.43} \cdot L^{\text{var}}_{hp,cp,k} \quad \forall\ hp \in HP,\ cp \in CP,\ k \in \tag{4-188}$$

The volume of the insulation has to be determined (Eq. 4-189 and Eq. 4-190), in order to calculate the insulation cost.

$$V^{ins,CSHS}_{hp,cp,k} = \pi \cdot \Big(\big(d^{CSHS}_{hp,cp,k} / 2 + th^{pipe,CSHS}_{hp,cp,k} + th^{ins,CSHS}_{hp,cp,k} \big)^2 - \big(d^{CSHS}_{hp,cp,k} / 2 + th^{pipe,CSHS}_{hp,cp,k} \big)^2 \Big) \cdot L^{\text{var}}_{hp,cp,k} \quad \forall\ hp \in HP,\ cp \in CP,\ k \in K \tag{4-189}$$

$$V^{ins,HSCS}_{hp,cp,k} = \pi \cdot \Big(\big(d^{HSCS}_{hp,cp,k} / 2 + th^{pipe,HSCS}_{hp,cp,k} + th^{ins,HSCS}_{hp,cp,k} \big)^2 - \big(d^{HSCS}_{hp,cp,k} / 2 + th^{pipe,HSCS}_{hp,cp,k} \big)^2 \Big) \cdot L^{\text{var}}_{hp,cp,k} \quad \forall\ hp \in HP,\ cp \in CP,\ k \in K \tag{4-190}$$

Finally, the cost of a pipeline is the sum of the material cost, installation cost, right-of-way cost, and the insulation cost of the pipe.

$$c^{pipe,dir} = c^{P1} \cdot \sum_{hp,cp,k} \left(w_{hp,cp,k}^{tot,dir,CSHS} + w_{hp,cp,k}^{tot,dir,HSCS} \right) + c^{P2} \cdot \left(pipe_{hp,cp,k}^{inst,CSHS} + pipe_{hp,cp,k}^{inst,HSCS} \right)$$
$$+ c^{P3} \cdot \sum_{hp,cp,k} 2 \cdot y_{hp,cp,k} \cdot L_{hp,cp} + c^{P4} \cdot \sum_{s,icue} \left(V_{hp,cp,k}^{ins,CSHS} + V_{hp,cp,k}^{ins,HSCS} \right) \qquad (4\text{-}191)$$

4.5.2 Illustrative Case study 4

This case study is presented showing a testing of the model and discussing the basic relationships during optimisation regarding Total Site. The input data for Total Site included the supply T_S and target T_T temperatures, heat capacity flow rates FC, and the heat transfer coefficients of each stream (Table 4-6). Two types of heat exchangers were considered. A double pipe heat exchanger was used for heat exchange between the process stream and the external utility, having a fixed-charge coefficient of 121.4 k€ and a variable-charge coefficient of 0.193 k€/m^2, whilst for matches between the process streams and between the process streams and the intermediate utilities a fixed-plate shell and tube heat exchanger with a fixed-charge coefficient of 46.0 k€ and a variable-charge coefficient of 2.742 k€/m^2 were used. The data was taken from 2008, however updated to 2012 prices by applying the Chemical Engineering Plant Cost Index – CEPCI (Chemical Engineering, 2012). The depreciation was determined for 15y. Three intermediate utilities were considered: i) high pressure-, ii) medium pressure-, and iii) low pressure steam. The temperature range for each intermediate utility is presented in Table 4-6. After performing Heat Integration, the additional heating/ cooling requirements were supplied by hot oil and cooling water as external utilities (Table 4-6). Investment for heat exchangers was modified by a factor for increased steam pressure. 10 % and 15 % higher investment for piping was assumed for medium pressure steam and high pressure steam, respectively.

Table 4-6: Input data for Case study 4

PROCESS STREAMS					
Process	Stream/Type	T_S/°C	T_T/°C	FC/kW°C^{-1}	h/kWm^{-2}°C^{-1}
Process 1	H1P1/hot	350	200	15	0.33
	C1P1/cold	2	80	15	0.45
Process 2	H1P2/hot	50	20	16	0.40
	C1P2/cold	0	150	25	0.38
			UTILITIES		
Utility	Type		T^{lo}/°C	T^{up}/°C	h/kWm^{-2}°C^{-1}
Intermediate	Low-pressure steam		120	148	10
Intermediate	Medium-pressure steam		148	208	10.5
Intermediate	High-pressure steam		208	252	11
			T^{in}/°C	T^{out}/°C	
External	Hot oil		377	377	0.8
External	Cooling water		0	10	0.8
UTILITIES					
				Fixed charge coefficient/ k€	Variable cost coefficient
Investment for a heat exchanger between process streams and intermediate utility				46	2.742/ k€ m^{-2}
Investment for a heat exchanger between process streams and external utility				121.4	0.193/ k€ m^{-2}

Investment for pump	2.2	8.9 €/kWh
PIPELINE		
Thermal conductivity of insulation (Devki Energy Consultancy, 2006)	0.03	W/(m.°C)
Friction factor of pipeline	Direct heat transfer	0.015
	Indirect heat transfer-steam	0.0188
	Indirect heat transfer-condensate	0.011
Pipe cost per unit weight (Alibaba, 2014)	1.3	k€/t
Installation cost (McAllister, 2014)	0.26	
Right-of-way cost (McAllister, 2014)	80	k€/km
Insulation cost	0.3	k€/m^3

The pump efficiency was 0.45 and the electricity cost 0.1 €/kWh. In regard to economic analysis, a 15y lifetime was considered, 20% tax rate, 5% discount rate and 2 % inflation were assumed, resulting in a 7 % interest rate.

4.5.2.1 *Results*

A comparison was performed between the direct and indirect heat transfers. Table 4-7 presents the comparison for 0.5 km distance, when the condensate recovery was 100%. The ΔW_{ENPV} is the expected net present value, Q^{HU} the hot utility load, Q^{CU} the cold utility load, Q^{REC} the heat recovery load within each process, Q^{REC_TS} is the process-to-process heat recovery, I the investment, c^{OP_sav} the net present value of savings in operating cost over the entire lifetime, D net present value of the depreciation over the entire lifetime.

Table 4-7: Comparison of direct and indirect (100% condensate recovery) heat recovery at 0.5 km

Process-to-process heat transfer	ΔW_{ENPV} /k€	Q^{HU}/kW	Q^{CU}/kW	Q^{REC}/kW	Q^{REC_TS}	I/k€	c^{OP_sav} / k€	D/ k€
Direct	38,525.0	2,198.2	-	P1: 1,170 P2:480.	1071.8	**I= 1,014.6** I^{HEN}=689.6 I^{PIPE}= 320.6 I^{PUMP}=4.402	39,416.4	123.2
Indirect	38,214.6	2,211. 6	-	P1: 1,170 P2:480	1,066.6	**I= 1,167.0** I^{HEN}= 950.4 I^{PIPE}= 212.2 I^{PUMP}=4.404	39,239.9	141.7
Difference	310.4	-13.4	-	0	5.2	-152.4	176.5	-18.5
Difference/%	0.8	-0.6	-	0	0.5	-15	0.45	15

As can be seen in Table 4-7 the direct heat transfer between processes results have a somewhat higher ΔW_{ENPV} . This was due to better process-to-process integration when direct heat transport was applied. It results in higher energy savings and also lower investment by 152.4 k€ than in the indirect heat transfer case. The pipe cost decreased when indirect heat exchange was applied by 108.4 k€ (34 %); however, it did not outweigh the increased investment cost for heat exchangers that was 260.8k€ (38 %) higher in the case of indirect heat exchange. It should be noted that in the case of direct heat exchange only one heat exchanger was necessary, whilst in the case of indirect heat exchange there are two heat exchangers: i) from the hot process stream of one process to the intermediate utility stream and ii) from the intermediate utility stream to the cold process stream of another process. Moreover, the temperature difference as a driving force for heat exchange was for the indirect heat exchange exchangers, generally speaking, half of those for direct heat exchange, due to the temperature level of the intermediate utility. Lower temperature difference thus resulted in an increase of heat transfer area and consequently an increase in the investment for heat exchangers. Therefore, it should be noted that an investment increase when considering indirect process-to-process heat exchange is generally twofold: i) because of the higher number of heat exchangers required and ii) due to lower temperature differences.

The sum of the depreciations over the entire lifetime increases due to higher investment for indirect process-to-process heat exchange. However, the higher depreciation leads to a higher tax decrease (as the depreciation is deducted from incomes).

When changing the distances between the processes the trade-offs also moved in a different direction. Table 4-8 presents the results when the distance between processes was 2 km. It can be concluded that even at greater distances the direct heat exchanges resulted in higher ΔW_{ENPV}.

Table 4-8: Comparison of direct and indirect (100% and 70 % condensate recovery) heat recovery at 2 km

Process-to-process heat transfer	ΔW_{ENPV} /k€	Q^{HU}/kW	Q^{CU}/kW	Q^{REC}/kW	Q^{REC_TS}	I/k€	c^{OP_sav} / k€	D/ k€
a) Direct	37,370.2	2,222.3	-	P1: 1,170 P2:480.	1,047.6	***I*= 1974.2** I^{HEN}= 689.7 I^{PIPE}= 1280.1 I^{PUMP}=4.402	39,104.6	239.8
b) Indirect (100% condensate recovery)	36,787.7	2,280.6	-	P1: 1,170 P2:480	1,024.6	***I*=1776.7** I^{HEN}=933.4 I^{PIPE}=838.8 I^{PUMP}=4.411	38,348.7	215.8
c) Indirect (70% condensate recovery)	35,908.9	2,346.5	-	P1: 1,170 P2:480	956.1	***I*=1811.7** I^{HEN}=970.5 I^{PIPE}=836.7 I^{PUMP}=4.411	37,500.6	220.0
Difference b-a	**-582.5**	**58.3**	**-**	**0**	**-23.0**	**-197.5**	**-755.9**	**24.0**
Difference b-a /%	**-1.6**	**2.3**	**-**	**0**	**-2.2**	**-10.0**	**-1.93**	**10.0**
Difference c-b	-878.8	65.9	-	0	-68.5	35	-848.1	4.2
Difference c-b /%	-2.4	2.9	-	0	-6.7	1.9	-2.2	1.9

From Table 4-8 it could be seen that with the increase the distance difference between the two options was higher compared to the case with the smaller distance (Table 4-7). As could be seen the difference was reversed between hot utility consumption at this distance. This was achieved due to lower heat recovery and higher heat losses when applying indirect heat exchange. Heat losses of indirect exchange were increased due to the usually higher temperature within the pipeline. It should be noted that heat losses occurred during transfer in pipelines (partly recovered by condensate recovery) were also covered by hot utility. This led to an additional heat exchanger for the preheating of condensate. In the case of the direct heat exchanger, the hot utility covered only the demand of a cold stream that had not been covered by heat recovery. The heat recovery had decreased due to heat losses. Therefore, in the case of direct heat exchange, the heat losses resulted in an increase of most probably the already existing heat exchanger and not necessarily in an additional heat exchanger. The overall investment of direct heat exchange was higher compared to the indirect one. This was mainly a consequence of higher investment in the pipe. It was also a result of larger diameters (31.4 cm) in both directions when a direct heat exchanger was applied, compared to those pipelines when indirect heat exchange was considered, where the larger diameter was only for one steam main (33.9 cm), whilst the condensate pipeline was significantly smaller (7.1 cm). The investment in pumps was somewhat higher, when indirect exchange was considered as pressure drop in these pipes leading also to a loss of temperature potential; however, the investment and, moreover, the difference between investment in pumps was relatively low and could be neglected.

Furthermore, the influence of the condensate recovery rate was also investigated (Table 4-8). As expected, when the condensate recovery was lower, the hot utility consumption had increased by 65.9 kW as the process-to-process heat recovery decreased by 68.5 kW. It should be noted that the increase in the hot utility consumption was somewhat lower compared to process-to-process heat transfer decrease. This is a result of somewhat lower heat demand of condensate preheating due to decreased rate of recovery. Additional heating was required for fresh water pre-heating, which could be covered by a hot process stream. The investment for heat exchangers increased due to an additional heat exchanger for preheating and smaller temperature differences within the heat exchangers.

4.5.3 Case study 5

This case study consisted of two processes - Process 1 included three hot and two cold streams and Process 2 two hot and two cold streams. Three different intermediate utilities and two external utilities were available. The input data for those streams and utilities are presented in Table 4-9.

Table 4-9: Input data for Case study 5

		PROCESS STREAMS			
Process	Stream/Type	T_S/°C	T_T/°C	FC/kW°C^{-1}	h/kWm^{-2}°C^{-1}
Process 1	H1P1/hot	350	200	15	0.35
	H2P1/hot	342	210	14	0.33
	H3P1/hot	330	192	12	0.30
	C1P1/cold	27	80	10	0.45
	C2P1/cold	0	150	8	0.38
Process 2	H1P2/hot	50	30	8	0.4
	H2P2/hot	40	20	12	0.4
	C1P2/cold	-13	85	30	0.4
	C2P2/cold	-20	150	25	0.3
		UTILITIES			
Utility	Type		T^{lo}/°C	T^{up}/°C	h/kWm^{-2}°C^{-1}
Intermediate	Low-pressure steam		120	148	10
Intermediate	Medium-pressure steam		148	208	10.5
Intermediate	High-pressure steam		208	252	11
			T^{in}/°C	T^{out}/°C	
External	Hot oil		377	377	0.8
External	Cooling water		0	10	0.8
		INVESTMENT			
				Fixed charge coefficient/ k€	Variable cost coefficient
Investment for a heat exchanger between process streams and intermediate utility				46	2.742/ k€ m^{-2}
Investment for a heat exchanger between process streams and external utility				121.4	0.193/ k€ m^{-2}
Investment for pump				2.2	8.9 €/kWh
		PIPELINE			

Thermal conductivity of insulation (Devki Energy Consultancy, 2006)	0.03	W/(m.°C)
Friction factor of pipeline	Direct heat transfer	0.015
	Indirect heat transfer-steam	0.0188
	Indirect heat transfer-condensate	0.011
Pipe cost per unit weight (Alibaba, 2014)	1.3	k€/t
Installation cost (McAllister, 2014)	0.26	
Right-of-way cost (McAllister, 2014)	80	k€/km
Insulation cost	0.3	k€/m^3

The pump efficiency was 0.45 and the electricity cost 0.1€/kWh. In regard to economic analysis a 15y lifetime was considered, 20% tax rate, 5% discount rate, and 2% inflation.

4.5.3.1 *Results for indirect heat transfer*

The synthesis was performed at different distances from 1km to 6km between the two processes in order to perform sensitivity analyses of external utility consumption, heat recovery within and between processes, and economics. Figure 4-22 presents the expected net present value ΔW^{ENPV}, enthalpy flow of heat recovery within processes (ΔH^{rec} in Figure 4-22), hot utility consumption (ΔH^{HU} in Figure 4-22) and enthalpy flow of heat recovery between two processes ($\Delta H^{\mathrm{rec\_TS}}$ in Figure 4-22), depending on the distance L between the processes. Note that the level of heat integration within the processes did not change with the distance, whilst the $\Delta H^{\mathrm{rec\_TS}}$ was decreasing and ΔH^{HU} increasing. As a consequence, the ΔW^{ENPV} decreased and was reduced by 6 % at 6 km compared to the one at 1 km.

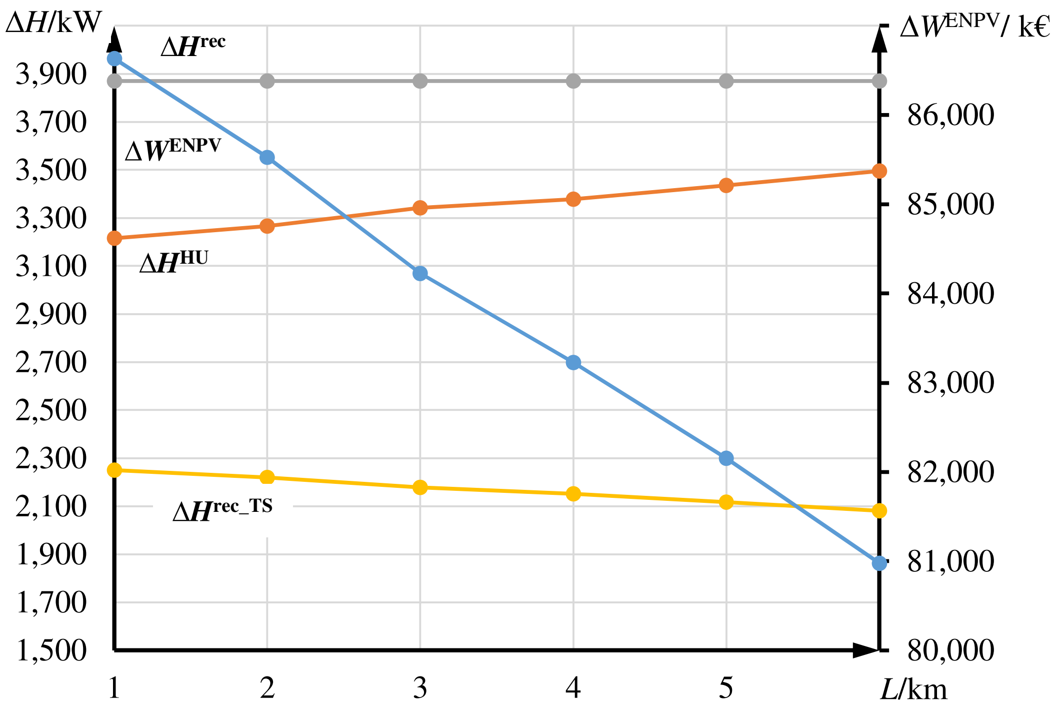

Figure 4-22: Enthalpy flow-rate of indirect process-to-process heat exchange together with external hot utility consumption depending of a distance between processes for 100% condensate recovery

Figure 4-23 presents an analysis of the involved investment. As expected, the total investment I was larger at higher distances. The major contribution to the increased investment was the increase of investment in the pipeline (I^{pipe} in Figure 4-23), whilst the investment of HEN

(I^{HEN} in Figure 4-24) and the one of the pump (I^{pump} in Figure 4-24) did not vary notably with distance. From Figures 4-23 and 4-24 it could be concluded that the decrease in ΔW^{ENPV} depending on the distance was twofold. It was firstly a consequence of decreased heat recovery resulting in higher operating cost, and secondly, due to increased investment, mainly for the pipeline. From Figure 4-24 it could be seen that at about 3.5 km for Case study 5 the fraction of the pipeline investment within the overall investment prevailed. Thus, in general it can be concluded that the fraction of pipeline investment increased with the distance, whilst the one of HEN gradually decreased.

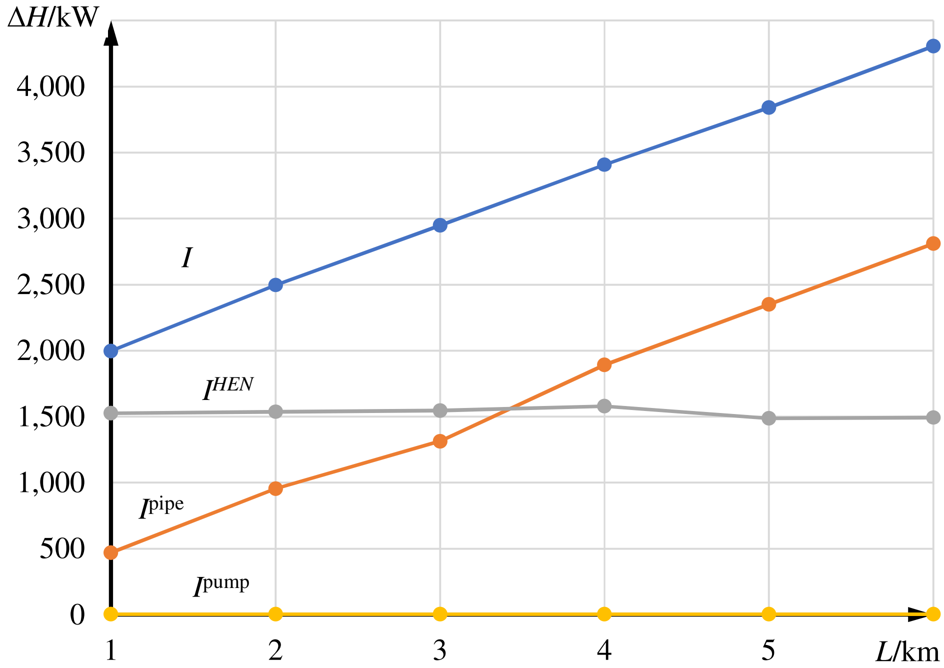

Figure 4-23: Investment distribution between heat exchangers, pipeline and pumps depending on the distance between processes, when condensate heat recovery is 100 %

The presented results were obtained under the assumption of 100 % condensate recovery. In reality, the assumption of 100 % condensate recovery is quite unrealistic. Therefore, an analysis at 70 % condensate recovery was performed in order to evaluate its effect on the economic performance. Figure 4-24 presents a comparison between the situations when the heat recovery was 100 % and when 70 %. The heat recovery between processes was decreased and the hot utility requirement increased enabling coverage of the fresh water preheating demand. The ΔW^{ENPV} was therefore decreased, on average by approximately 1,800 k€, which represented 2.1 % reduction. Therefore, the effect of the condensate recovery could not be neglected, as even 70 % of condensate recovery presents a high recovery rate.

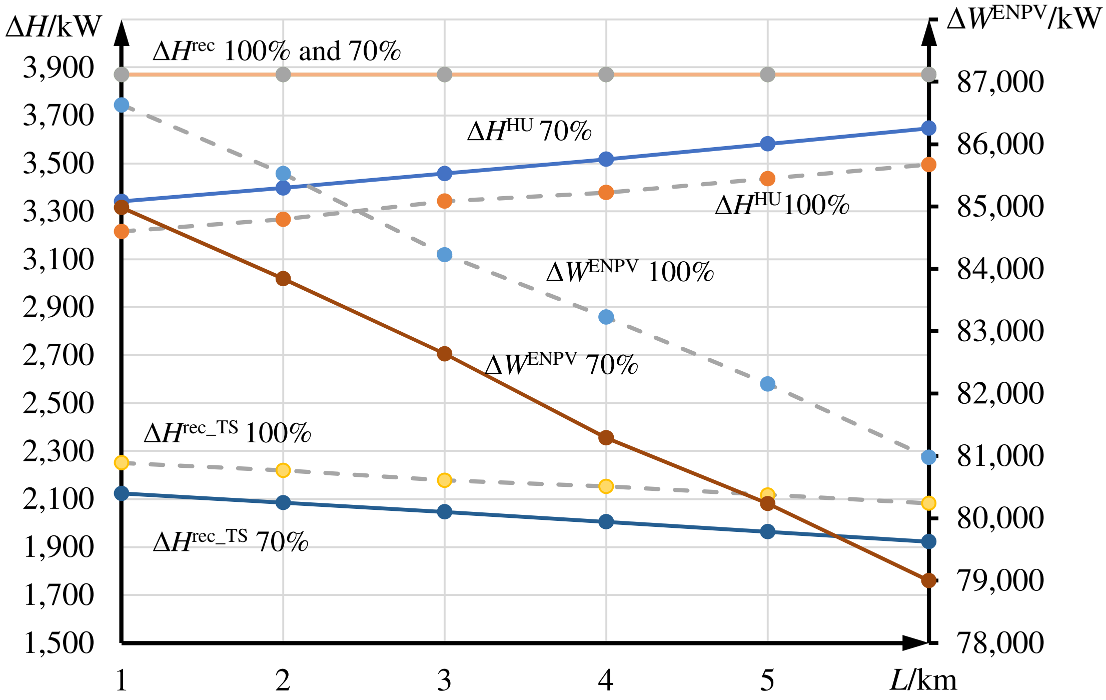

Figure 4-24: Comparison of the expected net present value, hot utility consumption, heat exchange within and between processes when condensate recovery is 100 % or 70 %

4.5.3.2 *Results for direct heat transfer*

The direct heat transfer was evaluated between processes. As can be seen in Figure 4-25, the ΔW^{ENPV} decreased with any increase of distance.

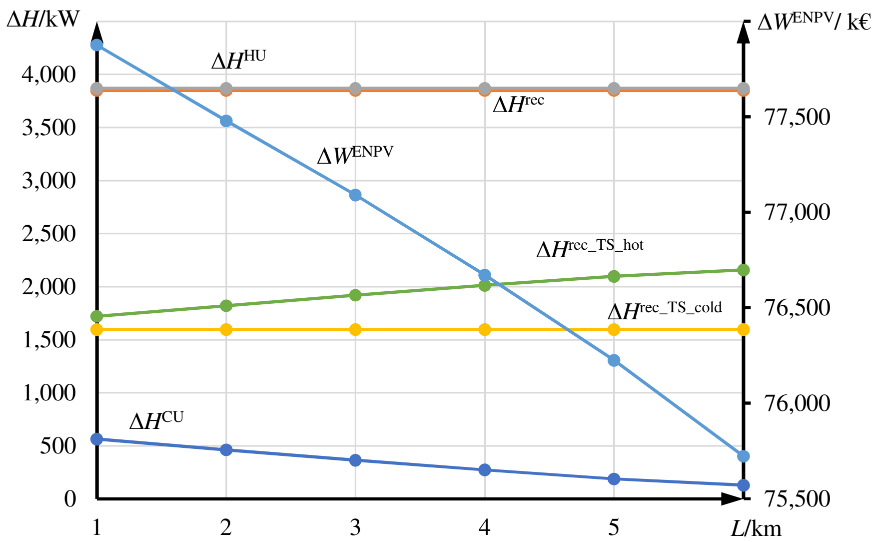

Figure 4-25: Enthalpy flow-rate of direct process-to-process heat exchange together with external hot utility consumption depending of a distance between processes

The hot utility consumption and heat recovery within processes did not change by the variation of the distance. The cold utility consumption decreased when increasing the distances between processes. This is a result of higher heat losses in longer pipelines, providing some cooling. This decrease of cold utility consumption can be seen in Figure 4-25 as the difference between the heat transferred from the hot process stream $\Delta H^{rec\_TS\_hot}$ and that to the cold stream $\Delta H^{rec\_TS\_cold}$. Note that the first one represents the amount of heat transfer without heat loss. This cooling effect can provide some advantage for cooling by pipelines at larger distances. However, the expected net present value with the distance is significantly decreasing. In this case when direct heat transfer is applied it can be seen that the fraction of the pipeline investment becomes predominant already at a 2 km distance between the processes.

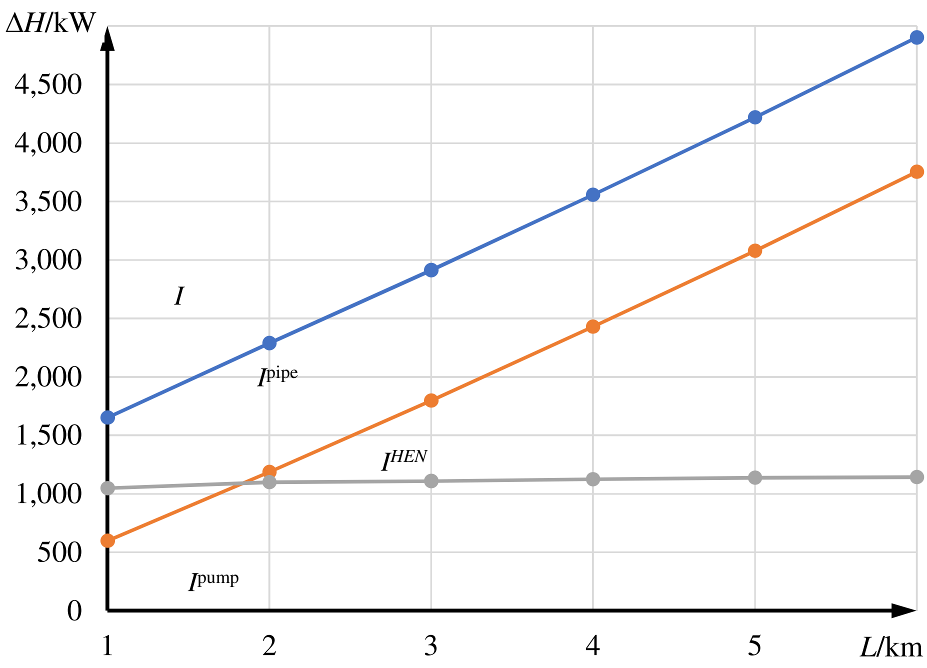

Figure 4-26: Enthalpy flow-rate of indirect process-to-process heat exchange together with external hot utility consumption depending of a distance between processes for 100% condensate recover

4.5.3.3 Comparison between indirect and direct heat transfers

Figure 4-27 presents the comparison between direct and indirect process-to-process heat exchanges. For Case study 5 the ΔW^{ENPV} was higher for indirect heat transfer ΔW^{ENPV_INDIR} at any distance between processes compared to the direct ΔW^{ENPV_DIR}. The heat recoveries within processes ($\Delta H^{rec,DIR}$ – direct heat exchange; $\Delta H^{rec,INDIR}$ – indirect heat exchange) were constant and of the same level in both the studied heat exchange modes. The heat recovery between processes was higher for indirect process-to-process heat transfer $\Delta H^{rec\_TS,INDIR}$ compared to the direct $\Delta H^{rec\_TS,DIR}$ one. Consequently, the hot utility consumption for indirect heat transfer $\Delta H^{HU,INDIR}$ was lower compared to the direct one $\Delta H^{HU,DIR}$. When applying indirect heat exchange, there was no cold utility consumption, whilst performing a direct heat exchange between streams of different processes resulted in some cold utility consumption $\Delta H^{CU,DIR}$. It should be noted that an upper limit on heat loss in the pipeline had been set according to the following Eqs. 4-192 and 4-193.

$$Q_{HP,CP,k}^{loss\_CSHS} = Ech_{hp}/5 \cdot \left(1\text{-}0.85^{L^{HP,CP}}\right) \qquad \forall hp \in HP,\ cp \in CP,\ k \in K \qquad (4\text{-}192)$$

$$Q_{HP,CP,k}^{loss\_HSCS} = Ech_{hp}/5 \cdot \left(1\text{-}0.85^{L^{HP,CP}}\right) \qquad \forall hp \in HP,\ cp \in CP,\ k \in K \qquad (4\text{-}193)$$

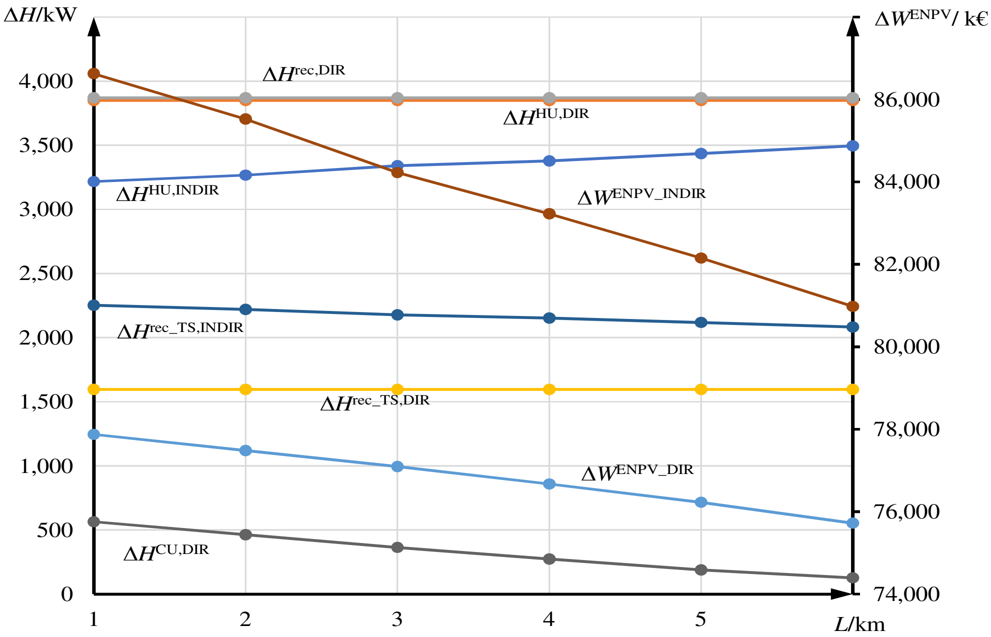

Figure 4-27: Comparison of the expected net present value, heat recovery and hot utility consumptions between indirect and direct process-to-process heat exchange depending on distance

By comparing the investment distribution between direct I^{DIR} and indirect I^{INDIR} process-to-process heat exchange it can be seen in Figure 4-28 that for shorter distances the investment was higher for indirect, whilst for longer distances the investment was higher for direct process-to-process heat exchange.

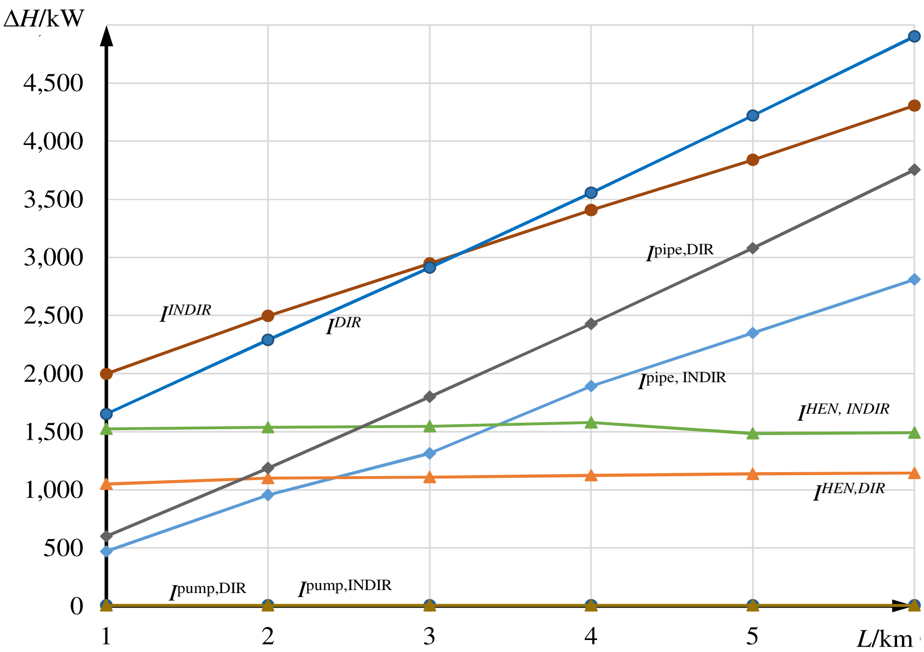

Figure 4-28 Comparison of the investment distribution between indirect and direct process-to-process heat exchange depending on distance

The HEN investment was higher for indirect heat exchange $I^{HEN, INDIR}$ compared to direct $I^{HEN,DIR}$, whilst pipe investment was higher for direct $I^{pipe,DIR}$ compared to indirect $I^{pipe,INDIR}$ heat exchange at any distance. The difference in pump investment ($I^{pump,DIR}$ – direct heat exchange and $I^{pump,INDIR}$ – indirect heat exchange) was negligible and did not contribute to the difference between both overall investments. It can be seen that at direct heat exchange the pipe investment took a higher proportion of the overall investment at shorter distances (less than 2 km), whilst for indirect heat transfer larger distances (more than 3 km). Figure 4- 29 presents corresponding HENs when considering direct or indirect heat exchanges between processes. The reason for the better result obtained for indirect heat exchange was due to its advantage of connecting more than only one hot and one cold stream. Despite the opportunity for heat recovery between all the hot streams of Process 1 and all cold streams of Process 2 only one pipeline was economically viable.

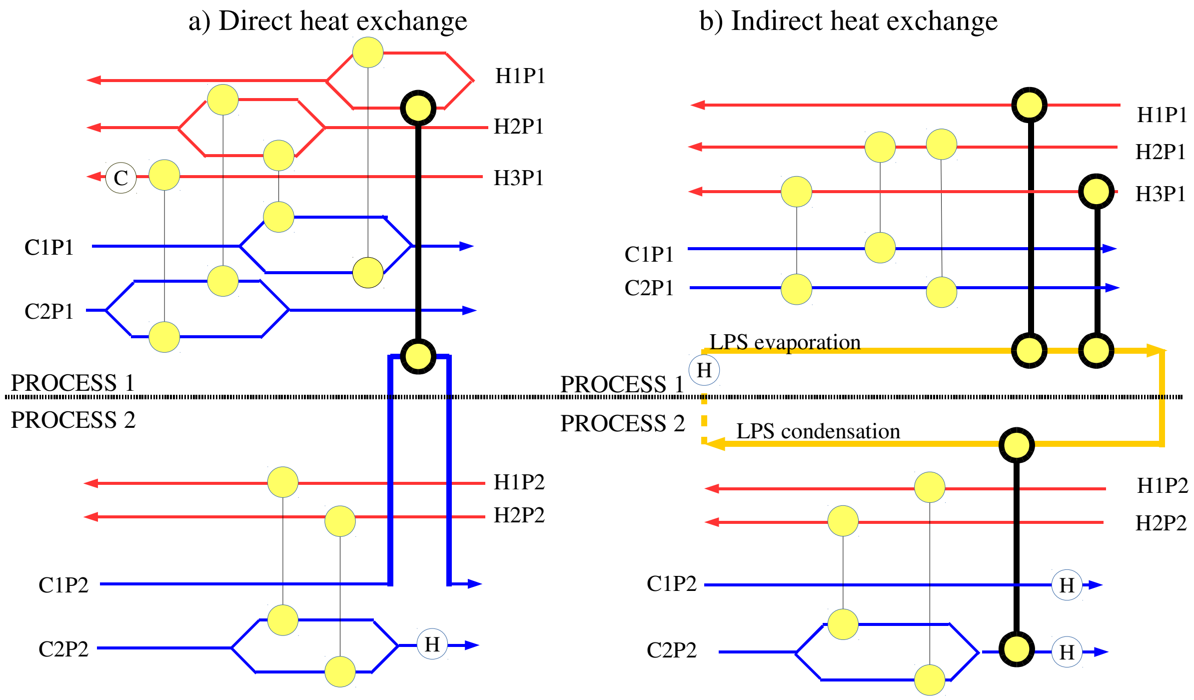

Figure 4-29: Heat Exchanger Networks for Total Site, when the distance is 2 km for a) direct and b) indirect process-to-process heat exchange

5 Synthesis of distillation columns sequence and their HENs over an entire lifetime

Optimally designing distillation columns in order to ensure energy efficiency is a complex task, which has a significant effect on process profitability, since separation processes require large amounts of utilities. In fact, the energy requirements for separation processes represent quite a high rate of overall world energy consumption. Similarly as during the heat integration, there are two main directions for distillation columns synthesis. One direction is the thermodynamic approach. Descriptions about sequencing the distillation columns, and about the heat integration of distillation columns, can be found in different sources - for example (Smith, 2005).

An example of retrofit design regarding methanol plant was presented by Demirel (2006) by applying a Column Grand Composite Curve and an Exergy Loss Profile. Soares Pinto et al. (2011) developed a novel approach for temperature-enthalpy profile when determining a target for the usage of side condensers and side reboilers, based on a thermodynamic analysis. They introduced a minimum driving force, which was considered as an exergy loss distribution of the existing column similar to temperature driving force in the case of HEN. By applying the thermodynamic approach, the target for processes is set. However, the rate of integrating the distillation column and HEN depends on the trade-off between the operating cost and the capital cost.

A mathematical programming approach was developed, in order to establish this trade-off. For example, Novak et al. (1996) presented a compact superstructure for the optimisation of distillation column's sequence integrated with its heat exchanger network. A nonlinear short-cut method was applied, in order to overcome the problems with singularities (1999). A combination of state task network and state equipment network superstructure was suggested for this purpose. A nonlinear disjunctive programming model was proposed for the synthesis of the heat integrated distillation column sequence. Another problem relating to solving MINLP problems is to ensure a feasible initial guess for the optimisation, on which the solution can be highly dependent, not to mention that the objective function and constraints usually have to be continuously differentiable twice. An alternative method for solving these problems is the natural hybrid evolutionary/local search method. Using this approach, the continuous design parameters for the units the local search method are applied, whilst for the optimisation procedure regarding the heat exchanger design an evolutionary optimisation procedure can be used (Fraga & Žilinskas, 2003). Proios et al. (2005) presented a generalised modular framework for the heat integrated distillation column. It is a three-stage systematic procedure that uses logical modelling in order to generate tight and accurate structural models. Grossmann et al. (2005) presented a rigorous model for the synthesis of a complex distillation column. Two models were described - a mixed-integer nonlinear model and a generalised disjunctive programming model. Both models applied tray-by-tray formulation. However, these models are quite complex. A novel approach for obtaining solution for the heat integrated distillation column sequence is the genetic algorithm (Wang and Li, 2010) for the non-sharp separation of the components.

5.1 Methodology

The aim of this work was to optimise distillation columns sequence when integrated with their heat exchanger network over an entire lifetime. A multi-period mixed-integer nonlinear programming (MINLP) model was applied based on the single-period model developed by

Novak and Kravanja (1996). The superstructure applied was a compact distillation superstructure, where each separation task is represented by a distinct distillation column. As the role of optimisation is to optimise the sequence of separation tasks, the solution for the optimisation is the optimal path of the distillation sequence. For the integration of a heat exchanger network (HEN), a one-stage HEN superstructure developed by Yee and Grossmann (1990) was integrated within the distillation superstructure. In this model each hot stream, representing condensation at the top of the distillation column, can be potentially matched with each cold stream, representing evaporation at the bottom of the column. The overall model's superstructure was presented in Novak et al. (1996).

As highlighted earlier, the utilities prices vary quite quickly. In order to account for these variations, future utility price projections, based on past price fluctuations, were forecast. The past price profiles for utilities were determined by applying the data and methodology described in Ulrich and Vasudevan (2006), for price basis the data from Index Mundi (2013) has been applied, and CEPCE factors has been taken from Chemical Engineering (2012). There are 5 scenarios due to the uncertainty of the projections, Figure 5-1. The neutral scenario 3 is based on the average utility prices; a more pessimistic scenario is 4, which is determined as the average of the utility prices above the overall average; a more optimistic scenario is 2, which is obtained as the average of the utility prices below the overall average; and the extreme scenarios (1 and 5) are determined as the averages above the scenarios 4 and 2.

The distillation sequence synthesis model previously developed by Novak et al. (1996) and the single-period model for the synthesis of HEN (Yee and Grossmann, 1990) were merged together and converted into a multi-period optimisation model, in order to account for utility prices variations. The synthesis of distillation column sequence, integrated within its heat exchanger network, was thus performed simultaneously.

In order to convert the model to multi-period, the following performance and operational variables x were disaggregated and indexed over a set of periods $i \in I$ so that they may vary throughout a lifetime: minimum number of trays $N_{DIST,i}^{\min}$,theoretical number of trays $N_{DIST,i}^{t}$,minimum reflux ratio $R_{DIST,i}^{\min}$, actual reflux ratio, $R_{DIST,i}^{ac}$,average volatility, $\alpha_{DIST,i}^{av}$, temperature of the hot stream $T_{H,k,i}$,temperature of the cold stream $T_{C,k,i}$,heat surplus of hot stream $Q_{H,k,i}$,heat demand of cold stream $Q_{C,k,i}$, amount of heat exchanged between hot and cold stream $Q_{H,C,k,i}$, temperature difference between hot and cold streams at stage k $\Delta T_{H,C,k,i}$, temperature difference between hot and cold stream at stage k+1 $\Delta T_{H,C,k+1,i}$, mass flow F_i, mass flow of component FC_i, temperature T_i, pressure P_i, vapour pressure VP_i, cold utility demand Q_i^{cool} ,hot utility demand Q_i^{heat} , heat capacity flow-rate of hot stream $FCP_{H,i}$ heat capacity flow-rate of cold stream $FCP_{C,i}$,heat duty of reboiler $Q_{HP,i}$,and heat duty of condenser $Q_{CP,i}$.

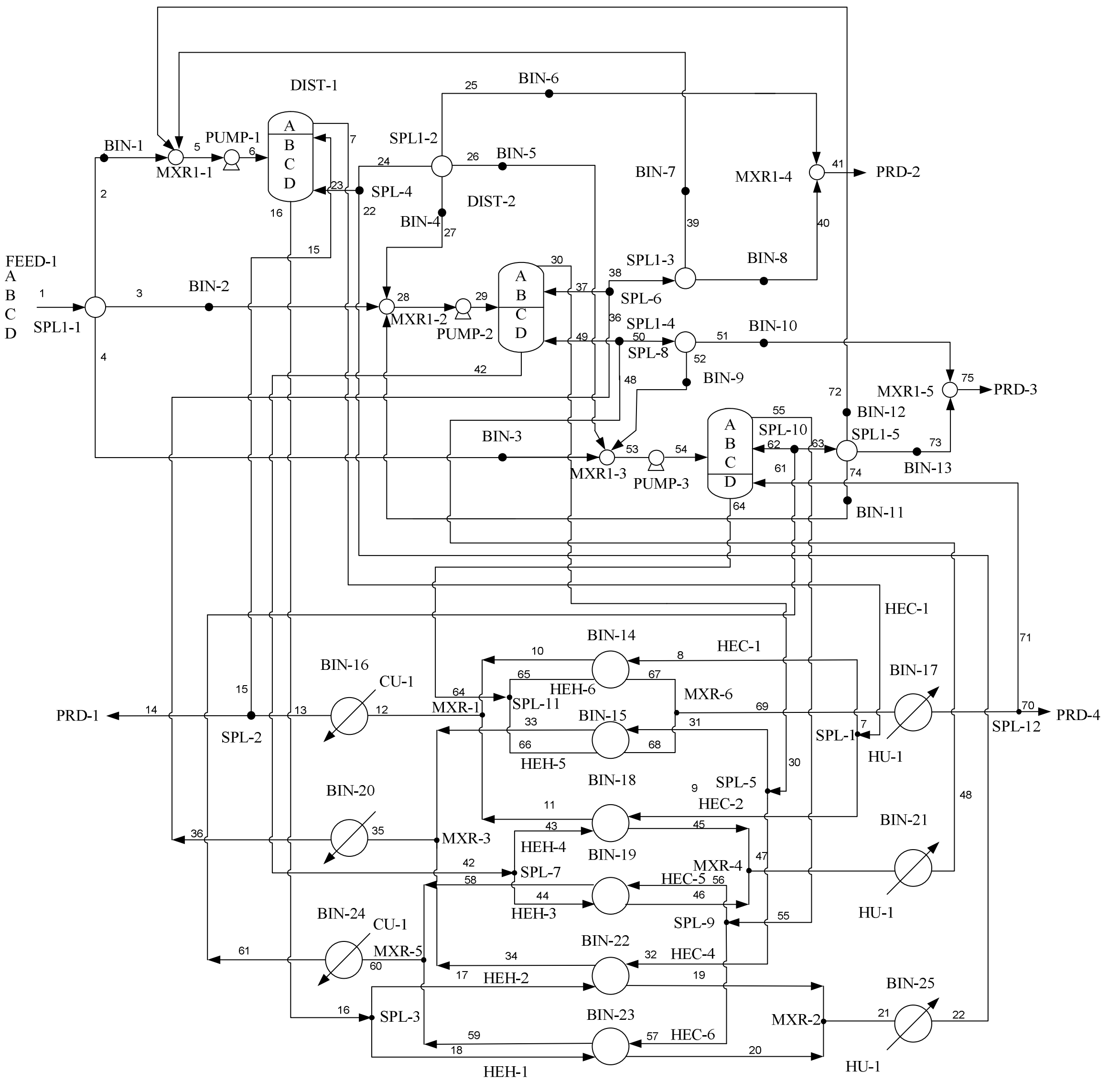

Figure 5-1: Superstructure for optimisation of distillation column sequence with its heat exchanger network (Novak et al., 1996)

As these variables would be changing throughout the periods, the optimal design may be different from one year to another. However, in practice, once the distillation columns and the HEN are installed, the design variables d (distillation column diameters, numbers of trays, reflux rates, and heat exchanger areas) are constant over the entire lifetime. In order that these variables suit all the future periods, their maximal values have to be selected and minimised within the objective function:

$$R^{ac}_{dist,i} \geq R^{\min}_{dist,i} \qquad \forall dist \in DIST \tag{5-1}$$

$$N^{ac}_{dist} \geq \frac{N^{t}_{dist,i}}{E_{dist}} \qquad \forall dist \in DIST \tag{5-2}$$

$$D_{dist} \geq \sqrt{\frac{4 \cdot F_{out,dist,i} \cdot (1 + R^{ac}_{dist,i})}{1.61 \cdot \pi} \sqrt{\sum_{comp} (M_{comp} \cdot \frac{FC_{out,dist,comp,i}}{F_{out,dist,i}}) \cdot \frac{R \cdot T_{out,dist,i}}{p}}} \qquad \forall dist \in DIST \tag{5-3}$$

$$A_{H,C,k} \geq \frac{Q_{H,C,k,i}}{U_{H,C} \cdot 0.5 \cdot (\Delta T_{H,C,k} + \Delta T_{H,C,k+1})} \qquad \forall h \in H,\ c \in C,\ k \in K \qquad (5\text{-}4)$$

The Net Present Value was selected as the objective function, in order to consider utility price variations and the value of money.

5.2 Case study 6

In the case study the separation sequence of four component system - benzene (38.585 %), toluene (29.230 %), O-xylene (21.973 %) and diphenyl (10.212 %) - was synthesized simultaneously with the heat integrated HEN. The sharpness of the distillation was set at 0.995. The inlet flow of the mixture was 0.05 kmol/s at a temperature of 374 K and the inlet pressure was 0.1 MPa. The efficiency of the distillation was 0.85. There were two available utilities: hot utility at 700 K with the heat transfer coefficient h = 4,500 J/(s m^2 K) and cold utility at 299 K with h = 1,200 J/(s m^2 K). There were two types of heat exchangers. Double pipe exchangers were used to exchange heat between the heat excess regarding the condensation of one column, with the heat requirement regarding evaporation of the other column. The fixed cost coefficient for these exchangers was 59.8 k\$ and the variable cost 3.565 k\$/m^2. Shell-and-tube exchangers were assumed for the utility to distillation heat exchange. The fixed cost coefficient of these exchangers was 157.8 k\$ and the variable cost was 0.251 k\$/m^2.

The actual-to-minimum reflux ratio was set at 1.35 as can be found in the literature (Tham, 2009). The optimal scheme obtained is presented in Figure 5-2. It follows the sequence where separation of the most volatile component always occurs first. Heat exchange takes place between the condenser of the third column and the evaporator of the first column.

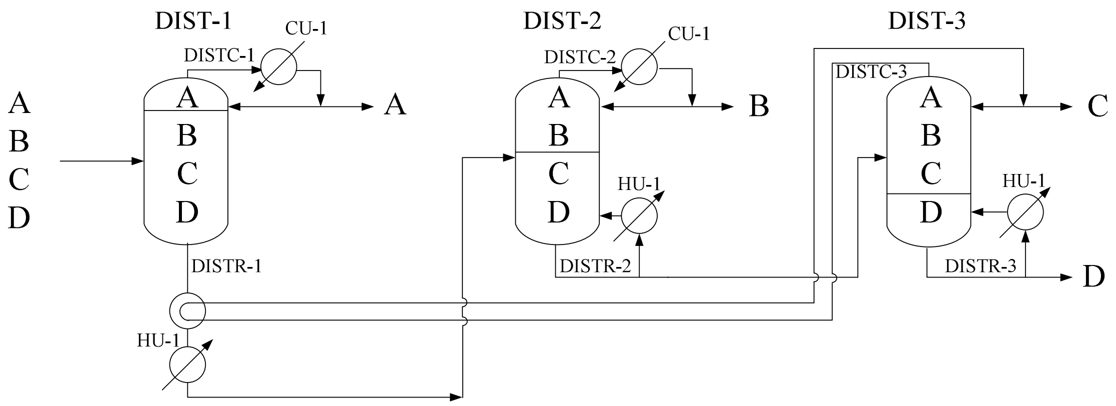

Figure 5-2: Distillation column optimal design with its HEN

The solution obtained with an actual-to-minimum reflux ratio of 1.35 was compared to the solution obtained, where the actual reflux ratio was optimised. The solution yielded a ratio what was 0.01 greater than the minimum reflux ratio. Table 5-1 presents the NPV of the mentioned optimisations at different future forecasted price scenarios. A comparison between the solutions obtained by different optimisation is presented in Table 5-2. As can be seen from Table 5-2, the utility consumption was significantly reduced when the reflux ratio was optimised and future utility prices were considered.

Table 5-1:Expected NPV for the optimisations at different future forecasted price scenarios.

Optimisation	NPV	NPV1	NPV2	NPV3	NPV4	NPV5
Current prices (R_{ac}=1.35 R_{min})	1.220	-48.002	-65.241	-84.314	-114.298	-237.746
Price projection (R_{ac}=R_{min}+0.01)		-19.905	-34.553	-50.759	-76.229	-181.131
ΔNPV		26.097	30.688	33.555	38.078	119.615

As the reflux ratio decreased, the number of trays in the columns had to be increased in order to maintain the same sharpness of separation. As the reflux ratio was decreasing the amounts of the distillate and condensate returned to the distillation were decreasing, which led to a decrease in the heating/cooling requirements and, therefore, smaller areas of the heat exchanger were appropriate. As a consequence, the HEN cost was reduced whilst the investment in the distillation columns due to a higher number of trays was increased.

Table 5-2: Comparison between solutions obtained by optimisation when considering the current prices of utilities and R_{Dist}^{ac} =1.35 $R_{Dist}^{\min}$ with the solution, when future utility prices are considered with the $R_{Dist}^{ac} = R_{Dist}^{\min}$ +0.01

Optimisation	Q^{heat} MJ/s	Q^{cool} MJ/s	N_{Dist}^{ac}	R_{Dist}^{ac}	$A_{H,C,k}$ /m^2	C_{DIST} /k\$	C_{HEN} /k\$
Current prices (R_{ac}=1.35 R_{min})	3.821	3.427	N_{Dist-3}^{ac} = 23 N_{Dist-2}^{ac} = 27 N_{Dist-1}^{ac} = 27	R_{Dist-3}^{ac} = 0.131 R_{Dist-2}^{ac} = 1.910 R_{Dist-1}^{ac} = 2.377	$A_{DISTC-3,DISTR-1,k}$ = 51.99 $A_{DISTC-2,CU-1,k}$ = 31.17 $A_{DISTC-1,CU-1,k}$ = 68.94 $A_{HU-1,DISTR-3,k}$ = 4.89 $A_{HU-1,DISTR-2,k}$ = 5.58 $A_{HU-1,DISTR-1,k}$ = 5.65	462.89	1,063.32
Price projection (R_{ac}=R_{min}+0.01)	3.224	2.830	N_{Dist-3}^{ac} = 27 N_{Dist-2}^{ac} = 52 N_{Dist-1}^{ac} = 53	R_{Dist-3}^{ac} = 0.107 R_{Dist-2}^{ac} = 1.425 R_{Dist-1}^{ac} = 1.771	$A_{DISTC-3,DISTR-1,k}$ = 50.89 $A_{DISTC-2,CU-1,k}$ = 25.97 $A_{DISTC-1,CU-1,k}$ = 56.57 $A_{HU-1,DISTR-3,k}$ = 4.83 $A_{HU-1,DISTR-2,k}$ = 4.65 $A_{HU-1,DISTR-1,k}$ = 4.41	677.355	1,054.42

A trade-off between the investment and operating cost was established by applying maximisation of the net present value. The investment was calculated for the distillation columns and their heat exchanger network. The operating cost was defined as the cost for utilities only. The solution, when considering current utility prices and the 15 y lifetime of the process, yielded to NPV of 21,920 k\$, which corresponded to the 113,556 k\$ for annual operating cost and the 1,730 k\$ for investment: 677 k\$ for distillation columns, and 1,053 k\$ for HEN.

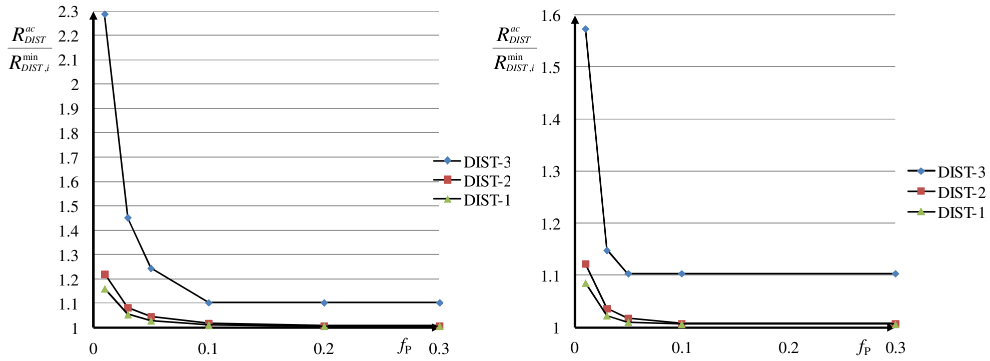

a) b)

Figure 5-3:Optimal-to-minimum reflux ratio as a function of a multiplication factor regarding the current utility price, fP, for the lifetimes of the distillation columns a) 5 y and b) 15y.

As can be seen, that proportion of the operating costs relative to the investment was very high. It resulted in a high level of integrating of the process with very small reflux ratios already in the distillation columns when considering current utility prices. The difference between the minimal reflux ratio and the optimal reflux ratio was quite small. In most of the cases it almost hit the lower bound. It can be concluded, that for this case study, even at significantly decreased utility prices the proportion of the operating costs relative to investment remained high. This affects the optimal-to-minimum reflux ratio, being significantly smaller than suggested in most of the literature (1.2 to 1.5).

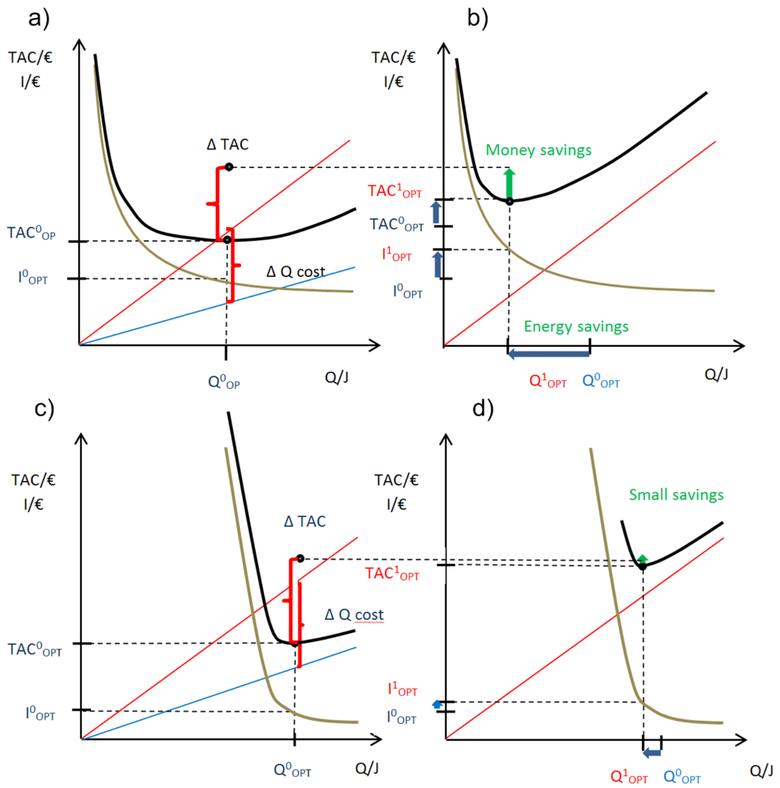

Figure 5-4: Trade-off between the operating cost and investment, presenting the savings as a result of planning for an entire lifetime, a) at current energy prices, b) future energy prices, when saving is potentially high, and c) at current and c) future prices when the potential is low.

Figure 5-4a shows the optimal point obtained regarding current energy prices (blue line) whilst Figure 5-4b displays a shift in the trade-offs towards higher investment and lower energy consumption when future energy prices (red line) are considered. However, the optimal point in Figure 1a is underestimated as its design features higher energy consumption for which much higher energy cost would be charged in the future - see an increase of TAC (total annual cost) based on the red energy cost line. As due to this increase the actual TAC would be higher than the one obtained at higher energy prices (Figure 5-4b), the difference between the two could be regarded as potential saving, expected when the synthesis is perform regarding future rather than current energy prices. The potential savings achieved by optimising the entire lifetime would be high in those cases when the current prices of energy were low and therefore the operating cost would be low compared to the investment (Figure 5-4b). In contrast, if the trade-off between operating cost and investment were already tight at the current energy prices, the potential savings accounting for increased prices in the future would be low (Figure 5-4c-d). Note that HENs would be typical examples as they have rather high potentials for saving energy, whilst heat integrated distillation sequences with high energy/investment ratios would provide poorer possibilities for energy improvements based on future prices.

6 Process synthesis for entire lifetime

The annual production of methanol is above 40 Mt and still shows a growth tendency with approximately 4 % increase each year (Aasberg-Petersen et al., 2013). It is used as a feed for producing a range of chemicals such as acetic acid and formaldehyde amongst others. There are many different raw materials utilised for methanol production; e.g. a mixture of natural gas and biomass can be used (Li et al., 2010), or methane by applying the Ammonia-Oxidizing Bacteria process (Taher and Chandran, 2013). A different approach for utilising steel-work off-gases, either with or without the addition of a biomass, for the production of methanol was presented recently by Lundgren et al. (2013). Despite different possible sources methanol is still mainly produced from natural gas. However, the production from coal is increasing significantly, especially in regions where natural gas is unavailable or is expensive, e.g. in China (Aasberg-Petersen et al., 2013). Due to the sharp competition between various raw materials - mainly between natural gas and coal - the design of a methanol production plant should be performed by considering several aspects. A proper trade-off between operating costs and investment should be established for obtaining an optimal process design. Kordabadi and Jahanmiri (2005) used a genetic algorithm for designing a methanol plant under varying conditions in regard to the length and temperature of a stage in within a two-stage methanol synthesis reactor. A super-structural approach to the synthesis of a methanol process was presented some time ago by Kravanja and Grossmann (1990), by applying a MINLP model using PROSYN – a MINLP process synthesizer.

The fluctuations of future prices can be handled using mathematical programming by considering either deterministic or stochastic approaches. In the former case, the variations are uniquely determined through known relationships amongst different states, whilst in the stochastic approach the ranges of values and probability distributions are assigned to uncertain future prices. Different strategies for handling uncertainties have been proposed to date and different uncertain parameters considered, e.g. demand, feed composition, temperature, conversion factor. Other varying parameters that have a significant impact on an optimal solution are the fluctuating prices of raw materials, electricity, products, and utilities. The prices of these quantities have shown significant variations in the past. Therefore, it is unrealistic to expect constant prices during a whole process´ total lifespan. A multi-period MINLP model has been developed in order to cope with these issues. A stochastic approach has been applied due to the uncertainty of the price forecast, and different prices projections have been derived at based on historical prices.

6.1 Methodology

6.1.1 Process flow-sheet

The aim of this work was to optimise the process of methanol production from hydrogen and carbon monoxide over an entire lifespan by accounting for the varying prices of raw materials, products, electricity, and both hot and cold utilities. The process flowsheet for the production of methanol is presented in Figure 6-1. Two arrangements for raw material feed compression are included in the flowsheet, either with one-stage compression or two-stage compression with a cooler in-between. In the first case, the operating temperature of the compressor might be outside the optimal operating conditions. In the second approach the optimal operating conditions for each compressor can be achieved, however, with increased investment. The raw material then follows, being cooled down to a required temperature in order to be fed into a reactor. Two alternative types of reactors with different conversion factors are available from which one has to be selected during optimisation. After synthesis of the methanol, separation should be performed using flash. The liquid outlet of the flash contains mainly methanol and the vapour consists mainly of unreacted raw material - H_2 and CO. An additional stream for reflux is also included in the flowsheet.

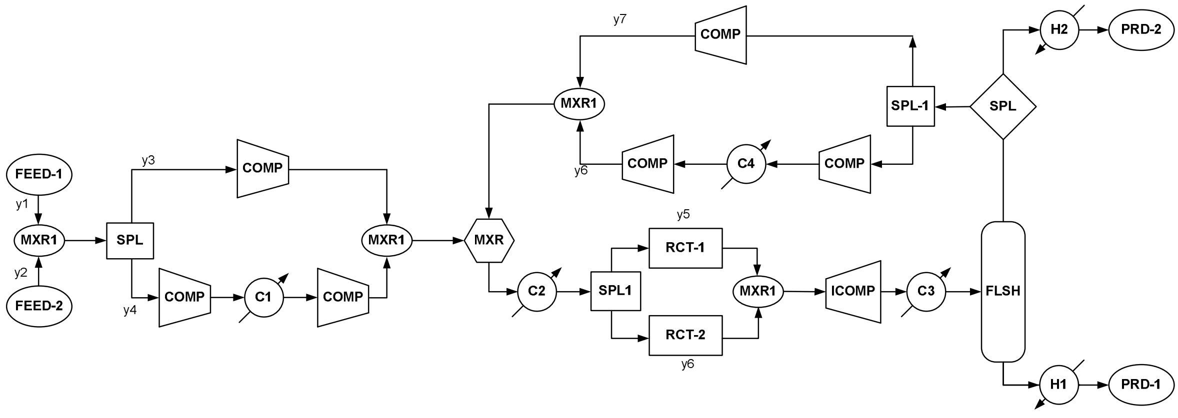

Figure 6-1: Superstructure of methanol production from H_2 and CO_2 (Kravanja and Grossmann, 1990)

Compared to the initial process flowsheet presented by Kravanja and Grossmann (1990) the valve after the reaction stage has been supplemented by a turbine (ICOMP in Figure 6-1) in order to produce electricity. In this way the electricity consumption/ production is also considered. Furthermore, the direct usage of shaft-work has also been considered rather than converting shaft-work to electricity and utilising it for operating the compressor. This assumption is reasonable as on the market there are producers offering combined equipment consisting of a turbine connected through a shaft to a compressor. In this way not only Heat Integration but Energy Integration can also be performed simultaneously.

6.1.2 Prices forecasting

A price forecast is required in order to achieve an optimal design over a whole lifespan, when the economic conditions vary. There are attempts being made to forecast prices over a longer term for crude oil prices and also commodities (Kolesnikov, 2013). However, the methodology of obtaining the results from a forecast is often unrevealed. Therefore, a relatively simple approach for price forecasting based on the historical prices has been developed. Since the uncertainty of the forecast is high, different scenarios for the forecast are proposed for electricity and natural gas prices, and the methanol price. The feed for methanol production is syngas, which can be produced from several different sources such as biomass or coal. However, the more common process used is still the reforming of natural gas (Coskata, 2014). The price of feed has been determined as the price of hydrogen when applying the methodology as described Yang and Ogden (2007), where the price of hydrogen is determined according to the capital cost required for reforming, the capacity of the process, the hydrogen yielded during the process, and the prices of natural gas. The historical prices of methanol were taken from Methanex (2013). The electricity prices were taken according to the Statistical Office of the Republic Slovenia (2013), and for the hot and cold utilities, the connections between the energy prices when the fuel is used to produce a utility assumed to be natural gas. The utility prices were determined by applying the methodology described by Ulrich and Vasudevan (2006) for considering the forecasted price of natural gas, CEPCI inflation factor, and some technological data, e.g. the pressure and the auxiliary boiler steam capacity (kg/s) for process steam and water heat capacity when cooling water (m^3/s).The historical prices for natural gas were taken from IndexMundi (2013) and the CEPCI inflation factor from Chemical Engineering (2012).

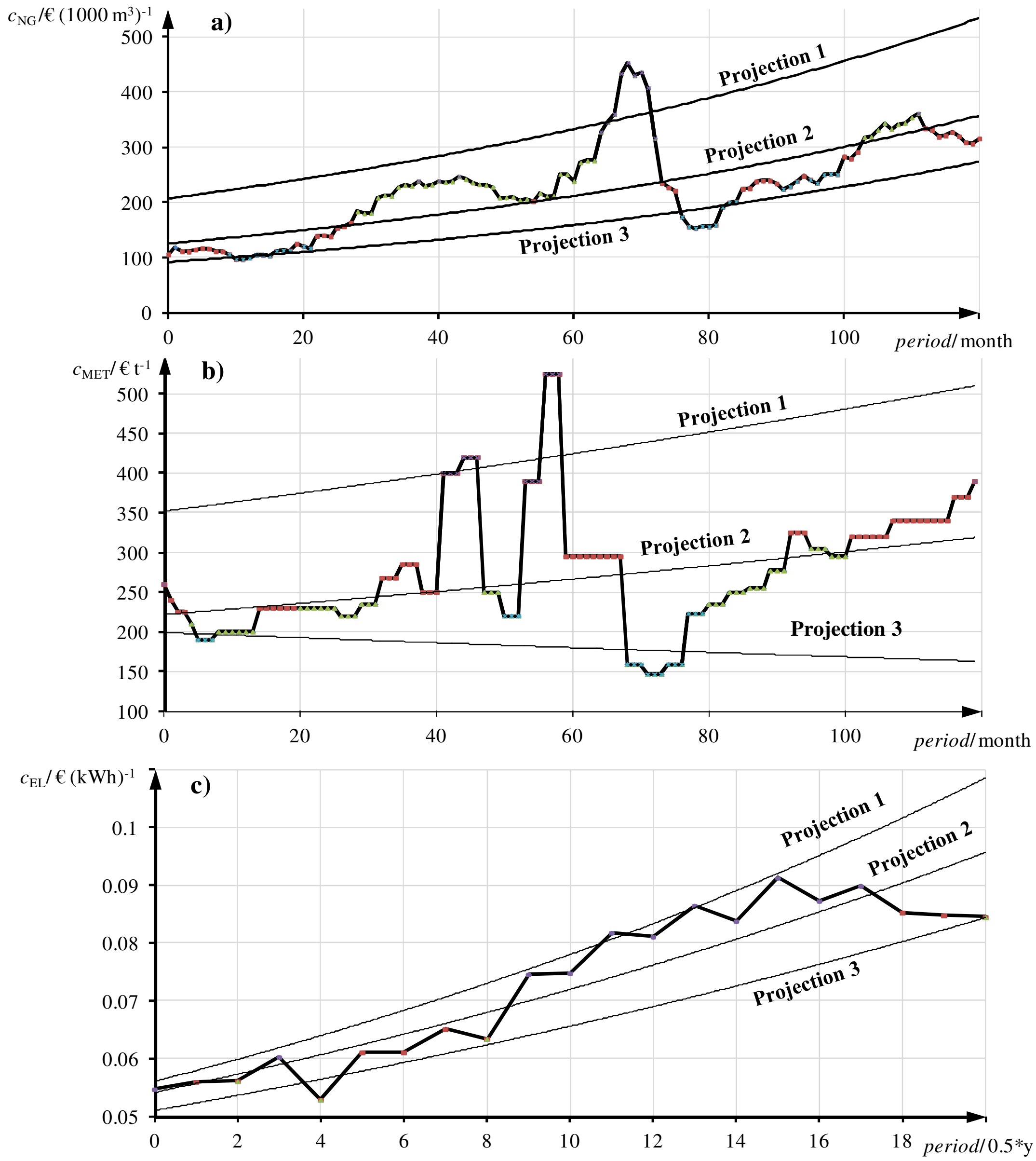

Figure 6-2: Bases for utility forecasting for a) natural gas prices, b) methanol and c) electricity

After obtaining historical prices a forecast was made for the prices in the following way. The middle Projection 2 was taken as the average of all the prices, and the function fitted to the point was used to provide the forecast. The other two projections were selected by obtaining the average of the points above / below Projection 2. After this step, the procedure was repeated for a price greater/ less than the prices of the above / below average of Projection 2. The highest prices represent Projection 1 and the lowest Projection 3. The probabilities assigned to the projections were 0.5 for Projection 2 and 0.25 for Projections 1 and 3 according to Gaussian distribution. The bases of the price forecasting for each assumed fluctuation price is presented in Figure 6-3.

6.2 Case study 7

The production of methanol was fixed at 1 kmol/s and the temperature of the product set at 127 °C. The feed consisted of 65 % H_2, 30 % CO, and 5% CH_4. Hot utility steam at 177 °C was considered and cold water as a cold utility with an inlet temperature of 10 °C and an outlet temperature of 22 °C. 8,500 h/y of annual working hours was assumed, a tax rate of 20 % and an interest rate 7 % (including 2 % inflation). The bases for price forecasting are those presented in Figure 2. The fixed cost for reactor 1 was 7,500 k\$, 9,750 k\$ for reactor 2, 750 k\$ for the compressors, and 97.5 k\$ for the heat-exchangers. The variable cost coefficient for reactor 1 was 375 k\$/m^3, for reactor 2 450 k\$/m^3, and for the compressor 1,312.5 \$/(kW).

Table 6-1: Economic comparison of process designs when considering forecasted prices and current prices

	ENPV/ M\$	*I* / M\$	Q^{CU}/ MW	Q^{HU}/ MW	Q^{REC}/ MW	P^{EL}/ MW	V^{RCT}/ m^3	q^{FEED}/ kmol s^{-1}	q^{REF}/ kmol s^{-1}
Synthesis,when considering forecasted prices	686.74	102.65	43.65	0	10.22	51.41	51.27	3.63	11.37
Synthesis, when considering current prices	678.96	115.64	53.91	0	9.78	63.34	47.11	3.48	9.81
Difference	7.78	-12.99	-10.260	-	0.44	-11.93	4.16	0.15	1.56
Difference / %	1.15	-24.7	-19.03	-	4.5	-18.8	8.8	4.3	15.9

Table 6-1 shows the comparisons between the syntheses of the processes when considering the current and the forecasted prices. As can be seen, the design obtained when assuming the forecasted prices economically outperforms that of the current prices, as the Expected Net Present Value (*ENPV*) of the current design when considering current prices increased by 1.15 %. Note that in both cases the optimisation resulted in a threshold problem, as there was no hot utility consumption QHU. However, the Heat Integration (amount of recovered heat is Q^{REC} in Table 6-1) resulted in significantly lower consumption of cold utility Q^{CU} (19 %). The higher electricity price resulted in a lower consumption of electricity P^{EL}, especially for the compression of the feed (18.8 %). As a consequence, the outlet pressure and temperature from compressor 1 were significantly reduced, which led to less efficient operating conditions for reactor 2 (RCT-2, Figure 6-3). This worsening of the reactor conditions was compensated for by a higher consumption of the feed q^{FEED} (4.3 %), a higher reflux rate q^{REF} (15.9 %), and a higher reactor volume V^{RCT} (8.8 %). However, despite this compensation the overall conversion of CO to CH_3OH decreased (from 32.92 % to 31.34 %). At a higher reflux rate the electricity consumption for compressor 2 increased somewhat (COMP-2, Figure 6-3). Due to the higher reflux rate the heat-recovery increased by 4.5 %. However, higher investment for HEN was required and two heat exchangers were relocated (Figure 6-3). Note that the total investment decreased, despite the increase in the reactor volume and heat exchanger areas. The main savings came from the reduced investment occurred in regard to compressor 1 (COMP-1, Figure 6-3).

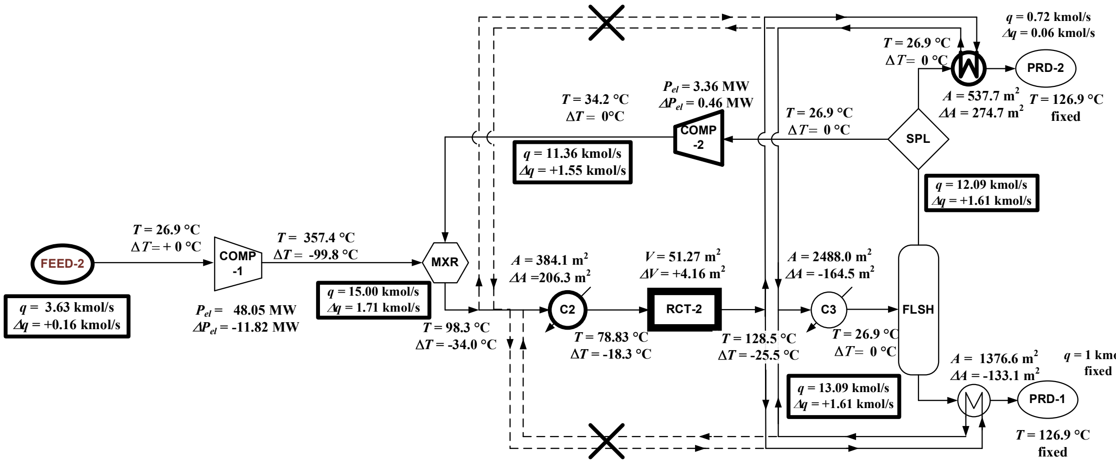

Figure 6-3:Comparison between the design obtained by optimisation when considering the forecasted prices for raw materials, products, utilities, and electricity when compared to the result of optimisation assuming current prices.

The consumption of raw materials increased and electricity decreased because the escalation of electricity prices had a more negative effect on the process economics than the escalation of the raw material price. When evaluating the distribution of the costs (Figure 6-4a), it can be seen, that the raw material cost represented the highest fraction of the expenditure. However, when the potential for saving was determined, the distribution significantly changed (Figure 6-4b). Note that the potential saving of a quantity (raw material, electricity, cold utility, and investment) was determined as a difference in that quantity's value identified at the current price solution and that at the future price solution, multiplied by its forecasted price. Figure 4b indicates that the overall potential savings would be 107,000 k$ and that the highest potential saving were associated with the electricity cost (226,000 k$) and then the cold utility cost (118,000 k$). This is why the utility and electricity costs were decreased when accounting for the forecasted prices.

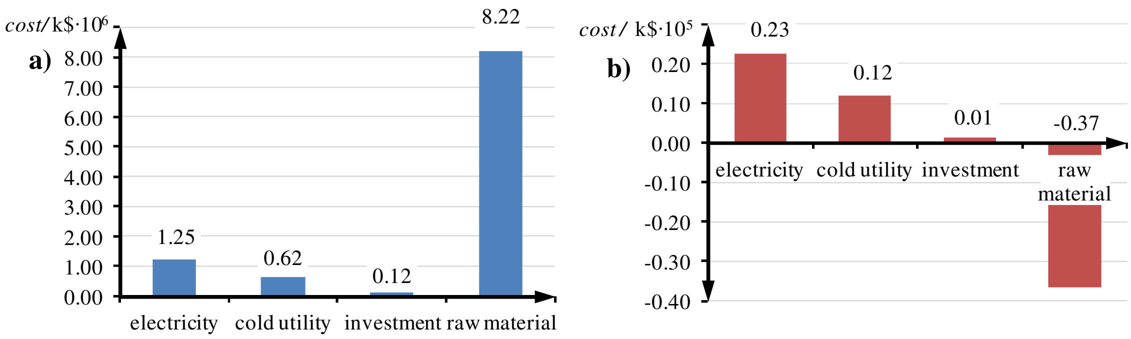

Figure 6-4: Distribution of the a) expenditures and b) distribution of potential savings for raw material, cold utility, electricity costs, and investment

7 Conclusions

The following conclusion were obtained regarding each case studied.

Heat exchanger network- no extension

Two drawbacks of the methods optimising HENs have been addressed . The first one is that the optimisations were usually carried out on a yearly basis although the duration of a HEN's lifetime has a significant effect on the optimal solution. The second drawback is the use of constant current prices for utilities, although these prices are expected to fluctuate and with a high probability of rising in the future. This again can have a significant effect on the optimal solution. In order to overcome these drawbacks multi-period deterministic and stochastic models for the MINLP synthesis of HEN have been proposed. They are based on future projections for utility prices throughout the whole lifetime of HEN.

The results obtained by solving two case studies indicate the significant effect of a lifetime on the optimal solution. It was observed when fixed utility prices were used, that over the lifetime the cumulative utility cost increased and that the trade-offs between operating cost and investment moved towards smaller utility loads and larger investment. This was even more evident, when the optimisation was carried out with future projections for utility prices. A longer lifetime and a higher projection for future utility prices had a synergistic effect on lowering the utility cost and increasing the investment. Consequently, significant savings in utility cost can be obtained with some additional investment. A multi-period optimisation approach with future utility prices for entire lifetimes was applied and compared to a single-period with current fixed prices. These savings after taxes cumulated over the HEN lifetime reduced by the incremental investment correspond to the incremental net present value which was chosen as the main economic criteria within the objective function. In addition, the economic viability of HEN designs with higher investment cost as a result of considering future projections for utility prices over the entire lifetime were also evaluated by an Incremental internal rate of return, Discounted payback, and Lifetime discounted return on investment. The incremental net present value proved to be the most suitable optimisation criterion since its maximisations lead to HEN designs with the highest benefits obtained over their entire lifetimes. The results indicate that incremental investment may not be economically viable for pessimistic price projections, if the lifetime of HEN considered is too short. However, for normal lifetime durations and the most likely price projections, the additional investments would be almost certainly justified. Nevertheless, the economic viability is case dependent. In Case Study 2 we could see that all the HEN designs with long lifetimes were economically viable for all the considered future price scenarios. The stochastic approach can be applied for the simultaneous consideration of future price projections and their probabilities.

The multi-period approach with future price projections is important for sustainable HEN designs with higher heat recovery and, consequently, with lower utility consumption. The decreased utility requirement makes these HEN designs less sensitive to future fluctuations in utility prices.

Heat exchanger network-extensions

There is always a high uncertainty of the forecast and, therefore, an additional investment related to the higher future utility prices may not be credibly justified, especially if it is implemented at the beginning. In order to reduce the risk associated to premature additional investments, initial investment is constrained, allowing for future extensions. The constraint that is imposed to the investment at the beginning of the lifetime prevents the initial investment from exceeding the one that would be obtained by the optimisation with current utility prices. An extension in the future should be implemented only when sufficiently higher utility prices are coming to be the reality. This approach allows decision makers to react based on the actually realised energy prices rather than the forecasted ones, thus reducing the risk. By applying the optimisation with forecasted energy prices, more robust HEN designs can be obtained, which can be adapted to future prices, when necessary, with lower expenses and yet better heat recovery. In Case study 1 and 2 improvements up to about 50 k€ can be achieved when HEN design are optimised by the proposed stochastic optimisation model considering future utility prices and allowing for future extension.

The risk related to the variations of utility prices can be further reduced by the proper selection of the risk tolerance applied in the risk-free optimisation criterion – the Certainty Equivalent. As can be concluded from Case study 1, even when the risk tolerance is low, the extensions are still economically viable as the Certainty Equivalent at risk tolerance 25 k€ was 12.52 k€. However, at high risk tolerance 200 k€ the Certainty Equivalent was significantly higher 47.70 k€ and almost reaches the Incremental Expected Net Present Value of 54.3 k€. The Case study 2 illustrates the improvements of HEN design related to possible extensions. The savings were in the range from 11.9 k€ to 17.6 k€, which is not very significant. However, they indicate a potential for achieving more significant improvements related to the synthesis of larger HEN designs with more combinatorial opportunity. Another conclusion is that by applying maximisation of Net Present Value significantly better results can be obtained than with minimisation of Total Annual cost - about 27 % with future prices and extensions and 29 % with current energy prices.

Total Site-sequential approach

The Heat Integration within a Total Site shows a significant potential for energy recovery. However, an optimal design has a significant influence on the economic viability. It is even more crucial to obtain a proper design for a heat exchanger network within a Total Site, as the heat is transferred twice: (i) from hot streams to intermediate utilities, and (ii) from intermediate utilities to cold streams. Both heat transfers require heat exchangers and also a pipeline for connecting the source and sink sides in which additional pressure/temperature drops and heat losses occur. Therefore, the trade-off between investment and operating cost is even sharper.

In this work a stochastic multi-period MINLP model was developed for the synthesis of a Total Site and the optimisation of its heat recovery. The results of the case study indicated that it is necessary to account for:

- All interactions between source and sink HENs and the pipeline, which gives rise to the use of the simultaneous approach. The *ENPV* in the case study presented was increased by 7.9 % and a 14.2 % reduction in external hot utility consumption was achieved.
- Pipeline investment, as the fraction of the pipeline investment within the total investment cannot be neglected; in the presented case study presented it was up to 20.6%.
- Optimisation of pressure levels, as it can significantly improve *ENPV* when compared to the cases with fixed pressure levels. In the case study *ENPV* was increased by 9.8 % and external hot utility reduced by 31.6 %.
- Future prices of energy as they can have additional impact on the trade-off between investment and operating cost. Together with the optimisation of pressure levels when applying simultaneous optimisation of source and sink sides including the pipeline, it gave rise to the 19.7 % increase of *ENPV* and even to the 46.4 % reduction of external

hot utility. It alone contributed to 6.7 % of the total improvement in *ENPV* and 10.9 % of the total increase in heat recovery.

- Heat losses, as it represent up to 4.4 % when no preheating was considered, whilst in the case of incomplete recovery of the condensate it increased by up to 12.9 %.
- Pressure drops simultaneously with the evaluation of pipe diameters. In the case study they were less significant; however, as they reached almost 1 bar in certain pipelines, they already reduced the heat content of steam and caused temperature drops of utility supply at the sink site, which influenced somewhat the trade-off between investment and external utility consumption. Note that accounting for all heat losses and pressure/temperature drops in the Total Site can have a significant impact on the economic performance.

The proposed approach improves the modelling of Total Site in many respects in order to obtain more realistic solutions and can therefore help significantly the efficiency of the decision making about the Total Site design. In the future a better optimization of pipeline layout needs to be developed as it might have a significant impact on a Total Site performance.

Total Site-simultaneous approach

Two strategies both applying mixed integer nonlinear programming model have been presented for the optimisation of Total Site Heat Integration Network. It addresses couple of issues of Total Site synthesis, presented by Chew et al., 2013. The sequential model employing a two-step approach, determining heat integration on process level first and afterwards on the Total Site scale, followed the traditional way of performing Total Site heat integration. The second way of obtaining results was by applying the simultaneous optimisation on both the process and the Total Site levels. Applying the latter approach can lead to a significantly better result with lower Total Annual Cost - by 26.3 % in the case study presented. However, applying the simultaneous model on large-scale problems might be very hard or even impossible since the complexity as the problem increases rapidly with the number of processes and process streams included in the analysis. In these cases the sequential approach would be more useful. There are two modes considered for process-to-process heat recovery: i) Direct, by extending the cold process stream by pipeline from one process to another and back in order to exchange heat with the hot process stream of the other process and ii) indirect, via utilisation of intermediate utility. From the case studies presented it can be concluded that the direct mode of transfer is an economically more attractive option, when only one hot and one cold process streams are included in the heat recovery between processes at any distance. However, when more than one hot or cold process stream is involved in Total Site Heat Integration the indirect transport mode can be more favourable when considering the economical aspect. The condensate recovery rate should be taken into account when optimising Total Site as it can affect the final result significantly. A sensitivity analysis regarding distances between processes indicated that investment in pump and heat exchangers does not vary significantly by altering the distance between processes, whilst it has a great impact on the pipe investment.

Distillation column sequence with its HEN

Synthesising the distillation column sequence simultaneously with its HEN was optimised over the whole lifetime of the process by applying a multi-period mixed-integer nonlinear programming model. The degree of integration depends on the trade-off between the operating costs and the investment. The presented case study reflected the need for optimising the reflux ratios separately for each column. Applying an empirical actual-to-minimal ratio within the range of 1.2 - 1.5 is problematic, as it does not even reflect the optimal trade-off at the current prices for utilities. It can also be concluded that when the proportion of operational costs with respect to investment is low, the trade-off between the operating costs and the investment is more sensitive to utility prices and, hence, future utility prices also, and shifts more towards smaller utility consumption and higher investment than in those cases when the proportion is high, as was the case during the example problem.

Process synthesis- methanol

A synthesis of a methanol process scheme under varying economic conditions was performed by applying a stochastic MINLP model. The solutions obtained indicate that it is reasonable to apply the developed model because it enables higher profitability when future forecasted prices are considered, rather than the current ones. The case study showed that the design obtained at current prices had 1.15% lower *ENPV* when recalculated by considering future prices, than the *ENPV* of the design obtained at future prices.

Another important conclusion is that all the price variations should be considered simultaneously, as separate influences might be determined incorrectly. The simultaneous approach enables the obtaining of appropriate trade-offs between costs, income, and investment. As can be seen from the case study by increasing electricity and utility prices, their consumptions decreased. However, this was not the case with the raw material consumption, which increased even if its price increased. It is recommended that a distribution of potential savings regarding expenditures should be considered rather than a distribution of expenditure when evaluating the impacts of future cost variations. An important revelation from the research is that the trade-off obtained by considering future prices simultaneously is the one that determines whether the process would operate at higher or lower efficiencies. It is interesting to note that in the above case study the trade-off when considering future prices was established for the solution with lower consumptions of both electricity and cold utility, but with higher raw material usage and a notable reduction in the overall reaction conversion.

References

[1] Aaltola, J., 2002, Simultaneous synthesis of flexible heat exchanger network. Applied Thermal Engineering, 22(8), 907-918.

[2] Aasberg-Petersen, K., Nielsen, C. S., Dybkjaer, I., Perregaard, J., 2013. Large Scale Methanol Production from Natural Gas., <www.topsoe.com/sites/default/files/topsoe_large_scale_methanol_prod_paper.ashx_.pdf>, accessed 11.11.2014

[3] AccountingExplained, 2014. Discounted Payback Period <accountingexplained.com/managerial/capital-budgeting/discounted-payback-period> accessed 11.11.2014.

[4] Aguilar, O., Perry, S., Kim, J.-K., Smith, R., 2007, Design and Optimization of Flexible Utility Systems Subject to Variable Conditions: Part 1: Modelling Framework. Chemical Engineering Research and Design , 85(8), 1136-1148.

[5] Aguilar, O., Perry, S., Kim, J.-K., Smith, R., 2007, Design and Optimization of Flexible Utility Systems Subject to Variable Conditions: Part 2: Methodology and Applications. Chemical Engineering Research and Design, 85(8), 1149-1168.

[6] Al-Mayyahi, M. A., Hoadley, A. F., Rangaiah, G., 2013, A novel graphical approach to target CO2 emissions for energy resource planning and utility system optimization. Applied Energy, 104(0), 783-790.

[7] Awudu, I. Zhang, J., 2013, Stochastic production planning for a biofuel supply chain under demand and price uncertainties. Applied Energy, 103(0), 189-196.

[8] Azad, A. V., Amidpour, M., 2011, Economic optimization of shell and tube heat exchanger based on constructal theory. Energy , 36(2), 1087-1096.

[9] Bagajewicz, M., Rodera, H., 2000, Energy savings in the total site heat integration across many plants. Computers and Chemical Engineering, 24(2-7), 1237-1242.

[10] Bahadori, A., Vuthaluru, H. B., 2010, A simple correlation for estimation of economic thickness of thermal insulation for process piping and equipment. Applied Thermal Engineering, 30(2-3), 254-259.

[11] Bandyopadhyay, S., Varghese, J., Bansal, V., 2010, Targeting for cogeneration potential through total site integration. Applied Thermal Engineering , 30(1), 6-14.

[12] Björk, K.-M., Westerlund, T., 2002, Global optimization of heat exchanger network synthesis problems with and without the isothermal mixing assumption. Computers and Chemical Engineering, 26(11), 1581-1593.

[13] Chemical Engineering, 2012. Economic Indicators. <www.chemengonline.com/business_and_economics/economic_indicators.html>, accessed 11.11.2014

[14] Chen, C.-L., Lin, C.-Y., 2012, Design of Entire Energy System for Chemical Plants. Industrial and Engineering Chemistry Research, 51(30), 9980-9996.

[15] Chen, J., 1987. Comments on improvements on a replacement for the logarithmic mean. Chemical Engineering Science , 42(10), 2488-2489.

[16] Chew, K. H., Klemeš, J. J., Wan Alwi, S. R., Manan, Z. A., 2013, Industrial implementation issues of Total Site Heat Integration. Applied Thermal Engineering , 61(1), 17-25.

[17] Coskata, Process overview, 2013, <www.coskata.com/process/?source=7E352957-657F-44D4-8CEC-3FCA8BBB2D7C>, accessed 21. 03. 2013.

[18] Demirel, Y., 2006, Retrofit of Distillation Columns Using Thermodynamic Analysis. Separation Science and Technology,41, 791-817.

[19] Dhole, V. R., Linnhoff, B., 1993, Total site targets for fuel, co-generation, emissions, and cooling. Computers and Chemical Engineering, 17, Supplement 1(0), S101 - S109.

[20] Dipama, J., Teyssedou, A., Sorin, M., 2008, Synthesis of heat exchanger networks using genetic algorithms. Applied Thermal Engineering, 28(14-15),1763-1773.

[21] Duran, M., Grossmann, I., 1986; An outer-approximation algorithm for a class of mixed-integer nonlinear programs. Mathematical Programming, 36(3), 307-339.

[22] Engineering Toolbox, 2013. Cylinder or Pipe - Conductive Heat Loss. <www.engineeringtoolbox.com/conductive-heat-loss-cylinder-pipe-d_1487.html>, accessed 11.11.2014

[23] Fodor, Z., Varbanov, P., Klemeš, J., 2010, Total site targeting accounting for individual process heat transfer characteristics. Chemical Engineering Transanctions, 21, 49-54.

[24] Fraga, E., Žilinskas, A., 2003. Evaluation of hybrid optimization methods for the optimal design of heat integrated distillation sequences. Advances in Engineering Software, 34(2), 73-86.

[25] Ghannadzadeh, A., Perry, S., Smith, R., 2012, Cogeneration targeting for site utility systems. Applied Thermal Engineering , 43(0), 60-66.

[26] Grossmann, I. E., Aguirre, P. A., Barttfeld, M., 2005, Optimal synthesis of complex distillation columns using rigorous models. Computers and Chemical Engineering , 29(6), 1203-1215.

[27] Hackl, R., Harvey, S., 2013, Framework methodology for increased energy efficiency and renewable feedstock integration in industrial clusters. Applied Energy , 112(0), 1500-1509.

[28] Halasz, L. Nagy A.B., Ivicz T., Friedler F., 2002, Optimal retrofit design and operation of the steam-supply system of a chemical complex. Applied Thermal Engineering , 22(8), 939-947.

[29] Hipólito-Valencia, B. J., Lira-Barragán L. F., Ponce-Ortega, J. M., Serna-Gonzáles, M., El-Halwagi, M. M., 2014, Multiobjective design of interplant trigeneration systems. AIChE Journal, 60(1), 213-236.

[30] Index Mundi, 2013.<www.indexmundi.com>, accessed 10.10.2013

[31] Index Mundi, 2012.<www.indexmundi.com>, accessed 21.07.2012

[32] Isafiade, A., Fraser, D., 2010, Interval based MINLP superstructure synthesis of heat exchanger networks for multi-period operations. Chemical Engineering Research and Design , 88(10), 1329-1341.

[33] Kecebas, A., Alkan, M. A., Bayhan, M., 2011, Thermo-economic analysis of pipe insulation for district heating piping systems. Applied Thermal Engineering, 31(17-18), 3929-3937.

[34] Kim, S. H., Yoon, S.-G., Chae, S. H., Park, S., 2010, Economic and environmental optimization of a multi-site utility network for an industrial complex. Journal of Environmental Management , 91(3), 690-705.

[35] Klemeš, J. J., Kravanja, Z., 2013, Forty years of Heat Integration: Pinch Analysis (PA) and Mathematical Programming (MP). Current Opinion in Chemical Engineering, 2(4), 461-474.

[36] Klemeš, J., Dhole V. R., Raissi K., Perry S. J., Puigjaner L, 1997, Targeting and design methodology for reduction of fuel, power and CO_2 on total sites. Applied Thermal Engineering, 17, 993-1003.

[37] Klemeš, J., Friedler, F., Bulatov, I., Varbanov, P., 2010, Sustainability in the process industry – Integration and optimization. New York: USA, 362.

[38] Kocis, G. R., Grossmann, I. E., 1987. Relaxation strategy for the structural optimization of process flow sheets. Industrial and Engineering Chemistry Research, 26(9), 1869-1880.

[39] Kolesnikov, I., 2013. Crude Oil Price Forecast: Long Term to 2025: Data and Charts.

[40] Kordabadi, H., Jahanmiri, A., 2005. Optimization of methanol synthesis reactor using genetic algorithms. Chemical Engineering Journal , 108(3), 249-255.

[41] Kovač Kralj, A., Glavič, P., Krajnc, M., 2002, Waste heat integration between processes. Applied Thermal Engineering , 22(11), 1259-1269.

[42] Kovač Kralj, A., Glavič, P., Kravanja, Z., 2005. Heat integration between processes: Integrated structure and MINLP model. Computers and Chemical Engineering, 29(8), 1699-1711.

[43] Kravanja, S., Kravanja, Z., Bedenik, B. S., 1998, The MINLP optimization approach to structural synthesis. Part I: A general view on simultaneous topology and parameter optimization. International Journal for Numerical Methods in Engineering, 43(2), 263-292.

[44] Kravanja, Z., Grossmann, I., 1990, Prosyn-an MINLP process synthesizer. Computers and Chemical Engineering , 14(12), 1363-1378.

[45] Kravanja, Z. Grossmann, I., 1994, New developments and capabilities in prosyn An automated topology and parameter process synthesizer. Computers and Chemical Engineering , 18(11-12), 1097-1114.

[46] Kravanja, Z., 2010, Challenges in sustainable integrated process synthesis and the capabilities of an MINLP process synthesizer MipSyn. Computers and Chemical Engineering , 34(11), 1831-1848.

[47] Kruczek, T., 2013, Determination of annual heat losses from heat and steam pipeline networks and economic analysis of their thermomodernisation. Energy , 62(0), 120-131.

[48] Laukkanen, T., Tveit, T.-M. and Fogelholm, C.-J., 2012, Simultaneous heat exchanger network synthesis for direct and indirect heat transfer inside and between processes. Chemical Engineering Research and Design , 90(9), 1129-1140.

[49] Lewin, D. R., 1998, A generalized method for HEN synthesis using stochastic optimization II.: The synthesis of cost-optimal networks. Computers and Chemical Engineering , 22(10), 1387-1405.

[50] Lewin, D. R., Wang, H., Shalev, O., 1998, A generalized method for HEN synthesis using stochastic optimization I. General framework and MER optimal synthesis. Computers & Chemical Engineering , 22(10), 1503-1513.

[51] Li, H., Hong, H., Jin, H., Cai, R., 2010, Analysis of a feasible polygeneration system for power and methanol production taking natural gas and biomass as materials. Applied Energy , 87(9), 2846-2853.

[52] Liew, P. Y., Wan Alwi R. H., Varbanov P. S., Manan Z. A., Klemeš J., 2012, A numerical technique for Total Site sensitivity analysis. Applied Thermal Engineering , 40(0), 397-408.

[53] Linnhoff, B., Eastwood A., 1997, Overall site optimisation by Pinch Technology. Chemical Engineering Research and Design , 75, Supplement(0), S138 - S144.

[54] Linnhoff, B., Flower, J. R., 1978, Synthesis of heat exchanger networks: I. Systematic generation of energy optimal networks. AIChE Journal, 24(4), 633-642.

[55] Linnhoff, B., Hindmarsh, E., 1983. The pinch design method for heat exchanger networks. Chemical Engineering Science, 38(5), 745-763.

[56] Linnhoff B., Townsend D.W., Boland D., Hewitt G.F., Thomas B.E.A., Guy A.R., Marsland R.H., 1982. A user guide on process integration for the efficient use of energy. Rugby, U.K.: IChemE [revised edition published in 1994].

[57] Lundgren, J. Ekborn K., Hulteberg C., Larsson M., Grip C.-E., Nilsson L., Tuna P., 2013, Methanol production from steel-work off-gases and biomass based synthesis gas. Applied Energy , 112(0), 431-439.

[58] Luo, X., Zhang, B., Chen, Y., Mo, S., 2012, Operational planning optimization of multiple interconnected steam power plants considering environmental costs. Energy, 37(1), 549-561.

[59] Maréchal, F., Kalitventzeff, B., 1999, Targeting the optimal integration of steam networks: Mathematical tools and methodology. Computers and Chemical Engineering , 23, Supplement(0), S133 - S136.

[60] Matsuda, K., Tanaka, S., Endou, M., Iiyoshi, T., 2012, Energy saving study on a large steel plant by total site based pinch technology. Applied Thermal Engineering, 43(0), 14-19.

[61] Mavromatis, S., Kokossis, A., 1998, Conceptual optimisation of utility networks for operational variations-I. targets and level optimisation. Chemical Engineering Science , 53(8), 1585-1608.

[62] Mavromatis, S., Kokossis, A., 1998. Conceptual optimisation of utility networks for operational variations-II. Network development and optimisation. Chemical Engineering Science, 53(8), 1609-1630.

[63] McAllister, E., 2014. Pipeline rules of thumb handbook.. eight edition ed., Gulf Professional Publishing.Elsevier, Oxford, UK.

[64] Mehleri, E., Sarimveis, H., Markatos, N., Papageorgiou, L., 2013. Optimal design and operation of distributed energy systems: Application to Greek residential sector. Renewable Energy , 51(0), 331-342.

[65] Mertanex Corporation, M., 2013. Methanol price. <www.methanex.com/our-business/pricing>, accessed 12.10.2013

[66] Mizutani, F. T., Pessoa F. L. P., Queiroz E.M., Haunan S., Grossmann I. E., 2003, Mathematical Programming Model for Heat-Exchanger Network Synthesis Including Detailed Heat-Exchanger Designs. 1. Shell-and-Tube Heat-Exchanger Design. Industrial and Engineering Chemistry Research, 42(17), 4009-4018.

[67] Mizutani, F. T., Pessoa F. L. P., Queiroz E.M., Haunan S., Grossmann I. E., 2003. Mathematical Programming Model for Heat-Exchanger Network Synthesis Including Detailed Heat-Exchanger Designs. 2. Network Synthesis. Industrial and Engineering Chemistry Research, 42(17), 4019-4027.

[68] Mulhall, R. A. and Bryson, J. R., 2014. Energy price risk and the sustainability of demand side supply chains. Applied Energy , doi:10.1016/j.apenergy.2014.01.018

[69] Nayyar, M. L., 2000. Piping handbook. McGraw-Hill.

[70] Nemet, A., Klemeš, J. J., Kravanja, Z., 2012, Minimisation of a heat exchanger networks' cost over its lifetime. Energy, 45(1), 264-276.

[71] Nemet, A., Klemeš, J. J., Kravanja, Z., 2013, Optimising entire lifetime economy of heat exchanger networks. Energy, 57(0), 222-235.

[72] Novak Pintarič, Z., Kravanja, Z., 2006, Selection of the Economic Objective Function for the Optimization of Process Flow Sheets. Industrial and Engineering Chemistry Research, 45(12), 4222-4232.

[73] Novak Pintarič, Z., Kasaš, M., Kravanja, Z., 2013, Sensitivity analyses for scenario reduction in flexible flow sheet design with a large number of uncertain parameters. AIChE Journal, 59(8), 2862-2871.

[74] Novak, Z., Kravanja, Z., Grossmann, I., 1996. Simultaneous synthesis of distillation sequences in overall process schemes using an improved minlp approach. Computers & Chemical Engineering, 20(12), 1425-1440.

[75] Papandreou, V.,Shang, Z., 2008. A multi-criteria optimisation approach for the design of sustainable utility systems. Computers and Chemical Engineering , 32(7), 1589-1602.

[76] Perry R. H., Green. D., 2007, Perry's Chemical Engineers' Handbook, 8th Edition. McGraw Hill, New York, United States.

[77] Perry, S., Klemeš, J. J., Bulatov, I., 2008, Integrating waste and renewable energy to reduce the carbon footprint of locally integrated energy sectors. Energy, 33(10), 1489-1497.

[78] Pinto, F. S., Zemp, R., Jobson, M., Smith, R., 2011, Thermodynamic optimisation of distillation columns. Chemical Engineering Science , 66(13), 2920-2934.

[79] Proios, P., Goula, N. F., Pistikopoulos, E. N., 2005, Generalized modular framework for the synthesis of heat integrated distillation column sequences. Chemical Engineering Science, 60(17), 4678-4701.

[80] Sahu, G. C. Bandyopadhyay, S., 2012, Mathematically Rigorous Algebraic and Graphical Techniques for Targeting Minimum Resource Requirement and Interplant Flow Rate for Total Site Involving Two Plants. Industrial and Engineering Chemistry Research, 51(8), 3401-3417.

[81] Shang, Z. Kokossis, A., 2004, A transhipment model for the optimisation of steam levels of total site utility system for multiperiod operation. Computers and Chemical Engineering , 28(9), 1673-1688.

[82] Shang, Z. Kokossis, A., 2005, A systematic approach to the synthesis and design of flexible site utility systems. Chemical Engineering Science , 60(16), 4431-4451.

[83] Statistical office of Republic of Slovenia, 2013. Prices of Energy Sources - Old Methodology Data.<pxweb.stat.si/pxweb/Database/Environment/18_energy/02_18175_energy_prices/18613_energy_prices_old/18613_energy_prices_old.asp>, accessed 5.10.2013.

[84] Smith, R., 2005, Chemical Process Design and Integration. John Wiley and Sons, Ltd.

[85] Soltani, H., Shafiei, S., 2011, Heat exchanger networks retrofit with considering pressure drop by coupling genetic algorithm with LP (linear programming) and ILP (integer linear programming) methods. Energy, 36(5), 2381-2391.

[86] Soršak, A., Kravanja, Z., 1999. Simultaneous MINLP synthesis of heat and power integrated heat exchanger networks. Computers and Chemical Engineering, 23, Supplement(0), S143 - S147.

[87] Soršak, A., Kravanja, Z., 2004. MINLP retrofit of heat exchanger networks comprising different exchanger types. Computers and Chemical Engineering, 28(1-2), 235-251.

[88] Stovall, T., 1981. Evaluation of steam pipeline, In: Department of Energy, OAK RIDGE National Laboratory, Engineering Technology Division, Department of Energy,Contract NQ. W-7405-eng-26.

[89] Taher, E., Chandran, K., 2013. High-Rate, High-Yield Production of Methanol by Ammonia-Oxidizing Bacteria. Environmental Science and Technology, 47(7), 3167-3173.

[90] Taylor, N. W., Jones, P. H., Kipp, M. J., 2014. Targeting utility customers to improve energy savings from conservation and efficiency programs. Applied Energy, 115(0), 25-36.

[91] Thomson, G. W., 1946, The Antoine Equation for Vapor-pressure Data. Chemical Reviews, 38(1), 1-39.

[92] TLV, 2013. Pipe Sizing by Pressure Loss for Steam. <http://www.tlv.com/global/TI/calculator/steam-pipe-sizing-by-pressure-loss.html>, accessed 20.10.2013

[93] Townsend, D. W., Linnhoff, B., 1983. Heat and power networks in process design. Part II: Design procedure for equipment selection and process matching. AIChE Journal, 29(5), 748-771.

[94] Ugursal, V. I., 2013. Energy consumption, associated questions and some answers. Applied Energy, 130, 783-792.

[95] Ulrich, G., Vasudevan, P., 2006. How to Estimate Utility cost? Chemical Engineering, April. <www.che.com/technical_and_practical/2798.html>, accessed 12.03.2011.

[96] Varbanov, P., Doyle, S., Smith, R., 2004. Modelling and Optimization of Utility Systems. Chemical Engineering Research and Design , 82(5), 561-578.

[97] Varbanov, P., Perry, S., Klemeš, J., Smith, R., 2005. Synthesis of industrial utility systems: cost-effective de-carbonisation. Applied Thermal Engineering , 25(7), 985-1001.

[98] Velasco-Garcia, P., Varbanov, P. S., Arellano-Garcia, H. & Wozny, G., 2011. Utility systems operation: Optimisation-based decision making. Applied Thermal Engineering, 31(16), 3196-3205.

[99] Verheyen, W., Zhang, N., 2006. Design of flexible heat exchanger network for multi-period operation. Chemical Engineering Science , 61(23), 7730-7753.

[100] Viguri Fuente, J. R., 2013 Chemical Process Design, Subject 7 Equipment Sizing and Costing,<ocw.unican.es/ensenanzas-tecnicas/procesos-quimicos-defabricacion/materiales/Subject%207.%20Equipment%20Sizing%20and%20Costing%20OCW.pdf>. accessed: 20.11.2013.

[101] Viswanathan, J., Grossmann, I., 1990, A combined penalty function and outer-approximation method for MINLP optimization. Computers and Chemical Engineering , 14(7), pp. 769-782.

[102] Wan AlwiS. R., Rozali N. E. M., Abdul-Manan, Z., Klemeš, J. J., 2012, A process integration targeting method for hybrid power systems. Energy , 44(1), 6-10.

[103] Wang, X.-H., Li, Y.-G., 2010. Stochastic GP synthesis of heat integrated nonsharp distillation sequences. Chemical Engineering Research and Design , 88(1), 45-54.

[104] Yang C., Ogden J., 2007, Advanced Energy Pathways (AEP) Project, Task 4.1 Technology Assessments of Vehicle Fuels and Technologies, Public Interest Energy Research (PIER) Program, California Energy Commission, <steps.ucdavis.edu/People/cyang/aep/techology-assessments/AEP%20Tech %20Assessment%20-%20H2%20from%20NG.doc>, accessed 20.03.2013., California Energy Commission.

[105] Yee, T., Grossmann, I., 1990. Simultaneous optimization models for heat integration II. Heat exchanger network synthesis. Computers and Chemical Engineering, 14(10), 1165-1184.

[106] Yeomans, H., Grossmann, I. E., 1999. Nonlinear disjunctive programming models for the synthesis of heat integrated distillation sequences. Computers and Chemical Engineering , 23(9), 1135-1151.

[107] Zhang, B. J., Luo, X. L., Chen, X. Z., Chen, Q. L., 2013. Coupling Process Plants and Utility Systems for Site Scale Steam Integration. Industrial and Engineering Chemistry Research, 52(41), 14627-14636.

[108] Zhang, J., Liu P., Zhou Z., Ma L., Zheng L, Ni W., 2014, A mixed-integer nonlinear programming approach to the optimal design of heat network in a polygeneration energy system. Applied Energy, 114(0), 146-154.

[109] Zhang, N., Smith, R., Bulatov, I., Klemeš, J. J., 2013. Sustaining high energy efficiency in existing processes with advanced process integration technology. Applied Energy, 101(0), 26-32.

[110] Zhou, Z., Zhang J., Liu P., Zheng L., Georgiadis M.C., Pisticopoulus E N., 2013, A two-stage stochastic programming model for the optimal design of distributed energy systems. Applied Energy, 103(0), 135-144.

[111] Zhu, H., Huang, W.,Huang, G., 2014, Planning of regional energy systems: An inexact mixed-integer fractional programming model. Applied Energy, 113(0), 500-514.

Curicullum vitae

PERSONAL INFORMATION

Andreja Nemet

Kapca, Glavna ulica 2, SI-9220 Lendava (Slovenia)

+386 2 576 1502

nemeta@gmail.com

Sex Female | Date of birth 04 September 1984 | Nationality Slovenian

EDUCATION AND TRAINING

01 October 2010 – Present

PhD training
University of Maribor, Faculty of Chemistry and Chemical Engineering, Maribor (Slovenia)
Synthesis of processes and process subsystem for entire lifetime

01 March 2010 – 28 February 2013

PhD training
University of Pannonia, Faculty of Information Technology, Veszprém (Hungary)
Optimisation and integration of renewable energy generation and management options

01 October 2003 – 16 December 2009

Chemical engineer (equivalent to Master Degree)
University of Maribor, Faculty of Chemistry and Chemical Engineering, Maribor, (Slovenia)
Chemical engineering

1999 – 2003

Secondary School
Bilingual Secondary School Lendava (Slovenia)

WORK EXPERIENCE

May 2009 – September 2009

Diploma work
University of Maribor, Faculty of Chemistry and Chemical Engineering, Maribor (Slovenia)
Anaerobic digestion of mixture of Japanese knotweed (Polygonum Cuspidatum) and chicken manure treated with fungus Pleurotus Ostreatus

01 February 2008 – 31 March 2008

Study Praxis
Nafta Petrochem d.o.o, Lendava (Slovenia)
Analysis of melamine-urea-phenol formaldehyde adhesives.

PERSONAL SKILLS

Mother tongue(s) Slovenian, Hungarian

Other language(s)

	UNDERSTANDING		SPEAKING		WRITING
	Listening	Reading	Spoken interaction	Spoken production	
English	B2	B2	C1	C1	C1

Levels: A1/A2: Basic user - B1/B2: Independent user - C1/C2: Proficient user
Common European Framework of Reference for Languages

Communication skills: The communication skill I further developed in an international working group and also on the international conferences.

Organisational / managerial skills: Helped with the organization of CAPE Forum 2012 (Veszprém, Hungary)

Worked on different projects: see the list under title Projects

Job-related skills: Usage of gas chromatohraphy, FT-IR-a, usage of DSC

Computer skills: GAMS- General Algebraic Modeling System, MipSyn, Microsoft Office, internet

Other skills

Driving licence: B

ADDITIONAL INFORMATION

Projects

2010- 2012: EC FP7 project ‚Intensified Heat Transfer Technologies for Enhanced Heat Recovery– INTHEAT,

2011 – 2014: European Territorial Cooperation, Operational Programme Slovenia –Hungary project ECO HUB -Informational and educational eco-hub for supporting small and medium-sized enterprises in the integration, innovation, development and marketing of environmentally friendly products, processes and services

2012– 2013: Bilateral Project in cooperation with Joanneum Research – Graz,Initiationand Intensification of Cooperationin the Field of Energy and Resource Efficiency between Hungary and Austria.

2012 – 2016: EC FP7 project DISKNET Distributed Knowledge-Based Energy Saving Networks

Hungarian State and the European Union granted projectTÁMOP 4.2.2/B-10/1-2010-0025 „Tudományos képzés műhelyeinektámogatása a Pannon Egyetemen ”.

Hungarian State andthe European Union grantedproject TÁMOP-4.2.2.A-11/1/KONV-2012-0072 - Design and optimizationof modernization and efficient operation of energy supply and utilizationsystems using renewable energy sources and ICTs.

Research programme P2-0032 Process Systems Engineering and Sustainable Development

UNIVERZA V MARIBORU

FAKULTETA ZA KEMIJO IN KEMIJSKO TEHNOLOGIJO

Izjava doktorskega kandidata

Podpisana **Andreja Nemet**, vpisna številka **K3000274**

izjavljam,

da je doktorska disertacija z naslovom **Sinteza procesov in procesnih podsistemov za celotno življenjsko dobo (ang. Synthesis of processes and process subsystems for entire lifetime)**

- rezultat lastnega raziskovalnega dela,
- da predložena disertacija v celoti ali v delih ni bila predložena za pridobitev kakršnekoli izobrazbe po študijskih programih drugih fakultet ali univerz,
- da so rezultati korektno navedeni in
- da nisem kršil-a avtorskih pravic in intelektualne lastnine drugih.

Podpis doktorskega kandidata

Biography

COBISS Co-operative Online Bibliographic system & services COBISS

Andreja Nemet

Personal bibliography for the period 2009-2015

ARTICLES AND OTHER COMPONENT PARTS

1.01 Original scientific article

1. NEMET, Andreja, KLEMEŠ, Jiri, KRAVANJA, Zdravko. Mathematical programming approach to Total Site heate integration. V: KLEMEŠ, Jiri (ur.), VARBANOV, Petar (ur.), LIEW, Peng Yen (ur.). *24th European Symposium on Computer Aided Process Engineering : [ESCAPE-24, 15 to 18 June 2014, Budapest, Hungary]*, (Computer aided chemical engineering, ISSN 1570-7946, 33). Amsterdam ... [et al.]: Elsevier, cop. 2014, str. 1796-1800. [COBISS.SI-ID 18173718] tipologija 1.08 -> 1.01

2. NEMET, Andreja, KLEMEŠ, Jiri, KRAVANJA, Zdravko. Designing a Total Site for an entire lifetime under fluctuating utility prices. *Computers & chemical engineering*, ISSN 0098-1354. [Print ed.], Available online 18 July 2014, vol. , str. 1-24, doi: 10.1016/j.compchemeng.2014.07.004. [COBISS.SI-ID 18027798]

3. BOLDYRYEV, Stanislav, VARBANOV, Petar, NEMET, Andreja, KLEMEŠ, Jiri, KAPUSTENKO, Petro. Minimum heat transfer area for Total Site heat recovery. *Energy conversion and management*, ISSN 0196-8904. [Print ed.], 2014, vol. 87, str. 1093-1097, doi: 10.1016/j.enconman.2014.04.029. [COBISS.SI-ID 17797398]

4. NEMET, Andreja, KLEMEŠ, Jiri, KRAVANJA, Zdravko. Optimising entire lifetime economy of heat exchanger networks. *Energy*, ISSN 0360-5442. [Print ed.], 2013, vol. 57, str. 222-235, doi: 10.1016/j.energy.2013.02.046. [COBISS.SI-ID 16839702]

5. NEMET, Andreja, KLEMEŠ, Jiri, KRAVANJA, Zdravko. Life span production plant optimisation under varying economic conditions. V: VARBANOV, Petar (ur.). *PRES'13, the 16th International Conference on Process Integration, Modelling, and Optimisation for Energy Saving and Pollution Reduction, 29 September - 2 October, 2013, Rhodes, Greece*, (Chemical engineering transactions, ISSN 1974-9791, vol. 35, 2013). Milano: AIDIC, 2013, vol. 35, str. 103-108. [COBISS.SI-ID 17649174] tipologija 1.08 -> 1.01

6. NEMET, Andreja, KLEMEŠ, Jiri, KRAVANJA, Zdravko. Minimisation of a heat exchanger networks' cost over its lifetime. V: STEVANOVIC, Vladimir (ur.), STEFANOVIC, Gordana (ur.), RAŠKOVIĆ, Predrag (ur.). *The 24th International Conference on Efficiency, Cost, Optimization, Simulation and Environmental Impact of Energy, ECOS 2011*, (Energy, ISSN 0360-5442, Vol. 45, iss. 1 (2012)). Oxford: Elsevier, cop. 2012, vol. 45, iss. 1, str. 264-276, doi: 10.1016/j.energy.2012.02.049. [COBISS.SI-ID 16055574] tipologija 1.08 -> 1.01

7. NEMET, Andreja, KRAVANJA, Zdravko, KLEMEŠ, Jiri. Integration of solar thermal energy into processes with heat demand. *Clean technologies and environmental policy*, ISSN 1618-954X, June 2012, vol. 14, iss. 3, str. 453-463, doi: 10.1007/s10098-012-0457-6. [COBISS.SI-ID 15819798]

8. NEMET, Andreja, KLEMEŠ, Jiri, VARBANOV, Petar, KRAVANJA, Zdravko. Methodology for maximising the use of renewables with variable availability. V: KLEMEŠ, Jiri (ur.), GEORGIADIS, Michael C. (ur.), PISTIKOPOULOS, Efstratios N. (ur.). *Integration and Energy System Engineering, European Symposium on Computer-Aided Process Engineering 2011*, (Energy, ISSN 0360-5442, Vol. 44, iss. 1 (2012)). Oxford: Elsevier, cop. 2012, vol. 44, iss. 1, str. 29-37, doi: 10.1016/j.energy.2011.12.036. [COBISS.SI-ID 15816214] tipologija 1.08 -> 1.01

9. TABASOVÁ, Andrea, KROPÁČ, Jiří, KERMES, Vít, NEMET, Andreja, STEHLÍK, Petr. Waste-to-energy technologies : impact on environment. V: KLEMEŠ, Jiri (ur.), GEORGIADIS, Michael C. (ur.), PISTIKOPOULOS, Efstratios N. (ur.). *Integration and Energy System Engineering, European Symposium on Computer-Aided Process Engineering 2011*, (Energy, ISSN 0360-5442, Vol. 44, iss. 1 (2012)). Oxford: Elsevier, cop. 2012, vol. 44, iss. 1, str. 146-155, doi: 10.1016/j.energy.2012.01.014. [COBISS.SI-ID 16910102] tipologija 1.08 -> 1.01

10. NEMET, Andreja, KLEMEŠ, Jiri, VARBANOV, Petar, ATKINS, Martin, WALMSLEY, Michael. Total site methodology as a tool for planning and strategic decisions. V: 15th Conference Process Integration, Modelling and Optimisation for Energy Saving and Pollution Reduction, 25-29 August 2012, Prague, Czech Republic. VARBANOV, Petar (ur.).*PRES 2012*, (Chemical Engineering transactions, ISSN 1974-9791, Vol. 29, pt. 1,2 (2012)). Prague: ČSCHI: AIDIC, 2012, part 1, str. 115-120. [COBISS.SI-ID 16359702] tipologija 1.08 -> 1.01

11. NEMET, Andreja, KLEMEŠ, Jiri, KRAVANJA, Zdravko. Optimising a plant economic and environmental performace over a full lifetime. V: 15th Conference Process Integration, Modelling and Optimisation for Energy Saving and Pollution Reduction, 25-29 August 2012, Prague, Czech Republic. VARBANOV, Petar (ur.). *PRES 2012*, (Chemical Engineering transactions, ISSN 1974-9791, Vol. 29, pt. 1,2 (2012)). Prague: ČSCHI: AIDIC, 2012, part 2, str. 1435-1440. [COBISS.SI-ID 16360982] tipologija 1.08 -> 1.01

12. NEMET, Andreja, BOLDYRYEV, Stanislav, VARBANOV, Petar, KAPUSTENKO, Petro, KLEMEŠ, Jiri. Capital cost targeting of total site heat recovery. V: 15th Conference Process Integration, Modelling and Optimisation for Energy Saving and Pollution Reduction, 25-29 August 2012, Prague, Czech Republic. VARBANOV, Petar (ur.). *PRES 2012*, (Chemical Engineering transactions, ISSN 1974-9791, Vol. 29, pt. 1,2 (2012)). Prague: ČSCHI: AIDIC, 2012, part 2, str. 1447-1452. [COBISS.SI-ID 16361494] tipologija 1.08 -> 1.01

13. NEMET, Andreja, HEGYHÁTI, Máté, KLEMEŠ, Jiri, FRIEDLER, Ferenc. Increasing solar energy utilisation by rescheduling operations with heat and electricity demand. V: 15th Conference Process Integration, Modelling and Optimisation for Energy Saving and Pollution Reduction, 25-29 August 2012, Prague, Czech Republic. VARBANOV, Petar (ur.). *PRES 2012*, (Chemical Engineering transactions, ISSN 1974-9791, Vol. 29, pt. 1,2 (2012)). Prague: ČSCHI: AIDIC, 2012, part 2, str. 1483-1488. [COBISS.SI-ID 16361750] tipologija 1.08 -> 1.01

1.08 Published scientific conference contribution

14. BOLDYRYEV, Stanislav, VARBANOV, Petar, NEMET, Andreja, KLEMEŠ, Jiri, KAPUSTENKO, Petro. Minimum heat transfer area for total site heat recovery. V: 8th Conference on sustainable development of energy, water and environment systems, September 22-27, 2013, Dubrovnik. BAN, Marko (ur.), DUIĆ, Neven (ur.), GUZOVIĆ, Zvonimir (ur.).*Digital proceedings*, (CD Proceedings (Dubrovnik Conference on sustainable development of energy, water and environment systems), ISSN 1847-7178). Dubrovnik, 2013, str. 1-10. [COBISS.SI-ID 17305622]

15. ALAE-EDDINE, Barkaoui, YASSINE, Zarhoule, DUIĆ, Neven, KRAJAČIĆ, Goran, KLEMEŠ, Jiri, VARBANOV, Petar, NEMET, Andreja. Geothermal energy in Morocco : sustainability and environment impact. V: 8th Conference on sustainable development of energy, water and environment systems, September 22-27, 2013, Dubrovnik. BAN, Marko (ur.), DUIĆ, Neven (ur.), GUZOVIĆ, Zvonimir (ur.). *Digital proceedings*, (CD Proceedings (Dubrovnik Conference on sustainable development of energy, water and environment systems), ISSN 1847-7178). Dubrovnik, 2013, str. 1-13. [COBISS.SI-ID 17305366]

16. NEMET, Andreja, KLEMEŠ, Jiri, KRAVANJA, Zdravko. Designing a total site for an entire lifetime under fluctuating utility prices. V: 8th Conference on sustainable development of energy, water and environment systems, September 22-27, 2013, Dubrovnik. BAN, Marko (ur.), DUIĆ, Neven (ur.), GUZOVIĆ, Zvonimir (ur.). *Digital proceedings*, (CD Proceedings (Dubrovnik Conference on sustainable development of energy, water and environment systems), ISSN 1847-7178). Dubrovnik, 2013, str. 1-17. [COBISS.SI-ID 17304086]

17. NEMET, Andreja, KLEMEŠ, Jiri, KRAVANJA, Zdravko. Optimisation of heat exchangers network design over a full lifetime to improve economic potential of process heat recovery. V: 7 th Conference on Sustainable Development of Energy, Water and Environment Systems, Ohrid, Republic of Macedonia, July 1-7,2012. BAN, Marko (ur.).*Conference proceedings*. [S. l.: s. n.], 2012, str. 1-11. [COBISS.SI-ID 16147478]

18. NEMET, Andreja, ČUČEK, Lidija, VARBANOV, Petar, KLEMEŠ, Jiri, KRAVANJA, Zdravko. The potential of total site process integration and optimisation for energy saving and pollution reduction. V: 7 th Conference on Sustainable Development of Energy, Water and Environment Systems, Ohrid, Republic of Macedonia, July 1-7,2012. BAN, Marko (ur.). *Conference proceedings*. [S. l.: s. n.], 2012, str. 1-14. [COBISS.SI-ID 16146966]

19. NEMET, Andreja, KLEMEŠ, Jiri, KRAVANJA, Zdravko. Optimizacija ekonomske in okoljske uspešnosti podjetij skozi celotno življensko dobo. V: KRAVANJA, Zdravko (ur.), BRODNJAK-VONČINA, Darinka (ur.), BOGATAJ, Miloš (ur.). *Slovenski kemijski dnevi 2012, Portorož, 12.-14. september 2012 = Slovenian Chemical Days 2012, Portorož, September 12-14, 2012*. Maribor: FKKT, 2012, str. 1-7. [COBISS.SI-ID 16293398]

20. NEMET, Andreja, KLEMEŠ, Jiri, KRAVANJA, Zdravko. Minimisation of hen cost for entire life time. V: KRAVANJA, Zdravko (ur.), BRODNJAK-VONČINA, Darinka (ur.), BOGATAJ, Miloš (ur.). *Slovenski kemijski dnevi 2011, Portorož, 14-16 september 2011*. Maribor: FKKT, 2011, 11 str. [COBISS.SI-ID 15340822]

1.12 Published scientific conference contribution abstract

21. NEMET, Andreja, HOSNAR, Jernej, KLEMEŠ, Jiri, KRAVANJA, Zdravko. Synthesizing Total Site networks for direct and indirect inter-process heat exchange. V: *21st International Congress of Chemical and Process Engineering CHISA 2014 [and] 17th Conference PRES 2014, 23 - 27 August 2014, Praha, Czech Republic*. Praha: [s. n.], 2014, 1 str. [COBISS.SI-ID 18098454]

22. NEMET, Andreja, KLEMEŠ, Jiri, KRAVANJA, Zdravko. Optimising total site network under varying economic conditions. V: Slovenski kemijski dnevi 2013, Maribor, 10. in 12. september 2013. KRAVANJA, Zdravko (ur.), BRODNJAK-VONČINA, Darinka (ur.), BOGATAJ, Miloš (ur.). *Zbornik povzetkov referatov s posvetovanja*. Maribor: FKKT, 2013, str. 178. [COBISS.SI-ID 17165078]

23. NEMET, Andreja, KLEMEŠ, Jiri, KRAVANJA, Zdravko. Optimising plant economic and environmental performance over a full lifetime. V: 20th International Congress of Chemical and Process Engineering [and] 15th Conference PRES, 25 - 29 August 2012, Prague, Czech Republic. *CD-ROM of full texts*. Prague: [s. n.], cop. 2012, 1 str. [COBISS.SI-ID 16259350]

24. NEMET, Andreja, VARBANOV, Petar, KLEMEŠ, Jiri. An algorithm for determination of time slices with constant load for integration of renewable sources of energy. V: Veszprém Optimization Conference: Advanced Algorithms [also] VOCAL 2010, [Regional Centre of hungarian Academy of Sciences in Veszprém (VEAB), Hungary, December 13-15, 2010]. *VOCAL 2010 : program and abstracts*. Veszprém: Faculty of Information Technology, [2010], str. 46. [COBISS.SI-ID 14703894]

1.13 Published professional conference contribution abstract

25. ČUČEK, Lidija, VARBANOV, Petar, NEMET, Andreja, KLEMEŠ, Jiri, KRAVANJA, Zdravko. Extending potential of total site methodolgy for energy saving. V: Conference of Chemical Engineering = Műszaki Kémiai Napok'2012, 2012. április 24-26., Veszprém. *Konferencia kiadvány = Conference proceeding*. Veszprém: Pannon Egyetem, 2012, str. 132. [COBISS.SI-ID 16126230]

26. VARBANOV, Petar, NEMET, Andreja, KLEMEŠ, Jiri. Heat exchanger area targeting by an extended total site methodolgy. V: Conference of Chemical Engineering = Műszaki Kémiai Napok'2012, 2012. április 24-26., Veszprém. *Konferencia kiadvány = Conference proceeding*. Veszprém: Pannon Egyetem, 2012, str. 133-134. [COBISS.SI-ID16126486]

27. NEMET, Andreja, KLEMEŠ, Jiri, VARBANOV, Petar, KRAVANJA, Zdravko. Integrating renewables with varying availability to processes with heat demand. V: Conference of Chemical Engineering = Műszaki Kémiai Napok'2012, 2012. április 24-26., Veszprém. *Konferencia kiadvány = Conference proceeding*. Veszprém: Pannon Egyetem, 2012, str. 135-136. [COBISS.SI-ID 16126742]

MONOGRAPHS AND OTHER COMPLETED WORKS

2.11 Undergraduate thesis

28. NEMET, Andreja. *Anaerobna digestija mešanic japonskega dresnovca (polygonum cuspidatum) in piščančjega gnoja obdelanih z glivo pleurotus ostreatus : diplomska naloga*. Maribor: [A. Nemet], 2009. XVI, 67 str., ilustr. http://dkum.uni-mb.si/Dokument.php?id=12415. [COBISS.SI-ID 13783574]

2.13 Treatise, preliminary study, study

29. NEMET, Andreja, ČUČEK, Lidija, NOVAK-PINTARIČ, Zorka, KRAVANJA, Zdravko. *Design and optimization of modernization and efficient operation of energy supply and utilization systems using renewable energy sources and ICTs : report on project Contractor Agreement*. Maribor: Fakulteta za kemijo in kemijsko tehnologijo, 2015. 102 f., ilustr. [COBISS.SI-ID 18487318]

30. NEMET, Andreja, ANIČIĆ, Nemanja, KRAVANJA, Zdravko. *Anaerobna digestija piščančjega gnoja z dodatkom silaže in/ali oljnih usedlih : elaborat o opravljenem delu*. Maribor: Fakulteta za kemijo in kemijsko tehnologijo, 2014. 22 f., ilustr. [COBISS.SI-ID 17661462]

31. NEMET, Andreja, ČUČEK, Lidija, KRAVANJA, Zdravko. *Design and optimization of modernization and efficient operation of energy supply and utilization systems using renewable energy sources and ICTs : report on project Contractor Agreement*. Maribor: Fakulteta za kemijo in kemijsko tehnologijo, 2014. 52 f., ilustr. [COBISS.SI-ID 17662230]

32. NEMET, Andreja, BOTIĆ, Tanja, ČUČEK, Lidija, VAUKNER, Maja, NOVAK-PINTARIČ, Zorka, POHLEVEN, Franc, KRAVANJA, Zdravko. *Anaerobna digestija mešanic japonskega dresnovca (Polygonum Cuspidatum) in piščančjega gnoja obdelanih z glivo Pleurotus Ostreatus : poročilo o opravljenem delu za Perutnino Ptuj d.d.*. Maribor: Fakulteta za kemijo in kemijsko tehnologijo, Laboratorij za procesno sistemsko tehniko in trajnostni razvoj, 2010. 15 str., graf. prikazi. [COBISS.SI-ID 14030870]

PERFORMED WORKS (EVENTS)

3.15 Unpublished conference contribution

33. NEMET, Andreja, VARBANOV, Petar, KAPUSTENKO, Petro, DURGUTOVIĆ, Anes, KLEMEŠ, Jiri. *Capital cost targeting of total site heat recovery : training workshop at CAPE FORUM (Computer Aided Process Engineering) 26- 28 March 2012, Veszprém, Hungary*. Veszprém, 2012. [COBISS.SI-ID 15932182]

UNCLASSIFIED

34. KLEMEŠ, Jiri, VARBANOV, Petar, NEMET, Andreja. *Folyamatintegráció és optimalizálás*. Maribor: Kémia és Vegyészmérnöki Kara, 2014. 92 str., ilustr., graf. prikazi. ISBN 978-961-248-430-9. [COBISS.SI-ID 77415169]

35. KLEMEŠ, Jiri, VARBANOV, Petar, NEMET, Andreja. *Procesna integracija in optimizacija*. Maribor: Fakulteta za kemijo in kemijsko tehnologijo, 2014. 92 str., ilustr., graf. prikazi. ISBN 978-961-248-429-3. [COBISS.SI-ID 77412353]